R-06-120

Neutron data for accelerator-driven transmutation technologies

Annual Report 2005/2006

J Blomgren, L Nilsson, P Mermod, N Olsson,
S Pomp, A Öhrn, M Österlund
Department of Neutron Research, Uppsala University

October 2006

Svensk Kärnbränslehantering AB
Swedish Nuclear Fuel
and Waste Management Co
Box 5864
SE-102 40 Stockholm Sweden
Tel 08-459 84 00
+46 8 459 84 00
Fax 08-661 57 19
+46 8 661 57 19

ISSN 1402-3091
SKB Rapport R-06-120

Neutron data for accelerator-driven transmutation technologies

Annual Report 2005/2006

J Blomgren, L Nilsson, P Mermod, N Olsson,
S Pomp, A Öhrn, M Österlund
Department of Neutron Research, Uppsala University

October 2006

Summary

The project NATT, Neutron data for Accelerator-driven Transmutation Technology, is performed within the nuclear reactions group of the Department of Neutron Research, Uppsala University. The activities of the group are directed towards experimental studies of nuclear reaction probabilities of importance for various applications, like transmutation of nuclear waste, biomedical effects and electronics reliability. The experimental work is primarily undertaken at the The Svedberg Laboratory (TSL) in Uppsala, where the group is operating two world-unique instruments, MEDLEY and SCANDAL.

Highlights from the past year:

- Uppsala hosted the Tenth International Symposium on Neutron Dosimetry in June 2006. The conference is the largest in the world in the field.
- An EU project on nuclear data assessment for future reactors, including accelerator-driven systems, has been approved. Jan Blomgren, INF, is project coordinator.
- A network of European facilities for nuclear data measurements has been established via an EU Integrated Infrastructure Initiative. The neutron beam facility at TSL is one of nine facilities involved.
- Within the project, one PhD exam has been awarded.
- The number of masters level students in nuclear engineering has increased dramatically, and a course on nuclear power is presently the largest of all last-year engineering courses at Uppsala University.

Sammanfattning

Projektet NATT, Neutrondata för Acceleratordriven Transmutationsteknik, bedrivs inom kärnreaktionsgruppen vid institutionen för neutronforskning, Uppsala universitet. Gruppens verksamhet är inriktad mot experimentella studier av kärnfysikaliska reaktionssannolikheter för olika tillämpningsområden, som transmutation av kärnavfall, biomedicinska effekter och tillförlitlighet hos elektronik. Den experimentella verksamheten bedrivs huvudsakligen vid The Svedberglaboratoriet (TSL) i Uppsala, där gruppen driver två världsunika instrument, MEDLEY och SCANDAL.

Höjdpunkter från det gångna verksamhetsåret:

- Uppsala stod värd i juni 2006 för det tionde internationella symposiet om neutrondosimetri. Konferensen är världens största inom fältet.
- Ett EU-projekt om bedömning av kärndatabehoven för utveckling av framtida reaktorer, inklusive acceleratordrivna system, har beviljats. Jan Blomgren, INF, är projektets koordinator.
- Ett nätverk av europeiska faciliteter för kärndatamätningar har etablerats genom ett EU-projekt (Integrerat infrastrukturinitiativ). Neutronanläggningen vid TSL är en av nio involverade faciliteter.
- Inom projektet har en doktorand disputerat för doktorsexamen.
- Antalet grundutbildningsstudenter inom kärnkraft har ökat dramatiskt, och en kurs i kärnkraft är nu störst av alla sistaårskurser inom civilingenjörsprogrammen.

Contents

1 Background

1.1 The NATT project

The present project, Neutron data for Accelerator-driven Transmutation Technology (NATT), supported as a research task agreement by Statens Kärnkraftinspektion (SKI), Svensk Kärnbränslehantering AB (SKB), Ringhalsverket AB and Totalförsvarets forskningsinstitut (FOI), started 2002-07-01. The primary objective from the supporting organizations is to promote research and research education of relevance for development of the national competence within nuclear energy.

The aim of the project is in short to:

- promote development of the competence within nuclear physics and nuclear technology by supporting licenciate and PhD students,
- advance the international research front regarding fundamental nuclear data within the presently highlighted research area accelerator-driven transmutation,
- strengthen the Swedish influence within the mentioned research area by expanding the international contact network,
- provide a platform for Swedish participation in relevant EU projects,
- monitor the international development for the supporting organizations,
- constitute a basis for Swedish participation in the nuclear data activities at IAEA and OECD/NEA.

The project is operated by the Department of Neutron Research (INF) at Uppsala University, and is utilizing the unique neutron beam facility at the The Svedberg Laboratory (TSL) at Uppsala University.

In this document, we give a status report after the fourth year (2005-07-01–2006-06-30) of the project.

2 Introduction

Transmutation techniques in accelerator-driven systems (ADS) involve high-energy neutrons, created in the proton-induced spallation of a heavy target nucleus. The existing nuclear data libraries developed for reactors of today go up to about 20 MeV, which covers all available energies for that application; but with a spallator coupled to a core, neutrons with energies up to 1–2 GeV will be present. Although a large majority of the neutrons will be below 20 MeV, the relatively small fraction at higher energies still has to be characterized. Above about 200 MeV, direct reaction models work reasonably well, while at lower energies nuclear distortion plays a non-trivial role. This makes the 20–200 MeV region most important for new experimental cross section data /Blomgren 2002, 2004/.

Ten years ago, very little high-quality neutron-induced data existed in this energy domain. Only the total cross section /Finlay et al. 1993/ and the *np* scattering cross section had been investigated extensively. Besides this, there were data on neutron elastic scattering from UC Davis at 65 MeV on a few nuclei /Hjort et al. 1994/. Programmes to measure neutron elastic scattering had been proposed or begun at Los Alamos /Osborne et al. 2004/ and IUCF /Finlay et al. 1992/, with the former resulting in a publication on data on a few nuclei.

The situation was similar for (n,xp) reactions, where programmes have been run at UC Davis /Ford et al. 1989/, Los Alamos /Rapaport and Sugarbaker 1994/, TRIUMF /Alford and Spicer 1998/ and TSL Uppsala /Olsson 1995, Blomgren 1997/, but with limited coverage in secondary particle energy and angle. Better coverage had been obtained by the Louvain-la-Neuve group up to 70 MeV /Slypen et al. 1994/.

Thus, there was an urgent need for neutron-induced cross section data in the region around 100 MeV, which is an area where very few facilities in the world can give contributions. By international collaboration within an EU supported Concerted Action, which has been followed by the full scale projects HINDAS and EUROTRANS, the level of ambition for the present project has been increased, and the potential of the unique neutron beam facility at The Svedberg Laboratory in Uppsala has been well exploited.

During the last few years, the situation has improved dramatically, especially due to the HINDAS activities. At present, the nuclear data situation for ADS applications is relatively satisfactory up to 100 MeV. At 100 MeV, the hitherto most common energy at TSL, there are elastic neutron scattering data, neutron-induced light ion production data, neutron-induced activation, and fission cross sections available, in all cases on a series of nuclei. Some results have been published already, and there is a wealth of data under analysis and documentation. The present report will present some glimpses of this ongoing work.

Looking into the future, it can be envisioned that the coming 5–10 years will be devoted to similar activities at higher energies, i.e. up to 180 MeV, which is the highest neutron energy available at TSL. This has been made possible by the development of a new neutron beam facility, which is described below.

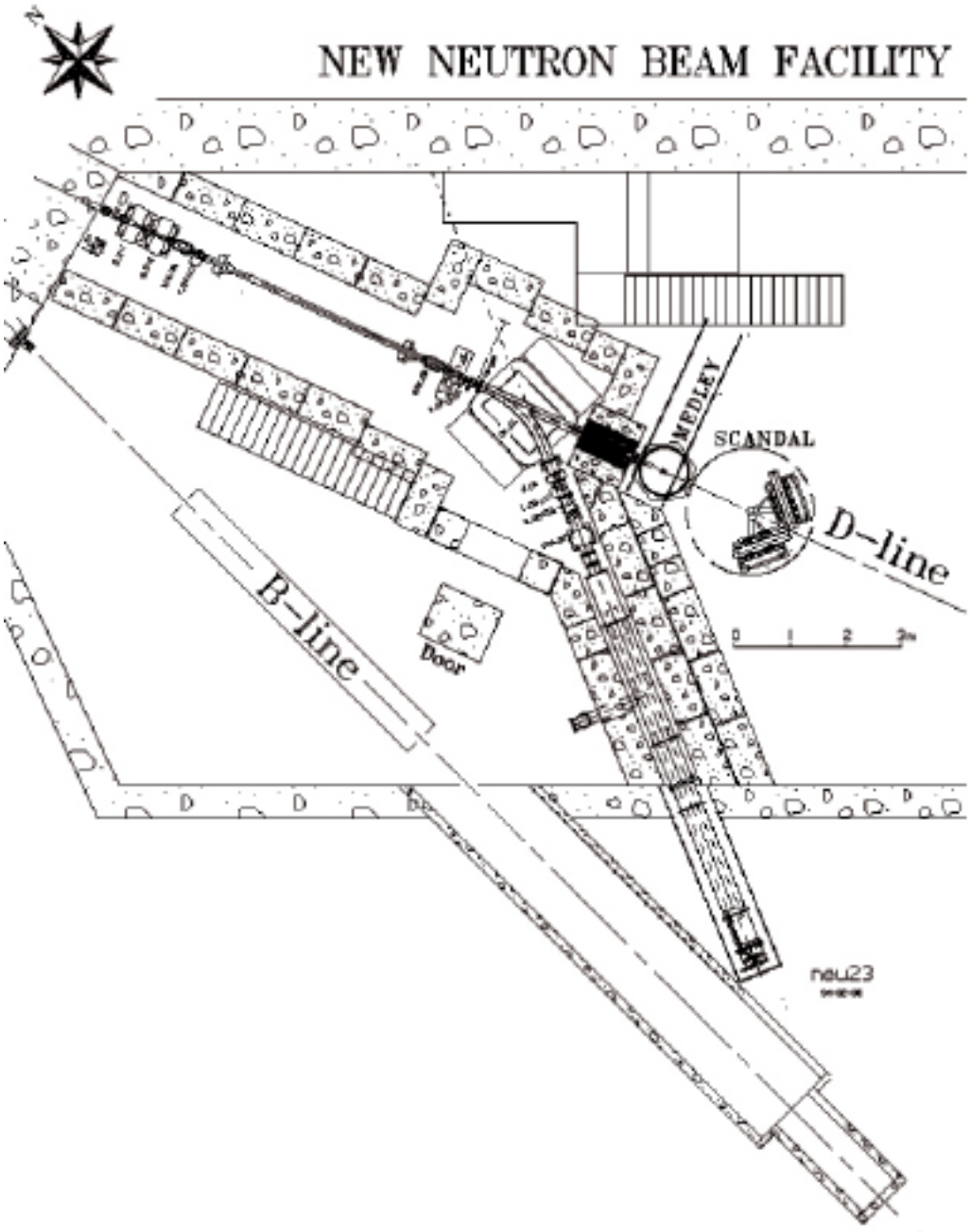

Figure 2-1. *The TSL neutron beam facility.*

3 Experimental setup and techniques

3.1 The TSL neutron beam facility

At TSL, quasi-monoenergetic neutrons are produced by the reaction $^{7}Li(p,n)^{7}Be$ in a ^{7}Li target bombarded by 50–180 MeV protons from the cyclotron, as is illustrated in Figure 2-1. After the target, the proton beam is bent by a dipole magnet into a concrete tunnel, where it is stopped in a well-shielded Faraday cup, used to measure the proton beam current. A narrow neutron beam is formed in the forward direction by a collimator with a total thickness of about one metre.

The energy spectrum of the neutron beam consists of a high-energy peak, having approximately the same energy as the incident proton beam, and a low-energy tail. About half of all neutrons appear in the high-energy peak, while the rest are roughly equally distributed in energy, from the maximum energy and down to zero. The thermal contribution is small. The low-energy tail of the neutron beam can be reduced using time-of-flight (TOF) techniques over the distance between the neutron source and the reaction target.

The relative neutron beam intensity is monitored by integrating the charge of the primary proton beam, as well as by using thin film breakdown counters, placed in the neutron beam, measuring the number of neutron-induced fissions in ^{238}U.

Two multi-purpose experimental setups are semi-permanently installed at the neutron beam line, namely MEDLEY and SCANDAL. These were described in detail in the annual report 1999/2000 of the previous KAT project, and only a brief presentation is given here.

3.2 The MEDLEY setup

The MEDLEY detector array /Dangtip et al. 2000/, shown in Figure 3-1, has been designed for measurements of neutron-induced light-ion production cross sections of relevance for applications within ADS and fast-neutron cancer therapy and related dosimetry. It consists of eight particle telescopes, installed at emission angles of 20–160 degrees with 20 degrees separation,

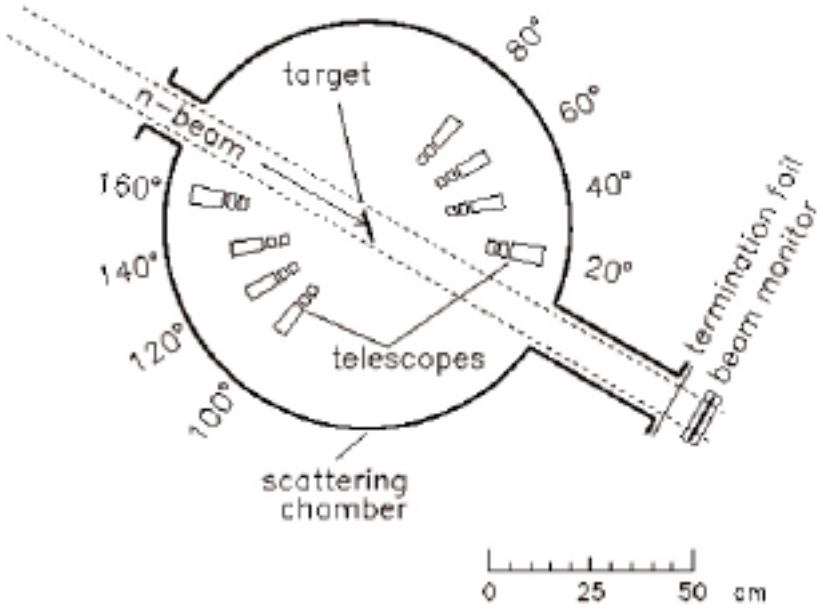

Figure 3-1. *The MEDLEY setup.*

in a 1 m diameter scattering chamber, positioned directly after the last neutron collimator. All the telescopes are fixed on a turnable plate at the bottom of the chamber, which can be rotated without breaking the vacuum.

Each telescope is a ΔE–ΔE–E detector combination, where the ΔE detectors are silicon surface barrier detectors with thicknesses of 50 or 60 μm and 400 or 500 μm, respectively, while the original E detector was a 50 mm long inorganic CsI(Tl) crystal. ΔE-ΔE or ΔE-E techniques are used to identify light charged particles (p, d, t, 3He, α). The chosen design gives a sufficient dynamic range to distinguish all charged particles from a few MeV up to more than 100 MeV.

During the present project year, the MEDLEY facility has been upgraded to work up to 180 MeV. This has been accomplished by replacing the previous CsI(Tl) detectors with thicker ones. The new facility is in operation, and will be the main instrument for the upcoming NEXT project.

3.3 The SCANDAL setup

The SCANDAL setup /Klug et al. 2002/ is primarily intended for studies of elastic neutron scattering, i.e. (n,n) reactions. Neutron detection is accomplished via conversion to protons by the H(n,p) reaction. In addition, (n,xp) reactions in nuclei can be studied by direct detection of protons. This feature is also used for calibration, and the setup has therefore been designed for a quick and simple change from one mode to the other.

The device is illustrated in Figure 3-2. It consists of two identical systems, in most cases located on each side of the neutron beam. The design allows the neutron beam to pass through the drift chambers of the right-side setup, making low-background measurements close to zero degrees feasible.

In neutron detection mode, each arm consists of a 2 mm thick veto scintillator for fast charged-particle rejection, a neutron-to-proton converter which is a 10 mm thick plastic scintillator, a 2 mm thick plastic scintillator for triggering, two drift chambers for proton tracking, a 2 mm thick ΔE plastic scintillator, which is also part of the trigger, and an array of 12 large CsI detectors for energy determination. The trigger is provided by a coincidence of the two trigger

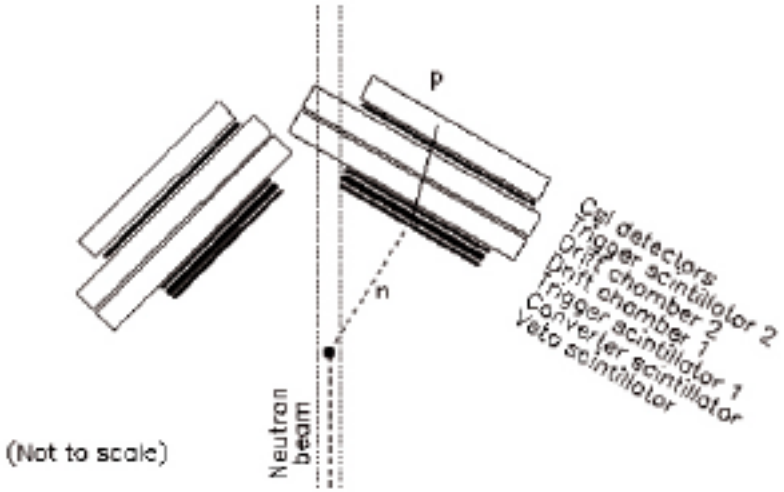

Figure 3-2. *The SCANDAL setup.*

scintillators, vetoed by the front scintillator. The compact geometry allows a large solid angle for protons emitted from the converter. Recoil protons are selected using the ΔE and E information from the plastic scintillators and the CsI detectors, respectively. The energy resolution is about 3.7 MeV (FWHM), which is sufficient to resolve elastic and inelastic scattering in several nuclei. The angular resolution is calculated to be about 1.4 degrees (rms) when using a cylindrical scattering sample of 5 cm diameter.

When SCANDAL is used for (n,xp) studies, the veto and converter scintillators are removed. A multitarget arrangement can be used to increase the target content without impairing the energy resolution, which is typically 3.0 MeV (FWHM). This multitarget box allows up to seven targets to be mounted simultaneously, interspaced with multi-wire

proportional counters (MWPC). In this way it is possible to determine in which target layer the reaction took place, and corrections for energy loss in the subsequent targets can be applied. In addition, different target materials can be studied simultaneously, thus facilitating absolute cross section normalization by filling a few of the multitarget slots with CH2 targets. The first two slots are normally kept empty, and used to identify charged particles contaminating the neutron beam.

3.4 Future activities

During 2004–05, the new neutron beam facility was taken into regular operation. The largest use is commercial, i.e. tests of the sensitivity of electronics concerning the neutron component of cosmic radiation. This is a rapidly growing reliability concern of the electronics industry, and it is commonly believed that this effect could terminate the further development of silicon-based circuit technology /Slayman 2004/ (Tang). This new facility has rapidly become the largest installation in Europe for this purpose, and the commercial potential is large. In combination with proton therapy of cancer, neutron irradiations of electronics provide adequate funding for the operation of TSL.

The new neutron beam facility provides a significantly higher intensity than the previous installation. This allows nuclear data experiments of high quality to be extended from the previous practical limit of 100 MeV up to the maximum energy of the facility, i.e. 180 MeV. This requires, however, a matching upgrade of the experimental devices. Both multipurpose experimental setups (MEDLEY and SCANDAL) are in principle possible to upgrade, i.e. the techniques as such can be expected to work also at higher energies. The cost, however, is very different. The MEDLEY setup is already under upgrade, since the cost is fairly limited, while upgrading of SCANDAL is pending due to financial limitations.

4 Results

4.1 Elastic scattering

A number of experimental observations seem to indicate that three-body forces exist in nuclei. Recent calculations /Witala et al. 1998/ have indicated that measurements of the differential cross section for elastic neutron-deuteron (*nd*) scattering in the 60–200 MeV range should be useful in searches for three-nucleon (*3N*) force effects. The *nd* elastic scattering differential cross section has been measured using both MEDLEY and SCANDAL at 95 MeV incident neutron energy. The results are presented in Figure 4-1 as the ratio between proton and deuteron production. It is evident that models based on inclusion of *3N* forces describe *nd* data in the angular region of the cross-section minimum very well, while models without 3N forces cannot account for the data. The MEDLEY data have previously been analyzed and published, and during the last year, additional data obtained with SCANDAL have been analyzed. The results corroborate the MEDLEY results, and a paper has recently been accepted for publication. A large publication, describing the experiments and analysis in detail is underway.

New experimental data on nitrogen, silicon, calcium, iron and yttrium are under analysis. Results on elastic scattering from carbon and lead have been published before. In the *nd* scattering experiment described above, also carbon and oxygen data were extracted as by-products due to normalization and the need for composed targets to study deuterium. This has resulted in more precise data on carbon than before, and on new data on oxygen, a nucleus hitherto not studied at this energy (see Figure 4-2).

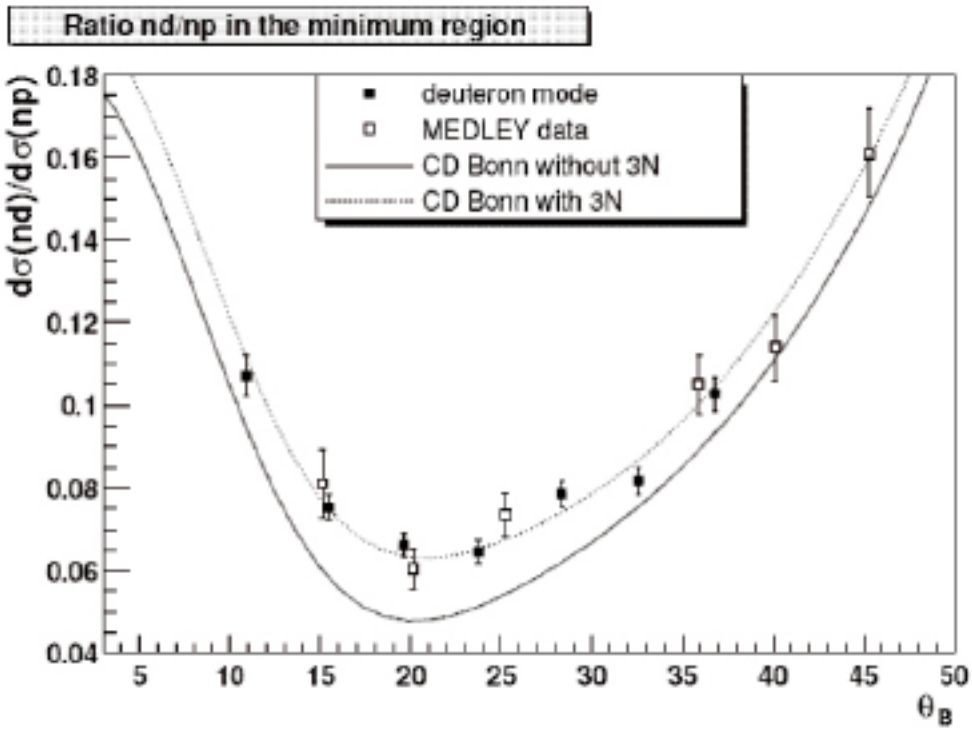

Figure 4-1. *The ratio of the neutron-deuteron and neutron-proton scattering cross sections at 95 MeV. The solid line is a theory prediction based on two-body forces only, while the dotted line includes three-body forces. Open symbols refer to previously published data with the MEDLEY setup, while filled symbols are the newly analyzed SCANDAL results.*

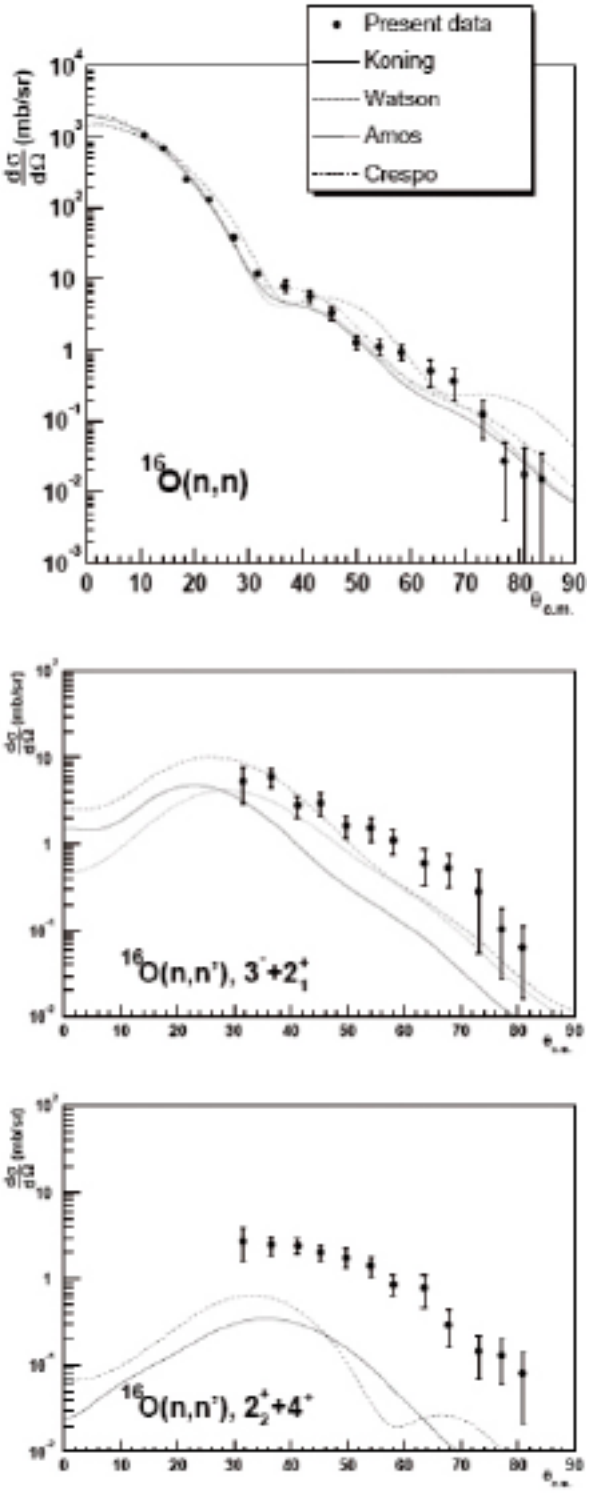

Figure 4-2. *Neutron scattering cross sections on oxygen at 95 MeV. The upper panel shows data for elastic scattering, while the two lower panels display cross sections for excited states. The lines refer to various theory predictions.*

The results on oxygen are particularly interesting from biological point of view. They have shown that conventional models for estimation of the biologic effects due to neutrons probably underestimate the biologic damage significantly, by as much as 30%.

4.2 (n,xlcp) reactions

In parallel with the other experiments mentioned above and below, data have been taken with the MEDLEY setup on light-ion production reactions. During the last years, results on oxygen, silicon, iron, lead and uranium have been published. Data on carbon, calcium, silver and molybdenum remain to be analyzed. Preliminary carbon data have been presented at an international conference.

4.3 (n,xn') reactions

We have a collaboration project with a group from Caen, France, on (n,xn') reactions. For these studies, a modified SCANDAL converter (CLODIA) has been designed and built in Caen. A large experiment on lead and iron targets was conducted in August 2004. This experiment is our deliverable in the EU 6th FWP EUROTRANS. Preliminary data were discussed at in informal project workshop in Uppsala recently, and will be presented at an international conference in April 2007.

4.4 Tagged neutron-proton scattering

Neutron-proton scattering is the reference cross section for fast-neutron reactions, i.e. it is the standard which all other cross sections are measured relative to. Besides our activities at TSL, we have been involved in a similar experiment at Indiana University Cyclotron Facility (IUCF), Bloomington, Indiana, USA. The results have recently been accepted for publication in Physical Review C.

4.5 Fission

We are working on the development of a setup for fission studies, based on MEDLEY in a revised geometric configuration. The setup has been tested and found to meet the specifications, and first experiments are in progress. One interesting feature of the new setup is that it allows a precise determination of the absolute cross section by measuring *np* scattering simultaneously. This is important, since only one previous experiment on high-energy fission has been performed with a reasonably good control of the absolute scale. Preliminary results have been presented at international conferences.

In addition, we have a long-term collaboration with a fission experiment group at Khlopin Radium Institute (KRI) in St. Petersburg, Russia (appendix V).

5 International activities

5.1 Collaborations

During 2005, the 6th EU framework program EUROTRANS started. Our group and our long-term collaborators from LPC Caen, France, have merged our activities in EUROTRANS, and we have a joint deliverable concerning (n,xn') reactions (see above).

Two new EU projects have been negotiated during the present project year. The four-year project EFNUDAT (European Facilities for Nuclear Data Measurements) aims at establishing a joint European infrastructure for nuclear data measurements by networking existing facilities. The role of INF is to provide access to The Svedberg Laboratory to other European users, and to coordinate the networking activities, i.e. organize workshops and training courses, as well as exchange programmes of technical staff. The total EU support is 2.4 M Euro, whereof 311,000 Euro is coordinated by UU/INF. The project involves 10 partners with 9 facilities in 7 countries.

INF is coordinating the two-year EU project CANDIDE (Coordination Action on Nuclear Data for Industrial Development in Europe). The project aims at enhancing the European collaboration on nuclear data for nuclear waste management. This will be accomplished via networking activities (workshops, training of young professionals in the nuclear power industry) and via an assessment of the status and needs of present and future nuclear data. The project involves 15 partners from 11 countries, spanning from very large business corporations (e.g. Electricité de France and Areva) to research centres and universities. The role of INF is to coordinate the entire project, to lead the development of a school for young professionals in the field, and to contribute experience in high-energy neutron experiments in the assessment. The total EU support to the project is 779,000 Euro.

5.2 Meetings and conferences

During the last year, Jan Blomgren has replaced Nils Olsson as Swedish representative in the OECD/NEA Nuclear Science Committee (NSC) and its Executive Group.

6 Administrative matters

6.1 Staff and students

During the project year, Jan Blomgren has been project leader, active on a 25–50% basis within the project. His other major activities are teaching and duties as director of studies, both at INF and the Swedish Nuclear Technology Center (SKC). Assistant professor (forskarassistent) Stephan Pomp has worked essentially full time within the project with research and student supervision. Associate professor (universitetslektor) Michael Österlund is involved in part-time research within the group. Leif Nilsson, retired professor, has been employed on about 10% time for student supervision.

Two PhD students are directly connected to and financed by the present project, Angelica Öhrn (born Hildebrand) and Philippe Mermod, which both are connected to the research school AIM (Advanced Instrumentation and Measurements).

6.2 Reference group

The reference group consists of Per-Eric Ahlström (SKB), Benny Sundström (SKI), Katarina Wilhelmsen (FOI) and Fredrik Winge (BKAB). Reference group meetings were held in Uppsala 2005-11-15 and 2006-06-08. Scientific and administrative reports on the progress of the project were given at the meetings.

In addition to this meeting, the progress of the work has continuously been communicated to the reference group members by short, written, quarterly reports.

6.3 New project – NEXT

A new nuclear data project, NEXT (Neutron Experiments for Transmutation), started July 1, 2006, and runs for four years. The project is similar to the present NATT project, but concentrating on light-ion production and fission studies at higher energies. The project is supported by Statens Kärnkraftinspektion (SKI), Svensk Kärnbränslehantering AB (SKB) and Ringhalsverket AB. Additional support is provided via the EU project EFNUDAT.

References

Alford W P, Spicer B M, 1998. Nucleon charge-exchange reactions at intermediate energy, Advances in Nuclear Physics 24, 1.

Blomgren J, 1997. The (n,p) reaction – Not So Boring After All? Proceedings from International Symposium on New Facet of Spin Giant Resonances in Nuclei, Tokyo, 1997, p. 70. (Invited talk).

Blomgren J, 2002. Experimental activities at high energies, Proceedings from an international symposium on Accelerator Driven Systems for Energy production and Waste Incineration: Physics, Design and Related Nuclear Data, Trieste, 2002, p. 327. (Invited talk)

Blomgren J, 2004. Nuclear data for accelerator-driven systems – Experiments above 20 MeV, Proceedings from EU enlargement workshop on Neutron Measurements and Evaluations for Applications, Bucharest, Romania, October 20–23, 2004 (invited).

Dangtip S, Atac A, Bergenwall B, Blomgren J, Elmgren K, Johansson C, Klug J, Olsson N, Alm Carlsson G, Söderberg J, Jonsson O, Nilsson L, Renberg P-U, Nadel-Turonski P, Le Brun C, Lecolley F-R, Lecolley J-F, Varignon C, Eudes Ph, Haddad F, Kerveno M, Kirchner T, Lebrun C, 2000. A facility for measurements of nuclear cross sections for fast neutron cancer therapy, Nucl. Instr. Meth. A452, 484.

Finlay R, Abfalterer W P, Fink G, Montei E, Adami T, Lisowski P W, Morgan G L, Haight R C, 1993. Neutron total cross sections at intermediate energies, Phys. Rev. C 47, 237.

Finlay R et al. 1992. Proposal to the NSF for support of CHICANE/Spectrometer System for the IUCF Cooler Ring.

Ford T D, Brady F P, Castaneda C M, Drummond J R, McEachern B, Romero J L, Sorenson D S, 1989. A large dynamic range detector for measurement of neutron-induced charged particle spectra down to zero degrees, Nucl. Instr. Meth. A274, 253.

Hjort E L, Brady F P, Romero J L, Drummond J R, Sorenson D S, Osborne J H, McEachern B, 1994. Measurements and analysis of neutron elastic scattering at 65 MeV, Phys. Rev. C 50, 275.

Klug J, Blomgren J, Atac A, Bergenwall B, Dangtip S, Elmgren K, Johansson C, Olsson N, Rahm J, Jonsson O, Nilsson L, Renberg P-U, Nadel-Turonski P, Ringbom A, Oberstedt A, Tovesson F, Le Brun C, Lecolley J-F, Lecolley F-R, Louvel M, Marie N, Schweitzer C, Varignon C, Eudes Ph, Haddad F, Kerveno M, Kirchner T, Lebrun C, Stuttgé L, Slypen I, Prokofiev A, Smirnov A, Michel R, Neumann S, Herpers U, 2002. SCANDAL – A facility for elastic neutron scattering studies in the 50–130 MeV range, Nucl. Instr. Meth. A489, 282.

Olsson N, 1995. Studies of spin-isospin excitations at TSL in Uppsala, Nucl. Phys. News 5, no. 2, 28.

Osborne J H, Brady F P, Romero J L, Ullmann J L, Sorenson D S, Ling A, King N S P, Haight R C, Rapaport J, Finlay R W, Bauge E, Delaroche J P, Koning A J, 2004. Phys. Rev. C 70, 054613.

Rapaport J, Sugarbaker E, 1994. Isovector excitations in nuclei, Ann. Rev. Nucl. Part. Sci. 44, 109.

Slayman C, 2004. Terrestial neutron single-event effects in workstations and servers, Proceedings of the 6th International Workshop on Radiation Effects on Semiconductor Devices for Space Applications, Tsukuba, Japan, October 6–8, 2004, p. 17.

Slypen I, Corcalciuc V, Ninane A, Meulders J P, 1994. Charged particles produced in fast neutron induced reactions ^{12}C in the 45–80 MeV energy range, Nucl. Instr. Meth. A337, 431.

Witala H, Glöckle W, Hüber D, Golak J, Kamada H, 1998. Cross section minima in elastic Nd scattering: Possible evidence for three-nucleon force effects, Phys. Rev. Lett. 81, 1183.

Appendix I

PHYSICAL REVIEW C **72**, 061002(R) (2005)

Evidence of three-body force effects in neutron-deuteron scattering at 95 MeV

P. Mermod, J. Blomgren,* A. Hildebrand, C. Johansson, J. Klug, M. Österlund, S. Pomp, and U. Tippawan
Department of Neutron Research, Uppsala University, Box 525, S-75120 Uppsala, Sweden

B. Bergenwall
Department of Neutron Research, Uppsala University, Box 525, S-75120 Uppsala, Sweden and Department of Radiation Sciences, Uppsala University, Sweden

L. Nilsson
Department of Neutron Research, Uppsala University, Box 525, S-75120 Uppsala, Sweden and The Svedberg Laboratory, Uppsala University, Sweden

N. Olsson
Department of Neutron Research, Uppsala University, Box 525, S-75120 Uppsala, Sweden and Swedish Defence Research Agency (FOI), Stockholm, Sweden

O. Jonsson, A. Prokofiev, and P.-U. Renberg
The Svedberg Laboratory, Uppsala University, Sweden

P. Nadel-Turonski
Department of Radiation Sciences, Uppsala University, Sweden and George Washington University, Washington, D.C., USA

Y. Maeda, H. Sakai, and A. Tamii
Department of Physics, University of Tokyo, Japan
(Received 17 June 2005; published 30 December 2005)

Recently, we have reported a measurement of the neutron-deuteron elastic scattering differential cross section at 95 MeV. In the present work, the previous results are confirmed with an independent measurement performed with another setup. The new data cover the full angular distribution by combining neutron detection and deuteron detection, and have an unprecedented precision in the region of the cross-section minimum, where three-nucleon forces are expected to be significant. The effect already identified in the previous measurement is clearly seen in the present data, which agree well with theoretical descriptions including three-nucleon forces.

DOI: 10.1103/PhysRevC.72.061002 PACS number(s): 21.45.+v, 25.10.+s, 25.40.Dn, 28.20.Cz

Nucleon-deuteron elastic scattering at intermediate energies is one of the most promising ways of investigating three-nucleon ($3N$) forces. The differential cross section for such a reaction can be calculated using refined nucleon-nucleon (NN) potentials [1–4] and solving the Faddeev equations [5]. By introducing a $3N$ potential—in this case the Tucson-Melbourne force [6]—into the Faddeev equations, it has been shown [7] that the presence of $3N$ forces should appear as a measurable effect in the angular range of the cross-section minimum. Another approach based on chiral perturbation theory (CHPT) gives similar predictions [8].

The effects of $3N$ forces, if present, should be seen in neutron-deuteron (nd) as well as in proton-deuteron (pd) scattering. Differential cross sections measurements for pd elastic scattering are numerous [9–18]. In contrast, there are few nd elastic scattering data at intermediate energies. The existing nd data sets are at 65 MeV [19], 95 MeV [20], 152 MeV [21], and 250 MeV [22]. At 65 MeV, the data are not able to resolve $3N$ force effects, which are expected to be small at this energy. At 95 and 152 MeV, the data favour the calculations including $3N$ forces. Finally, at 250 MeV, the data reveal an effect which is larger than predicted. At such energies, an ambiguity arises from the fact that relativistic effects are not taken into account by the theoretical descriptions. Thus, nd data around 100 MeV are well suited for investigating $3N$ forces: the effect is expected to be about 30% in the minimum region—large enough to be detected—whereas relativistic effects are not expected to contribute significantly.

The present data cover the full angular distribution at 95 MeV, the same energy as the MEDLEY data reported in Ref. [20]. They were obtained with the same neutron beam, and measured by the same research group, but with a completely different experimental setup. The detector setup used this time is SCANDAL (SCAttered Nucleon Detection AssembLy) [23], designed to detect neutrons for elastic scattering cross-section measurements by tracking recoil protons from converter plastic scintillators, with a possibility to remove the converters for detection of protons, and, in our case, also deuterons. One experiment was performed in neutron

*Corresponding author. Telephone: +46 18 471 3788. Email address: jan.blomgren@tsl.uu.se

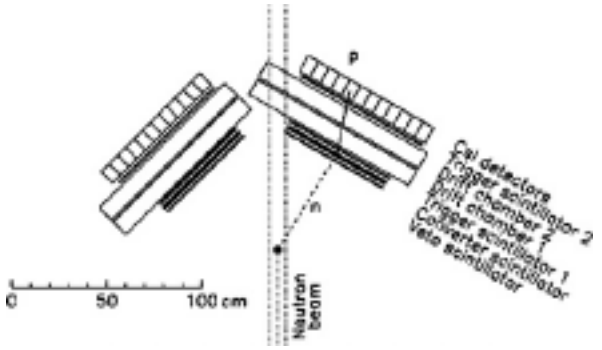

FIG. 1. Schematic layout of the SCANDAL setup [23]. In the present experiment (in neutron detection mode), the converter detector consisted of two plastic scintillators on each arm. A typical event is indicated.

detection mode and covers the angular range 15–100° for the neutron angle in the c.m. system. A second experiment was performed in deuteron detection mode, covering the angular range 105–158°, corresponding to the cross-section minimum.

The neutron beam was produced by the ^{7}Li$(p, n)^{7}$Be reaction at the neutron beam facility at The Svedberg Laboratory (TSL) in Uppsala before the upgrade of the facility. The high-energy peak in the neutron spectrum had an energy of 94.8 MeV, an FWHM of 2.7 MeV, and a flux of about 4×10^{4} n/(cm^{2} s) at the target position. The relative neutron fluence was monitored by two independent monitors based on the ^{238}U(n, f) reaction. The SCANDAL setup (see Fig. 1) consists of two identical arms that can be positioned on either side of the beam and rotated around the target position. Each arm can be equipped with a 2 mm thick veto scintillator for charged-particle rejection, two converter scintillators of 20 mm and 10 mm thickness for neutron-proton conversion, a 2 mm thick ΔE plastic scintillator for triggering, two drift chambers (DCH) giving two horizontal and two vertical positions for proton tracking, another 2 mm thick ΔE plastic scintillator for triggering, and an array of 12 CsI detectors. A full description of the SCANDAL setup and the TSL neutron beam facility is presented in Ref. [23].

The plastic scintillators and the CsI crystals were energy-calibrated by detecting recoil protons from *np* scattering at small angles, using the standard SCANDAL calibration procedure described in Ref. [23].

In neutron detection mode, the full setup was used, including veto, thick converter, and thin converter scintillators. The left arm was placed at −58° and the right arm at 32°. As

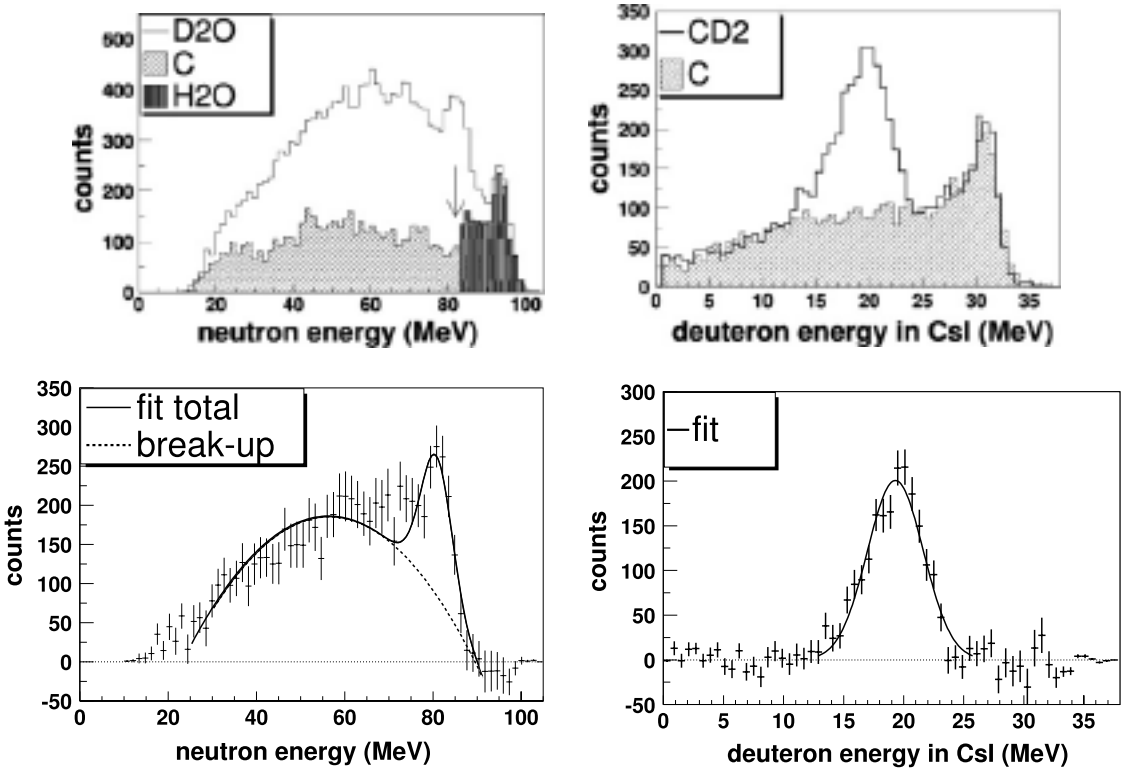

FIG. 2. Typical energy spectra for neutrons detected at 30° (left panels) and for deuterons detected at 32° (right panels). In the top left panel, the instrumental background has been subtracted. The bottom left panel shows the *nd* spectrum after subtraction of the oxygen content in D_2O and the contribution from elastic events converted in carbon (see text), fitted with a second degree polynomial plus a Gaussian in order to account for the deuteron breakup and elastic scattering, respectively. The bottom right panel shows the *nd* elastic peak after subtraction of the carbon content in CD_2 (in deuteron mode, break-up events are rejected by a particle identification cut). The error bars in the bottom panels are due to statistics.

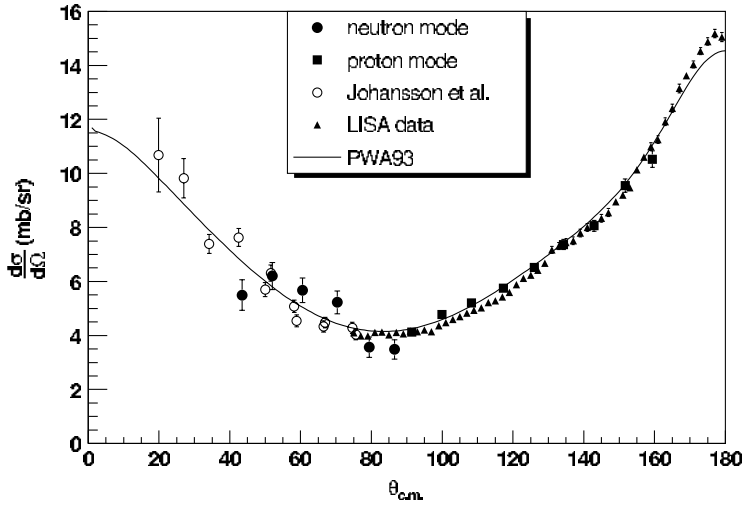

FIG. 3. The *np* differential cross section at 95 MeV. The error bars include both the statistical and systematic uncertainties. In neutron mode (filled circles), the data were normalized to the C(n, n) elastic scattering cross section [26] and can be compared with the Johansson *et al*. data [24] also taken with SCANDAL and normalized to the total *np* cross section. In proton mode (filled squares), the data were normalized to the LISA data [27] (filled triangles). The solid line represents the Nijmegen partial-wave analysis PWA93 [28].

targets, we used water (H_2O) and heavy water (D_2O) contained in cylindrical aluminium cans 8.5 cm in diameter, an empty can (EMPTY) for the instrumental background subtraction, and a graphite target cylinder 8 cm in diameter for normalization purposes. In a first-stage analysis, the data were treated on an event-by-event basis, selecting valid events the same way as described in detail in Ref. [24].

For the 12 angular bins of each arm defined by the 12 CsI crystals, the selected events were projected as neutron energy histograms. The spectra obtained with the H_2O, D_2O and EMPTY targets were normalized to the same neutron fluence—measured with the fission monitors and corrected for dead time. The instrumental background was eliminated by subtracting the EMPTY spectra from the H_2O and D_2O spectra. The oxygen background was canceled by subtracting the H_2O and D_2O spectra from each other, using also spectra from the graphite target [normalized to the same number of elastic events in O(n, n) and C(n, n) scattering] to simulate scattering from oxygen in the low-energy part of the spectra where *nd* and *np* scattering overlap. This is illustrated in the top left panel of Fig. 2, where the arrow indicates the end of the *np* peak, up to which the carbon spectrum is used. Additionnally, not shown in the figure is the subtraction of *nd* elastic events converted in carbon, which gives a contribution up to 10 MeV below the elastic peak [23,24]. The remaining *nd* spectra, as illustrated in the bottom left panel of the figure, were corrected for deuteron breakup by subtracting a second-order polynomian curve which was fitted to the break-up background. All these background subtraction procedures are not straightforward and will be described in more detail in a coming publication [25]. Finally, the elastic peaks were integrated to obtain the number of *np* and *nd* elastic events.

A correction for neutron multiple scattering and attenuation inside the target was applied as described in Ref. [24]. The data were corrected for the fraction of events due to low-energy neutrons, the CsI efficiency and the conversion efficiency, all these effects being slightly angle-dependent. The systematic uncertainty per point was typically $\pm 12\%$ and was heavily dominated by uncertainties in the oxygen and breakup background subtractions [25].

Differential cross sections were obtained for four sets of data: left and right arm with conversion in the thin and thick

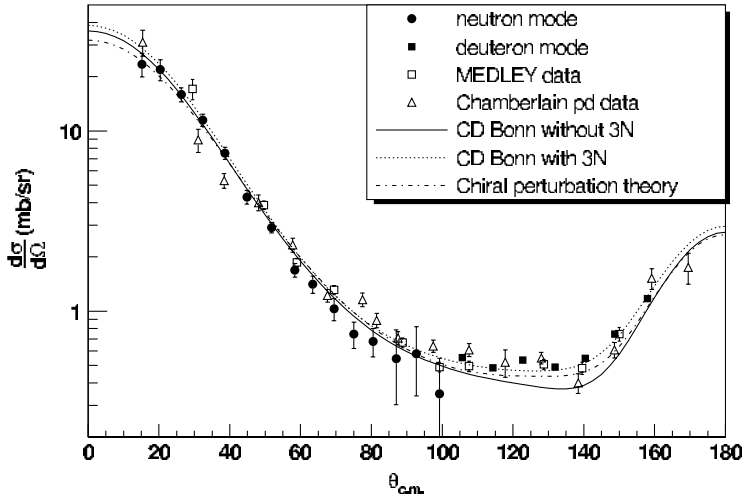

FIG. 4. The *nd* differential cross section at 95 MeV. The error bars include both the statistical and systematic uncertainties. In neutron mode (filled circles), the data were normalized to the C(n, n) elastic scattering cross section [26], and in deuteron mode (filled squares), the data were normalized to the *np* differential cross section (see Fig. 3). The present results are compared with the MEDLEY *nd* data [20] and Chamberlain and Stern *pd* data [10]. The theoretical curves are calculations using the CD-Bonn potential with (dotted line) and without (solid line) $3N$ forces [7], and CHPT calculations [8] (dashed line).

converter. Absolute normalization of these data was made relative to the $^{12}C(n, n)$ total elastic scattering cross section, handling the data from the graphite target the same way as in Ref. [26]. Knowing the total elastic cross section on carbon with an accuracy of $\pm 2.5\%$, as well as the relative neutron fluences and the relative number of nuclei inside the different targets with an accuracy better than $\pm 1\%$, the uncertainty in the normalization with this method was dominated by the quality of the fit to the $C(n, n)$ data and was estimated to be $\pm 4\%$. After normalization, the four sets of data were combined into one single set of data, reducing both the statistical and systematic uncertainties per point. The final *np* data are shown as filled circles in Fig. 3, and the *nd* data in Fig. 4. A good agreement between the present *np* data and the *np* data at the same energy measured by Johansson *et al.* [24]—which were normalized to the total *np* cross section—provides a valuable consistency check of our normalization method.

In deuteron detection mode (proton detection for *np* scattering), the veto and converter scintillators were removed from the SCANDAL arms used one at a time, disposed alternatively at 32° and -32° with respect to the beam. As targets, we used about 1 mm thick CD_2, CH_2 and graphite (C) target foils placed simultaneously inside a multitarget (MTGT) box (described in Ref. [23]). The MTGT multiwire proportional counter information was used to determine in which target the reaction took place. The data were sorted into 12 angular bins (one for each CsI). A time-of-flight criterion was applied to reject the low-energy part of the neutron spectrum. A cut in $\Delta E/E$ two-dimensional plots allowed to distinguish protons from deuterons.

For each angular bin, the remaining events were projected as energy spectra, as illustrated in the top right panel of Fig. 2. The *np* and *nd* peaks were obtained by subtracting the C spectra from the CH_2 and CD_2 spectra (see the bottom right panel of Fig. 2), and were integrated to obtain the number of elastic events.

Corrections were applied for the MTGT efficiency, the CsI efficiency, and the contamination from low-energy neutrons.

TABLE I. The measured *nd* elastic scattering differential cross section at 95 MeV incident neutron energy. In neutron detection mode, the data were normalized to the $C(n, n)$ total elastic scattering cross section [26], and in deuteron mode to the *np* differential cross section [27], in both cases with a normalization uncertainty of $\pm 4\%$. The uncertainty in the neutron c.m. angle is 0.5°.

$\theta_{\text{c.m.}}$ (degrees)	$\frac{d\sigma}{d\Omega}(\frac{mb}{sr})$	$\delta_{\text{stat}}(\frac{mb}{sr})$	$\delta_{\text{sys}}(\frac{mb}{sr})$
Neutron mode			
15.2	24.99	1.07	3.73
20.4	23.33	0.87	3.04
26.3	17.04	0.53	1.45
32.4	12.26	0.42	0.85
38.7	7.91	0.28	0.57
44.8	4.50	0.23	0.35
51.8	3.14	0.13	0.18
58.3	1.86	0.11	0.10
63.5	1.55	0.11	0.09
69.4	1.10	0.09	0.06
75.0	0.85	0.07	0.06
80.5	0.72	0.08	0.04
87.0	0.59	0.19	0.07
92.7	0.62	0.18	0.07
99.3	0.37	0.19	0.04
Deuteron mode			
105.7	0.552	0.010	0.014
114.3	0.484	0.009	0.012
122.8	0.535	0.010	0.013
131.9	0.488	0.010	0.013
140.4	0.548	0.013	0.014
148.8	0.744	0.016	0.019
158.0	1.172	0.025	0.034

The measurements beyond about 45° laboratory angle were discarded due to large energy losses inside the experimental setup. The systematic uncertainty per point was evaluated to typically $\pm 5\%$, due to uncertainties in the solid angle, the event selection and the corrections.

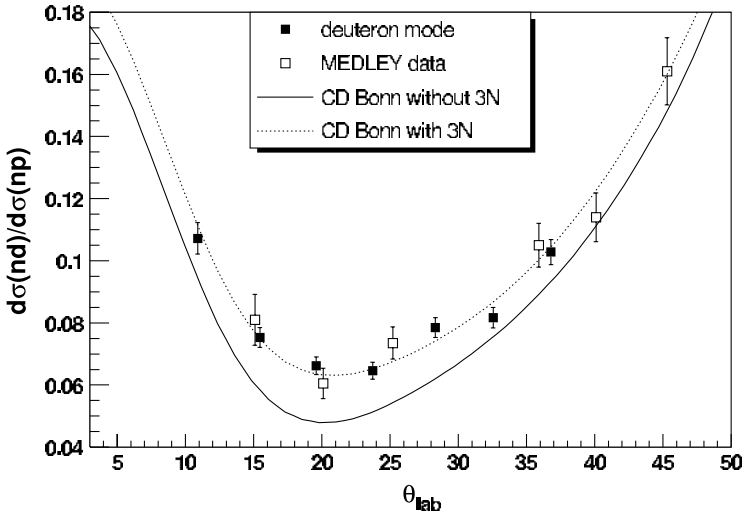

FIG. 5. Ratio of the *nd* cross section to the *np* cross section at 95 MeV in the minimum region, as a function of the detected particle angle in the laboratory. This ratio is independent of normalization uncertainties. The present results (filled squares) are compared with the MEDLEY results [20] (open squares), and with calculations based on the CD-Bonn potential with and without $3N$ forces [3,7].

The four sets of data—left and right arms placed on the left and right side of the beam—were independently normalized to the *np* scattering cross section, minimizing the χ^2 between the present *np* data and the high-quality LISA data [27]. This procedure gave an uncertainty of $\pm 4\%$ in the absolute normalization. Then, the four data sets were combined. The final *np* data are shown as filled squares in Fig. 3 and the *nd* data in Fig. 4 and in Table I, together with the data in neutron detection mode.

The present data are in very good agreement with the MEDLEY data [20] in both the forward and backward angular ranges. In the forward angular range (neutron mode), the data also agree well with the theoretical predictions. The $3N$ forces in this angular range are so weak compared to *NN* forces that the different predictions give very small differences, that cannot be resolved by the data. On the other hand, a comparison between *nd* and *pd* in this angular range could give information about Coulomb force effects, which are expected to be significant at forward angles [29].

At backward angles (deuteron mode), i.e., in the region of the *nd* cross-section minimum, the data agree fairly well with the Faddeev calculations including $3N$ forces with a reduced χ^2 of 3.7, and disagree spectacularly with the Faddeev calculations that do not include $3N$ forces with a reduced χ^2 of 44. In Fig. 5, we have plotted the ratio of the *nd* cross section to the *np* cross section, as a function of the deuteron/proton angle in the laboratory. This ratio has the advantage to be free from normalization uncertainties. Comparison between our data and the theoretical predictions for this ratio using the CD-Bonn potential gives a reduced χ^2 of 0.6 when $3N$ forces are included and 20 when they are not. The fact that the χ^2 is improved when considering the ratio indicates that the deviation is related to the normalization (here, the data were normalized to *np* scattering with an uncertainty of $\pm 4\%$ in the normalization). If we lower the absolute normalization for *nd* scattering by 4%, the χ^2 is reduced to a value close to one, as for the ratio (see Table II).

TABLE II. Reduced χ^2 between our data in deuteron mode and the different theoretical predictions.

	Without $3N$	With $3N$	CHPT
nd (Fig. 4)	44	3.7	18
$nd \cdot 0.96$	33	1.7	10
ratio *nd*/*np* (Fig. 5)	20	0.6	–

In conclusion, we have performed a new measurement of the *nd* scattering angular distribution at 95 MeV. The theoretical prediction based on Faddeev calculations using the CD-Bonn potential with $3N$ forces describes our data very well in the minimum region, while the same calculations without $3N$ forces are significantly off. The rest of the angular range is well described by all the calculations. This result, together with the previous MEDLEY data that observed the same behavior [20], can be interpreted as a strong evidence for $3N$ force effects.

We wish to thank the technical staff of the The Svedberg Laboratory for enthusiastic and skillful assistance. We are very thankful to E. Epelbaum, W. Glöckle, H. Kamada, and H. Witała for contributions concerning the theoretical part. We have appreciated the precious collaboration of K. Hatanaka and N. Kalantar-Nayestanaki. This work was supported by the Swedish Nuclear Fuel and Waste Management Company, the Swedish Nuclear Power Inspectorate, Ringhals AB, the Swedish Defence Research Agency and the Swedish Research Council.

[1] V. G. J. Stoks, R. A. M. Klomp, C. P. F. Terheggen, and J. J. de Swart, Phys. Rev. C **49**, 2950 (1994).
[2] R. B. Wiringa, V. G. J. Stoks, and R. Schiavilla, Phys. Rev. C **51**, 38 (1995).
[3] R. Machleidt, F. Sammarruca, and Y. Song, Phys. Rev. C **53**, R1483 (1996).
[4] R. Machleidt, Phys. Rev. C **63**, 024001 (2001).
[5] W. Glöckle, H. Witała, D. Hüber, H. Kamada, and J. Golak, Phys. Rep. **274**, 107 (1996).
[6] S. A. Coon and W. Glöckle, Phys. Rev. C **23**, 1790 (1981); S. A. Coon, M. D. Scadron, P. C. McNamee, B. R. Barrett, D. W. E. Blatt, and B. H. J. McKellar, Nucl. Phys. **A317**, 242 (1979).
[7] H. Witała, W. Glöckle, D. Hüber, J. Golak, and H. Kamada, Phys. Rev. Lett. **81**, 1183 (1998).
[8] E. Epelbaum, A. Nogga, W. Glöckle, H. Kamada, Ulf.-G. Meissner, and H. Witała, Phys. Rev. C **66**, 064001 (2002).
[9] H. Shimizu *et al*., Nucl. Phys. **A382**, 242 (1982).
[10] O. Chamberlain and M. O. Stern, Phys. Rev. **94**, 666 (1954).
[11] H. Sakai *et al*., Phys. Rev. Lett. **84**, 5288 (2000).
[12] G. Igo *et al*., Nucl. Phys. **A195**, 33 (1972).
[13] H. Postma and R. Wilson, Phys. Rev. **121**, 1229 (1961).
[14] K. Kuroda, A. Michalowicz, and M. Poulet, Nucl. Phys. **88**, 33 (1966).
[15] K. Sekiguchi *et al*., Phys. Rev. C **65**, 034003 (2002).
[16] K. Ermisch *et al*., Phys. Rev. C **68**, 051001(R) (2003).
[17] R. E. Adelberger and C. N. Brown, Phys. Rev. D **5**, 2139 (1972).
[18] K. Hatanaka *et al*., Phys. Rev. C **66**, 044002 (2002).
[19] H. Rühl *et al*., Nucl. Phys. **A524**, 377 (1991).
[20] P. Mermod *et al*., Phys. Lett. **B597**, 243 (2004).
[21] J. N. Palmieri, Nucl. Phys. **A188**, 72 (1972).
[22] Y. Maeda, Ph.D. thesis, University of Tokyo (2004), unpublished.
[23] J. Klug *et al*., Nucl. Instrum. Methods Phys. Res. A **489**, 282 (2002).
[24] C. Johansson *et al*., Phys. Rev. C **71**, 024002 (2005).
[25] P. Mermod *et al*., in preparation.
[26] J. Klug *et al*., Phys. Rev. C **68**, 064605 (2003).
[27] J. Rahm *et al*., Phys. Rev. C **63**, 044001 (2001).
[28] V. G. J. Stoks, R. A. M. Klomp, M. C. M. Rentmeester, and J. J. de Swart, Phys. Rev. C **48**, 792 (1993).
[29] A. Deltuva, A. C. Fonseca, and P. U. Sauer, Phys. Rev. C **71**, 054005 (2005).

SEE related studies at CELSIUS

Yu.Murin[1], J.Aichelin[2], Ch.Bargholtz[3], J.Blomgren[4], A.Budzanowski[5], M.Chubarov[1], B.Czech[5], C.Ekström[6], L.Geren[3], B.Jakobsson[7], A.Kolozhvari[6], O.Lozhkin[1], P.Nomokonov[8], N.Olsson[4], H.Persson[6], V.Plyushchev[1], I.Skwirczynska[5], H.H.K.Tang[9], P.-E.Tegner[3], L.Westerberg[6], I.Zartova[6], M.Zubkov[1], Y.Watanabe[10]

[1] V.G.Khlopin Radium Institute, 2-nd Murinsky 28, 194021, St.Petersburg, RU
[2] SUBATEX, University of Nantes, F-44307, Nantes, FR
[3] Department of Physics, Stockholm University, S-106 91, Stockholm, SE
[4] Department of Neutron Research, Angstrom Laboratory, Uppsala University Box 525, S-751 20, Uppsala, SE
[5]Institute of Nuclear Physics, 31-342 Krakow, PL
[6]The Svedberg Laboratory, Box 553, S-751 21, Uppsala, SE
[7] Department of Physics, University of Lund, Box 118, S-221 00, Lund, SE
[8] High Energy Laboratory, JINR, 141980, Moscow Region, Dubna, RU
[9] IBM T.J.Watson Research Center, NY 105 98, Yorktown Heights, USA
[10] Kyushu University, Kasuga 86-8580, JP

Introduction

Though the importance of cosmic radiation induced Single Event Effects (SEEs) in space electronics has been known for a long time, it was only in the last two decades that the impact of SEEs has also been recognized by the microelectronics industry that focuses on terrestrial applications [1,2]. The fundamental nuclear physics related to SEEs is in general understood [3]. The microscopic origin of SEEs is always traced down to the energy deposition from ionizing particles in a small, sensitive volume and subsequent charge released by a sensitive node of the device which can change the state of the curcuit. With this respect experimental measurements and theoretical simulations of the heavy recoils from nucleon-nucleus reactions are particularly important since the energy deposited by heavy recoils is a major source of secondary radiation. While in the past much effort has been devoted to the study of light particle emission (e.g. H and He isotopes) in intermediate-energy inelastic proton-nucleus collisions, very few experiments [5, 6] have been done to study the characteristics of slow recoils and especially to the yields and energy spectra of stable heavy recoils (eg. Al, Mg, etc.) - which are most effective in causing single event upsets (SEUs) in silicon chips. A major experimental difficulty in recoil work is that of identification of the heavy fragments - which have short ranges (of the order of 10 μm or less) - among other lighter reaction products in a standard setup in which the Si target is at rest in the laboratory system. The lack of direct measurements of recoil spectra (in the form of double differential cross sections) renders it difficult to make systematic checks on the standard nuclear reaction codes [3,7-9] used in the studies of SEE problems.

Experimental Setup at CELSIUS

An experimental setup has been developed at The Svedberg Laboratory (TSL), Uppsala, Sweden, to measure the production of recoil ions, using an inverse kinematics scheme. The setup is built at the CELSIUS nuclear accelerator and storage facility of TSL. It consists of four detector systems designed for the registration of reaction products emitted in collisions of 100-470A MeV Si ions with atoms of the internal hydrogen cryogenic cluster-jet target of CELSIUS. Secondary particles are registered simultaneously by the Small Angle Detector (SAD), Forward Wall Detector (FWD), Zero Angle Detector (ZAD), and the Spectator Tagging Detector (STD).

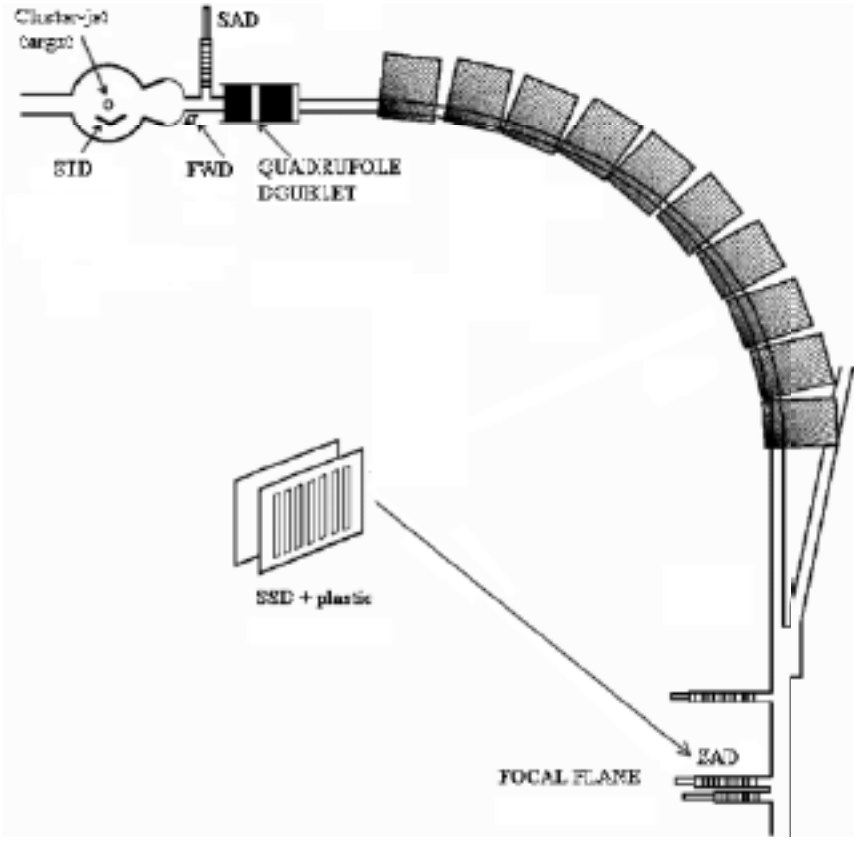

Figure 1: Layout of the experiments on Si+H and Si+D reactions at TSL

The Small Angle Detector (SAD) detects fragments of the Si ions emitted at angles $0.6^o - 1.1^o$ from the intersection point of the stored ion beam with the cluster-jet target of CELSIUS. Here the unique features of the CELSIUS cooled beam are fully exploited. SAD consists of a telescope with two 300 um custom-made silicon strip detectors (SSD) and a 5 mm thick plastic scintillator. The first SDD has circular and the second radial strips, with a total 16 of each type. Plastic scintillators are used as triggers of the readout cycle and for timing. The position of the particle registered simultaneously by both detectors is derived from the circular and radial strip numbers which identify one of the 512 pixels of SAD; the charge of the recoil is identified from SAD SSD pulse amplitude analysis. In the working position SAD is positioned to the minimum possible distance from the cooled beam of 12 mm.

The Zero Angle Detector (ZAD) is also a telescope made up of silicon strip detectors and plastic scintillator. Here we take the advantage of the technique developed at TSL [10] and use the quadrant after the cluster-jet target of CELSIUS as a magnetic spectrometer. ZAD is positioned at 22757 mm from the target, at the focal plane of the spectrometer [11]. As distinct from SAD, strips of ZAD make up the 32x32 rectangular net. Vertical strips of one of ZAD SSDs are used to register projectile-fragments, identify the charge (Z) and determine the position (X) of the hit point with respect to the nominal beam centerline. Electronic schemes of SAD and ZAD are identical. The Forward Wall Detector (FWD) [12] is used for the detection of light secondaries ($A < 5$) emitted within the polar angle of $3.9^o - 11.7^o$ in coincidence with the recoil registered by SAD. We used the CHICSi detector [13] for tagging the SAD data to the spectator-protons emitted within $60^o - 120^o$.

Experimental Results

A good quality 200A and 300A MeV Si beams were accelerated, cooled and stored by CELSIUS, with the fragment detectors located very close to the cooled beam. The experiments were conducted in November 2004 and April 2005 and the analysis of the experimental data obtained with the average Si ion beam current around 100 μA and hydrogen target thickness of around $2 * 10^(14)$ atoms/cm^2 for 200A and 300A MeV Si+H and Si+D reactions.

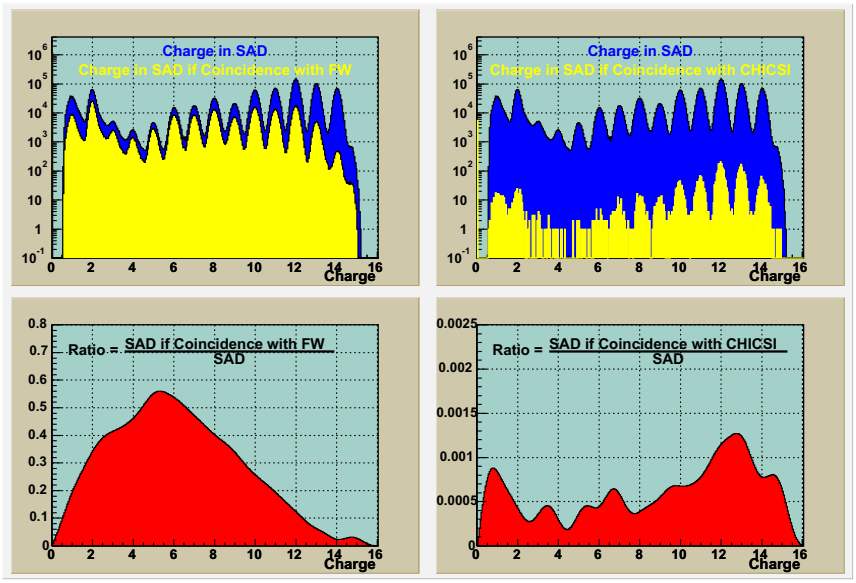

Figure 2: Charge distributions of recoils measured by SAD in study of 300A MeV Si+D reaction (see the text for details)

Figure 2 demonstrates charge distributions of recoils measured by us in a study of 300A MeV Si+D reaction. Here SAD inclusive data (dark colors) are confronted to that obtained in coinsedence with the hydrogen and helium isotopes registered by the FWD - (l.h.s.) and by the one of CHICSi telescopes (r.h.s). The bottom panels confront the the inclusive and semi-inclusive yields of recoils by showing the

ratios of the recoil rate production without and with the production of H,He or a low energetic spectator-like proton registered by the one of the telescopes of CHICSi. In the last case, one can argue that these events are attributed to the Si fragmentation induced by the quasi-free neutron of deuterium - a situation to a certain degree reproducing the practical SEE case. Results of complete analysis of the data are to appear soon.

ACKNOWLEDGMENTS

This work is supported by the International Scientific Technological Center (Project 1956)

References

[1] IBM J. Res. Dev. 40, No.1, 1996. (Special issue on terrestrial soft errors in microelectronic systems).

[2] MRS Bulletin vol. 28, Feb. 2003. (Special issue on Single Event Upsets in Microelectronics).

[3] Tang, H. H. K., IBM J. Res. Dev. 40, 91-107 (1996).

[4] Tang H. H. K. and Romero J.L., Hadron-Iduced Reactions: From Basic Research to New Technological Applications, AIP Conference Proceedings No. 392, 325-327 (1997).

[5] Romero J.L., Tang H.H.K., et al., Nucleon-Induced Secondaries: A Review and Future Experimental Developments, AIP Conference Proceedings No. 392, 655-658 (1997).

[6] Kwiatkowski K. et al., Phys.Rev.Lett. 50, 1648-1651 (1983).

[7] Tang H.H.K. et al., Phys. Rev C42, 1598-1622 (1990).

[8] Mashnik G., Gudima K.K., Sierk A.J., Prael R.E., "Improved Intranuclear Cascade Models for the Codes CEM2k and LAQGSM, LANL Report LA-UR-04-0039, Los Alamos (2004).

[9] Niita, K., Chiba, S. et al., Phys.Rev. C52, 2620-2635(1995).

[10] Chr. Bargholtz, K. Lindh et al., Nucl. Instr. Meth. A390, 160-166 (1997).

[11] Ringbom A., Tibell G. et al., Nucl. Instr. Meth. A373, 57-64 (1996).

[12] Budzanowski A. et al. Nucl.Instr.Meth. A482, 528-535 (2002).

[13] Jakobsson B., Nucl.Phys.News, 9, 22-27 (1999).

Contact e-mail: murin@hicx.phys.spbu.ru

Appendix III

PHYSICAL REVIEW C **73**, 034611 (2006)

Light-ion production in the interaction of 96 MeV neutrons with oxygen

U. Tippawan,[1,2] S. Pomp,[1,*] A. Ataç,[1] B. Bergenwall,[1,4] J. Blomgren,[1] S. Dangtip,[1] A. Hildebrand,[1] C. Johansson,[1] J. Klug,[1] P. Mermod,[1] L. Nilsson,[1,3] M. Österlund,[1] N. Olsson,[1,5] A. V. Prokofiev,[3] P. Nadel-Turonski,[4] V. Corcalciuc,[6] and A. J. Koning[7]

[1]*Department of Neutron Research, Uppsala University, Sweden*
[2]*Fast Neutron Research Facility, Chiang Mai University, Thailand*
[3]*The Svedberg Laboratory, Uppsala University, Sweden*
[4]*Department of Radiation Sciences, Uppsala University, Sweden*
[5]*Swedish Defence Research Agency, Stockholm, Sweden*
[6]*Institute of Atomic Physics, Heavy Ion Department, Bucharest, Romania*
[7]*Nuclear Research and Consultancy Group, Petten, The Netherlands*

(Received 19 January 2005; revised manuscript received 10 January 2006; published 23 March 2006)

Double-differential cross sections are reported for light-ion (p, d, t, ^{3}He, and α) production in oxygen induced by 96 MeV neutrons. Energy spectra are measured at eight laboratory angles from 20° to 160° in steps of 20°. Procedures for data taking and data reduction are presented. Deduced energy-differential and production cross sections are reported. Experimental cross sections are compared to theoretical reaction model calculations and experimental data at lower neutron energies in the literature. The measured proton data agree reasonably well with the results of the model calculations, whereas the agreement for the other particles is less convincing. The measured production cross sections for protons, deuterons, tritons, and α particles support the trends suggested by data at lower energies.

DOI: 10.1103/PhysRevC.73.034611 PACS number(s): 25.40.Hs, 25.40.Kv, 24.10.−i, 28.20.−v

I. INTRODUCTION

Fast-nucleon-induced reactions are useful is investigating nuclear structure, characterizing reaction mechanisms, and imposing stringent constraints on nuclear model calculations. Although oxygen is a light nucleus with doubly closed shells, it can be expected that many statistical assumptions hold for nucleon-induced reactions at several tens of MeV, because the level density at high excitation energies is sufficiently high that shell effects and other nuclear structure signatures are washed out. Light nuclei also have a low Coulomb barrier, implying that the suppression of charged-particle emission is weak. Therefore, nuclear reaction models for equilibrium and preequilibrium decay can be tested and benchmarked. Experimental data reported in the literature on reactions in oxygen at incident neutron energies of 27, 40, and 60 MeV [1,2] and between 25 and 65 MeV [3–5] offer possibilities for testing the predictions of reaction models.

In recent years, an increasing number of applications involving fast neutrons have been developed or are under consideration, e.g., radiation treatment of cancer [6–8], neutron dosimetry at commercial aircraft altitudes [9], soft-error effects in computer memories [10,11], accelerator-driven transmutation of nuclear waste and energy production [12,13], and determination of the response of neutron detectors [14]. Data on light-ion production in light nuclei such as carbon, nitrogen, and oxygen are particularly important in calculations of dose distributions in human tissue for radiation therapy at neutron beams, and for dosimetry of high-energy neutrons produced by high-energy cosmic radiation interacting with nuclei (nitrogen and oxygen) in the atmosphere [9,15]. When studying neutron dose effects in radiation therapy and at high altitude, it is especially important to consider oxygen, because it is the dominant element (65% by weight) in the average human tissue.

In this paper, we present experimental double-differential cross sections (inclusive yields) for protons, deuterons, tritons, ^{3}He, and α particles produced by 96 MeV neutrons incident on oxygen. The measurements have been performed at the cyclotron of The Svedberg Laboratory (TSL), Uppsala, using the MEDLEY experimental setup [16]. Spectra have been measured at eight laboratory angles, ranging from 20° to 160° in 20° steps. Extrapolation procedures are used to obtain coverage of the full angular range, and consequently energy-differential and production cross sections are deduced, the latter by integrating over energy and angle. The experimental data are compared to results of calculations with nuclear reaction codes and to existing experimental data at lower incident neutron energies.

The experimental methods are briefly discussed in Sec. II and data reduction and correction procedures are presented in Sec. III. The theoretical framework is summarized in Sec. IV. In Sec. V, the experimental results are reported and compared with theoretical and previous experimental data. Conclusions and an outlook are given in Sec. VI.

II. EXPERIMENTAL METHODS

The experimental setup and procedures for data reduction and corrections have been recently described in detail [17,18], and therefore only brief summaries are given here.

*Corresponding author: Tel. +46 18 471 6850, Fax. +46 18 471 3853, E-mail: stephan.pomp@tsl.uu.se

The neutron beam facility at TSL uses the ^{7}Li$(p,n)^{7}$Be reaction to produce a quasimonoenergetic neutron beam [19]. The lithium target was 8 mm thick in the present experiment and enriched to 99.98% in ^{7}Li. The 98.5 $\pm$ 0.3 MeV protons from the cyclotron impinge on the lithium target, producing neutrons with a full-energy peak of 95.6 $\pm$ 0.5 MeV with a full width at half maximum (FWHM) of 1.6 MeV. With a beam intensity of 5 μA, the neutron flux in the full-energy peak is about 5×10^4 neutrons/(s cm^2) at the target location. The collimated neutron beam has a diameter of 80 mm at the location of the target, where it is monitored by a thin film breakdown counter (TFBC) [20]. Relative monitoring was obtained by charge integration of the proton beam in a Faraday cup located in the proton beam dump. The two beam monitor readings were in agreement during the measurements.

The charged particles are detected by the MEDLEY setup [16]. It consists of eight three-element telescopes mounted inside a 100 cm diameter evacuated reaction chamber. Each telescope consists of two fully depleted ΔE silicon surface barrier detectors and a CsI(Tl) crystal. The thickness of the first ΔE detector (ΔE_1) is either 50 or 60 μm, while the second one (ΔE_2) is either 400 or 500 μm. They are all 23.9 mm in diameter (nominal). The cylindrical CsI(Tl) crystal, 50 mm long and 40 mm in diameter, serves as the E detector.

A 22 mm diameter 500 μm thick (cylindrical) disk of SiO_2 is used as the oxygen target. For the subtraction of the silicon contribution, measurements are performed using a silicon wafer having a 32×32 mm^2 quadratic shape and a thickness of 303 μm.

For absolute cross-section normalization, a 25 mm diameter and 1.0 mm thick polyethylene $(CH_2)_n$ target is used. The *np* cross section at 20° laboratory angle provides the reference cross section [21]. Instrumental background is measured by removing the target from the neutron beam. It is dominated by protons produced by neutron beam interactions with the beam tube and reaction chamber material, especially at the entrance and exit of the reaction chamber and in the telescope housings. Therefore, the telescopes at 20° and 160° are most affected.

The time-of-flight (TOF) obtained from the radio frequency of the cyclotron (stop signal for TDCs) and the timing signal from each of the eight telescopes (start signal) is registered for each charged-particle event. Typical count rates for target-in and target-out runs were 10 and 2 Hz, respectively. The dead time of the data acquisition system was typically 1–2% and never exceeded 10%.

III. DATA REDUCTION PROCEDURES AND CORRECTIONS

The ΔE-E technique is used to identify light charged particles ranging from protons to lithium ions. Good separation of all particles is obtained over their entire energy range, and particle identification is straightforward.

Energy calibration of all detectors is obtained from the data themselves [17,18]. Events in the ΔE-E bands are fitted with respect to the energy deposited in the two silicon detectors. This energy is determined from the detector thicknesses and tabulated energy loss values in silicon [22]. The ΔE_1 detectors are further calibrated and checked using a 5.48 MeV α source. The energy calibration of the CsI(Tl) detectors requires two parametrizations of the light output versus energy of the detected particle [16–18], one for hydrogen isotopes and another for helium isotopes. Supplementary calibration points are provided by the H(n,p) reaction, as well as transitions to the ground state and low-lying states in the ^{12}C$(n,d)^{11}$B, ^{16}O$(n,d)^{15}$N, and ^{28}Si$(n,d)^{27}$Al reactions. The energy of each particle is obtained by adding the energy deposited in each element of the telescope.

Low-energy charged particles are stopped in the ΔE_1 detector leading to a low-energy cutoff for particle identification of about 3 MeV for hydrogen isotopes and about 8 MeV for helium isotopes. The helium isotopes stopped in the ΔE_1 detector are nevertheless analyzed, and a remarkably low cutoff, about 4 MeV, can be achieved for the experimental α-particle spectra. These α-particle events could obviously not be separated from ^{3}He events in the same energy region, but the yield of ^{3}He is about a factor of 30 smaller than the α-particle yield in the region of 8 MeV, where the particle identification works properly. The assumption that the relative yield of ^{3}He is small is supported by the theoretical calculations in the evaporation peak region. In conclusion, the ^{3}He yield is within the statistical uncertainties of the α-particle yield for α energies between 4 and 8 MeV. A consequence of this procedure is that the ^{3}He spectra have a low-energy cutoff of about 8 MeV.

Knowing the energy calibration and flight distances, the flight time for each charged particle from target to detector can be calculated and subtracted from the measured total TOF. The resulting neutron TOF is used for selection of charged-particle events induced by neutrons in the main peak of the incident neutron spectrum.

Background events, collected in target-out runs and analyzed in the same way as target-in events, are subtracted from the corresponding target-in runs, with SiO_2 and silicon targets, after normalization to the same neutron fluence.

Because of the finite target thickness, corrections for energy loss and particle loss are applied to both targets individually. Details of the correction methods are described in Refs. [17,23]. The cross sections for oxygen are obtained after subtraction of the silicon data from the SiO_2 data with proper normalization with respect to the number of silicon nuclei in the two targets.[1]

Even if a great majority of the neutrons appear in the narrow full-energy peak at 95.6 MeV, a significant fraction (about 13%) belong to a tail extending toward lower energies, remaining after the TOF cut, see Fig. 1. The average neutron energy with the tail neutrons included is 94.0 MeV. The particle spectra have not been unfolded with the neutron energy distribution, because it is anticipated that the energy variation of the cross sections is rather weak in the energy range of interest. Furthermore, the data set is called 96 MeV (95.6) data, because the peak of the distribution is quite dominant and any structure observed at the high-energy end of the ejectile spectra is due to the peak of the neutron energy dsitribution.

[1] In the process of extracting the oxygen data, the silicon data of Ref. [17] were reanalyzed. In doing so, we adapted some changes and also found two mistakes. See Ref. [24] in this issue.

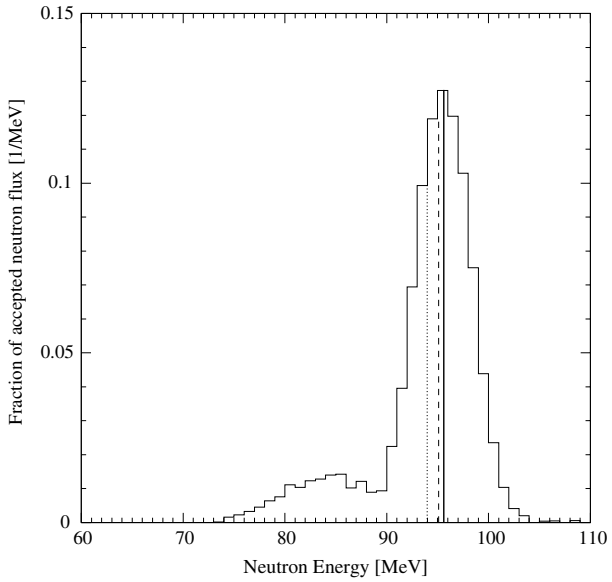

FIG. 1. Neutron energy distribution with TOF criterion applied derived from *np* scattering data at an angle of 20°. The peak (95.6 MeV), median (95.1 V), and average (94.0) are indicated by solid, dashed, and dotted vertical lines, respectively.

The *np* cross section, however, is measured at the peak of the distribution (95.6 MeV) and corrected for the tail contribution. The correction to 94.0 MeV is performed using the known energy dependence of the *np* cross section.

Other corrections of the data are performed in analogy with the similar experiment dealing with silicon and described in detail in [17]. The data and method for the efficiency correction of the CsI(Tl) detectors, reported in Ref. [19] and used in Ref. [17] and the present work, have recently [25] been corroborated by Monte Carlo calculations.

Absolute double-differential cross sections are obtained by normalizing the oxygen data to the number of recoil protons emerging from the CH_2 target. After selection of events in the main neutron peak and proper subtraction of the target-out and $^{12}C(n,p)$ background contributions, the latter taken from a previous experiment, the cross section can be determined from the recoil proton peak, using *np* scattering data [21]. All data have been normalized using the *np* scattering peak in the 20° telescope.

IV. THEORETICAL MODELS

The present data have been compared with nuclear theory predictions, computed with the two nuclear reaction codes GNASH [26,27] and TALYS [28]. While GNASH has been widely used during the last years, TALYS is a new code that has just been released in the public domain. The GNASH calculation is performed at a neutron energy of 100 MeV with parameters given in a recent evaluation for medical purposes [29] as described in Ref. [17]. Since oxygen is at the boundary of the mass range aimed for by the TALYS code, the code is described in some detail below.

Both GNASH and TALYS integrate direct, preequilibrium, and statistical nuclear reaction models into one calculation scheme and thereby give predictions for all the open reaction channels. Both codes use the Hauser-Feshbach model for sequential equilibrium decay and the exciton model for preequilibrium emission, though GNASH uses the one-component model, i.e., without isospin distinction of the excited nucleons, and TALYS uses the two-component model, see below. The angular distributions are obtained using the Kalbach systematics [30].

The purpose of TALYS is to simulate nuclear reactions that involve neutrons, photons, protons, deuterons, tritons, ^{3}He, and α particles in the 1 keV to 200 MeV energy range. Predicted quantities include integrated, single and double-differential cross sections, for both the continuum and discrete states, residue production and fission cross sections, γ-ray production cross sections, etc. For the present work, single- and double-differential cross sections are of interest. To predict these, a calculation scheme is invoked which consists of a direct + preequilibrium reaction calculation followed by subsequent compound nucleus decay of all possible residual nuclides calculated by means of the Hauser-Feshbach model.

For the optical model potentials (OMPs) of both neutrons and protons on ^{16}O up to 200 MeV, the global OMP of Ref. [31] was used. These potentials provide the necessary transmission coefficients for the statistical model calculations. Although the global neutron OMP has been validated for $A > 24$, at the high incident energy considered in this work, an adequate description of the basic scattering observables is expected, at least for the incident neutron channel and the high-energy inelastic scattering and charge-exchange leading to discrete states and the continuum. For the low-energy outgoing charged particles, the nonvalidated use of the global OMP may have larger consequences. Obviously, a system of a total of 17 nucleons can hardly be called statistical, and this shortcoming may be reflected in the prediction of some of the observables that concern low emission energies. For complex particles, the optical potentials were directly derived from the nucleon potentials using the folding approach of Watanabe [32]. Finally, since applying the charged-particle OMPs for nuclides as light as ^{16}O may be physically dubious, we renormalize the obtained OMP transmission coefficients with the empirical nonelastic cross sections of Ref. [33].

The high-energy end of the ejectile spectra are described by preequilibrium emission, which takes place after the first stage of the reaction but long before statistical equilibrium of the compound nucleus is attained. It is imagined that the incident particle creates step by step more complex states in the compound system and gradually loses its memory of the initial energy and direction. The default preequilibrium model of TALYS is the two-component exciton model [34,35]. A remark similar to that given above for the OMP applies: the two-component exciton model for nucleon reactions has been tested, rather successfully, against basically all available experimental nucleon spectra for $A > 24$ [34]. The current system, $A = 17$, falls outside that mass range and does not entirely qualify as a system that can be handled by fully statistical models such as the exciton model.

We recall the basic formula of Ref. [34] for the exciton model cross section,

$$\frac{d\sigma_k^{\mathrm{EM}}}{dE_k} = \sigma^{\mathrm{CF}} \sum_{p_\pi=p_\pi^0}^{p_\pi^{\mathrm{eq}}} \sum_{p_\nu=p_\nu^0}^{p_\nu^{\mathrm{eq}}} w_k(p_\pi, h_\pi, p_\nu, h_\nu, E_k) \times S_{\mathrm{pre}}(p_\pi, h_\pi, p_\nu, h_\nu), \quad (1)$$

where $p_\pi(p_\nu)$ is the proton (neutron) particle number and $h_\pi(h_\nu)$ the proton (neutron) hole number, σ^{CF} is the compound formation cross section, and S_{pre} is the time-integrated strength which determines how long the system remains in a certain exciton configuration. The initial proton and neutron particle numbers are denoted $p_\pi^0 = Z_p$ and $p_\nu^0 = N_p$ with $Z_p(N_p)$ being the proton (neutron) number of the projectile. In general, $h_\pi = p_\pi - p_\pi^0$ and $h_\nu = p_\nu - p_\nu^0$, so that the initial hole numbers are zero, i.e., $h_\pi^0 = h_\nu^0 = 0$, for primary preequilibrium emission. The preequilibrium part is calculated by Eq. (1), using $p_\pi^{\mathrm{eq}} = p_\nu^{\mathrm{eq}} = 6$, whereas the remainder of the reaction flux is distributed through the Hauser-Feshbach model. In addition, the never-come-back approximation is adopted.

The emission rate w_k for ejectile k with spin s_k is given by

$$w_k(p_\pi, h_\pi, p_\nu, h_\nu, E_k) = \frac{2s_k+1}{\pi^2\hbar^3}\mu_k E_k \sigma_{k,\mathrm{inv}}(E_k) \times \frac{\omega(p_\pi - Z_k, h_\pi, p_\nu - N_k, h_\nu, E_x)}{\omega(p_\pi, h_\pi, p_\nu, h_\nu, E^{\mathrm{tot}})}, \quad (2)$$

where $\sigma_{k,\mathrm{inv}}(E_k)$ is the inverse reaction cross section as calculated from the optical model, and ω is the two-component particle-hole state density. The full reaction dynamics that leads to Eq. (1) is described in Refs. [34,35]. We here restrict ourselves to the formulas given above since they contain the model- and parameter-dependent quantities. The expression for S_{pre} contains the adjustable transition matrix element M^2 for each possible transition between neutron-proton exciton configurations. A proton-neutron ratio of 1.6 for the squared internal transition matrix elements was adopted to give the best overall agreement with experiment, i.e., $M_{\pi\nu}^2 = M_{\nu\pi}^2 = 1.6M_{\pi\pi}^2 = 1.6M_{\nu\nu}^2 = 1.6M^2$. For ^{16}O, we use the following expression for the matrix element [34],

$$M^2 = \frac{0.6}{A^3}\left[6.8 + \frac{4.2\times10^5}{\left(\frac{E^{\mathrm{tot}}}{n} + 10.7\right)^3}\right], \quad (3)$$

where n is the exciton number. Partial level density parameters $g_\pi = Z/17$ and $g_\nu = N/17$ were used in the equidistant spacing model for the partial level densities. Finally, an effective surface interaction well depth $V = 12$ MeV [34] was used.

At incident energies above several tens of MeV, the residual nuclides formed after binary emission may have so large an excitation energy that the presence of additional fast particles inside the nucleus becomes possible. The latter can be imagined as strongly excited particle-hole pairs resulting from the first binary interaction with the projectile. The residual system is then clearly nonequilibrated, and the excited particle that is high in the continuum may, in addition to the first emitted particle, be emitted on a short time scale. This so-called multiple preequilibrium emission forms an alternative theoretical picture of the intranuclear cascade process, whereby the exact location and momentum of the particles are not followed, but instead the total energy of the system and the number of particle-hole excitations (exciton number). In actual calculations, the particle-hole configuration of the residual nucleus after emission of the ejectile, is reentered as an initial condition in Eq. (1). When looping over all possible residual configurations, the multiple preequilibrium contribution is obtained. In TALYS, multiple preequilibrium emission is followed up to arbitrary order; though for 96 MeV, only the secondary preequilibrium emission is significant.

It is well known that semiclassical models, such as the exciton model, have had some problems in describing angular distributions (essentially because the model is based on a compoundlike concept instead of a direct one). Therefore, as mentioned previously, the double-differential cross sections are obtained from the calculated energy spectra using the Kalbach systematics [30].

To account for the evaporation peaks in the charged-particle spectra, multiple compound emission was treated with the Hauser-Feshbach model. In this scheme, all reaction chains are followed until all emission channels are closed. The Ignatyuk model [36] has been adopted for the total level density to account for the damping of shell effects at high excitation energies.

For preequilibrium reactions involving deuterons, tritons, ^{3}He, and α particles, a statistical contribution from the exciton model is automatically calculated with the formalism described above. However, it is well known that for nuclear reactions involving projectiles and ejectiles with different particle numbers, mechanisms such as stripping, pickup, and knockout play an important role, and these directlike reactions to the continuum are not covered by the exciton model. Therefore, Kalbach has developed a phenomenological contribution for these mechanisms [37], which is included in TALYS. The advantages over the older method (which is included in GNASH) include a better consideration of the available phase space through normalized particle-hole state densities and a better empirical determination of the pickup, stripping, knockout strength parameters, enabled by the more extensive experimental database that is now available. It has recently been shown (see Table I of Ref. [38]) that for medium and heavy nuclides this method gives a considerable improvement over the older methods. The latter seemed to consistently underpredict neutron-induced reaction cross sections involving pickup of one or a few nucleons. In this paper, the two methods meet again, this time for the prediction of reactions on a light nucleus, and their performance will be compared in the next section.

V. RESULTS AND DISCUSSION

A. Experimental results

Double-differential cross sections of ^{16}O(n, $x$lcp) reactions, where lcp stands for light charged particle, at laboratory angles of 20°, 40°, 100°, and 140° for protons, deuterons, tritons, ^{3}He, and α particles are shown in Figs. 2–6, respectively. All angles are plotted with the same cross section scale for each

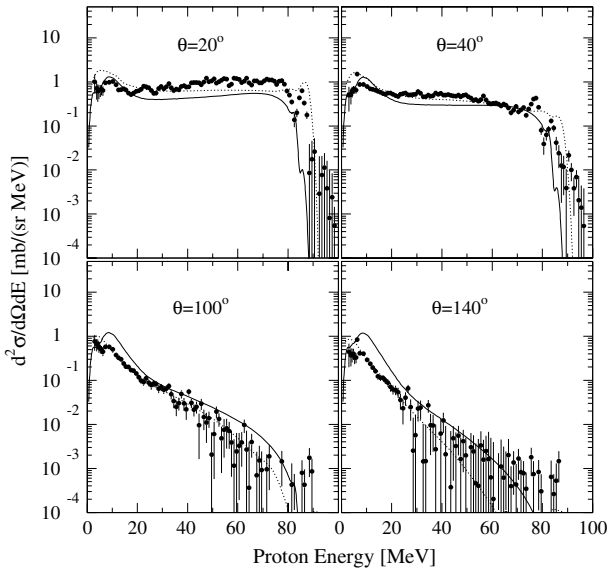

FIG. 2. Experimental double-differential cross sections (filled circles) of the O(n, px) reaction at 96 MeV at four laboratory angles. Curves indicate theoretical calculations based on GNASH (dotted) and TALYS (solid).

emitted particle to facilitate comparison of magnitudes. The choice of energy bin width depends on the energy resolution in the experiment, the thick target correction, and the acceptable statistics in each energy bin. The error bars in Figs. 2–6 represent statistical uncertainties only.

The overall relative statistical uncertainties of individual points in the double-differential energy spectra at 20° are typically 8% for protons, 13% for deuterons, 20% for tritons, 15% for ^{3}He, and 12% for α particles. As the angular

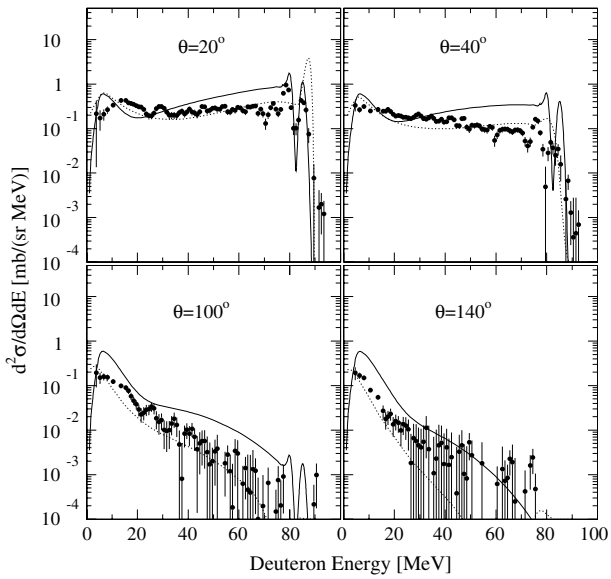

FIG. 3. Same as fig. 2, but for the O(n, dx) reaction.

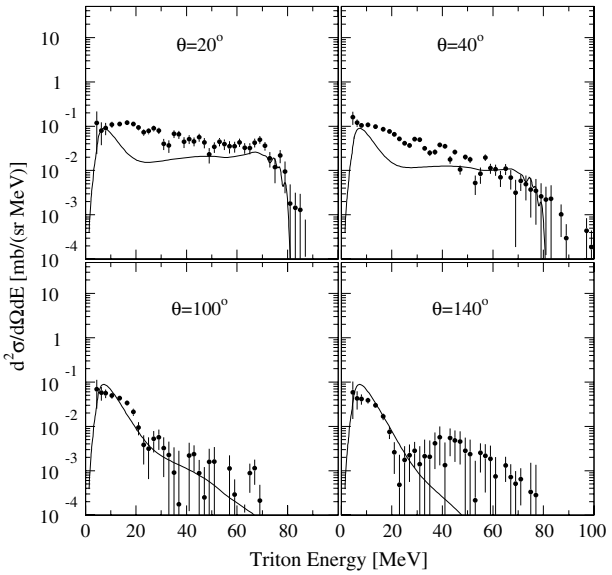

FIG. 4. Same as Fig. 2, but for the O(n, tx) reaction; curve indicates TALYS calculations.

distributions are forward-peaked, these values increase with angle. The systematic uncertainty contributions are due to thick target correction (1%–20%), collimator solid angle (1%–5%), beam monitoring (2%–3%), number of oxygen nuclei (0.1%), CsI(Tl) intrinsic efficiency (1%), particle identification (1%) and dead time (<0.1%). The uncertainty in the absolute cross section is about 5%, which is due to uncertainties in np scattering angle, contribution from the low-energy continuum of the ^{7}Li(p, n) spectrum to the np scattering proton peak (3%), reference np cross sections (2%) [21], statistics

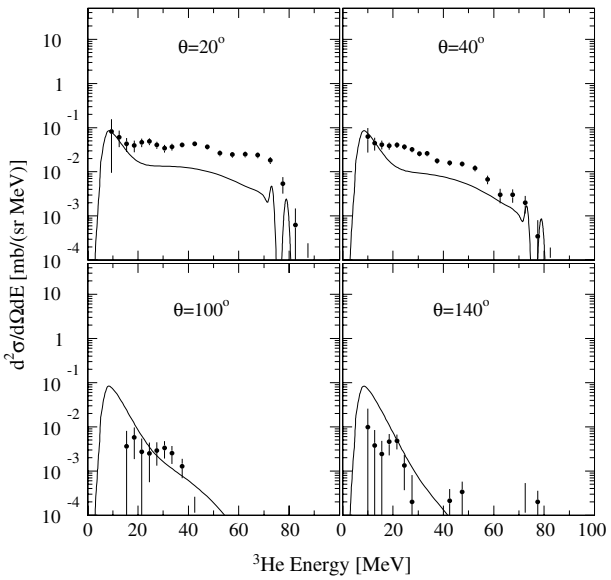

FIG. 5. Same as Fig. 2, but for O(n,^{3}Hex) reaction; curve indicates TALYS calculations.

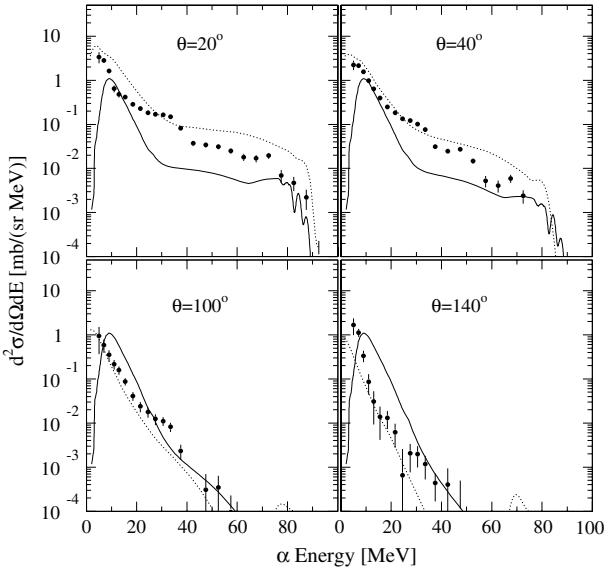

FIG. 6. Same as Fig. 2, but for the O(n,αx) reaction.

in the *np* scattering proton peak (2%), carbon contribution (0.1%), and number of hydrogen nuclei (0.1%).

From Figs. 2–6, it is obvious that the charged-particle emission at forward angles from 96 MeV neutron irradiation of oxygen is dominated by proton, deuteron, and α-particle channels. The yield of deuterons is about a factor of 3 lower than for protons, and the spectra of the two other particle types studied in this work (tritons and ^{3}He) are more than an order of magnitude weaker. All the spectra have more or less pronounced peaks at low energies (below 10–15 MeV), the angular distributions of which are not too far from isotropy except for α particles, where the yield at backward angles is about four times weaker than at 20°. The low-energy peak is not fully observed in the ^{3}He spectra because of the 8 MeV low-energy cutoff discussed in Sec. III.

All the particle spectra at forward angles show relatively large yields at medium-to-high energies. The emission of high-energy particles is strongly forward-peaked and hardly visible in the backward hemisphere. It is a sign of particle emission before statistical equilibrium has been reached in the reaction process. In addition to this broad distribution of emitted particles, the deuteron spectra at forward angles show narrow peaks corresponding to transitions to the ground state and low-lying states in the final nucleus, ^{15}N. These transitions are most likely due to pickup of weakly bound protons in the target nucleus, ^{16}O. A similar but less pronounced effect is observed in the proton spectra at forward angles. The structure observed in this case is due to transitions to Gamow-Teller states and other low-lying states with considerable single-particle strength [1].

B. Comparison with theoretical model calculations

In Figs. 2–6, the experimental results are presented together with theoretical model calculations. The GNASH calculations of Ref. [29] were done for protons, deuterons, and α particles, whereas the TALYS calculations discussed in Sec. IV were performed for all five particle types. The TALYS calculations include a transformation of the calculated cross sections to the laboratory system. Also in the GNASH code, a similar transformation from the c.m. to the lab system is performed using the kinematics of one-particle emission. Differences between data given in the laboratory and c.m. systems are particularly significant in this case, because oxygen is such a light nucleus.

Figure 2 shows that for protons above 25 MeV, both calculations give a reasonably good description of the spectra, although the calculated 20° cross sections, in particular the TALYS ones, fall below the experimental data. The low-energy statistical peak below 15 MeV in the spectra is considerably overpredicted by the two codes. The overestimate is particularly strong at backward angles for TALYS and at forward angles for GNASH.

The situation is quite different for the deuteron spectra (Fig. 3). None of the calculations account very well for the data, although the GNASH code gives a reasonable description of the angular dependence of the cross section. For the TALYS code, deviations between data and calculations of a factor of 2 or more are present. At forward angles, the high-energy part is strongly overestimated, in particular by the TALYS code, indicating problems in the hole-strength treatment. It is obvious, however, that efforts have been spent in these calculations to include individual hole-state strengths. Such strengths are not included in the GNASH calculations; nevertheless, the average behavior of the cross section at high energies is in fair agreement with the data. As seen in the proton spectra, the statistical peak is overpredicted by the TALYS calculations essentially at all angles, whereas the GNASH calculations seem to do a slightly better job in this case.

For tritons (Fig. 4), the TALYS calculation gives a fairly good description of the experimental data, except that it fails to account for an intensity bump around 15 MeV observed at forward angles.

The general trends of the forward-angle ^{3}He data (Fig. 5) are reasonably well described in the TALYS calculations, although the cross sections are underestimated by a large factor. At backward angles, the yield is very small and it is difficult to make quantitative comparisons.

The overall shapes of the α-particle spectra (Fig. 6) are reasonably well described by the two models. The GNASH calculations, however, overpredict the cross sections at forward angles and underpredict them at large angles, whereas the TALYS calculations do the opposite, i.e., underpredict at small angles and overpredict at large angles.

The ability of the models to account for the low-energy peak caused by the evaporation processes (and for α-particles also the 3α breakup of ^{12}C) is not impressive. In general, the models tend to overpredict the cross sections. However, keep in mind that the peak maximum is close to (for ^{3}He, below) the low-energy cutoff, which complicates the comparison. Another complication in this context is that the GNASH cross sections although given in the laboratory system, are calculated using the kinematics of one-particle emission [26,27] for the c.m.-to-lab transformation, which obviously is an approximation.

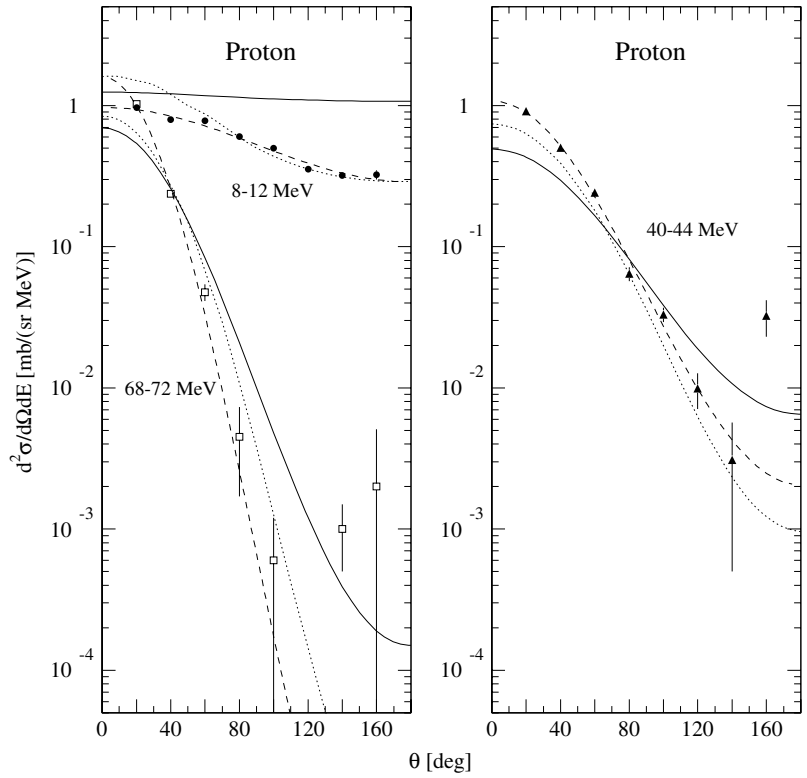

FIG. 7. Angular distributions of O(n, px) cross section at ejectile energies of 8–12 MeV (filled circles), 40–44 (filled triangles), and 68–72 (open squares). Dashed curves are fits to the data; dotted and solid curves represent calculations based on the GNASH and TALYS models, respectively.

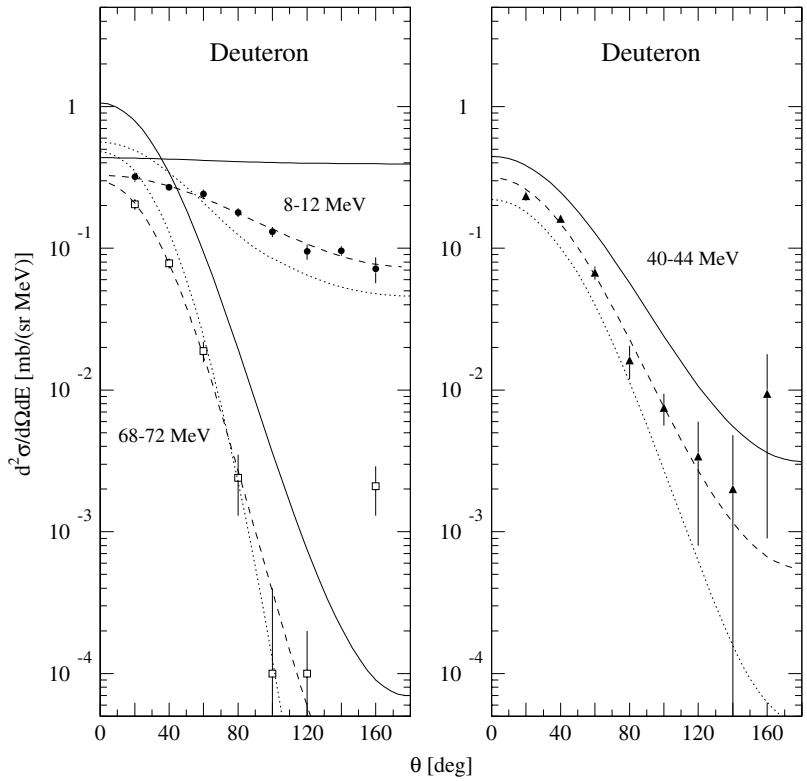

FIG. 8. Same as Fig. 7, but for the O(n, dx) cross section.

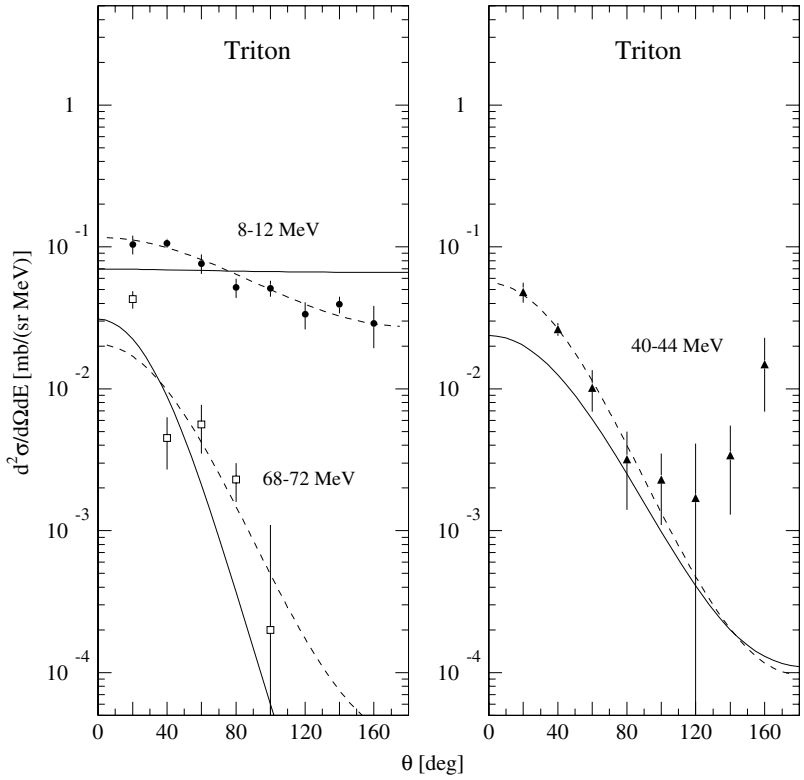

FIG. 9. Same as Fig. 7, but for the O(n, tx) cross section. No calculations based on the GNASH model are available for tritons.

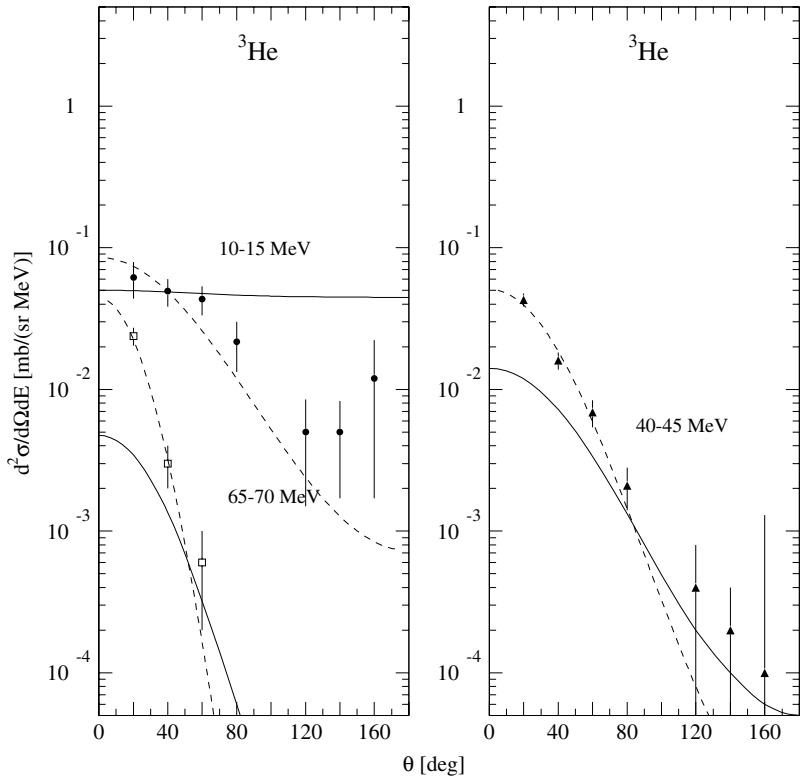

FIG. 10. Angular distributions of O(n,^{3}Hex) cross section at ejectile energies of 10–15 MeV (filled circles), 40–45 (filled triangles), and 65–70 (open squares). Dashed curves are fits to the data; solid curves represent TALYS calculations.

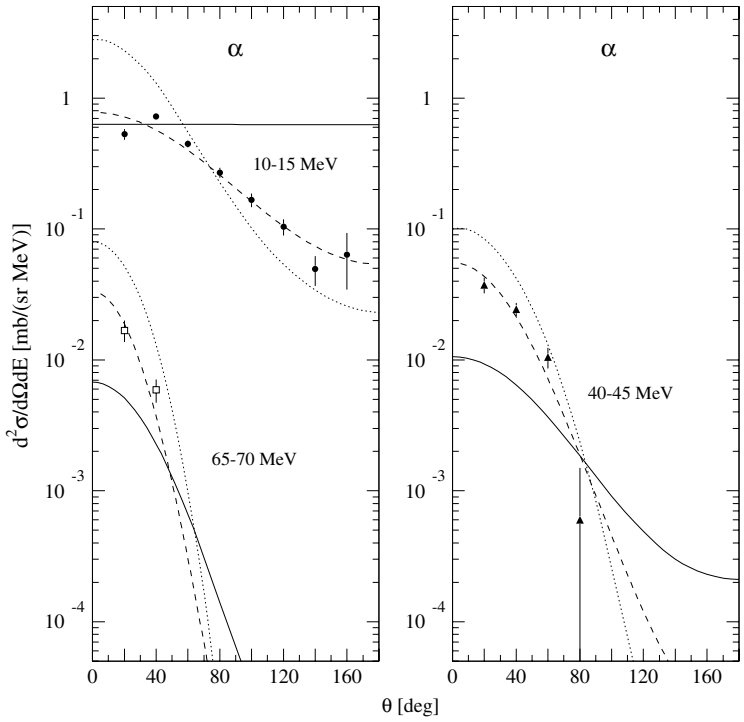

FIG. 11. Same as Fig. 10, but for the O(n,αx) cross section. Dotted curves represent GNASH calculations.

Experimental angular distributions at low, medium, and high ejectile energies are shown in Figs. 7–11 for protons, deuterons, tritons, ^{3}He, and α particles, respectively. The angular distributions are fitted by a simple two-parameter function, $a \exp(b \cos\theta)$ [30]. The data are compared with angular distributions calculated on the basis of the GNASH and TALYS models. In general, the TALYS model gives a weaker angular dependence than the data, whereas the GNASH model, although being closer to the data, tends to give a slightly steeper angular variation.

A conspicuous deviation from the experimental angular distribution is seen for the TALYS prediction at the lowest outgoing energies, e.g., at 8–12 MeV, in Fig. 7. We think this is attributed to wrong partial spectrum contributions to the total spectrum. The slightly forward-peaked angular distribution suggests that the spectrum at these emission energies is not as compound-dominated as the TALYS calculation suggests. Instead secondary, and even tertiary, preequilibrium emission may not be negligible even in the evaporation peak. Multiple preequilibrium emission is taken into account in TALYS but only contributes at somewhat higher emission energies. A way to make multiple preequilibrium (processes) relatively more important is to reduce the compound nucleus emission contribution, but we find that the predicted evaporation peak is rather insensitive to parameter variations. Hence, this is an open problem for TALYS, which apparently has been solved for the GNASH calculation.

C. Integrated spectra

For each energy bin of the light-ion spectra, the experimental angular distribution is fitted by a simple two-parameter function, $a \exp(b \cos\theta)$ [30], as exemplified in the previous section (Figs. 7–11). This allows extrapolation of double-differential cross sections to very forward and very backward angles. In this way, coverage of the full angular range is obtained. By integration of the angular distribution,

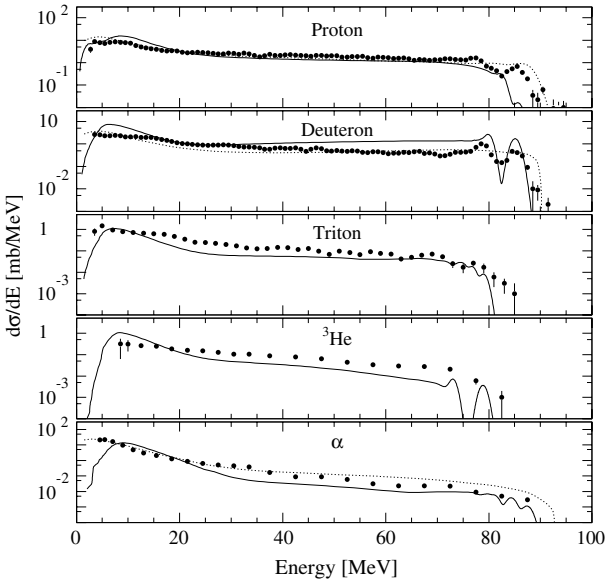

FIG. 12. Experimental energy-differential cross sections (filled circles) for neutron-induced p, d, t, ^{3}He, and α production at 96 MeV. Curves indicate theoretical calculations based on GNASH (dotted) and TALYS (solid).

energy-differential cross sections ($d\sigma/dE$) are obtained for each ejectile. These are shown in Fig. 12 together with theoretical calculations. For all ejectiles, both calculations give a fair description of the energy dependence. Both calculations are in good agreement with the proton experimental data over the whole energy range, although the calculations for (n,p) reactions to discrete states underestimate the data. A study of the spectroscopic strengths for these states would be welcome. Concerning the deuteron spectra, the GNASH calculations are in good agreement with the data, whereas the TALYS code gives cross sections a factor of 2 or more larger than the experimental ones at energies above 30 MeV. In the case of α particles, the GNASH calculation tends to overpredict the high-energy part of the spectrum, and the TALYS calculations fall below the data above an α-particle energy of 25 MeV. The energy dependence of the triton and ^{3}He spectra are well described by the TALYS code; but in both cases, the calculation falls below the data above about 20 MeV.

The production cross sections are deduced by integration of the energy-differential spectra (see Table I). To be compared with the calculated cross sections, the experimental values in Table I have to be corrected for the undetected particles below the low-energy cutoff. This is particularly important for ^{3}He because of the high cutoff energy. The corrections obtained with TALYS seem to be too small in some cases, in particular for the $(n,x\alpha)$ production cross section. As illustrated in Fig. 12 (bottom panel), the TALYS curve falls well below the experimental $d\sigma/dE$ data in the 4–7 MeV region.

The proton, deuteron, triton, and α-particle production cross sections are compared with previous data at lower energies [5] in Fig. 13. There seems to be general agreement between the trends of the previous data and the present data points. The curves in this figure are based on a GNASH calculation [29].

TABLE I. Experimental production cross sections for protons, deuterons, tritons, ^{3}He, and α particles from the present work, and theoretical calculations.

σ_{prod}	Experiment[a] (mb)	Experiment [cutoff corr.][b]		Theoretical calculation	
		GNASH	TALYS	GNASH	TALYS
(n,px)	224 ± 11	248	231	259.9	221.7
(n,dx)	72 ± 4	80	73	73.4	131.3
(n,tx)	20 ± 1	–	20	–	10.6
$(n,^3\text{He}x)$	6.9 ± 0.6	–	8.7	–	8.2
$(n,\alpha x)$	132 ± 7	218	132	224.7	88.4

[a]Obtained with cutoff energies of 2.5, 3.0, 3.5, 8.0, and 4.0 MeV for $p,d,t,$ ^{3}He, and alpha particles, respectively.
[b]Data corrected for energy cutoffs, using GNASH [29] and TALYS calculations of the present work.

VI. CONCLUSIONS AND OUTLOOK

In the present paper, we report an experimental data set on light-ion production in oxygen induced by 96 MeV neutrons. Experimental double-differential cross sections ($d^2\sigma/d\Omega dE$) are measured at eight angles between 20° and 160°. Energy-differential ($d\sigma/dE$) and production cross sections are obtained for the five types of outgoing particles. Theoretical

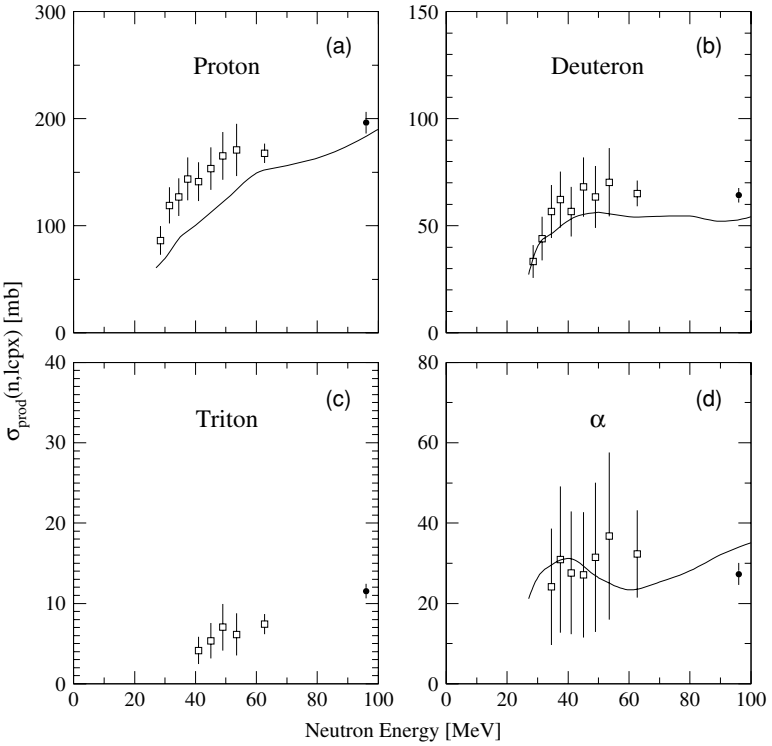

FIG. 13. Neutron-induced (a) proton, (b) deuteron, (c) triton, and (d) α-particle production cross section as a function of neutron energy. Full circles are from the present work; open circles are from previous work [5]. Curves are based on GNASH calculation. Data and calculations correspond to cutoff energies of 6 MeV for protons and deuterons and 12 MeV for tritons and α particles. Note that cutoff energies are different from those in Table I.

calculations based on nuclear reaction codes including direct, preequilibrium, and statistical models generally give a good account of the magnitude of the experimental cross sections. For proton emission, the shape of the spectra for the double-differential and energy-differential cross sections are well described. The calculated and the experimental α-particle spectra are also in fair agreement, with the exception of the high-energy part, where the GNASH model predicts higher yield and the TALYS model lower yield than experimentally observed. For the proton evaporation peak, the global TALYS calculation overestimates the data. A future activity should be an adjustment of the responsible OMP and level density parameters (as was done in the case of GNASH) instead of relying on a full global prediction. For the other complex ejectiles (deuteron, triton, and ^{3}He) there are important differences between theory and experiment in what concerns the shape of the spectra at various angles. We think this is due to the use of statistical models, such as the Hauser-Feshbach model and the preequilibrium exciton model, in mass ranges where these models become suspect and to the absence of a breakup model in the theoretical analysis. Apart from the aforementioned breakup model, predictions of emission of α-particles may be particularly sensitive to a correct knockout model and the use of adequate complex particle optical model potentials. Stripping and knockout models, level densities, optical models, and omission of breakup reactions may all add up to problems for something as light as oxygen. This needs to be studied in much more detail. Finally, the magnitude of the angle-integrated cross sections is reasonably well accounted for.

For the further development of the field, data at even higher energies are requested. The results suggest that the MEDLEY facility, which was used in the present work, should be upgraded to work also at 180 MeV, i.e., the maximum energy of the TSL neutron beam facility. At present, a new neutron beam facility is under commissioning at TSL [39], covering the same energy range, but with a projected intensity increase of a factor 5. This will facilitate measurements at energies higher than in the present work.

ACKNOWLEDGMENTS

The authors thank the Svedberg Laboratory for excellent support. U.T. expresses his gratitude to the Thai Ministry of University Affairs and to the International Program in the Physical Sciences at Uppsala University. This work was supported by the Swedish Natural Science Research Council, the Swedish Nuclear Fuel and Waste Management Company, the Swedish Nuclear Power Inspectorate, Ringhals AB, the Swedish Defence Research Agency, and the Swedish International Development Authority.

[1] G. A. Needham, F. P. Brady, D. H. Fitzgerald, J. L. Romero, J. L. Ullmann, J. W. Watson, C. I. Zanelli, N. S. P. King, and G. R. Satchler, Nucl. Phys. **A385**, 349 (1982).

[2] T. S. Subramanian, J. L. Romero, F. P. Brady, D. H. Fitzgerald, R. Garrett, G. A. Needham, J. L. Ullmann, J. W. Watson, C. I. Zanelli, D. J. Brenner, and R. E. Prael, Phys. Rev. C **34**, 1580 (1986).

[3] S. Benck, I. Slypen, J. P. Meulders, and V. Corcalciuc, Eur. Phys. J. A **3**, 149 (1998).

[4] S. Benck, I. Slypen, J. P. Meulders, and V. Corcalciuc, Eur. Phys. J. A **3**, 159 (1998).

[5] S. Benck, I. Slypen, J. P. Meulders, and V. Corcalciuc, Phys. Med. Biol. **43**, 3427 (1998).

[6] R. Orecchia, A. Zurlo, A. Loasses, M. Krengli, G. Tosi, S. Zurrida, P. Zucali, and U. Veronesi, Eur. J. Cancer **34**, 459 (1998).

[7] D. L. Schwartz, J. Einck, J. Bellon, and G. E. Laramore, Int. J. Radiat. Oncol. Biol. Phys. **50**, 449 (2001).

[8] G. E. Laramore and T. W. Griffin, Int. J. Radiat. Oncol. Biol. Phys. **32**, 879 (1995).

[9] D. T. Bartlett, R. Grillmaier, W. Heinrich, L. Lindborg, D. O'Sullivan, H. Schraube, M. Silari, and L. Tommasino, in *Radiation Research, Vol. 2: Proceedings of Eleventh International Congress of Radiation Research, Dublin, Ireland, 18–23 July 1999*, edited by M. Moriarty, C. Mothersill, C. Seymour, M. Edington, J. F. Ward, and R. J. M. Fry (Allen Press, Lawrence, KS, 2000), p. 759; see also *Proceedings of the International Conference on Cosmic Radiation and Aircrew Exposure, Dublin, Ireland, July 1–3, 1998*, Radiat. Prot. Dosimetry **86(4)** (1999).

[10] Single-Event Upsets in Microelectronics, topical issue, edited by H. H. K. Tang and N. Olsson, Mater. Res. Soc. Bull. **28** (2003).

[11] M. B. Chadwick and E. Normand, IEEE Trans. Nucl. Sci. **46**, 1386 (1999).

[12] High and Intermediate Energy Nuclear Data for Accelerator-Driven Systems (HINDAS), European Contract FIKW-CT-2000-00031, coord. J. P. Meulders.

[13] A. Koning, H. Beijers, J. Benlliure, O. Bersillon, J. Blomgren, J. Cugnon, M. Duijvestijn, Ph. Eudes, D. Filges, F. Haddad, S. Hilaire, C. Lebrun, F.-R. Lecolley, S. Leray, J.-P. Meulders, R. Michel, R.-D. Neef, R. Nolte, N. Olsson, E. Ostendorf, E. Ramström, K.-H. Schmidt, H. Schuhmacher, I. Slypen, H.-A. Synal, and R. Weinreich, J. Nucl. Sci. Tech. Suppl. **2**, 1161 (2002).

[14] R. A. Cecil, B. D. Anderson, and R. Madey, Nucl. Instrum. Methods **161**, 439 (1979).

[15] J. Blomgren and N. Olsson, Radiat. Prot. Dosim. **103(4)**, 293 (2003).

[16] S. Dangtip, A. Ataç, B. Bergenwall, J. Blomgren, K. Elmgren, C. Johansson, J. Klug, N. Olsson, G. Alm Carlsson, J. Söderberg, O. Jonsson, L. Nilsson, P.-U. Renberg, P. Nadel-Turonski, C. Le Brun, F. R. Lecolley, J. F. Lecolley, C. Varignon, Ph. Eudes, F. Haddad, M. Kerveno, T. Kirchner, and C. Lebrun, Nucl. Instrum. Methods Phys. Res. A **452**, 484 (2000).

[17] U. Tippawan, S. Pomp, A. Ataç, B. Bergenwall, J. Blomgren, S. Dangtip, A. Hildebrand, C. Johansson, J. Klug, P. Mermod, L. Nilsson, M. Österlund, N. Olsson, K. Elmgren, O. Jonsson, A. V. Prokofiev, P.-U. Renberg, P. Nadel-Turonski, V. Corcalciuc, Y. Watanabe, and A. Koning, Phys. Rev. C **69**, 064609 (2004).

[18] U. Tippawan, Ph.D. thesis, Chiang Mai University, 2004 (unpublished).

[19] J. Klug, J. Blomgren, A. Ataç, B. Bergenwall, S. Dangtip, K. Elmgren, C. Johansson, N. Olsson, S. Pomp, A. V. Prokofiev, J. Rahm, U. Tippawan, O. Jonsson, L. Nilsson, P.-U. Renberg, P. Nadel-Turonski, A. Ringbom, A. Oberstedt, F. Tovesson, V. Blideanu, C. Le Brun, J. F. Lecolley, F. R. Lecolley, M. Louvel, N. Marie, C. Schweitzer, C. Varignon, Ph. Eudes, F. Haddad, M. Kerveno, T. Kirchner, C. Lebrun, L. Stuttgé, I. Slypen, A. Smirnov, R. Michel, S. Neumann, and U. Herpers, Nucl. Instrum. Methods Phys. Res. A **489**, 282 (2002).

[20] A. N. Smirnov, V. P. Eismont, and A. V. Prokofiev, Radiat. Meas. **25**, 151 (1995).

[21] J. Rahm, J. Blomgren, H. Condé, S. Dangtip, K. Elmgren, N. Olsson, T. Rönnqvist, R. Zorro, O. Jonsson, L. Nilsson, P.-U. Renberg, A. Ringbom, G. Tibell, S. Y. van der Werf, T. E. O. Ericson, and B. Loiseau, Phys. Rev. C **63**, 044001 (2001).

[22] J. F. Ziegler, TRIM code, version 95.4, IBM-Research, 1995.

[23] S. Pomp, Internal Note (unpublished).

[24] U. Tippawan, S. Pomp, A. Ataç, B. Bergenwall, J. Blomgren, S. Dangtip, A. Hildebrand, C. Johansson, J. Klug, P. Mermod, L. Nilsson, M. Österlund, N. Olsson, K. Elmgren, O. Jonsson, A. V. Prokofiev, P.-U. Renberg, P. Nadel-Turonski, V. Corcalciuc, Y. Watanabe, and A. Koning, Phys. Rev. C **73**, 039902(E) (2006).

[25] V. Blideanu, F. R. Lecolley, J. F. Lecolley, T. Lefort, N. Marie, A. Ataç, G. Ban, B. Bergenwall, J. Blomgren, S. Dangtip, K. Elmgren, Ph. Eudes, Y. Foucher, A. Guertin, F. Haddad, A. Hildebrand, C. Johansson, O. Jonsson, M. Kerveno, T. Kirchner, J. Klug, Ch. Le Brun, C. Lebrun, M. Louvel, P. Nadel-Turonski, L. Nilsson, N. Olsson, S. Pomp, A. V. Prokofiev, P.-U. Renberg, G. Rivière, I. Slypen, L. Stuttgé, U. Tippawan, and M. Österlund, Phys. Rev. C **70**, 014607 (2004).

[26] P. G. Young, E. D. Arthur, and M. B. Chadwick, Los Alamos National Laboratory Report No. LA-12343-MS, 1992, GNASH-FKK version gn9cp0, PSR-0125.

[27] M. B. Chadwick, P. G. Young, R. E. MacFarlane, and A. J. Koning, in *Proceedings of the Second International Conference on Accelerator-Driven Transmutation Technologies and Applications*, Kalmar, Sweden, 1996, edited by H. Condé (Gotab, Stockholm, 1997), p. 483.

[28] A. J. Koning, S. Hilaire, and M. C. Duijvestijn, TALYS-0.64 User Manual, December 5, 2004, NRG Report 21297/04.62741/P FAI/AK/AK.

[29] ICRU Report 63, International Commission on Radiation Units and Measurements, Bethesda, MD, March 2000.

[30] C. Kalbach, Phys. Rev. C **37**, 2350 (1988).

[31] A. J. Koning and J. P. Delaroche, Nucl. Phys. **A713**, 231 (2003).

[32] S. Watanabe, Nucl. Phys. **8**, 484 (1958).

[33] R. K. Tripathi, F. A. Cucinotta, and J. W. Wilson, Nucl. Instrum. Methods Phys. Res. B **117**, 347 (1996); R. K. Tripathi, F. A. Cucinotta, and J. W. Wilson, NASA Technical Paper 3621, January 1997.

[34] A. J. Koning and M. C. Duijvestijn, Nucl. Phys. **A744**, 15 (2004).

[35] C. Kalbach, Phys. Rev. C **33**, 818 (1986).

[36] A. V. Ignatyuk, G. N. Smirenkin, and A. S. Tishin, Sov. J. Nucl. Phys. **21**, 255 (1975).

[37] C. Kalbach, Users Manual for PRECO-2000, Duke University, 2001; Phys. Rev. C **71**, 034606 (2005).

[38] M. Kerveno, F. Haddad, Ph. Eudes, T. Kirchner, C. Lebrun, I. Slypen, J. P. Meulders, C. Le Brun, F. R. Lecolley, J. F. Lecolley, M. Louvel, F. Lefèbvres, S. Hilaire, and A. J. Koning, Phys. Rev. C **66**, 014601 (2002).

[39] S. Pomp, A. V. Prokofiev, J. Blomgren, C. Ekström, O. Jonsson, D. Reistad, V. Ziemann, N. Haag, A. Hildebrand, L. Nilsson, B. Bergenwall, C. Johansson, P. Mermod, N. Olsson, M. Österlund, and U. Tippawan, in *Proceedings of International Conference on Nuclear Data for Science and Technology, Santa Fe, NM, September 26–October 1, 2004*, AIP Conf. Proc. No. 769, edited by Robert C. Haight, Mark B. Chadwick, Toshihiko Kawano, and Patrick Talou (AIP, New York, 2005), p. 780.

Appendix IV

PHYSICAL REVIEW C **73**, 039902 (2006)

Erratum: Light-ion production in the interaction of 96 MeV neutrons with silicon [Phys. Rev. C 69, 064609 (2004)]

U. Tippawan, S. Pomp, A. Ataç, B. Bergenwall, J. Blomgren, S. Dangtip, A. Hildebrand, C. Johansson, J. Klug, P. Mermod, L. Nilsson, M. Österlund, N. Olsson, K. Elmgren, O. Jonsson, A. V. Prokofiev, P.-U. Renberg, P. Nadel-Turonski, V. Corcalciuc, Y. Watanabe, and A. Koning

(Received 10 January 2006; published 23 March 2006)

DOI: 10.1103/PhysRevC.73.039902 PACS number(s): 25.40.Hs, 25.40.Kv, 24.10.−i, 99.10.Cd

The data set presented in the above article uses both silicon and oxygen as target nuclei. In the process of extracting information on light-ion production induced by 96 MeV neutrons interacting with oxygen, of which the results are published in this issue [1], the silicon data have been reanalyzed. In doing so, we have adapted some changes and also found two mistakes.

(i) An improved analysis of the contributing neutron spectrum has lead to a change in the normalisation relative to the *np* cross section. Details are found in Ref. [1]. This leads to an increase of the cross sections by about 3%.
(ii) We found that an incorrect weight for the Si target was used. This leads to an increase in the cross sections by about 2%.
(iii) We found a mistake in the treatment of the alpha events stopping in the first ΔE detector. The solid angle for these events was not matched correctly with the other alpha events. This concerns only a fraction of the detected alpha events. However, due to the target corrections, which are large at these low energies, the effect on the production cross section for alpha particles is about 12%.

The total effect of the above changes is a change in the normalization leading to an increase of the cross sections of about 5–6%, except for the case of alpha particles where the additional change of the solid angle results in an increase of the production cross section by about 17%. The new production cross sections are given in Table I. Note that the total changes are within the errors quoted in the above paper, and that the errors given in Table I are statistical errors only.

We include revised versions of Figs. 9 and 10 of the above paper. The conclusions of the article are not affected. A revised data set has been submitted to the Experimental Nuclear Reaction Data (EXFOR) [4] database.

TABLE I. Experimental production cross sections for protons, deuterons, tritons, ^{3}He and alpha particles from the present work. Theoretical values resulting from GNASH and TALYS calculations are given as well. The experimental data in the second column have been obtained with cutoff energies of 2.5, 3.0, 3.5, 8.0, and 4.0 MeV for $p, d, t, ^3$He, and alpha particles, respectively. The third column shows data corrected for these cutoffs, using the GNASH calculation of the present work.

σ_{prod}	Experiment (mb)	Experiment (cutoff corr.)	GNASH (Ref. [3])	GNASH (present)	TALYS (present)
(n, px)	460 ± 23	531	670.3	701.9	558.3
(n, dx)	86 ± 4	94.5	77.0	109.6	107.6
(n, tx)	16.2 ± 0.9	18.9	–	15.0	13.1
$(n, ^3\text{He}x)$	8.3 ± 0.5	13.5	–	10.6	14.5
$(n, \alpha x)$	168 ± 8	207	175.8	202.4	146.8

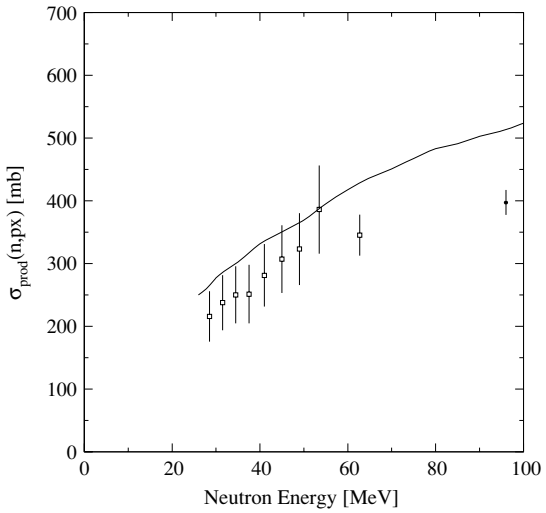

FIG. 1. Neutron-induced proton production cross section as a function of neutron energy. The full circle is from the present work, whereas the open circles are from previous work [2]. The curve is based on a GNASH calculation [3]. The data as well as the calculations correspond to a cutoff energy of 4 MeV. Note that the cutoff energy is different from that in Table I.

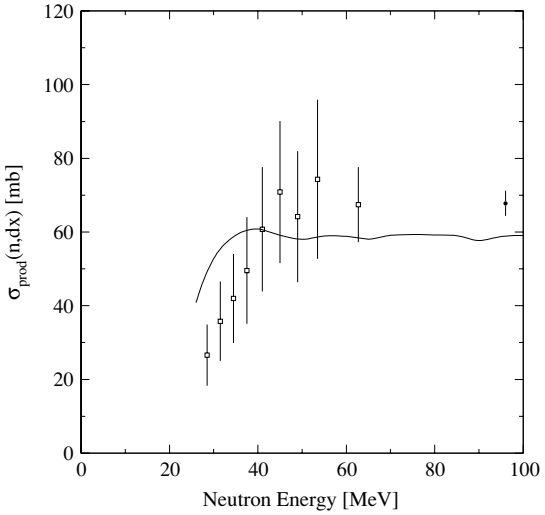

FIG. 2. Same as Fig. 9 for deuteron production, with a cutoff energy of 8 MeV.

[1] U. Tippawan, S. Pomp, A. Ataç, B. Bergenwall, J. Blomgren, S. Dangtip, A. Hildebrand, C. Johansson, J. Klug, P. Mermod, L. Nilsson, M. Österlund, N. Olsson, A. V. Prokofiev, P. Nadel-Turonski, V. Corcalciuc, and A. Koning, Phys. Rev. C **73**, 034611 (2006).

[2] S. Benck, I. Slypen, J. P. Meulders, and V. Corcalciuc, Nucl. Sci. Eng. **141**, 55 (2002).

[3] ICRU Report 63, International Commission on Radiation Units and Measurements, Bethesda, MD, March 2000.

[4] Experimental Nuclear Reaction Data (EXFOR), http://www.nndc.bnl.gov/exfor.

Appendix V

Nuclear Instruments and Methods in Physics Research A 562 (2006) 439–448

www.elsevier.com/locate/nima

Measurements of neutron-induced fission cross-sections of ^{205}Tl, ^{204,206,207,208}Pb and ^{209}Bi with a multi-section Frisch-gridded ionization chamber

I.V. Ryzhov[a], G.A. Tutin[a], A.G. Mitryukhin[a], V.S. Oplavin[a], S.M. Soloviev[a], J. Blomgren[b,*], P.-U. Renberg[c], J.P. Meulders[d], Y. El Masri[d], Th. Keutgen[d], R. Prieels[d], R. Nolte[e]

[a]*V.G. Khlopin Radium Institute, 2nd Murinski prospect 28, 194021 Saint-Petersburg, Russia Federation*
[b]*Department of Neutron Research, Uppsala University, Box 525, SE-751 20 Uppsala, Sweden*
[c]*The Svedberg Laboratory, Uppsala University, Box 533, SE-751 21 Uppsala, Sweden*
[d]*FNRS and Institute of Nuclear Physics, Université catholique de Louvain, B-1348 Louvain-la-Neuve, Belgium*
[e]*Physikalisch-Technische Bundesanstalt, D-38116 Braunschweig, Germany*

Received 14 February 2006; received in revised form 8 March 2006; accepted 9 March 2006
Available online 19 April 2006

Abstract

Neutron-induced fission cross-sections of ^{205}Tl, ^{204,206,207,208}Pb and ^{209}Bi have been measured in the energy range from 30 to 180 MeV. The measurements were performed with quasi-monoenergetic neutron beams using a multi-section Frisch-gridded ionization chamber. The neutron-induced fission cross-sections of ^{238}U were used as reference data. The experimental techniques are described in detail as well as the data processing. The results are compared with existing experimental data.

PACS: 25.85.Ec; 29.40.Cs

Keywords: ^{205}Tl; ^{204,206,207,208}Pb; ^{209}Bi; Neutron-induced fission cross-sections; Ionization chamber

1. Introduction

A motivation of this work stems from the nuclear data needs for accelerator-driven systems (ADS). Nowadays, ADS have gained the worldwide attention as a possibility to address such problems as transmutation of nuclear waste, energy amplification, incineration of weapon plutonium, etc. Feasibility studies of ADS require nuclear data on neutron-induced reactions within a wide incident energy range including the so-called intermediate energies, i.e., between 20 and 200 MeV [1]. In particular, data on neutron-induced fission of spallation target materials (W, Pb and Bi) are of interest, because the fission reactions may influence the nuclear heating of the target, its prompt and residual radioactivity, its radiation resistance (in the case of solid target), etc.

Another aspect of this work concerns the ^{209}Bi (n, f) cross-section, which has been recommended as a secondary neutron cross-section standard [2]. Bismuth-based neutron fluence monitors, being insensitive to low-energy (<25 MeV) neutrons, are used in those experiments, where the low-energy neutron background is difficult to determine [3,4]. Meanwhile, the present uncertainty of the ^{209}Bi (n, f) standard is rather large, so further improvement of the standard is necessary.

The data on neutron-induced fission of nuclei in the lead-bismuth region are important not only for practical applications, but also for fundamental nuclear physics. In particular, one can expect a manifestation of nuclear shell effects in the fission of nuclei in the vicinity of the double

*Corresponding author. Tel.: +46 18 471 3788; fax: +46 18 471 3853.
E-mail addresses: ryzhov@atom.nw.ru (I.V. Ryzhov), jan.blomgren@tsl.uu.se (J. Blomgren).

0168-9002/$ - see front matter © 2006 Elsevier B.V. All rights reserved.
doi:10.1016/j.nima.2006.03.021

magic nucleus ^{208}Pb. These effects were evident in proton- and deuteron-induced fission of sub-actinides at low excitation energies [5]. However, the most interesting compound nucleus ^{208}Pb cannot be formed in reactions with protons and deuterons due to the absence of appropriate (stable) target nuclides. Notice that this problem can easily be resolved in neutron experiments with ^{207}Pb targets.

This paper describes measurements of neutron-induced fission cross-sections of ^{205}Tl, ^{204,206,207,208}Pb and ^{209}Bi carried out in the neutron energy range from 30 to 180 MeV. The experiments were performed with quasi-monoenergetic neutron beams using a multi-section Frisch-gridded ionization chamber (MFGIC). Some results have previously been presented [6,7]. In this paper, the emphasis will be put on the fission chamber performance and the data processing. The obtained results are compared with existing experimental data for ^{nat}Pb and ^{209}Bi.

2. Neutron beam facilities

The measurements were performed using the neutron sources of the Louvain-la-Neuve (LLN) cyclotron facility CYCLONE, Louvain-la-Neuve, Belgium [8] and of The Svedberg Laboratory (TSL), Uppsala, Sweden [9]. In both facilities, the ^{7}Li (p, n) reaction was used to produce a quasi-monoenergetic neutron beam. At the LLN facility, a 5 mm thick natural lithium target (92.5% of ^{7}Li and 7.5% of ^{6}Li) was bombarded by protons with beam current of about 10 μA. In the TSL experiments, 4–15 mm thick lithium targets (enriched to 99.98% in ^{7}Li) were exposed to proton bombardment with a beam current from 1 to 10 μA. At both laboratories, protons passing through the neutron production targets were deflected into a Faraday cup, while neutrons were guided to the experimental rooms through a system of collimators.

The neutron spectrum from the ^{7}Li (p, n) reaction at 0° consists of a high-energy peak and a continuum of lower energy neutrons. The high-energy peak corresponds to the ^{7}Li (p, n) ^{7}Be (g.s. and 0.43 MeV first excited state) reaction, while the low-energy tail originates from more complicated physical processes, such as the three-body breakup reaction ^{7}Li (p, n ^{3}He)α. Examples of quasi-monoenergetic neutron spectra obtained at the LLN [10] and the TSL [11] neutron facilities are shown in Fig. 1. The present measurements were performed with the following neutron peak energies: 32.8, 45.3 and 59.9 MeV (at LLN) and 34.7, 46.3, 65.4, 96.0, 133.6 and 173.9 MeV (at TSL).

The MFGIC was typically positioned at a distance of about 10 m from the Li-targets. The diameter of the neutron beam at this position was about 10 cm with a fluence of high-energy peak neutrons (“peak neutrons”) in the range from 10^{3} to 10^{4} s^{-1} cm^{-2} depending on the incident proton energy and Li-target thickness.

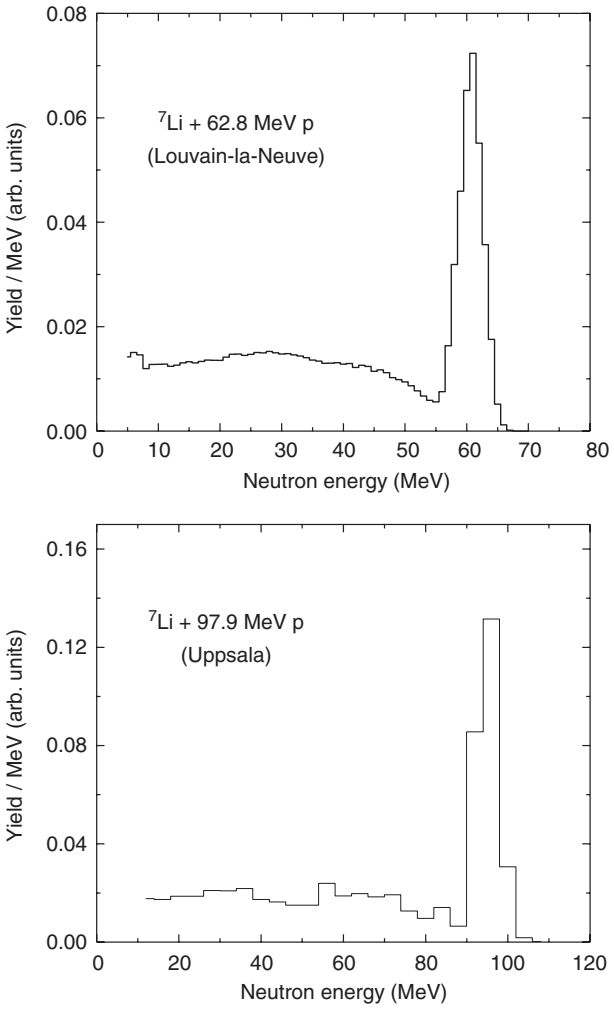

Fig. 1. Neutron spectra produced by the ^{7}Li (p, n) reaction at the LLN [10] (4 mm thick Li target + 62.8 MeV protons) and the TSL [11] (8 mm thick Li target + 97.9 MeV protons) accelerator facilities. The first spectrum (from the LLN) is normalized to unit neutron yield, while the second one (from the TSL) is normalized so that the peak area is unity.

3. Fission fragment detector

3.1. Chamber construction

A schematic drawing of the multi-section Frisch-gridded ionization chamber is displayed in Fig. 2. The electrode assembly consists of seven sections. Each section comprises two single gridded ionization chambers with a common cathode, two grids and two anodes. Two adjacent sections are separated by a common anode. The cathodes and anodes are duralumin foils, 50 μm thick, sandwiched between two 1 mm thick duralumin rings with inner and outer diameters of 140 and 170 mm, respectively. The choice of the electrode material was based on two considerations. First, the duralumin foil is flexible enough to be stretched without surface irregularities. Second, the

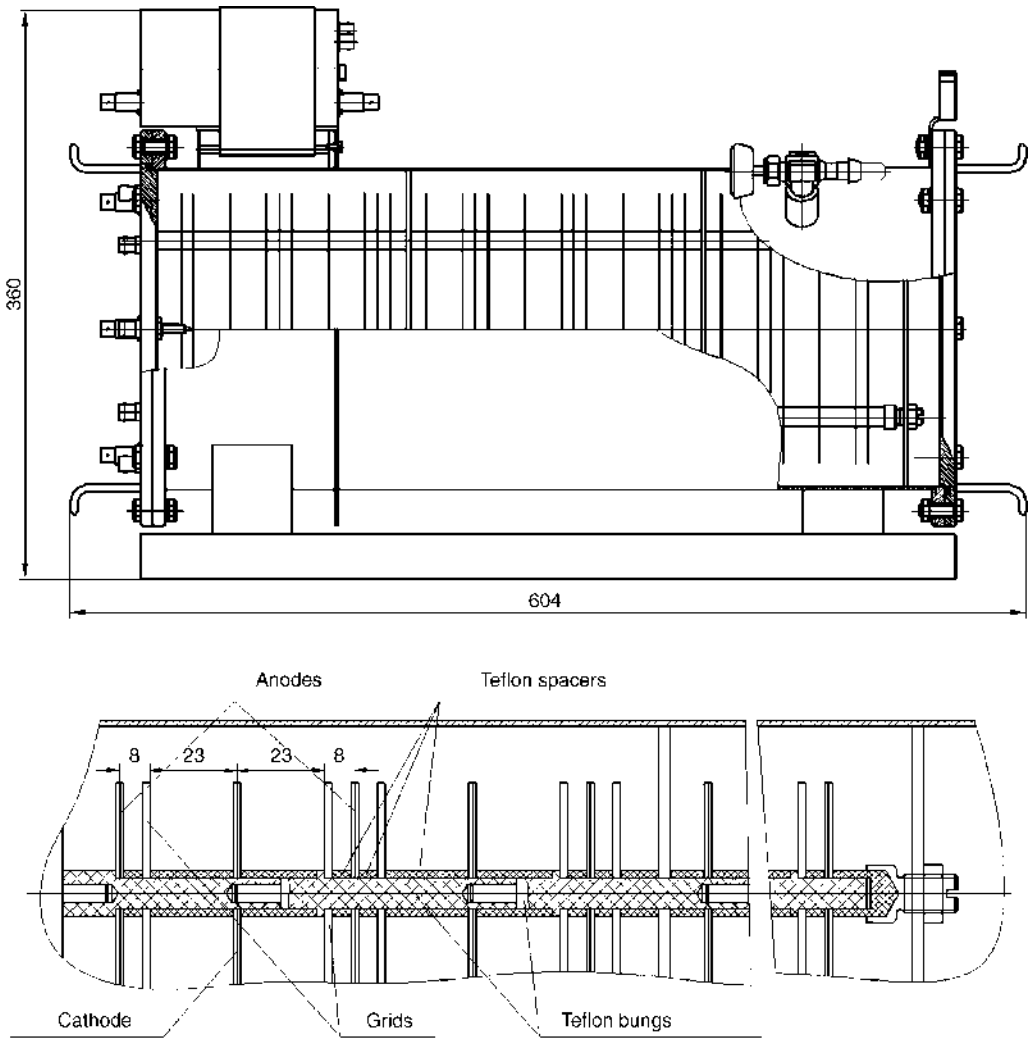

Fig. 2. Schematic view of the multi-section Frisch-gridded ionization chamber (MFGIC). Dimensions are in mm.

impurity of duralumin with heavy fissile elements is low. As a mass spectrometric analysis revealed, the duralumin foils have a thorium and uranium content of about 0.34 and 1.06 μg/g, respectively. The grids are made of gilded molybdenum wires of 80 μm in diameter spaced by 1.25 mm. The wires are mounted in parallel on the stainless steel rings using a spot weld. The calculated inefficiency of the grid shielding is about 0.04 [12].

The electrode assembly is housed in a cylindrical, 1 mm thick stainless-steel shell, of 200 mm diameter and 520 mm long. The electrodes are held together with four sectional teflon rods sandwiched between the chamber lids. As shown at the bottom of Fig. 2, each rod consists of electrode supporting bungs and spacers. Such a design enables a quick access to any electrode, and if required, its replacement. The distance between the anode and the grid is 8 mm. The cathode to grid distance is 23 mm. The gas mixture was composed of 90% argon and 10% methane (P-10). The chamber operates at atmospheric pressure without a continuous gas flow.

3.2. Targets

The fissile targets have been fabricated by the sample preparation group of the Khlopin Radium Institute. The target list includes ^{205}Tl, ^{204,206,207,208}Pb (enriched in its basic isotope), ^{209}Bi and ^{nat}U. The sub-actinide targets were made of pure metals, whereas the uranium target was prepared from $^{nat}UF_4$. All the materials were deposited on both sides of each cathode foil by thermal vacuum evaporation. The diameter of each target was 80 mm with the deposit uniformity better than 10%. For metallic targets, the total deposit masses were determined by weighing. The uranium target mass was measured by

alpha counting. The relative uncertainties of the fissile masses are less than 2%. Characteristics of the targets are given in Table 1.

3.3. Electronic treatment of the signals

Fig. 3 shows a block diagram of the electronics used to process the signals from the MFGIC. Each section of the detector operates as a double Frisch-gridded ionization chamber described in detail in Ref. [13]. It generates two signals for one fission event. One signal, proportional to the fission fragment energy, is taken from an anode using a low-noise, charge-sensitive preamplifier (PA). To simplify the scheme, the alternate anodes are connected together, so only two spectroscopy channels (instead of 14) are used to treat the anode signals from all sections. In principle, such a connection of the anodes can result in a pile-up of the anode signals from different sections. However, the probability of an accidental coincidence is negligibly small at the counting rates ($<10\,s^{-1}$) characteristic of the present experiments. After the pre-amplification, the anode signal is amplified, shaped (with time constants $\tau_{int} = \tau_{diff} = 1\,\mu s$) and fed to a peak sensing analog-to-digital converter (ADC). The other signal is taken from the cathode. This signal is a function of the fragment energy and emission angle relative to the normal on the cathode [13]. In addition, the cathode signal is used for the timing purposes. Seven fast preamplifiers, having rise time $\leqslant 20\,ns$ for detector with capacitance of 100 pF, accept the cathode signals and deliver separate preamplifier outputs for timing and pulse-height measurements. The spectroscopy signals from the cathode PAs are processed like those from the anode ones. A coded number of the ADC channels, triggered by the anode and cathode signals, is used to identify the section where the fission event took place, as well as the target orientation with respect to the neutron beam direction (the forward- or backward-facing).

The timing outputs of the cathode FPAs are fed to respective timing filter amplifiers (TFA) with shaping time constants $\tau_{int} = \tau_{diff} = 20\,ns$. Seven constant fraction discriminators follow the TFAs. Their outputs are mixed in a logic fan-in/fan-out and then split into two branches. One pulse starts a time-to-digital converter (TDC), while the other one triggers a gate and delay generator. The master gate signals with a width of 10–15 μs are fed to the ADCs to ensure that every digitized signal pulse-height will have an associated timing signal. The TDC is stopped with the cyclotron RF signal put in coincidence with a delayed gate signal generated from a cathode signal. The data reading is done (via CAMAC) with a computer-based

Table 1
Characteristics of the fissile targets

Target	Compound	Percentage (%)	Areal mass (mg/cm^2)
^{205}Tl	Metal	99.8	1.38/1.40
^{204}Pb	Metal	66.5	0.52/0.55
^{206}Pb	Metal	90.4	0.98/1.10
^{207}Pb	Metal	93.2	0.96/0.98
^{208}Pb	Metal	99.0	0.88/1.08
^{209}Bi	Metal	100.0	1.14/0.87
^{238}U	UF_4	99.3	0.21/0.20

The areal mass is given for the forward/backward oriented targets.

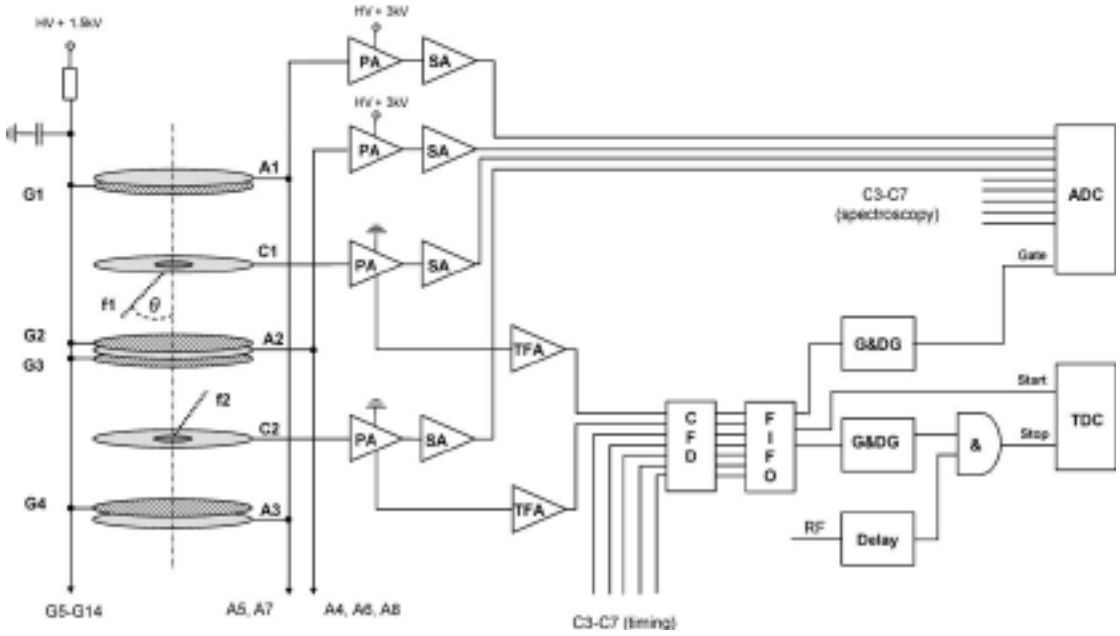

Fig. 3. Block diagram of the electronic set-up.

data acquisition system. The data are stored event by event on a hard disk.

4. Data analysis and corrections

To discriminate fission events caused by peak neutrons from those induced by low-energy "tail" neutrons time-of-flight (TOF) techniques were used. Typical distributions of fission events over relative neutron time-of-flight are given in Fig. 4. The TOF distributions have a frame–overlapping structure due to a high frequency (13–25 MHz) of the proton bunches impinging on the neutron production target. The numbers of fission events induced by peak neutrons were extracted for all the targets using a decomposition procedure detailed in Ref. [14]. These data were then corrected for the fragment losses due to the self-absorption in the fissile deposits (K_{abs}) and the pulse height threshold (K_{th}). In a parallel plate ionization chamber, the former correction is calculated (see, e.g., Ref. [15]) as follows:

$$K_{abs} = 1 - (t/2R)(1 + B/3)^{-1}, \quad (1)$$

where B is the angular anisotropy coefficient, t the thickness of the deposit and R the average range of the fission fragments in the deposited material. These corrections range within 1.7–10.5% depending on the target

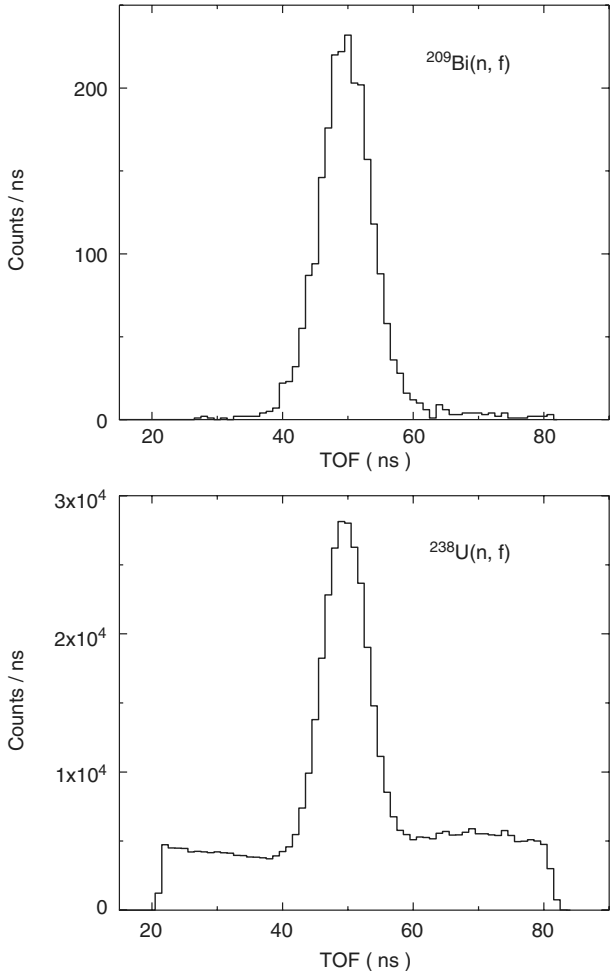

Fig. 4. Distributions of ^{209}Bi and ^{238}U fission events over time intervals between "start" and "stop" signals related to the fragment detection and the cyclotron RF, respectively (see the block diagram in Fig. 3). Neutrons were produced at the LLN accelerator facility by bombarding 5 mm thick Li target with 48.5 MeV protons.

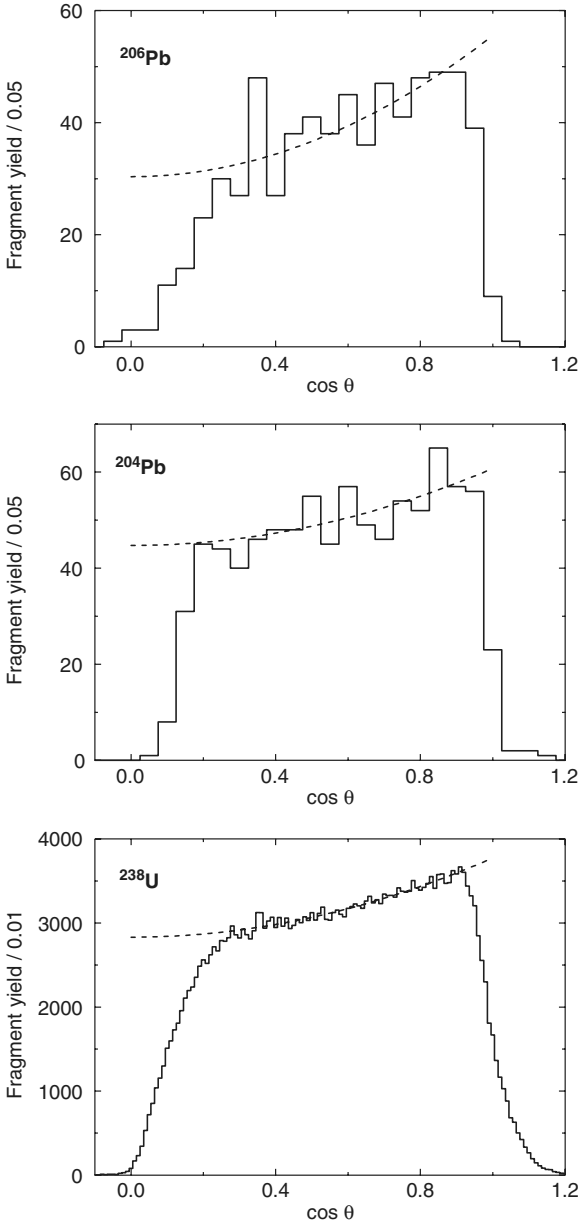

Fig. 5. Angular distributions of forward emitted fragments measured for the ^{204,206}Pb (n, f) and ^{238}U (n, f) reactions at neutron energy of 45.3 MeV.The distributions were fitted (in the cosine range 0.3–0.9) with a function $W(\theta) \propto 1 + B\cos^2\theta$, where B is the angular anisotropy coefficient.

orientation, its thickness and incident neutron energy. Due to the linear momentum transferred (LMT) to the fissioning nuclei, the average range of the forward-emitted fragments is larger than that of the backward-emitted ones. For the same reason, the forward and backward anisotropy coefficients differ from each other as well as the normalized (to target mass) count rates of forward- and backward-emitted fragments. Note that the measured forward/backward count rate ratios depend slightly on incident neutron energy and lie in the interval from 1.02 to 1.18. To account for the influence of LMT on the K_{abs} values, we have calculated the fragment ranges for both emission directions using our experimental data on fragment energy distributions and the SRIM code [16]. The angular anisotropy coefficients were obtained from angular distributions of forward- and backward-emitted fragments. (The angle determination technique has been described in detail elsewhere [13]). Examples of fragment distributions versus emission angle θ (with respect to the neutron beam direction) are given in Fig. 5. To derive the anisotropy coefficients, the data were fitted in the undistorted region ($0.3 \leqslant |\cos\theta| \leqslant 0.9$) with a function $W(\theta) \propto 1 + B\cos^2\theta$.

The determination of K_{th} is complicated by the presence of the low-energy background in the energy spectra of fission fragments. The background is due to light charged particles, which are produced by incident neutrons in the counting gas and upstream materials. As shown in Ref. [17], an ionization chamber with Frisch grids (apart from a simple parallel-plate ionization chamber) allows a considerable suppression of the background. The discrimination principle is based on the fact that fission fragments and light charged particles give different ratios of anode to cathode signal pulse-heights, and thus may be separated from each other by off-line processing. To find the K_{th} values, we have used the "cleared" energy spectra of fission fragments with constant linear extrapolation from about 27 MeV to zero fragment energy.

The fission cross-section ratios of various nuclides to U were obtained for both the forward- and the backward-facing targets as follows:

$$\frac{\sigma_i}{\sigma_U} = \frac{N_{f,i}}{N_{f,U}} \cdot \frac{m_U}{m_i} \quad (2)$$

Here $N_{f,i}$ is the number of "peak" fission events, corrected for K_{abs} and K_{th} as described above; m is the number of target nuclei; the subscript i denotes one of six nuclides under study (^{205}Tl, $^{204,206–208}$Pb or ^{209}Bi). The resulting ratios were obtained as a linear average of the "forward" and "backward" ratios. Fission cross-section ratios for the pure lead isotopes ^{204}Pb, ^{206}Pb and ^{207}Pb to ^{238}U were obtained taking into account the isotope composition of the targets. The absolute neutron-induced fission cross-sections were obtained using the ^{238}U(n, f) cross-section standard [2].

In fact, the above-described procedure implies the neutron fluence measurements through a reference reaction ^{238}U (n, f). The validity of this procedure was estimated in a cross-check measurement performed at the LLN neutron beam facility. In this experiment, the fluence of 59.9 MeV neutrons has been simultaneously determined with the MFGIC and a fission chamber monitor (FCM) calibrated relative to a proton recoil telescope [8]. The FCM and MFGIC were positioned at distances of 6 and 10.2 m, respectively. The fluence measurements were compared taking into account the divergence of the neutron beam (the $1/r^2$ law) and the neutron losses in the air. The results of the intercomparison were found to be consistent within 3%.

5. Results and discussion

Measured neutron-induced fission cross-sections of ^{205}Tl, $^{204,206–208}$Pb, ^{209}Bi and their total uncertainties are given in Table 2. The first column contains the mean energies of the neutron peaks with the corresponding half-widths. The data for ^{nat}Pb calculated from the

Table 2
Neutron-induced fission cross-sections of ^{205}Tl, $^{204,206–208,nat}$Pb and ^{209}Bi

E_n (MeV)	Fission cross-section (mb)						
	^{205}Tl	^{204}Pb	^{206}Pb	^{207}Pb	^{208}Pb	^{nat}Pb[a]	^{209}Bi
32.8±1.8	0.004±0.003	0.26±0.04	0.047±0.009	0.028±0.009	0.012±0.006	0.027±0.011	0.245±0.023
34.7±1.4	0.025±0.017	0.46±0.13	0.08±0.04	0.035±0.024	0.029±0.022	0.048±0.025	0.37±0.07
45.3±1.5	0.125±0.011	2.19±0.09	0.67±0.03	0.426±0.023	0.252±0.018	0.418±0.025	2.19±0.07
46.3±1.1	—	2.58±0.15	0.79±0.06	0.51±0.04	0.28±0.04	0.49±0.05	2.70±0.12
59.9±1.2	0.57±0.05	7.5±0.4	2.96±0.17	2.24±0.13	1.38±0.09	2.04±0.14	8.04±0.36
65.4±0.9	0.97±0.08	11.1±0.7	5.1±0.3	3.28±0.22	2.33±0.17	3.32±0.24	12.3±0.7
96.0±1.4	4.73±0.26	30.3±1.7	15.2±0.9	11.2±0.6	8.2±0.5	10.9±0.7	28.8±1.7
133.6±1.9	7.9±0.7	46.2±3.4	24.2±1.8	18.2±1.4	14.3±1.1	18.0±1.5	43.3±3.3
173.9±1.9	11.1±1.6	61.7±4.8	38.7±3.1	35.3±2.5	23.9±1.8	30.5±2.4	66.6±3.8

The average neutron peak energies E_n are given with their half-widths calculated from the energy losses of protons in the lithium targets. The data total uncertainties are given as standard deviations.

[a]The data were derived from the cross-sections of separate lead isotopes.

cross-sections of separate lead isotopes are also given in Table 2. The cross-section uncertainties include the uncertainties of the measured cross-section ratios and of the cross-section standard [2].

Fig. 6 shows the fission cross-section of six target nuclides versus incident neutron energy. All the data obtained at the LLN neutron facility agree well with the ones obtained at the TSL at low neutron energies. The

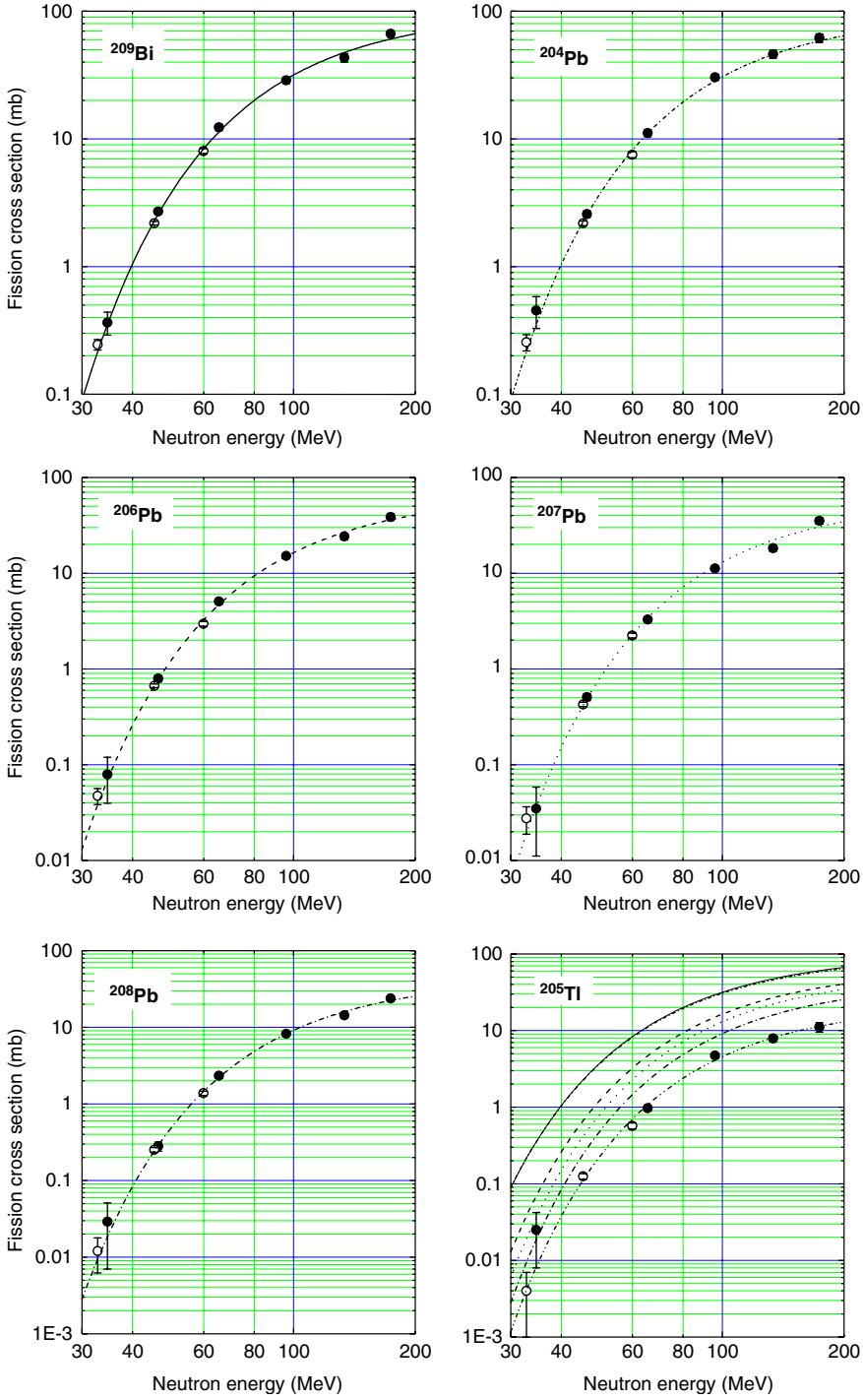

Fig. 6. Neutron-induced fission cross-sections of ^{205}Tl, $^{204,206-208}$Pb and ^{209}Bi measured at the LLN (open circles) and the TSL (solid circles) neutron beam facilities. The plotted curves are the data fits using a function $p_1 \exp(-(p_2/E_n)^{3/2})$, where E_n is the incident neutron energy. The parameters p_1 and p_2 are given in Table 3. For an easy comparison, the fits of the Pb and Bi data are reproduced in the ^{205}Tl panel.

Table 3
Parameters used to fit the present data (see Fig. 6) with a function $p_1 \exp(-(p_2/E_n)^{3/2})$

Parameter	Target nuclide					
	^{205}Tl	^{204}Pb	^{206}Pb	^{207}Pb	^{208}Pb	^{209}Bi
p_1	23.1	96.4	66.6	59.0	44.7	100.2
p_2	138.1	109.5	135.3	131.6	136.2	110.0

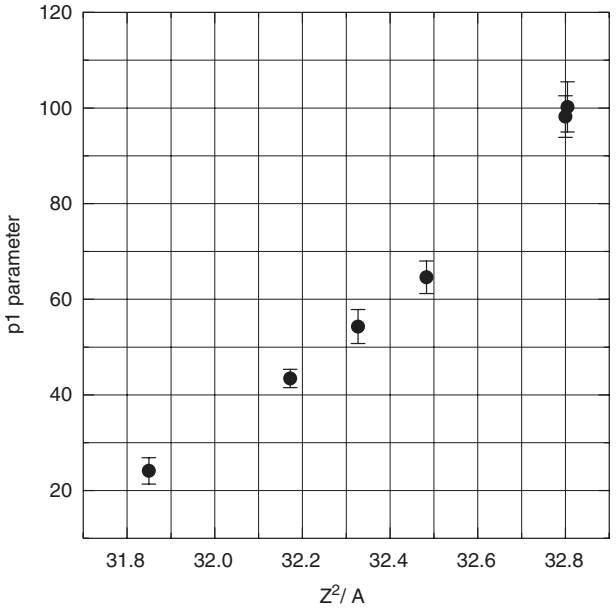

Fig. 7. Parameter p_1 of the (n, f) cross-section parameterizations (see Table 3) versus the fissility parameter Z^2/A of the composite nucleus.

curves plotted in Fig. 6 are fits to the experimental data using a function $p_1 \exp(-(p_2/E_n)^{3/2})$. The corresponding parameters are given in Table 3. All the fits are compared in the panel with the thallium data (Fig. 6). From this comparison, a strong dependence of the fission cross-section on the fissility parameter Z^2/A of the composite nucleus is clearly seen in Fig. 7.

The neutron-induced fission cross-sections of ^{nat}Pb and ^{209}Bi obtained in this work are compared with other experimental data in Figs. 8 and 9. The bulk of the data was obtained at "white" source neutron beam facilities: at the LANCE/WNR facility by Staples et al. [18] and at the GNEIS facility by Shcherbakov et al. [19]. In addition, there are data obtained with quasi-monoenergetic neutron beams by Nolte et al. [20] and by Smirnov et al. [21]. One can see that our data for both ^{209}Bi and ^{nat}Pb agree well with the data of Shcherbakov et al. [19] practically over all neutron energies where a comparison is possible. The data of Staples et al. [18] at neutron energies above 50 MeV are consistent (both for ^{209}Bi and ^{nat}Pb) with the present data as well as with the data of Shcherbakov et al. [19]. The data

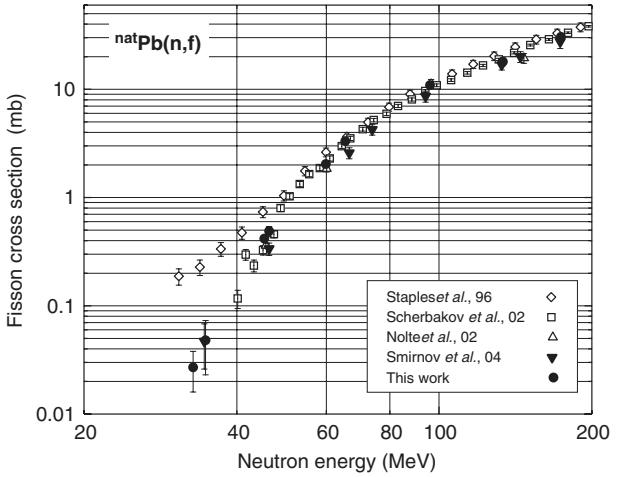

Fig. 8. Neutron-induced fission cross-sections of ^{nat}Pb obtained in the present work in comparison with other experimental data [18–21].

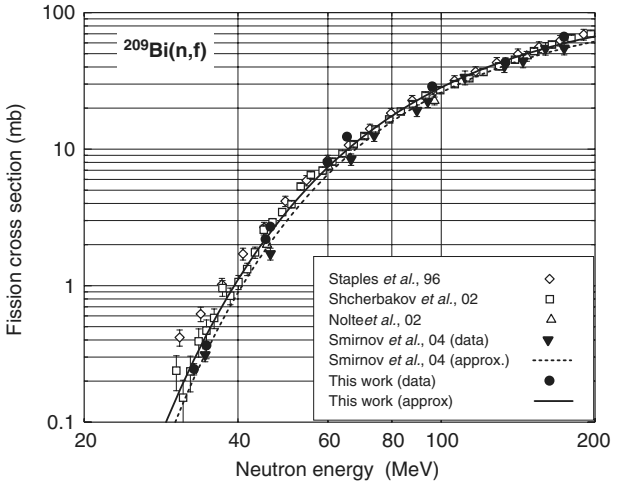

Fig. 9. Measured neutron-induced fission cross-sections of ^{209}Bi compared to other experimental data [18–21]. The data from Refs. [18,19] are given with regard to the recommended standard uncertainties [2]. The dashed line shows the cross-section parameterization of Smirnov et al. [21], the solid line corresponds to the parameterization obtained in the present work (see the text).

of Nolte et al. [20] lie somewhat below the present data but are consistent with them within the stated uncertainties. At neutron energies below 50 MeV, there is a large discrepancy between our data and the data of Staples et al. [18]. In particular, the cross-sections of ^{209}Bi and ^{nat}Pb measured by Staples et al. [18] at 35 MeV exceed the present data by two and four times, respectively. Also seen is a systematic deviation of the data of Smirnov et al. [21] from our data at neutron energies above 40 MeV.

As mentioned above, the neutron-induced fission cross-section of ^{209}Bi was adopted as a secondary standard [2], so the bismuth data require a particular attention. Recently,

the standard parameterization was revised by Smirnov et al. [21]. A new parameterization suggested in Ref. [21] is shown in Fig. 9 by the dashed line. It is apparent that this parameterization is in rather poor agreement with all the available experimental data over the 35–200 MeV neutron energy range: the corresponding χ^2/v value (calculated without the data of Staples et al. [18] at neutron energies below 45 MeV) is as large as 5.1. This disagreement is due to that the data of Shcherbakov et al. [19] as well as the data of Staples et al. [18] (these data are very close to the Shcherbakov's ones at energies above 45 MeV) were not taken into consideration by Smirnov et al. [21]. The new standard parameterization of Smirnov et al. [21] was based on their own data and the data of Nolte et al. [20]. It is not clear why Smirnov et al. [21] used such a reduced experimental database. We can only note that the data of Shcherbakov et al. [19] were incorrectly quoted by Smirnov et al. [21] (see Fig. 9 in Ref. [21]): the true data at low neutron energies are 2–3 times below the quoted ones.

Since the data obtained at the LANCE/WNR and the GNEIS facilities make up about 70% of the existing experimental database for ^{209}Bi, we have taken them into consideration. A parameterization based on the whole data set (excluding the data of Staples et al. [18] at $E_n < 45$ MeV) is shown in Fig. 9 by the solid line. The fitted function $p_1 \exp(-(p_2/E_n)^{p_3})$ was taken from Ref. [21]. It yields a χ^2/v value of 1.9 with the following parameters: $p_1 = 123.4$, $p_2 = 135.6$ and $p_3 = 1.27$. Note that the present parameterization is only valid in the neutron energy range from 30 to about 200 MeV. In order to fit the data set extended to lower and higher neutron energies (see, e.g., the data from Ref. [22] and Refs. [18,23], respectively) a more sophisticated fitting function will be necessary.

The present parameterization differs from the one suggested by Smirnov et al. [21] by about 10–15% in the 50–150 MeV range. It is notable, however, that the shapes of the two resulting functions are in fair agreement. To some extent it can be a normalization effect. Note that different normalization techniques have been used for the various experiments discussed. The present results and the data of Smirnov et al. [21] were normalized to the ^{238}U (n, f) cross-section standard, while Nolte et al. [20] normalized to n–p scattering (except one data point at 97 MeV) and Shcherbakov et al. [19] to the ^{235}U (n, f) cross-section. Thus, work to establish accurate cross-section standards is highly motivated.

Acknowledgments

The authors wish to thank the operating crews of the Louvain-la-Neuve and the Uppsala cyclotron facilities for the excellent beams they provided for these experiments. The participants from Khlopin Radium Institute (I.V.R., G.A.T. and A.G.M.) would like to thank the Université catholique de Louvain and Uppsala University for the kind hospitality they received during their stays in Belgium and Sweden, respectively.

This work was partially supported by the International Science and Technology Centre (Project #1309).

References

[1] A.J. Koning, J.-P. Delaroche, O. Bersillon, Nucl. Instr. and Meth. A 414 (1998) 49.
[2] A.D. Carlson, S. Chiba, F.-J. Hambsch, N. Olsson, A.N. Smirnov, IAEA Report INDC (NDC)-368, Vienna, 1997, Proceedings of the International Conference on Nuclear Data for Science and Technology, 1997, part II, Trieste, Italy, p.1223.
[3] W. Glasser, R. Michel, S. Neumann, H. Schuhmacher, V. Dangendorf, R. Nolte, U. Herpers, A.N. Smirnov, I.V. Ryzhov, A.V. Prokofiev, P. Malmborg, D. Kollár, J.P. Meulders, J. Nucl. Sci. Tech. 1 (Suppl. 2) (2002) 373.
[4] R. Michel, W. Glasser, U. Herpers, H. Schuhmacher, H.J. Brede, V. Dangendorf, R. Nolte, P. Malmborg, A.V. Prokofiev, A.N. Smirnov, I.V. Ryzhov, J.P. Meulders, M. Duijvestijn, A. Koning, Proceedings of International Conference on Nuclear Data for Science and Technology, Santa Fe, NM, USA, 2004, AIP Conference Proceedings, vol.769, p.861.
[5] A.V. Ignatyuk, G.N. Smirenkin, M.G. Itkis, S.I. Mulgin, V.N. Okolovich, Sov. J. Part. Nucl. 16 (1985) 307;
A.V. Ignatyuk, G.N. Smirenkin, M.G. Itkis, S.I. Mulgin, V.N. Okolovich, Fiz. Elem. Chastits At. Yadra 16 (1985) 709 (in Russian).
[6] G.A. Tutin, I.V. Ryzhov, V.P. Eismont, A.G. Mitryukhin, V.S. Oplavin, S.M. Soloviev, J. Blomgren, H. Condé, N. Olsson, P.-U. Renberg, Proceedings of International Conference on Nuclear Data for Science and Technology, Santa Fe, NM, USA, 2004, AIP Conference Proceedings, vol.769, p.937.
[7] I.V. Ryzhov, G.A. Tutin, V.P. Eismont, A.G. Mitryukhin, V.S. Oplavin, S.M. Soloviev, J.P. Meulders, Y. El Masri, Th. Keutgen, R. Prieels, R. Nolte, Proceedings of International Conference on Nuclear Data for Science and Technology, Santa Fe, NM, USA, 2004, AIP Conference Proceedings vol.769, p.684.
[8] H. Schuhmacher, H.J. Brede, V. Dangendorf, M. Kuhfuss, J.P. Meulders, W.D. Newhauser, R. Nolte, Nucl. Instr. and Meth. A 421 (1999) 284.
[9] J. Klug, J. Blomgren, A. Ataç, B. Bergenwall, S. Dangtip, K. Elmgren, C. Johansson, N. Olsson, S. Pomp, A. Prokofiev, J. Rahm, U. Tippawan, O. Jonsson, L. Nilsson, P.-U. Renberg, P. Nadel-Turonski, A. Ringbom, A. Oberstedt, F. Tovesson, V. Blideanu, C. Le Brun, J.-F. Lecolley, F.-R. Lecolley, M. Louvel, N. Marie, C. Schweitzer, C. Varignon, Ph. Eudes, F. Haddad, M. Kerveno, T. Kirchner, C. Lebrun, L. Stuttgé, I. Slypen, A. Smirnov, R. Michel, S. Neumann, U. Herpers, Nucl. Instr. and Meth. A 489 (2002) 282.
[10] R. Nolte, private communication.
[11] S. Pomp, A.V. Prokofiev, J. Blomgren, O. Byström, C. Ekström, N. Haag, A. Hildebrand, C. Johansson, O. Jonsson, P. Mermod, L. Nilsson, D. Reistad, N. Olsson, P.-U. Renberg, M. Österlund, U. Tippawan, D. Wessman, V. Ziemann, Proceedings of International Conference on Nuclear Data for Science and Technology, Santa Fe, NM, USA, 2004, AIP Conference Proceedings, vol.769, p.780.
[12] O. Bunemann, T.E. Cranshaw, J.A. Harvey, Can. J. Res. A 27 (1949) 191.
[13] G.A. Tutin, I.V. Ryzhov, V.P. Eismont, A.V. Kireev, H. Condé, K. Elmgren, N. Olsson, P.-U. Renberg, Nucl. Instr. and Meth. A 457 (2001) 646.
[14] V.P. Eismont, A.V. Kireev, I.V. Ryzhov, G.A. Tutin, H. Condé, K. Elmgren, S. Hultqvist, Proceedings of the Second International Conference on Accelerator Driven Transmutation Technologies and Applications, vol.2, Kalmar, Sweden, 1997, p.618.
[15] D.B. Gayther, Metrologia 27 (1990) 221.
[16] J.F. Ziegler, J.P. Biersack, U. Littmark, The Stopping and Range of Ions in Solids, Pergamon Press, New York, 1985.
[17] V.P. Eismont, A.V. Kireev, I.V. Ryzhov, S.M. Soloviev, G.A. Tutin, H. Condé, K. Elmgren, N. Olsson, P.-U Renberg, Proceedings of

Third International Conference on Accelerator Driven Transmutation Technologies and Applications, Praha, Czech Republic, 1999, http://www.fjfi.cvut.cz/con_adtt99/a_confer/a_info/list_pap.htm, Mo-O-C7.

[18] P. Staples, P.W. Lisowski, N.W. Hill, Bull. Am. Phys. Soc. 40 (1995) 962;
P. Staples, private communication (1996).

[19] O. Shcherbakov, A. Donets, A. Evdokimov, A. Fomichev, T. Fukahori, A. Hasegawa, A. Laptev, V. Maslov, G. Petrov, S. Soloviev, Y. Tuboltsev, A. Vorobyev, J. Nucl. Sci. Tech. 1 (Suppl. 2) (2002) 230.

[20] R. Nolte, M.S. Allie, P.J. Binns, F.D. Brooks, A. Buffler, V. Dangendorf, K. Langen, J.P. Meulders, W.D. Newhauser, F. Ross, H. Schuhmacher, J. Nucl. Sci. Tech. 1 (Suppl. 2) (2002) 311.

[21] A.N. Smirnov, V.P. Eismont, N.P. Filatov, J. Blomgren, H. Condé, A.V. Prokofiev, P.U. Renberg, N. Olsson, Phys. Rev. C 70 (2004) 054603.

[22] P.E. Vorotnikov, L.S. Larionov, Sov. J. Nucl. Phys. 40 (1984) 552;
P.E. Vorotnikov, L.S. Larionov, Yad. Fiz. 40 (1984) 867 (in Russian).

[23] V.I. Goldanskiy, V.S. Penkina, E.Z. Tarumov, Zh. Eksp. Teor. Fiz. 29 (1955) 778 (in Russian).

Experimental neutron data above 20 MeV: What can be done? What should be done?

J. Blomgren,
Department of Neutron Research
Uppsala University
Sweden

Abstract

The nuclear data needs of the most important applications involving neutrons above 20 MeV are reviewed. The present status of experimental data is outlined, and future possibilities are discussed.

1 Applications involving neutrons above 20 MeV

The interest in high-energy neutron data is rapidly growing since a number of potential large-scale applications involving fast neutrons are under development, or have been identified. These applications primarily fall into three sectors; nuclear energy and waste management, nuclear medicine and radiation effects on electronics.

The recent development of high-intensity proton accelerators has resulted in ideas to use sub-critical reactors, fed by neutrons produced in spallation processes maintained by external proton beams, for transmutation of spent fuel from nuclear power reactors or incineration of nuclear weapons material. Incineration by such accelerator-driven systems (ADS) might result in less problematic handling of fissile material. New nuclear data are needed for feasibility assessments of these techniques. For reviews of recent nuclear data activities in this field, see, e.g., refs. [1, 2, 3].

Conventional radiation treatment of tumours, i. e., by photons or electrons, is a cornerstone in modern cancer therapy. Some rather common types of tumours, however, cannot be treated successfully using these modalities. For some of these, good treatment results have been obtained with neutron therapy [4]. The nuclear data situation and prospects for future development is outlined in ref. [5]

During the last few years, it has become evident that electronics in aircrafts suffer effects from neutrons generated by cosmic radiation interacting in the upper atmosphere [6, 7, 8, 9]. For instance, a neutron could induce a nuclear reaction in the silicon substrate of a memory device, releasing free charge, which could flip one or more memory units. Similar effects causing soft- and/or hardware damage have recently been identified also at ground level.

Finally, neutrons at commercial aircraft altitudes induce significant radiation doses to the crew [10]. In fact, the largest average doses to personnel in civil work are obtained in aviation.

For all the applications mentioned above, an improved understanding of neutron interactions is needed. Moreover, neutron-induced nuclear reactions are also important for fundamental physics reasons. Recently, the *np* scattering cross section at intermediate energies has been under intense debate (for a review, see Ref. [11]).

The np scattering cross section is of utmost importance for applications because it is used for normalization of nuclear data measurements. It is also of great fundamental importance, because np scattering data are being used for determinations of the pion-nucleon coupling constant, i.e., the absolute strength of the strong interaction in the nuclear sector. This coupling constant is of great relevance not only to basic nuclear physics, but also on a cosmological scale.

A second area of fundamental interest is studies of three-nucleon force effects. Recent calculations [12] has indicated that measurements of the differential cross section for elastic nd scattering in the 60–200 MeV range should be useful in searches for three-nucleon ($3N$) force effects. The neutron-deuteron (nd) elastic scattering differential cross section has been measured at 95 MeV incident neutron energy. Models based on inclusion of $3N$ forces describe nd data in the angular region of the cross-section minimum very well, while models without $3N$ forces cannot account for the data [13, 14].

2 The nuclear data situation

2.1 Importance of various applications

When judging the importance of these various applications, different sets of criteria can be used, and the importance of various nuclear data activities can be judged differently depending on the basis of the comparison. The largest activity does not necessarily have the most severe nuclear data needs. The three most important applications are - to my judgement - accelerator-driven systems for waste incineration (ADS), single-event effects in electronics (SEE) and neutron therapy for cancer treatment (NT).

Transmutation of nuclear waste and electronics effects are both of importance to commercial industries with turnovers exceeding national budgets. Accelerator-driven systems for transmutation is on a research stage, and a possible future industry implementation is probably more than twenty years into the future. Single-event effects in electronics constitute already an important reliability issue, and it is rapidly growing. Experts in the field predict that this effect is at present the most likely candidate to halt the rapid progress of silicon-based circuit technology [15, 16].

Fast neutron cancer therapy represents a relatively stable niche modality, with about a dozen facilities running worldwide. Dose effects to aviation personnel, and even in space environments, is an activity of limited size.

Another basis of comparisons is how large the data needs are. In ADS, the data needs develop over time. Initially, some basic data were needed for the assessment whether this was worth continued attention. At present, the nuclear data research is on a level where data needed for the design of a demonstration facility should be the target. If plans for a full-scale plant or a close-to-full-scale prototype mature, the nuclear data needs evolve even further, and if industry deployment becomes a reality, a massive nuclear data campaign will be motivated.

Concerning electronics reliability, the problem itself is already large and it can become huge, but this does not necessarily mean that the nuclear data needs are extremely large. These effects are caused by a limited number of nuclear reactions in only a few elements, and therefore the total nuclear data research needed is relatively limited.

The same holds for dose effects in neutron therapy and civil aviation. Also there, there are a limited number of reactions on a few nuclei that contribute essentially the entire dose.

A third basis for comparison is the role of fast neutrons. In ADS, a vast majority of the neutrons are at traditional reactor energies, i.e., below a few MeV. Neutrons

above 20 MeV represent a small fraction of the externally produced neutrons, on a percent level or less. Still, the importance of these fast neutrons is larger than their share of the total number, because these fast neutrons can multiply into a large number of low-energy neutrons, and very fast neutrons can cause considerable materials damage, and they constitute an important radiation protection problem. To first order, the neutrons produced by the proton beam via spallation reactions display a $1/E$ spectrum, while the capability of neutrons to cause damage (and to multiply themselves) essentially goes as the energy. Thus, to first order neutrons at all energies should be of about equal importance. One has to remember, however, that this holds for the spallation neutrons only. In a typical design concept, it is assumed that each accelerator-produced neutron should induce a nuclear reaction chain releasing 20–50 neutrons. Thus, the spallation neutrons constitute only a few percent of the total neutron population in a hybrid accelerator-target-reactor system.

Concerning single-event effects, the neutrons only play the role of a villain. They induce unwanted disturbances of the system, while for ADS and neutron therapy, they are indispensible. In fact, fast neutrons are the most important in NT, where they are responsible for the entire effect.

Still another comparison is provided by fiscal realities. In the realm of ADS, there are relatively good possibilities to get funding from various sources. Nuclear data for SEE studies have so far received very limited financial resources, and it is not likely that this will change dramatically when it comes to direct support for nuclear data experiments. Here there is, however, a possibility for indirect funding. By providing in-beam tests of components on a commercial scale, resorces for nuclear data experiments can be obtained. In the NT field, the financial situation is no reason for joy. Here, the eternal dilemma of funding of interdisciplinary research comes into play. The physics community considers this to be service to medicine, which should be payed by the end users, and the medical community claims these activities to be nuclear physics and should be financed as such.

Finally, we need to consider which data to study for the development of the various applications. The needs are the smallest for SEE. The effects are caused by neutron-induced production of charged particles in silicon. With present technologies, heavy ions (HI), i.e., lithium ions and heavier are causing the main effects. With future technology development, also light ions can become important. Because these effects are caused by the natural cosmic-ray neutron spectrum, which has a $1/E$ energy distribution, in combination with a decrease of the total cross section at high energies, the importance goes down at high energies. At low energies, the neutron energy is insufficient to induce reactions that can cause an upset. Therefore, 5–500 MeV seems to be the relevant interval, with the largest importance in the 20–100 MeV range.

In neutron therapy, about half the dose comes from neutron-proton scattering, taking place in the water in the body. Although there has been some debate recently about the np scattering cross section at backward angles, this is not very important for this particular application. Most of the remaining dose is due to neutron-induced light ion production in the body, and finally, the recoils due to elastic scattering give a small dose, however of large biologic significance. The most common elements in the body are hydrogen, oxygen, carbon, nitrogen and calcium, together constituting more than 90 % of the body. If including also phosphorus, about 99 % is accounted for. Thus, it is only a few elements that need to be studied. At present, clinical treatments are carried out up to 70 MeV, so the interesting range is up to about that energy. It might still be wise to extend these studies to slightly higher energies, because future optimization of NT might point towards higher treatment energies.

Application	ADS	SEE	NT
Tendency	Slow growth	Rapid growth	Steady state
Role of fast n	Small but important	Disturbance	Does all the job
En (MeV)	0–1000	10–500	20–100
Targets	Many	Si	C, N, O, Ca
Reactions	Many	(n,HI), (n,LI)	(n,LI), (n,n)
Funding	Good	Direct: bad Indirect: possible	Bad

Table 1: Summary of the nuclear data needs for the largest applications involving fast neutrons. See the text for details.

2.2 Nuclear data status

It is a fairly limited class of reactions that are of interest for the further development of the applications under consideration. These are elastic scattering, inelastic neutron emission, light ion production, heavy ion production and fission.

Elastic scattering has been studied on a range of nuclei up to 96 MeV. At present, ten nuclei have been studied and results are either published or underway [17]. An overall uncertainty of about 5 % has been achieved. A novel normalization method has been established that allows elastic scattering data to be normalized absolutely to about 3 % uncertainty [18]. This method, however, works only for elastic scattering. Feasibility studies have shown that the technique as such works up to about 200 MeV, so these studies can be extended up in energy.

An experimental programme on inelastic neutron emission, i.e., (n,xn') reactions, is in progress [19]. Data have been taken on lead and iron, and the method as such seems to work. It is too early to quote a final uncertainty in the results, but 10 % seems feasible.

Data on light ion production has been acquired on about ten nuclei at 96 MeV, and analysis is in progress [20, 21]. At present, about half the data set has been published. Normalization has been obtained by simultaneous detection of np scattering at an angle where the cross section uncertainty can be estimated to about 5 %, which is the dominating uncertatinty in the final light ion production cross sections. These studies are presently being extended to 180 MeV, with a first in-beam test late autumn 2005.

Fission cross sections have been studied at many facilities up to about 200 MeV energy. The energy dependencies of the cross sections agree fairly well in shape, but the absolute scale differs by up to 15 %. It is at present not clear what causes this. One possibility is the normalizations used. Another possible cause is that the sensitivity to low-energy neutrons is not under control for some of the experiments. Dedicated experiments to remedy this situation are underway.

In principle, fission cross sections can be measured up to several GeV using white beams with a very high initial proton energy, like at the CERN-nTOF facility [22]. The neutron beam intensity is very low, but the cross sections are large and it is possible to detect a major fraction of the fission fragments, resulting in reasonable statistical precision. A major problem, however, is normalization, since the beam intensity is very difficult to monitor at these very high energies.

There are only a few examples of other fission data than cross sections. This means that important fission parameters, like angular distributions, yields, etc., essentially remain to be investigated at high neutron energies.

Reaction	Status	Uncertainty
(n,n)	Done up to 100 MeV	5 %
	Can be done up to 200 MeV	
(n,xn')	Underway at 100 MeV	10 %
	Can be done up to 200 MeV	
(n,LI)	Done up to 100 MeV	5 %
	Up to 200 MeV underway	
(n,f)	Cross sections up to 200 MeV	15 %
	Possible up to 5 GeV	
	Absolute scale problem	
	$d\sigma/d\Omega$, yields, etc. remaining	
	Overall limitation: normalization	5 %

Table 2: Summary of the nuclear data situation for the most important neutron-induced nuclear reactions above 20 MeV. See the text for details.

3 Future possibilities

As was discussed in the previous section, the prospects for development in the near future, i.e., within ten years, can be summarized to extension to about 200 MeV of ongoing work on elastic scattering, inelastic neutron emission and light ion production at around 100 MeV, and fission studies of other parameters than the cross section.

If looking a bit further into the future, we can allow ourselves to be more visionary. To my opinion, the single most important problem to solve if we want a significant development of the field is normalization. At present, we inevitably end up with an uncertainty of about 5 %, because we have to normalize to something, typically np scattering, which is known to - at best - 5%, and it is difficult to see how this can be radically improved upon in a short term with present techniques.

I consider energy resolution to be the second largest problem, with intensity on third place. These two are, however, to a large degree coupled. If you aim for good neutron-beam energy resolution, you have to pay by poor intensity and vice versa. It is presently close to inconceivable to produce neutrons at high energies with a resolution better than 1 MeV with a reasonable intensity. The limited intensity puts severe constraints on the detection, in such a way that the detection often has to be performed with techniques that sacrifice resolution for efficiency, resulting in a final resolution of a few MeV. This means that only in a few rare cases, resolved final states can be studied.

Recently, a way out of this dilemma has been proposed. At CERN, planning is ongoing for a beta-beam facility [23]. The background is that neutrino physics has progressed rapidly the last few years, with the discovery of neutrino oscillations as the most visible example. Up to now, essentially all accelerator-produced neutrinos have been muon neutrinos, being the final product of pion decay. Electron neutrinos are much more difficult to produce in large amounts, because they require a nuclear beta decay for their creation.

At the proposed CERN beta-beam facility, production of suitable beta-emitting nuclei should be undertaken in an ISOLDE-like facility, and the produced nuclei should be post-accelerated to very high energy by a series of accelerators, the final one being SPS. After acceleration, the ions are directed to a decay ring of race-track shape. At these very high energies, hundreds of GeV per nucleon, there is a very strong Lorentz boost, which means that the neutrino is emitted very close to the

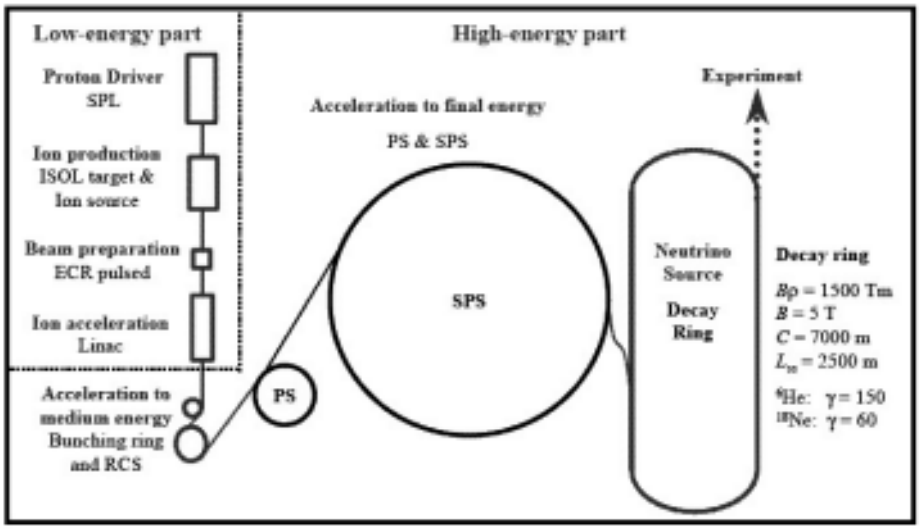

Figure 1: Overview of the proposed CERN beta-beam facility.

beam direction in the laboratory system, in spite of that the emission is isotropic in its moving reference frame. Thereby, intense neutrino beams can be produced. The idea is to build the decay ring so that one straight section points towards a distant neutrino detector to allow studies of electron neutrino oscillations.

Intense neutron beams could be a spin-off from that facility. It has been proposed to use two production targets, one for nuclei suited for neutrino emission in the decay ring, and one for beta-delayed neutron emitters. Some unstable neutron-rich nuclei can beta decay to a nucleus that promptly emits a neutron (a process which by the way is of utmost importance to the stability of nuclear power reactors). This neutron has typically an energy of a few hundred keV in its rest frame. By accelerating the beta-delayed neutron emitters up to a few hundred MeV per nucleon, the Lorentz boost is sufficient to focus the beam to reasonable dimensions. All this can be done in parallel with the primary objective, since the accelerators for the neutrino emitters have a long cycle with a low duty factor. Thus, for most of the time there is no injection into the synchrotrons for neutrino emitter acceleration, and then the production targets can be used for beta-delayed neutron emitter production.

The resulting neutron beam has an energy in the 100–500 MeV range with an energy resolution of about 1 MeV, and intensities of about 10^{11} n/s are estimated. This should be compared with 10^{6} for present-day technology, i.e., an improvement by a factor 100 000 (!). With such intensities, only imagination sets the limit for what can be achieved.

First and foremost, such intensities are not too far from what has been used in proton beam experiments for fundamental nuclear physics. This opens opportunities to study, e.g., the role of isospin in nuclei by conducting a carefully selected set of experiments where information from experiments with neutrons could be combined with previous information from proton-induced reactions. Many types of fundamental physics issues hitherto inaccessible to experiments could be within reach to address. This is such a large field that it deserves its own workshop.

If we now restrict the discussion to nuclear data for applications and turn to my problem list above, it seems feasible that we can address all of them through one experimental trick: tagging. If we use the neutron beam directly for experiments we have essentially only solved the intensity problem, but the other two remain;

we end up in a 1 MeV resolution due to the inherent energy spread, and we are still plagued by the normalization problem. Tagging means that we produce a secondary neutron beam of less intensity, but with much better known intensity. One candidate reaction is to let neutrons scatter from a hydrogen target, and the recoil proton is detected. Since this is a two-body final state, detection of the associated proton means that a neutron must have been scattered to the corresponding direction. Thereby, the normalization problem can be circumvented, since we count the neutrons one by one through the associated particle. If this tagging is performed with a high resolution, both in energy and angle, we can also know the neutron energy event by event far better than the initial neutron beam energy resolution. If the tagging is performed with a magnetic spectrometer, the tagger can be made rather insensitive to the ambient background, and a proton energy resolution of better than 100 keV can be obtained, resulting in a comparable neutron energy resolution.

With reasonable estimates on tagger parameters, 10^4 tagged neutrons with an energy resolution of 100 keV should be possible to reach, given the beam intensity above. This might sound like a poor intensity, but with such a resolution, final states can be well resolved, which means that already a small number of events will result in a good precision. Moreover, since the intensity can be determined to about 1 % in a typical tagger system, the accuracy is far better than what can be obtained today. In cases when the demands on energy resolution are not as stringent, a thicker tagger target can be used, resulting in increased intensity. This goes faster than linear, because with a worse resolution, the intensity at the tagger is increased, thicker secondary experimental targets can be used, and the detection limitations are less severe. Therefore, even with resolutions that are on the limit to be possible untagged today, we might have tagged beams of intensities exceeding what is presently available in a not too distant future.

To conclude, the rumours of the death of nuclear data research seem to be greatly exaggerated...

Acknowledgments

The information from Mats Lindroos is gratefully acknowledged. This work was financially supported by the Swedish Nuclear Fuel and Waste Management Company, the Swedish Nuclear Power Inspectorate, Ringhals AB, Forsmarks Kraftgrupp AB, the Swedish Defense Research Agency, the Swedish Nuclear Safety and Training Centre, and the European Union.

References

[1] A. Koning, *et al.*, J. Nucl. Sci. Tech., Suppl. **2** (2002) 1161.

[2] J. Blomgren, in Proceedings of Workshop on Nuclear Data for Science & Technology: Accelerator Driven Waste Incineration, Trieste, Italy, Sept. 10-21, 2001, eds. M. Herman, N. Paver, A. Stanculescu, ICTP lecture notes **12** (2002) 327.

[3] J. Blomgren, Nuclear data for accelerator-driven systems - Experiments above 20 MeV, in Proceedings of EU enlargement workshop on Neutron Measurements and Evaluations for Applications, Bucharest, Romania, October 20-23, 2004.

[4] A. Wambersie, P. Pihet, H.G. Menzel, Radiat. Prot. Dosim. **31** (1990) 421.

[5] J. Blomgren and N. Olsson, Radiat. Prot. Dosim. **103(4)** (2003) 293.

[6] H.H.K. Tang, IBM J. Res. Develop. **40** (1996) 91.

[7] Single-Event Upsets in Microelectronics, topical issue, eds. H.H.K. Tang and N. Olsson, Mat. Res. Soc. Bull. **28** (2003).

[8] J. Blomgren, B. Granbom, T. Granlund, N. Olsson, Mat. Res. Soc. Bull. **28** (2003) 121.

[9] J. Blomgren, Nuclear Data for Single-Event Effects, in Proceedings of EU enlargement workshop on Neutron Measurements and Evaluations for Applications, Budapest, Hungary, November 5-8, 2003. EUR Report 21100 EN, Luxembourg: Office for Official Publications of the European Communities, ISBN 92-894-6041-5, European Communities, 2004.

[10] D.T. Bartlett, R. Grillmaier, W. Heinrich, L. Lindborg, D. O'Sullivan, H. Schraube, M. Silari, L. Tommasino, Radiat. Res. Cong. Proc. **2** (2000) 719. See also the entire issue of Radiat. Prot. Dosim. **86(4)**, (1999).

[11] Proceedings of Workshop on "Critical Points in the Determination of the Pion-Nucleon Coupling Constant", Uppsala, June 7-8, 1999, ed. J. Blomgren. Phys. Scr. **T87** (2000).

[12] H. Witała, *et al.*, Phys. Rev. Lett. **81** (1998) 1183.

[13] P. Mermod, *et al.*, Phys. Lett. **B 597** (2004) 243.

[14] P. Mermod, *et al.*, accepted for publication in Phys. Rev. C.

[15] H.H.K. Tang, private communication.

[16] C. Slayman, in Proceedings of the 6th International Workshop on Radiation Effects on Semiconductor Devices for Space Applications, Tsukuba, Japan, October 6-8, 2004, p. 17.

[17] A. Hildebrand, *et al.*, AIP Conference Proceedings **769** (2005) 853.

[18] J. Klug, *et al.*, Phys. Rev. C **68**, 064605 (2003).

[19] F.-R. Lecolley, private communication.

[20] V. Blideanu, *et al.*, Phys. Rev. C **70** (2004) 014607.

[21] U. Tippawan, *et al.*, Phys. Rev. C **69**, 064609 (2004).

[22] L. Tassan-Got, private communication.

[23] The CERN beta-beam working group, http://cern.ch/beta-beam.

PW-14

A New Neutron Beam Facility for SEE Testing

Alexander V. Prokofiev, Stephan Pomp, Jan Blomgren, Olle Byström, Curt Ekström, Dag Reistad, Udomrat Tippawan, Dan Wessman, Volker Ziemann, and Michael Österlund

***Abstract*—A new quasi-monoenergetic neutron beam facility has been constructed at The Svedberg Laboratory in Uppsala, Sweden. The new facility has been designed specifically to provide optimal conditions for testing of single-event effects in electronics. Key features include a neutron energy range of 20 to 175 MeV, high fluxes, user flux control, flexible neutron field size and shape, and spacious and easily accessible user area. Results of beam characterization measurements are reported.**

***Index Terms*—neutron beams, neutron detectors, neutron radiation effects, neutron sources**

I. Introduction

AMONG the different components in the cosmic rays, neutrons are the predominant cause of single-event effects (SEE) in electronics from sea level up to operating altitudes for commercial aircraft [1, 2]. Testing of neutron-induced SEE using the natural flux of cosmic neutrons is time-consuming. To speed up the measurements, one needs to use neutron beams produced with particle accelerators. The procedures for the accelerated testing of memory devices are summarized in the recent JESD89 standard [3]. According to this standard, two types of neutron facilities are recommended for SEE testing: white-spectrum facilities and mono-energetic ones.

White-spectrum neutron facilities, e.g., in Los Alamos [4], Vancouver [5], CERN [6], and St. Petersburg [7], are based on neutron production in a massive target of heavy material (tungsten or lead) irradiated by a proton beam with energies in the region from several hundred MeV to several GeV. Such facilities possess neutron spectra that more or less resemble the natural one at sea level. In order to correct for the differences between the facility spectrum and the natural spectrum at the location of interest, one needs to assume a certain "SEE excitation function", i.e., the energy dependence of the SEE cross-section. However, the behaviour of this function is not sufficiently studied, and different functional forms and parameters are suggested (see, e.g., Refs. [8, 9]). Moreover, the excitation function may vary significantly for different types of SEE, as well as for different technologies, as shown recently by Yahagi *et al.* [8]. Thus, the results of the white-spectrum testing are inevitably model-dependent. This drawback could in principle be eliminated by determining the energy of the neutron that caused SEE using time-of-flight (TOF) techniques, but this would require the ability to read out large computer chips (e.g., multi-MB memories) within a few nanoseconds, which is hardly possible nowadays. On the other hand, the SEE excitation function can be measured at monoenergetic neutron facilities. Then, the SEE rate can be obtained by integration of the obtained excitation function weighted with the atmospheric neutron spectrum. Furthermore, knowledge of the SEE excitation function may shed light upon the nature of the SEE that in turn might be useful when assessing how to deal with the problem. In short, monoenergetic SEE testing is capable to yield more information than white-spectrum testing.

The JESD89 standard [3] suggests that the monoenergetic testing is performed with four nominal neutron energies of 10-20, 50, 100, and 150 MeV. In the energy region above about 20 MeV, a truly monoenergetic neutron beam is not feasible in a strict sense. For certain nuclear reactions, however, there is a strong dominance of neutrons in a narrow energy range. Therefore, such neutron sources are often called "quasi-monoenergetic". The most popular neutron production reaction above 20 MeV is ^{7}Li(p,n)^{7}Be. It is used, e.g., at quasi-monoenergetic neutron facilities in Louvain-la-Neuve [10], Cape Town [11], Davis [12], Takasaki [13], and Saitama [14].

There is a long-term experience in high-energy neutron production at The Svedberg Laboratory (TSL). A neutron facility was built first in the late 1980s [15, 16] and remained in operation until 2003. In 2003-2004, a new facility was constructed that has been optimized for the SEE testing. Emphasis was put on high neutron beam intensity in combination with flexibility in energy and neutron field shape.

II. Technical Specification

The facility uses the ^{7}Li(p,n)^{7}Be reaction to produce a quasi-monoenergetic neutron beam. The proton beam is provided by the Gustaf Werner cyclotron with energies variable in the 25-180 MeV range. The energy of the resulting peak neutrons is controllable in the 20-175 MeV range. This makes TSL the only laboratory in the world offering full monoenergetic neutron testing according to the JESD89 standard [3].

Manuscript received April 7, 2005.

A. V. Prokofiev, O. Byström, C. Ekström, D. Reistad, D. Wessman, and V. Ziemann are with The Svedberg Laboratory, Uppsala University, Box 533, S-751 21 Uppsala, Sweden (corresponding author's phone: +46 18 471 38 50; fax: +46 18 471 38 33; e-mail: Alexander.Prokofiev@tsl.uu.se).

S. Pomp, J. Blomgren, and M. Österlund are with the Department of Neutron Research, Uppsala University, Box 525, S-751 20 Uppsala, Sweden (e-mail: Stephan.Pomp@tsl.uu.se).

U. Tippawan is with the Fast Neutron Research Facility, Chiang Mai University, Thailand (e-mail: udomrat@fnrf.science.cmu.ac.th).

A drawing of the neutron-beam facility is shown in Fig. 1. The proton beam is incident on a target of lithium, enriched to 99.99% in ^{7}Li. The available targets are 1, 2, 4, 8, and 24 mm thick. Proton energy loss in the target amounts to 2-6 MeV depending on the incident proton energy and target thickness. The targets are rectangular in shape, 20×32 mm^2, and are mounted in a remotely controlled water-cooled copper rig. An additional target position contains a fluorescent screen viewed by a TV camera, which is used for beam alignment and focusing. Downstream of the target, the proton beam is deflected by a magnet into a 10-m long dumping line, where it is guided onto a heavily shielded water-cooled graphite beam dump.

The neutron beam is formed geometrically by a cylindrically shaped iron collimator block, 50 cm in diameter and 100 cm long, with a hole of variable size and shape. The collimator is surrounded by concrete to form the end wall of the production line towards a user area. Thereby, efficient shielding from the production target region is achieved. A modular construction of the collimator allows the user to select the diameter of the neutron beam. The available collimator openings are 2, 3, 5.4, 10, 15, 20, and 30 cm in diameter. In addition, a quadratically shaped opening with 1-cm side is available, intended for testing of a separate component without affecting the rest of an electronic board. Other collimator openings in the 0-30 cm range can be provided upon request. The time needed to change the opening size is typically about 30 min.

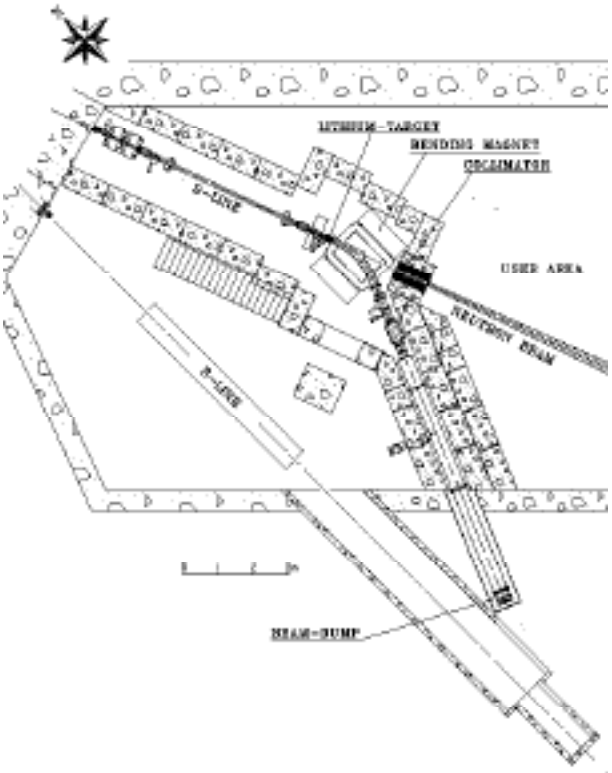

Fig. 1. Drawing of the new neutron beam facility. The neutron beam, produced in the lithium target, continues along the D-line.

The user area extends from 3 to 15 m downstream of the lithium target. Positions located closest to the target are used for high-flux testing of compact objects, with achievable fluxes about an order of magnitude higher compared to the old TSL neutron facility [15, 16], for the same target thickness, proton energy and current. Remote positions may be used to irradiate large objects, up to 1 m in diameter, e.g., entire computers or aircraft navigation systems. Beam currents of up to 10 μA can be used for energies below 100 MeV. Above 100 MeV, the achievable beam current is about a factor of 10 lower. The resulting lower neutron flux can be partly compensated by using thicker lithium targets.

The user area, situated at a level of 12 m below the ground, is connected by Ethernet and coaxial cables, about 100 m long, to counting rooms, which are located at the ground level. A user can vary the neutron flux according to the needs of the specific test. The whole user area is accessible before and immediately after irradiation, because the dose rate from residual β- and γ-rays is only slightly above the natural radiation level.

III. Characterization of the Facility

The first neutron beam at the new facility was delivered in 2004. Since then, commissioning runs have been performed, including measurements of neutron flux, spectra, and profile.

The measured neutron energy spectra are shown in Fig. 2a-d for peak energies of 21.8 (a), 46.5 (b), 94.7 (c), and 142.7 MeV (d). The peak energies are chosen in compliance with recommendations of the JESD89 standard [3]. In all the cases, the spectrum is dominated by a peak situated a few MeV below the energy of the primary protons and comprising about 40% of the total number of neutrons. Neutron spectra have been obtained by measuring elastic *np*-scattering with the Medley setup [17]. More details about the method of the neutron spectrum measurements may be found in Ref. [18].

Fig. 2 includes a comparison of the measurements with the systematics by Prokofiev *et al.* [19] for the three higher energies (Fig. 2b-d). The systematics is not applicable at the lowest beam energy (Fig. 2a). Instead, an evaluation of Mashnik *et al*. [20] was employed for the description of the neutron spectrum. The differential cross-section for high-energy peak neutron production at 0° was obtained by multiplication of the total cross-section of the ^{7}Li(p,n)^{7}Be reaction [20] with the "index of forwardness" from the systematics of Uwamino *et al*. [21]. The experimental data agree with the calculations except for the low-energy tail region in the 21.8-MeV spectrum where the model overpredicts the yield of neutrons with energies above 5 MeV by about 40%.

The presence of the low-energy “tail” in the neutron spectra makes it necessary to introduce a correction to measured SEE rates. The correction method, based on an unfolding procedure, is described, e.g., in Ref. [9].

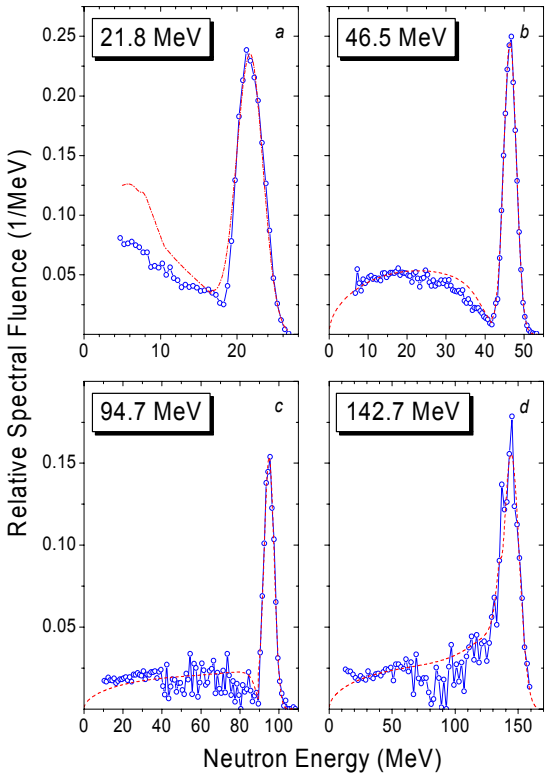

Fig. 2. The neutron spectra at 0º for different peak neutron energies (see Table I for incident proton energies and ^{7}Li target thicknesses). Symbols connected by a solid line represent experimental data obtained in the present work. Predictions are shown as dashed lines (see text).

Table I summarizes the main features of the measured spectra and the achieved neutron flux. The latter is measured with a monitor based on a thin-film breakdown counter (TFBC) [22]. Another monitoring option is provided by an ionization chamber. Both monitors utilize neutron-induced fission of ^{238}U with the well-known cross-section adopted as neutron flux standard [23]. In addition, the neutron flux is indirectly monitored by a Faraday cup, which integrates the current of protons collected at the beam dump.

The measured contamination of the neutron beam at the user area due to interactions of the primary protons with beam transport elements, e.g., the target frame, did not exceed 0.2%. Such interactions lead to a minor surplus of neutrons in the user area, because charged particles produced near the lithium target and upstream are removed by the deflection magnet. The relative contamination of protons with energies above 15 MeV in the neutron beam is about 10^{-5} for a proton beam energy of 98 MeV.

Figure 3 shows a horizontal beam profile for 142.7-MeV neutrons, measured at a distance of 4.77 m from the lithium target. The measurement was performed by counting neutron-induced SEE in a set of memory chips positioned across the beam [24].

TABLE I
NEUTRON BEAM PARAMETERS

Proton beam energy (MeV)	^{7}Li target thick-ness (mm)	Proton beam current (μA)	Result-ing average energy of peak neutrons (MeV)	Fraction of neutrons in the mono-energetic peak (%)		Peak neutron flux (10^{5} cm^{-2} s^{-1})
				Meas-ured	Calc-ulated	
24.68 ± 0.04	2	10	21.8	~50	--	1.3
49.5 ± 0.2	4	10	46.5	39	36	2.9
97.9 ± 0.3	8	5	94.7	41	39	4.6
147.4 ± 0.6	24	0.6	142.7	55[b)]	40	2.1

[a]The fluxes refer to the entrance of the beam line to the user area.
[b]Upper limit due to poor energy resolution.

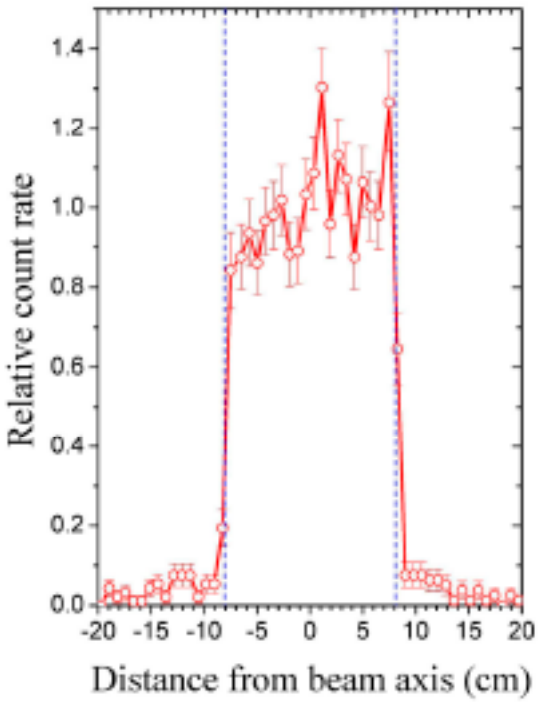

Fig. 1. The horizontal beam profile for 142.7-MeV neutrons, measured at the distance of 4.77 m from the lithium target. Vertical dashed lines represent boundaries of the beam expected from the geometry of the collimator.

IV. CONCLUSIONS AND OUTLOOK

A new neutron beam facility has been constructed at TSL and has put into regular operation for commercial electronics testing. The facility is capable to deliver neutrons in the 20-175 MeV range. Work is in progress for development of neutron fields with energies lower than 20 MeV.

ACKNOWLEDGMENT

We would like to thank all the staff at The Svedberg Laboratory for the excellent work in building this new facility. We are thankful to M. Olmos for providing us with the beam profile data.

REFERENCES

[1] J.F. Ziegler, IBM J. Res. Develop. 40, 19 (1996).
[2] Mater. Res. Soc. Bull. 28 (2003).
[3] JEDEC Standard: Measurements and Reporting of Alpha Particles and Terrestrial Cosmic Ray-Induced Soft Errors in Semiconductor Devices. JESD89, August 2001.
[4] P.W. Lisowski *et al.,* Nucl. Sci. Eng. 106, 208 (1990).
[5] E.W. Blackmore *et al.,* Improved Capabilities for Proton and Neutron Irradiation at TRIUMF, NSREC'2003, Monterey, IEEE Radiation Effects Data Workshop, p. 149, 2003.
[6] C. Borcea *et al.,* J. Nucl. Sci. Tech., Suppl. 2, p. 653 (2002).
[7] N.K. Abrosimov *et al.,* Nucl. Instr. Meth. **A** 242, 121 (1985).
[8] Y. Yahagi *et al.,* Proc. 42nd Annual IEEE International Reliability Physics Symposium, 25-29 April 2004, Phoenix, AZ, p. 669.
[9] M. Olmos *et al.,* Unfolding Procedure for SER Measurements Using Quasi-Monoenergetic Neutrons, Accepted for presentation at International Reliability Physics Symposium (IRPS'2005), San Jose, California, April 17-21, 2005, paper SE03.
[10] H. Schuhmacher *et al.,* Nucl. Instrum. Meth. Phys. Res. A 421*,* 284 (1999).
[11] R. Nolte *et al.,* Nucl. Instrum. Meth. Phys. Res. A 476, 369 (2002).
[12] F.P. Brady, Can. J. Phys. 65, 578 (1987).
[13] M. Baba *et al.,* Nucl. Instrum. Meth. Phys. Res. A 428, 454 (1999).
[14] N. Nakao *et al.,* Nucl. Instrum. Meth. Phys. Res. A 420, 218 (1999).
[15] H. Condé *et al*., Nucl. Instrum. Meth. Phys. Res. A 292, 121 (1990).
[16] J. Klug *et al.*, Nucl. Instrum. Meth. Phys. Res. A 489, 282 (2002).
[17] S. Dangtip *et al*., Nucl. Instrum. Meth. Phys. Res. A 452, 484 (2000).
[18] S. Pomp *et al*., AIP Conf. Proc. 769, 780-783 (2005).
[19] A.V. Prokofiev *et al*., J. Nucl. Sci. Techn., Suppl. 2, 112 (2002).
[20] S.G. Mashnik *et al*., LANL Report LA-UR-00-1067 (2000).
[21] Y. Uwamino *et al*., Nucl. Instrum. Meth. Phys. Res. A 389, 463 (1997).
[22] A.N. Smirnov *et al*., Radiat. Meas. 25, 151 (1995).
[23] A.D. Carlson *et al*., Proc. Int. Conf. on Nuclear Data for Science and Technology, Trieste, Italy, May 19-24, 1997, Part II, p. 1223.
[24] M. Olmos, priv. comm.

REFERENCE CROSS SECTIONS RELEVANT FOR NEUTRON DETECTORS

J. Blomgren*
Department of Neutron Research
Uppsala University
Box 525, S-751 20 Uppsala, Sweden
E-mail: Jan.Blomgren@tsl.uu.se

Neutron detection inevitably proceeds via nuclear reactions, making nuclear cross section data of major importance in the determination of neutron detector properties in general, and efficiency determination in particular. Up to about 20 MeV, the cross section data base is fairly advanced, and the codes for, e.g., determination of scintillator properties produce results with uncertainties on the level of a few percent. Above 20 MeV, the scarcity of nuclear data results in much larger uncertanties in model calculations of detector performances.

The data base above 20 MeV is meagre, but this is not the only problem. It also contains severe discrepancies for the most important cross sections. In this energy domain, the neutron-proton (*np*) scattering cross section is used as primary standard. The *np* scattering database contains discrepancies up to about 10 %. Since essentially all other cross sections are measured relative to *np* scattering, this means that most data have similar uncertainties. In the talk, the present status of reference cross sections in general and *np* scattering in particular is outlined, and recent experiments to elucidate the problems are presented. Moreover, the data situation concerning fast-neutron fission as reference is discussed.

International Workshop on Fast Neutron Detectors and Applications
April, 3 - 6, 2006
University of Cape Town, South Africa

*Speaker.

1. Introduction

To measure a cross section, the intensity of the beam has to be known. For charged beams, this is a straight-forward affair, but to determine a neutron beam intensity is actually very difficult.

A charged particle interacts with the electrons of the atom. Thereby it is possible to build systems where every particle gives a signal when passing through a detector, and hence it is a relatively simple task to determine the beam intensity by just counting pulses. Another option is to stop particles via their energy loss - which is also an effect of interaction with the atomic electrons - and finally measure the collected charge.

Neutrons interact by the strong interaction only, and they are uncharged. This means that there is no way you can build a device which produces a signal for each particle that passes, and you cannot stop neutrons in a controlled way. Detection of neutrons always has to proceed via a nuclear reaction, releasing charged particles, which can subsequently be detected. The problem is that there is no way to determine a nuclear cross section from theory only with a reasonable precision. This means we end up in circular reasoning.

Let us assume we want to use neutron-proton (np) scattering for neutron detection. Counting the protons emanating from a hydrogenous material is a simple task, but we need to know the cross section to derive the number of incoming neutrons. To measure that cross section, however, we need to know the number of incident neutrons. Are there no ways out of this vicious circle?

In fact, there are a few tricks which can be used, but they are all associated with large difficulties. The standard procedure is therefore to determine a single cross section using all these painstaking methods, and subsequently this cross section is used as reference, i.e., other cross section measurements are measured relative to it. The only three techniques available are presented below:

1. *Tagged beams.* The methodologically simplest method is probably to use tagged beams, but this does not necessarily mean it is the simplest technique in real life. For a few reactions, detection of the residual nucleus can be used to verify the neutron production. An example is the D(d,n)^{3}He reaction. By detecting the kinetic energy and direction of the residual ^{3}He nucleus, the energy and angle of the neutron is known. In addition, the detection of a ^{3}He nucleus implies that there must be a neutron, i.e., the ^{3}He nucleus serves as a "tag" on the neutron. With this technique, "beams" of really low - but well-known - intensity can be produced. This beam can subsequently be used for cross section measurements.

2. *Combination of total and differential hydrogen cross sections.* The total cross section, i.e., the probability that a neutron interacts at all with a target nucleus, is a quantity that can be determined without knowledge of the absolute beam intensity. This integral cross section is related to the attenuation of a neutron beam, which means that a relative measurement of the beam intensity before and after a target is sufficient.

   In the case of hydrogen, the total cross section is completely dominated by elastic np scattering, which accounts for more than 99 % of the total cross section. A relative measurement of the np scattering angular distribution can thereby be normalized to agree with the total np cross section, and thus an absolute np differential cross section can be obtained.

3. *Combination of total, reaction and differential elastic cross sections.* The differential elastic cross section of a nucleus can be determined absolutely by a combination of total and reaction cross section measurements, together with a relative measurement of the differential elastic cross section. Both the total cross section and the reaction cross section can be determined in relative measurements of beam attenuation. The only important difference is the geometry used. The integrated elastic cross section can then be derived as the difference of the total and reaction cross sections. The elastic differential cross section on almost any nucleus falls dramatically with angle. Thus, by covering a moderately wide range at forward angles, essentially all the elastic differential cross section is covered. Thereby, the differential cross section can be related to the integrated elastic cross section.

The primary standard reference cross section for fast neutrons is *np* scattering. Instead of trying to measure a certain cross section on an absolute scale, a typical experiment would be designed to measure the *ratio* of that cross section versus *np* scattering. This facilitates the experimental work immensely.

Although proton recoil detection from *np* scattering is the most commonly used normalization technique, not all reactions are well suited to be measured against *np* scattering. Therefore, secondary standards have been proposed. This is particularily true for fission studies, for which ^{209}Bi, ^{235}U and ^{238}U have been used. Fission is very useful for beam intensity monitoring, because the products to detect, the fission fragments, can hardly be created due to any type of background, and they are easily separated from other types of products created in the target, like α particles.

A major risk with relative measurements is that if the reference cross section is incorrect, all other data measured relative to it will be equally off. It turns out that for neutrons above 50 MeV, there have been quite some problems with both the primary and the secondary standards lately.

2. Neutron-proton scattering

The *np* scattering cross section - in particular at 180° (c.m.), which corresponds to proton emission at 0° in the lab - is frequently used to normalize measurements of other neutron-induced cross sections, i.e., it is the primary standard cross section. In addition, it plays an important role in fundamental physics, because it can be used to derive a value of the absolute strength of the strong interaction in the nuclear sector, commonly expressed as the pion-nucleon coupling constant, $g^2_{\pi NN}$ (see Ref. [1] for a review). Large uncertainties for such an important cross section are therefore unacceptable.

Unfortunately, there are severe discrepancies in the data base on *np* scattering in the 100–1000 MeV range [2], and uncertainties of 10 % or more are common. These discrepancies concern both the shape of the angular distributions and the absolute normalization, and in fact there is no combination of two major experiments that agree. The experimental data discussed in the present paper are representative to the situation, but there are many more data sets available.

The *np* scattering data base was until recently dominated by the Bonner et al. data ($160-800$ MeV) from Los Alamos [3] and essentially all evaluations and theory work in the field were fitted to those results. Recently, the results of two high-precision experiments, at TSL Uppsala at 96 MeV [4] and 162 MeV [5], and at PSI [6] ($200-580$ MeV), have been published. The Uppsala

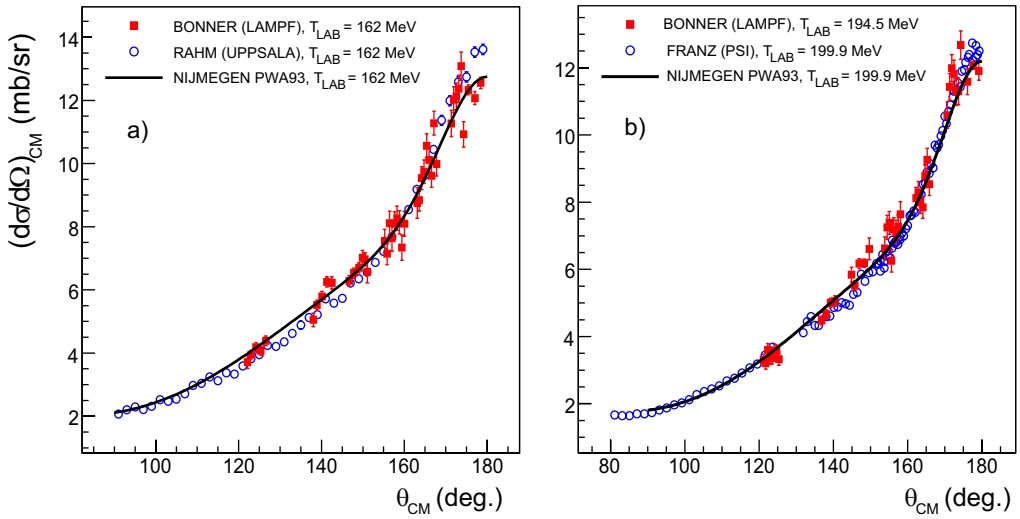

Figure 1: Comparison of *np* scattering differential cross section measurements (left panel) from Uppsala [4] and Los Alamos [3], and (right) from PSI [6] and Los Alamos near 200 MeV. The Los Alamos data are in each case represented by closed squares and the other data by open circles. The experimental results are compared to the Nijmegen PWA93 [9] partial wave analysis solution. The Los Alamos data have been renormalized by factors of 1.092 (left) and 1.078 (right) to bring them into agreement with the PWA. The PSI cross sections have been similarly normalized here, while the reported absolute cross section scale for the Uppsala data has been retained.

and PSI experiments agree in shape (which is a rather weak function of beam energy), but not in absolute magnitude, and both show a steeper angular distribution at backward angles than the Bonner data. The different absolute scale can, however, be attributed to different normalization methods. If the same normalization procedure is applied to the two sets, they are in agreement. Thus, there is a problem of inconsistencies in magnitude as well as in shape at the most backward angles (see fig. 1).

All the experiments above were performed using magnetic spectrometers for proton recoil detection and a neutron beam of unknown intensity, i.e., all data sets have been normalized after the experiment. The Uppsala data were normalized to the total cross section, while the other two experiments were normalized to a pion-production reaction. The latter method can only be used above 275 MeV (the pion production threshold) and it depends on several corrections of unknown precision.

Recently, the entire problem has been addressed at IUCF with a novel technique [7, 8]. Tagged neutrons have been produced at 194 MeV using the D(p,n)^{2}He reaction, where ^{2}He denotes two protons in a $^1S_0$ state, i.e., by detecting two correlated low-energy protons, the energy and direction of the outgoing neutron was identified event-by-event. Proton recoils from these tagged neutrons impinging on a scintillator target were detected in a large scintillator array equipped with wire chamber tracking.

The results are shown in fig. 2. The new tagged IUCF data ("present experiment" in the figure) agree well with a PWA fitted to the shape (but not magnitude) of the Bonner data. If believing

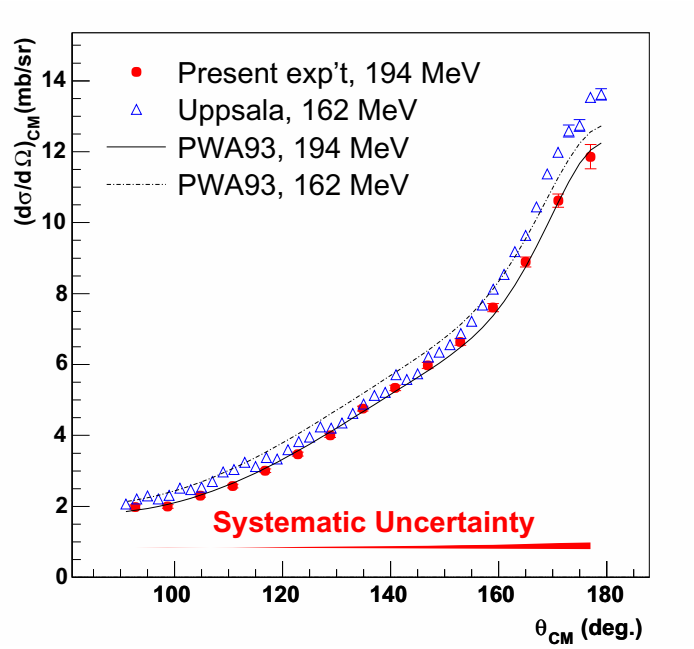

Figure 2: Absolute differential cross section from the IUCF experiment at 194 MeV [7, 8], compared with data from TSL Uppsala [5] and with PWA calculations [9] at two relevant energies. The figure is taken from ref. [8], i.e., "present experiment" refers to ref. [8]. The error bars on the present results are statistical (including background subtraction), while the shaded band represents all systematic uncertainties, including those in the overall normalization.

the new tagged data (and my personal opinion is that they are probably the best data available), it can be conluded that the normalization technique used by the TSL Uppsala group is in good agreement with the new IUCF data. As mentioned previously, the Los Alamos and PSI data need significant renormalization to agree with the PWA that describes the IUCF data well (see fig. 1). Thus, normalization to the total *np* cross section seems to be a better technique than using pion production as reference.

The shape of the angular distribution, however, is in better agreement with the Bonner data than the Uppsala and PSI experiments. To clear up this controversy once for all, it would be valuable to find an explanation why two recent experiments (Uppsala and PSI) agree internally in shape with a steeper angular distribution, but only at the most backward angles. For almost all the angular range, all the experiments agree in shape. Moreover, producing a too steep angular distribution is not straight-forward; most experimental problems tend to reduce steepness. It is proposed in a forthcoming IUCF publication [8] that this could be due to either not taking the neutron beam divergence properly into account or to a mismatch of the proton recoil solid angles near zero degrees in the laboratory system. Investigations of this effect for the Uppsala data are underway.

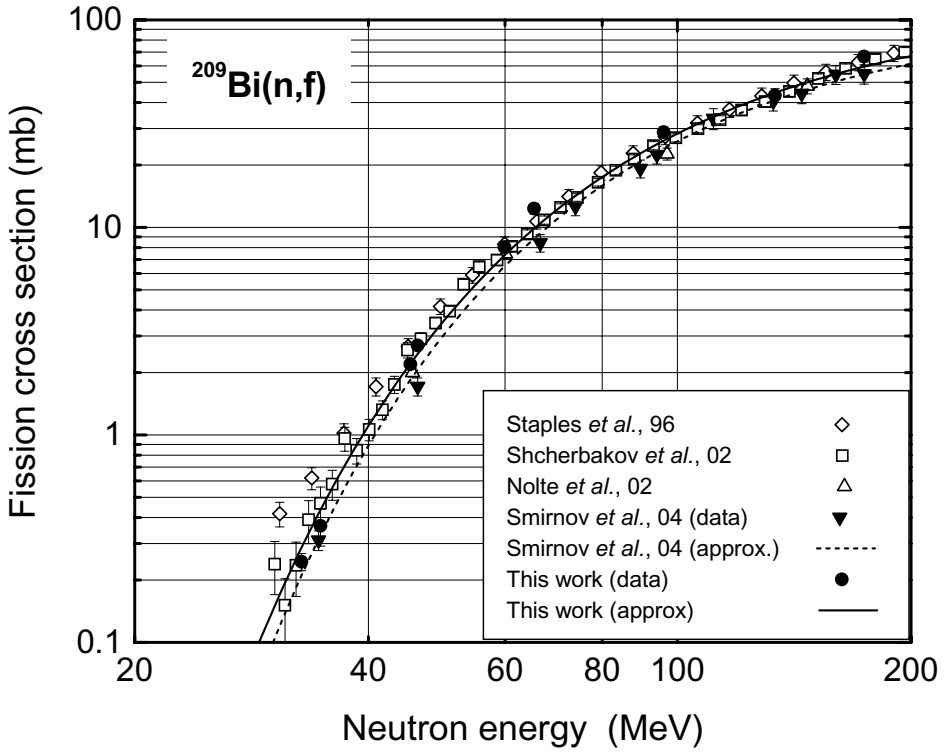

Figure 3: Measured neutron-induced fission cross sections of ^{209}Bi [13, 14, 15, 16, 17]. The figure is taken from ref. [13], i.e., "present experiment" refers to ref. [13]. The data from Refs. [16, 17] are given with regard to the recommended standard uncertainties [10]. The solid and dashed lines show the cross section parameterizations of Ryzhov et al. [13] and of Smirnov et al. [14], resp.

3. Fission

When it comes to fission cross section data, not much is available above 20 MeV. As described above, fission chambers are frequently used for beam monitoring. As long as relative monitoring is the only ambition, precise knowledge of the cross section is not very important. General technical reliability is more important. One critical issue, however, is the presence of thermal neutrons. The thermal neutron content in a fast-neutron beam is often unknown, and so is the ambient thermal background. Moreover, this thermal background is often not stable, and therefore fissile nuclides are preferentially not used for fast-neutron monitoring. Thus, ^{238}U is more often used than ^{235}U.

The readily available nuclides ^{232}Th and ^{238}U both have fission thresholds of about 1 MeV. The next lighter elements that are available for realistic applications are lead and bismuth, the heaviest stable elements, which have effective fission thresholds of about $20-30$ MeV. In between bismuth and thorium, all elements have rather short halflives and are therefore difficult to handle and hard to obtain in useful quantities. This limits the practical possibilities to detectors with thresholds either in the 1 or 20 MeV range.

For applications of very fast neutrons, above 20 MeV, it is often of interest to have a high threshold to reduce the influence of neutrons below 20 MeV. For such applications, the ^{209}Bi(n,f) cross section has been recommended as a secondary neutron cross section standard [10]. Bismuth-based neutron fluence monitors, being insensitive to low-energy (< 25 MeV) neutrons, are used in experiments where the low-energy neutron background is difficult to determine [11, 12].

Meanwhile, the present uncertainty of the ^{209}Bi(n,f) standard is rather large (see fig. 3), so further improvement of the standard is necessary. In a recent paper, Ryzhov et al. [13] presents a parametrization to the existing data. A similar parametrization has previously been proposed by Smirnov et al. [14]. These two parameterization differ by about $10-15$ % in the $50-150$ MeV range. It is notable, however, that the shapes of the two resulting functions are in fair agreement. To some extent it can be a normalization effect. It should be noted that different normalization techniques have been used for the various experiments in the data base. The data of Ryzhov et al. [13] and of Smirnov et al. [14] were normalized to the ^{238}U(n,f) cross section standard, while Nolte et al. [15] normalized to *np* scattering (except one point at 97 MeV) and Shcherbakov et al. [16] to the ^{235}U(n,f) cross section.

It should be pointed out that the experiments normalized to ^{235}U and ^{238}U are implicitly normalized to something else, because these cross sections cannot be determined absolutely. Some of the high-energy fission data on uranium isotopes are normalized using *np* scattering as reference, but some data have used other methods, sometimes of unknown quality. I have chosen to use the data situation for lead and bismuth as an illustration, but the data quality is similar for uranium. Also there, 10 % uncertainties are common.

Thus, work to establish accurate cross section standards is highly motivated. For instance, at TSL Uppsala a project is underway in which the ^{238}U(n,f) cross section will be measured relative to *np* scattering using the same detectors and target (two layers, ^{238}U with a CH_2 backing) for simultaneous detection of proton recoils and fission fragments. With such a technique, some of the systematic uncertainties of previous experiments cancel.

4. Conclusions

Both the primary and the secondary standards have large uncertainties. Up to now, it has been reasonable to ascribe $5-10$ % uncertainty to the *np* scattering cross section and $10-15$ % to the best-known fission cross sections. There are hopes that the situation for *np* scattering can be improved upon. A recent experiment has shed new light on the problem. If follow-up investigations can elucidate the origin of previous discrepancies in the data base, it might be possible to arrive at a 3 % uncertainty in *np* scattering. This could in turn allow fission cross sections to be determined to about 5 % uncertainty. New high-precision experiments are most welcome to allow us to reach this goal.

Acknowledgments

This work was financially supported by the Swedish Nuclear Fuel and Waste Management Company, the Swedish Nuclear Power Inspectorate, Ringhals AB, Forsmarks Kraftgrupp AB, the Swedish Defense Research Agency, the Swedish Nuclear Safety and Training Centre, and the European Union.

References

[1] Proceedings of Workshop on "Critical Points in the Determination of the Pion-Nucleon Coupling Constant", Uppsala, June 7-8, 1999, ed. J. Blomgren. Phys. Scr. **T87** (2000).

[2] J. Blomgren, N. Olsson, J. Rahm, Phys. Scr. **T87**, 33 (2000).

[3] B.E. Bonner, J.E. Simmons, C.L. Hollas, C.R. Newsom, P.J. Riley, G. Glass, Mahavir Jain, Phys. Rev. Lett. **41**, 1200 (1978).

[4] J. Rahm, J. Blomgren, H. Condé, S. Dangtip, K. Elmgren, N. Olsson, T. Rönnqvist, R. Zorro, O. Jonsson, L. Nilsson, P.-U. Renberg, A. Ringbom, G. Tibell, S.Y. van der Werf, T.E.O. Ericson, B. Loiseau, Phys. Rev. **C63**, 044001 (2001).

[5] J. Rahm, J. Blomgren, H. Condé, S. Dangtip, K. Elmgren, N. Olsson, T. Rönnqvist, R. Zorro, A. Ringbom, G. Tibell, O. Jonsson, L. Nilsson, P.-U. Renberg, T.E.O. Ericson, B. Loiseau, Phys. Rev. **C57**, 1077 (1998).

[6] J. Franz, E. Rössle, H. Schmitt, L. Schmitt, Phys. Scr. **T87**, 14 (2000).

[7] M. Sarsour, T. Peterson, M. Planinic, S.E. Vigdor, C. Allgower, B. Bergenwall, J. Blomgren, T. Hossbach, W.W. Jacobs, C. Johansson, J. Klug, A.V. Klyachko, P. Nadel-Turonski, L. Nilsson, N. Olsson, S. Pomp, J. Rapaport, T. Rinckel, E.J. Stephenson, U. Tippawan, S.W. Wissink, Y. Zhou, Phys. Rev. Lett. **94** (2005) 082303.

[8] M. Sarsour, T. Peterson, M. Planinic, S.E. Vigdor, C. Allgower, B. Bergenwall, J. Blomgren, T. Hossbach, W.W. Jacobs, C. Johansson, J. Klug, A.V. Klyachko, P. Nadel-Turonski, L. Nilsson, N. Olsson, S. Pomp, J. Rapaport, T. Rinckel, E.J. Stephenson, U. Tippawan, S.W. Wissink, Y. Zhou, Measurement of the Absolute Differential Cross Section for np Elastic Scattering at 194 MeV, submitted to Phys. Rev. C.

[9] V.G.J. Stoks, R.A.M. Klomp, M.C.M. Rentmeester, and J.J. de Swart, Phys. Rev. C **48**, 792 (1993).

[10] A.D. Carlson, S. Chiba, F.-J. Hambsch, N. Olsson, and A.N. Smirnov, IAEA Report INDC (NDC)-368, Vienna, 1997; Proc. Int. Conf. on Nuclear Data for Science and Technology, Trieste, Italy, 1997, Part II, p.1223.

[11] W. Glasser, R. Michel, S. Neumann, H. Schuhmacher, V. Dangendorf, R. Nolte, U. Herpers, A.N. Smirnov, I.V. Ryzhov, A.V. Prokofiev, P. Malmborg, D. Kollár, J.P. Meulders, J. Nucl. Sci. Tech. Suppl. 2, vol. 1 (2002) 373.

[12] R. Michel, W. Glasser, U. Herpers, H. Schuhmacher, H.J. Brede, V. Dangendorf, R. Nolte, P. Malmborg, A.V. Prokofiev, A.N. Smirnov, I.V. Ryzhov, J.P. Meulders, M. Duijvestijn, and A. Koning, Proc. Int. Conf. on Nuclear Data for Science and Technology, Santa Fé, NM, USA, 2004, AIP Conf. Proc. **769** (2005) 861.

[13] I.V. Ryzhov, G.A. Tutin, A.G. Mitryukhin, S.M. Soloviev, J. Blomgren, P.-U. Renberg, J.-P. Meulders, Y. El Masri, Th. Keutgen, R. Preels, R. Nolte, Measurement of neutron-induced fission cross sections of ^{205}Tl, ^{204,206,207,207}Pb and ^{209}Bi with a multi-section Frisch-gridded ionization chamber, accepted for publication in Nucl. Instr. Meth. A.

[14] A.N. Smirnov, V.P. Eismont, N.P. Filatov, J. Blomgren, H. Condé, A.V. Prokofiev, P.U. Renberg, and N. Olsson, Phys. Rev. C70 (2004) 054603.

[15] R. Nolte, M.S. Allie, P.J. Binns, F.D. Brooks, A. Buffler, V. Dangendorf, K. Langen, J.P. Meulders, W.D. Newhauser, F. Ross, and H. Schuhmacher, J. Nucl. Sci. Tech. Suppl. 2, vol. 1 (2002) 311.

[16] O. Shcherbakov, A. Donets, A. Evdokimov, A. Fomichev, T. Fukahori, A. Hasegawa, A. Laptev, V. Maslov, G. Petrov, S. Soloviev, Y. Tuboltsev, and A. Vorobyev, J. Nucl. Sci. Tech. Suppl. 2, vol. 1 (2002) 230.

[17] P. Staples, P. W. Lisowski, and N. W. Hill, Bull. Am. Phys. Soc. **40** (1995) 962; P. Staples, private communication (1996).

SCANDAL - A FACILITY FOR ELASTIC NEUTRON SCATTERING STUDIES IN THE 50–130 MeV RANGE

J. Blomgren[*1], **J. Klug**[1,5], **P. Mermod**[1], **L. Nilsson**[1], **S. Pomp**[1], **A. Öhrn**[1], **Michael Österlund**[1], **A.V. Prokofiev**[2], **U. Tippawan**[1,3], **J.F. Lecolley**[4], **F.R. Lecolley**[4], **N. Marie-Noury**[4], **I. Sagrado-Garcia**[4], **G. Ban**[4], **G. Iltiss**[4], **J.-M. Fontbonne**[4]

[1] *Department of Neutron Research, Uppsala University, Sweden*
[2] *The Svedberg Laboratory, Uppsala University, Sweden*
[3] *Fast Neutron Research Facility, Chiang Mai University, Thailand*
[4] *LPC, ISMRA et Université de Caen, CNRS/IN2P3, France*
[5] *Forschungszentrum Rossendorf, Dresden, Germany*
E-mail: Jan.Blomgren@tsl.uu.se

A facility for detection of scattered neutrons in the energy interval 50 − 130 MeV, SCANDAL (SCAttered Nucleon Detection AssembLy), is part of the standard detection system at the 20-180 MeV neutron beam facility of the The Svedberg Laboratory, Uppsala. It has primarily been used for studies of elastic neutron scattering, but it has been employed for (n,p) and (n,d) reaction experiments as well. Results of recent experiments are presented to illustrate the performance of the spectrometer.

Recently, the facility has been upgraded to perform also (n,Xn') experiments. For this purpose, a new converter, CLODIA, has been developed and installed. Preliminary results of the commissioning of CLODIA will be presented.

International Workshop on Fast Neutron Detectors and Applications
April, 3 - 6, 2006
University of Cape Town, South Africa

[*] Speaker.

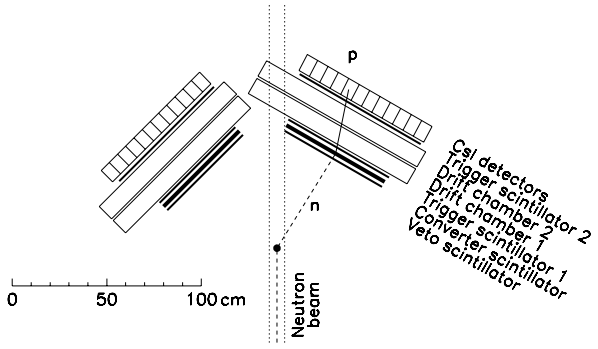

Figure 1: Overview of the SCANDAL setup.

1. Introduction

The development of new large-scale applications involving fast neutrons motivates nuclear data research. This applies to transmutation of spent nuclear fuel [1, 2, 3], neutron therapy of cancer tumours [4] and upsets in electronics [5, 6].

The SCANDAL (SCAttered Nucleon Detection AssembLy) setup [7] at The Svedberg Laboratory has been developed to meet some of these demands. The device has been designed for neutron elastic scattering experiments in the 50 − 130 MeV range, but can be used also for charged-particle detection in the same energy interval. In the present paper, the focus is on the device. Thus, examples of the performance in various experiments are presented, while the physics results are presented elsewhere.

The neutron beam facility and the SCANDAL setup at The Svedberg Laboratory, Uppsala, Sweden, have recently been described in detail [7], and therefore only a brief description is given here. Neutrons are produced by the ^{7}Li(p,n) reaction. The low-energy tail of the source-neutron spectrum is suppressed by time-of-flight techniques. After the target, the proton beam is bent into a well-shielded beam dump. A system of three collimators defines a 9 cm diameter neutron beam at the scattering target.

SCANDAL consists of two identical systems (see fig. 1). When used for neutron detection, they are normally placed to cover 10 − 50° and 30 − 70°, respectively. The energy of the scattered neutrons is determined by measuring the energy of proton recoils from a plastic scintillator, and the angle is determined by tracking the recoil proton. Each arm consists of a 2 mm thick veto scintillator for fast charged-particle rejection, a 10 mm thick neutron-to-proton converter scintillator, a 2 mm thick plastic scintillator for triggering, two drift chambers for proton tracking, a 2 mm thick ΔE plastic scintillator that is also part of the trigger, and an array of CsI detectors for energy determination of recoil protons produced in the converter by *np* scattering. The trigger is provided by a coincidence of the two trigger scintillators, vetoed by the front scintillator. The total excitation energy resolution varies with CsI crystal, but is on average 3.7 MeV (FWHM). The angular resolution is in the 1.0 − 1.3° (rms) range.

When used for charged particle detection, the veto and converter scintillators are removed and a multi-target system is used to increase the count rate without deteriorating the energy resolution.

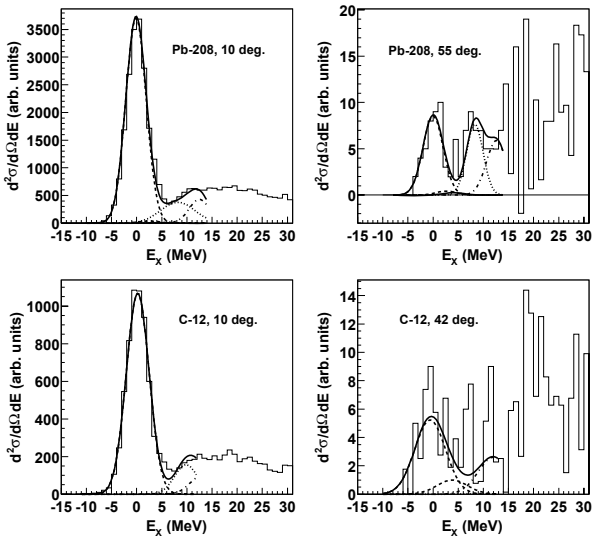

Figure 2: Excitation energy spectra for elastic neutron scattering from ^{12}C and ^{208}Pb at 96 MeV incident neutron energy, together with Gaussians representing known excited states.

2. Elastic neutron scattering

The main use of SCANDAL up to now has been elastic neutron scattering studies at 96 MeV. Examples of spectra on ^{12}C and ^{208}Pb [8] are presented in fig. 2. As can be seen, the ground states are resolved. It is also evident that the cross section drops rapidly with angle. At the largest angles, around 70°, about one count per run week is obtained.

3. (n,p) studies

For transmutation applications, data on neutron-induced light-ion reactions are of importance, especially for assessment of materials damage in future accelerator-driven systems (ADS). Therefore, studies of (n,xlcp), where lcp denotes light charged particles, have been performed at 96 MeV on iron, lead and uranium [9].

The MEDLEY facility [11] has been designed for such studies (see the contribution by Pomp et al.), but SCANDAL can be used to obtain additional information. The MEDLEY system operates in vacuum, which allows measurements of particle emission down to very low energies, and all light ions can be detected. SCANDAL operates in air, with the consequence that there is a 30 MeV low-energy threshold for protons, and helium isotopes can hardly be detected at all. Nevertheless, the very large acceptance of SCANDAL makes it interesting for part of the emission spectrum. At backward angles, the high-energy proton emission is very weak, and in those regions SCANDAL can provide added value. An example is given in fig. 3.

4. Neutron-deuteron scattering

Neutron-deuteron scattering at intermediate energies has recently been identified as a good

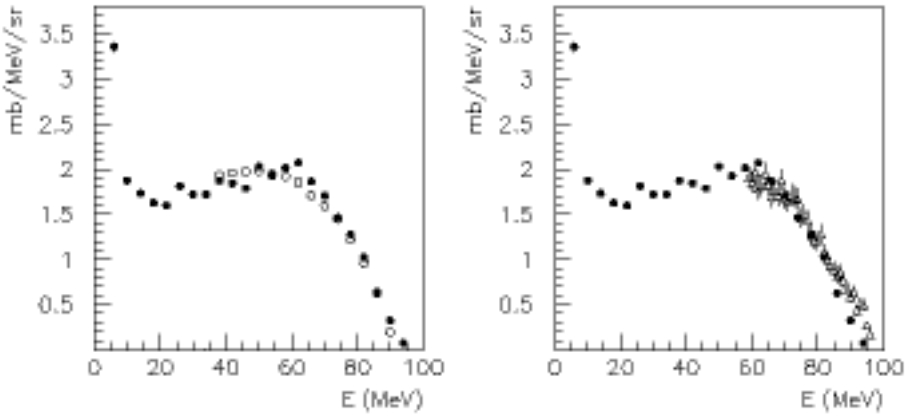

Figure 3: Left panel: Fe(n,Xp) double-differential cross sections measured with the MEDLEY setup at 20 ° (full circles), compared to the SCANDAL results (open circles). Right panel: The same data compared to those from Ref. [10] (open triangles).

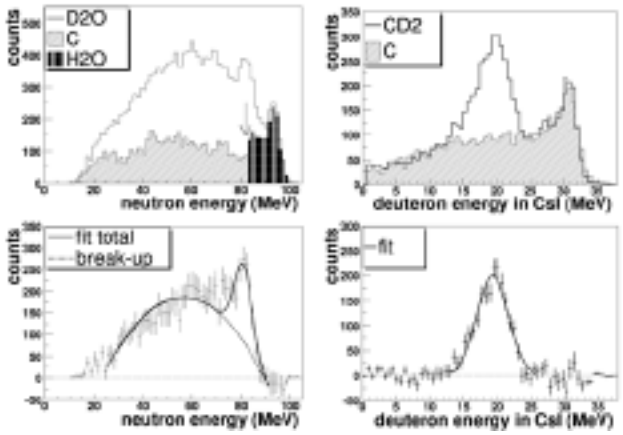

Figure 4: Typical energy spectra in *nd* scattering experiments, showing neutrons detected at 30° (left panels) and deuterons detected at 32° (right panels). The bottom left panel shows the *nd* spectrum after subtraction of the oxygen content in D_2O. The bottom right panel shows the nd elastic peak after subtraction of the carbon content in CD_2. The error bars in the bottom panels are due to statistics.

case for studies of three-body effects in nuclei [12]. The full *nd* angular distribution has been covered by two separate SCANDAL experiments. Forward angles have been studied by neutron detection, using heavy water targets for the signal, and light water targets for background. In addition, graphite targets were used for normalization. Backward angles were studied by deuteron detection, using CD_2 discs for signal, pure graphite targets for background subtraction and CH_2 targets for normalization.

Examples of spectra are presented in fig. 4. The final results show clear evidence of three-nucleon force effects [13, 14]. Data obtained with the MEDLEY setup [15] are in agreement with the SCANDAL results.

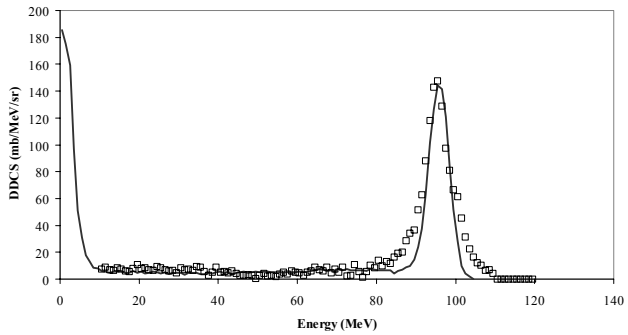

Figure 5: Preliminary results on Pb(n,Xn') at 95 MeV energy and 15° , shown with an MCNPX prediction (black line).

5. Inelastic neutron emission

Like neutron-induced light ion emission, inelastic neutron emission is of large importance in the assessment of materials damage in future ADS applications. Only one high-quality neutron-induced data set exists above 30 MeV, a measurement at 65 MeV of Fe, Sn and Pb(n,Xn') continuum cross sections at forward angles, however not beyond 30° and with a 15 MeV threshold [16].

The (n,Xn') setup is composed of two separated devices, the DECOI/DEMON scintillators at low neutron energies (10 − 50 MeV) and SCANDAL/CLODIA at high energies (40 − 100 MeV), the latter being similar to the 65 MeV system above. Low-energy neutrons interact with the hydrogen nuclei of the plastic scintillator DECOI, and scattered neutrons are then detected in the DEMON cell. Neutron identification is achieved via pulse-shape analysis [17], while the energy is derived from the time-of-flight of the scattered neutron between DECOI and DEMON. The upper threshold of 50 MeV is a consequence of the path-flight (100 cm) while the lower one is mainly due to the low energy (about 50 keV) of the recoiling proton detected in DECOI.

High-energy neutrons are detected by H(n,p) conversion in the CLODIA multi-layer converter, and the recoil protons are detected with SCANDAL. Neutron identification is achieved via rejection of incident charged particles using information from the veto scintillator and the first CLODIA drift chamber. The energy is derived from the tracking of the recoiling proton by several plastic scintillators and drift chambers, and the residual energy of those protons is measured in the SCANDAL CsI detectors. The low energy threshold of 40 MeV is due to recoiling proton energy losses in the several planes of the set-up before they reach the CsIs.

Preliminary results are presented in fig. 5. Error bars are not yet available. Nevertheless, the good agreement in the energy region where the two devices overlap can be consider as a test of the whole procedure. Moreover, the elastic cross-section Pb(n,n) derived from our preliminary results is in good agreement with a previous measurement perform at Uppsala [8]. In addition, MCNPX calculations using evaluated cross-sections calculated by GNASH for incident neutrons of 95 MeV with a Gaussian distribution ($\Delta E = 1.5$ MeV) reproduce the preliminary results.

Acknowledgments

This work was financially supported by the Swedish Nuclear Fuel and Waste Management Company, the Swedish Nuclear Power Inspectorate, Ringhals AB, Forsmarks Kraftgrupp AB, the Swedish Defense Research Agency, the Swedish Nuclear Safety and Training Centre, and the European Union.

References

[1] A. Koning, et al., J. Nucl. Sci. Tech., Suppl. **2** (2002) 1161.

[2] J. Blomgren, in Proceedings of Workshop on Nuclear Data for Science & Technology: Accelerator Driven Waste Incineration, Trieste, Italy, Sept. 10-21, 2001, eds. M. Herman, N. Paver, A. Stanculescu, ICTP lecture notes **12** (2002) 327.

[3] J. Blomgren, Nuclear data for accelerator-driven systems - Experiments above 20 MeV, in Proceedings of EU enlargement workshop on Neutron Measurements and Evaluations for Applications, Bucharest, Romania, October 20-23, 2004.

[4] J. Blomgren and N. Olsson, Radiat. Prot. Dosim. **103(4)** (2003) 293.

[5] J. Blomgren, B. Granbom, T. Granlund, N. Olsson, Mat. Res. Soc. Bull. **28** (2003) 121.

[6] J. Blomgren, Nuclear Data for Single-Event Effects, in Proceedings of EU enlargement workshop on Neutron Measurements and Evaluations for Applications, Budapest, Hungary, November 5-8, 2003. EUR Report 21100 EN, Luxembourg: Office for Official Publications of the European Communities, ISBN 92-894-6041-5, European Communities, 2004.

[7] J. Klug, et al., Nucl. Instr. Meth. **A 489**, 282 (2002).

[8] J. Klug, et al., Phys. Rev. C **68** (2003) 064605.

[9] V. Blideanu, et al., Phys. Rev. C **70** (2004) 014607.

[10] T. Rönnqvist, et al., Nucl. Phys. **A563** (1993) 225.

[11] S. Dangtip, et al., Nucl. Instr. Meth. **A452**, 484 (2000).

[12] H. Witała, W. Glöckle, D. Hüber, J. Golak, H. Kamada, Phys. Rev. Lett. **81** (1998) 1183.

[13] P. Mermod, et al., Phys. Rev. C **72** (2005) 061002(R).

[14] P. Mermod, et al., submitted to Phys. Rev. C.

[15] P. Mermod, et al., Phys. Lett. **B 597** (2004) 243.

[16] E.L. Hjort, et al., Phys. Rev. **C 53** (1996) 237.

[17] I. Tilquin, et al., Nucl. Inst. Meth. Phys. Res. **A 365** (1995) 446.

Appendix X

FAST-NEUTRON DIAGNOSTICS FOR TRANSMUTATION IN ACCELERATOR-DRIVEN SYSTEMS

Jan Blomgren* **and Moinul Habib**
Department of Neutron Research
Uppsala University
Box 525, S-751 20 Uppsala, Sweden
E-mail: Jan.Blomgren@tsl.uu.se

In critical reactors, the neutron energies extend up to a few MeV. The neutron diagnostics is commonly based on activation techniques and ssion ionization chambers. In accelerator-driven systems, the neutron spectrum will extend all the way up to the incident beam energy, i.e., several hundred MeV or even up to GeV energies. The high energy allows diagnostics with measurement techniques hitherto not used in reactor environments.

Such measurements are primarily connected to system safety and validation. It is shown that in-core fast-neutron diagnostics can be employed to monitor drifts in the position of incidence of the primary proton beam onto the neutron production target. Moreover, fast-neutron detection can be used to reveal temperature-dependent density changes in a liquid lead-bismuth target.

International Workshop on Fast Neutron Detectors and Applications
April, 3 - 6, 2006
University of Cape Town, South Africa

*Speaker.

1. Introduction

The basic idea of an accelerator-driven system (ADS) is to operate a sub-critical reactor driven by an accelerator that generates high-energy (around 1 GeV) charged particles (e.g. protons), which strike a heavy material target in the centre of the core. This bombardment leads to the production of a very intense neutron ux. Because the ssion multiplication chain reactions in a sub-critical core are not self-sustained, this external neutron source must be continuously supplied to the core.

An ADS is a highly integrated system, where neutrons are the driving agent of the processes involved. The present work is focused on whether detection of neutrons in various places could be used to reveal technical system properties. An extensive account of the present investigation is found in ref. [1]. To make the scope limited, some restrictions have been made. Neutron diagnostics at traditional critical reactor energies, i.e., up to 10 MeV, are not the primary aim of the present work. The primary focus of the present investigation is the potential to use very fast neutrons, above 10 MeV, to reveal technical properties of an ADS.

The more general issue of system validation is not explicitly discussed in the present work, but could potentially become an important by-product. In any ADS research experiment, measurements of neutron properties, like energy spectra, in various places can be used to validate the design as well as the input used in the simulations. Integral experiments can be used to verify the quality of, e.g., the nuclear data libraries used. Although the present work is focused on neutron diagnostics for system performance, the measurement techniques investigated could potentially, or even likely, be used for design validation.

When outlining the present project, a few boundary conditions were identi ed. The only source of the neutrons above 10 MeV is the spallation target, while neutrons below that energy can be created also in the blanket, primarily by ssion reactions. Thus, fast neutron diagnostics is primarily a means for target investigations. This in turn leads to important boundary conditions on the detection methods. In a realistic ADS, the target and blanket must be closely coupled, leaving little room for detectors. As a consequence, all diagnostics embedded in the system has to be performed with small-size equipment.

An alternative approach, not considered in the present work, is to use neutron guides out from the core to port holes where external detectors could be used. Such guides are in general interfering with the system, and are very dif cult to install after the system has been commissioned. Thus, they have to be very well motivated, and have to be part of the design already from the initial phase. There is, however, one particular neutron guide that will inevitably be installed in all ADS systems: the proton beam line. In it, neutrons produced in the target can escape the system. This so called neutron backstreaming can provide possibilities for high-quality diagnostics outside the core, thereby enabling use of much more sophisticated techniques than for in-core monitoring.

As has been discussed above, the only source of very fast neutrons is the target. Thus, fast-neutron diagnostics is a potential tool for investigation of target properties. It makes therefore sense to study the target parameters that can change during operation. This essentially limits the investigation to two properties. The position of incidence of the primary proton beam could move and the target density could change as a result of a higher temperature, in both cases resulting in a changed spatial or energy distribution of the neutron production. The former is possible in all ADS systems, while the latter is a real possibility only for liquid targets. In the present work, we

have used the SAD system [2] as reference. SAD uses solid targets only, but since the aim of the investigation is to study general features, we have taken the liberty to model a lower target density simply by arti cially forcing a reduced density in the simulation input.

2. Simulations

Simulations have been performed for the SAD system [2], which is a research project on ADS at low power. A 600 MeV proton accelerator is coupled to a core of fast-reactor MOX fuel (30/70 % Pu/U), with the beam entering from below. In principle, any system could have been simulated. One reason for using SAD is that it is a real project, underway to be installed, where possible results of the present work could be used. Also, an MC code based on MCNP [3] had already been developed, and thereby only minor changes of an existing code were needed for the present investigations.

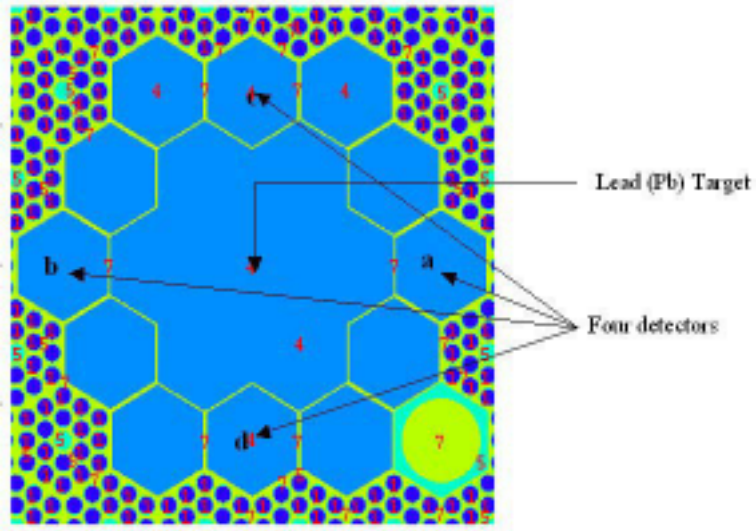

Figure 1: Horizontal cross sectional view of the SAD target. The distance between two opposite sides of each hexagonal target cell is 3.6 cm. Detector positions used in the simulations are indicated.

The SAD target consists of lead rods, 60 cm high with hexagonal cross sections (see g. 2). In the simulations, we have installed four detector chains (a-d). Note that the detector pair c-d is closer to the target centre than the a-b pair. Each chain has been divided into four vertical segments, numbered 1 to 4 from bottom to top.

3. Results

The effect of a displacement of the incident beam has been investigated by simulating the neutron emission from the target for two cases, one in which the beam hits the target centrally, and one with the beam moved 1 cm sideways towards detector a. In g. 2, the integrated neutron ux in the range from 20 to 600 MeV is presented. There is a signi cant increase at detector a and decrease at detector b and no changes at detector c and d. The ux ratio between detectors a and b

changes from 0.98± 0.01 to 1.57± 0.02. The errors quoted are statistical only. The magnitude of this change is in agreement with simple estimates in which the attenuation of neutrons is presumed to depend on the total cross section.

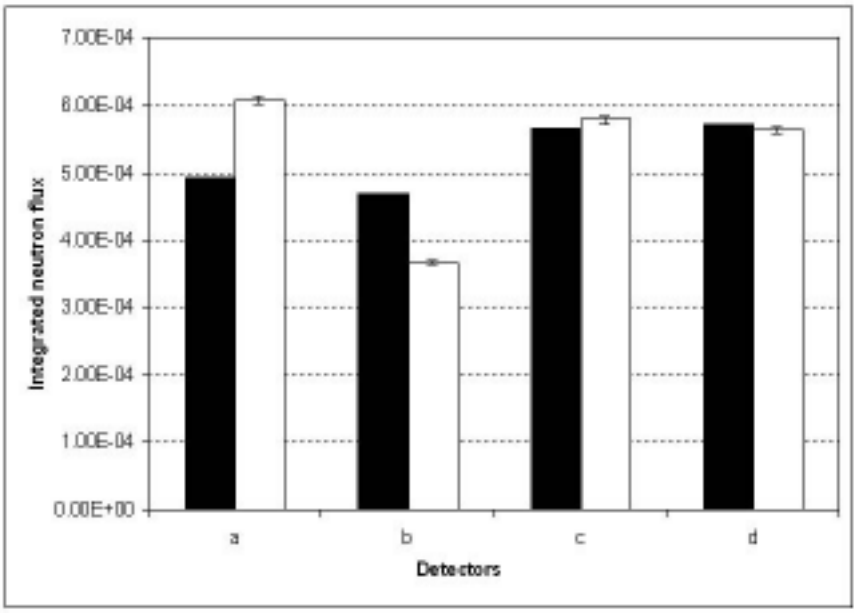

Figure 2: Neutron ux in the detectors a-d for central beam (lled bars) and for incident beam moved 1 cm towards detector a (un lled bars). The neutron ux refers to integration of the 20 to 600 MeV energy range. The ux scale is in arbitrary units. The errors presented are statistical only.

Thus, a beam position change of 1 cm results in a clear effect, but such a change is far larger than what is realistic. We have therefore computed the change due to a realistic move, 1 mm, which results in a ratio change of about 7%. Such a change can most likely be detectable. About 5% absolute uncertainty is achievable for a well-calibrated ssion detector. However, in our case only detection of relative changes are needed, and in that case 1-2% changes are relatively easy to detect. Thus, this could provide a beam position monitoring system.

The effect of a target density change is displayed in g. 3. It shows neutron emission spectra integrated from 20 to 600 MeV at four detector positions along a vertical detector chain, with detector 1 at the bottom and 4 at the top. The beam enters the target from below. The resulting total ux es show a notable change when the density is reduced by 10 %. The centroid of the production is moved upwards in the target, i.e., further into the material as consequence of the lower stopping power of the incident proton beam, as well as the reduced attentuation of the produced neutrons.

The neutron ux ratio between detector 1 and 4 is 1.20± 0.03 for normal target density, and 0.92± 0.03 for a density reduced by 10%. The ratio has a close to linear relation to the density, which means that the count rate ratio changes by about 2.3% for a 1% density change. Detection of a count rate ratio change of 1-2% should be possible with ssion-based detectors. Thus, density changes of about 1% are feasible to detect with such methods.

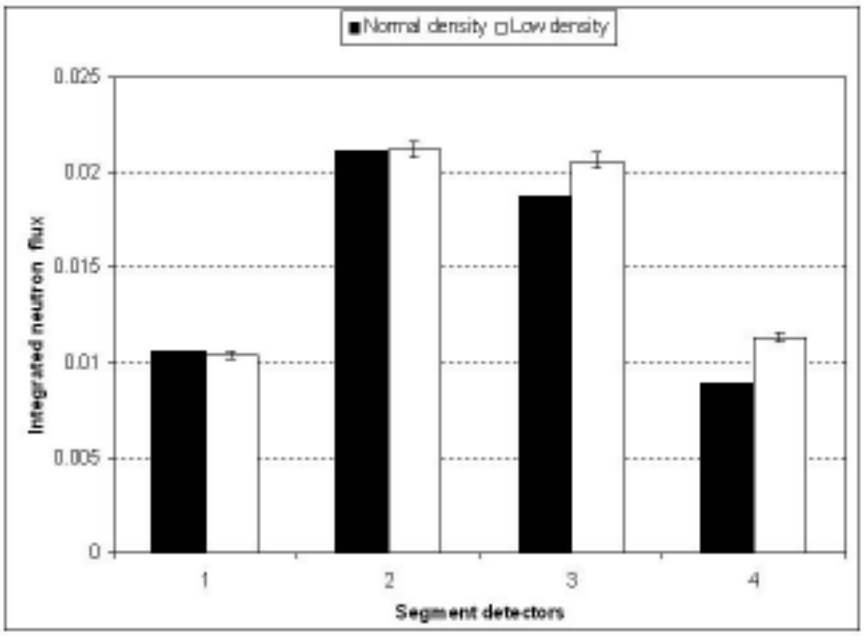

Figure 3: Integrated neutron ux of four segment detectors for normal density (lled bars) and reduced density (un lled bars). The errors given are statistical only.

4. Discussion and outlook

The choice of techniques for investigations of fast neutrons close to the target is to a large degree dictated by the environment, such as lack of space, very intense neutron ux, and in general hostile conditions. To our judgement, the most likely active detectors to be used are ssion ionization chambers. Such detectors are permanently installed in conventional critical power reactors (BWR), however primarily for thermal neutron monitoring. In the present application, fast neutrons are of main interest.

Fission-based detection of fast neutrons requires an element with a neutron energy threshold to be used. This poses some practical limitations. Thorium and uranium are elements that can be readily obtained in suf ciently large quantities. Both these have thresholds of about 1 MeV for neutron-induced ssion of the leading isotopes. The next lighter elements that are available for realistic applications are lead and bismuth, the heaviest stable elements, which have effective ssion thresholds of about 20-30 MeV. In between bismuth and thorium, all elements have rather short hal i ves and are therefore dif cult to handle and hard to obtain in useful quantities. This limits the practical possibilities to detectors with thresholds either in the 1 or 20 MeV range. For the former, the cross sections are large, resulting in high ef cienc y, but the relatively low threshold makes them sensitive also to a neutron ux range where the technical changes studied in the present work do not induce very large effects. Thus, the sensitivity might not be very high. On the other hand, for lead- or bismuth-based detection, the high thresholds make the detectors very sensitive for these effects, but the ssion cross section is smaller, making the detector itself less ef cient. Which solution to use for optimal performance in a practical implementation requires further studies.

If surrounding the target with ssion ionization chambers loaded with Pb/Bi and/or ^{238}U/^{232}Th, a 3D-picture of the neutron production could be provided. With such a system, the sideways and vertical movement of the incident beam could be detected. Using both Pb/Bi and ^{238}U/^{232}Th-based systems would also give a rough energy sensitivity. The detailed simulations of such a system and of suitable detector design constitute possible future work.

5. Acknowledgments

The collaboration with Per Seltborg on MCNP simulations is gratefully acknowledged. This work was nancially supported by the Swedish Nuclear Fuel and Waste Management Company, the Swedish Nuclear Power Inspectorate, Ringhals AB, Forsmarks Kraftgrupp AB, the Swedish Defense Research Agency, the Swedish Nuclear Safety and Training Centre, and the European Union.

References

[1] M. Habib, MCNPX simulations of fast neutron diagnostics for accelerator-driven systems, INF report UU-NF 05#09 (2005).

[2] Sub-critical Assembly at Dubna, http://www.SAD.dubna.ru

[3] J.F. Briesmeister, *MCNP - A General Monte Carlo N-Particle Transport Code*, Los Almos National Laboratory, version 4C, April, 2000.

FAST NEUTRON BEAMS - PROSPECTS FOR THE COMING DECADE

Jan Blomgren*
Department of Neutron Research
Uppsala University
Box 525, S-751 20 Uppsala, Sweden
E-mail: Jan.Blomgren@tsl.uu.se

The present status of neutron beam facilities above 20 MeV is reviewed. Presently, two main techniques for neutron production at these energies are used; white beams and quasi-monoenergetic beams. The performances of these two techniques are discussed, as well as the use of such facilities for measurements of nuclear data for fundamental and applied research. Recently, two novel ideas on how to produce extremely intense neuton beams in the 100-500 MeV range have been proposed. Decay in ight of beta-delayed neutron-emitting nuclei could provide beam intensities ve orders of magnitudes larger than present facilities. A typical neutron energy spectrum would be essentially mono-energetic, i.e., the energy spread is about 1 MeV with essentially no low-energy tail. A second option would be to produce beams of ^{6}He and dissociate the ^{6}He nuclei into α particles and neutrons. The basic features of these concept are outlined, and the potential for improved nuclear data research is discussed.

International Workshop on Fast Neutron Detectors and Applications
April, 3 - 6, 2006
University of Cape Town, South Africa

*Speaker.

1. Introduction

The interest in high-energy neutron data is rapidly growing since a number of potential large-scale applications involving fast neutrons are under development, or have been identi ed. This has motivated nuclear data research for transmutation of spent nuclear fuel [1, 2, 3], neutron therapy of cancer tumours [4] and upsets in electronics [5, 6]. In the present paper, present and future facilities for nuclear data production for these applications are discussed.

2. Present-day facilities for nuclear data measurements

At low energies (below 20 MeV or so), truly mono-energetic neutron beams can be produced. There are a few light-ion reactions, like D(d,n)^{3}He and T(d,n)^{4}He, which have positive Q-values and sizeable cross sections. Such a beam is strictly monoenergetic up to about 2 MeV incident deuteron energy. Above this energy, there is a possibility that the deuteron breaks up into a proton and a neutron. In reality, this is not a major obstacle until you get up to about 30 MeV neutron energy, because the T(d,n)^{4}He cross section is so large that the breakup neutrons form only a small low-energy tail. At even higher energies though, the T(d,n)^{4}He cross section is smaller, making the total yield too low for most measurements.

The largest neutron separation energy is about 20 MeV, making truly monoenergetic beams impossible to produce above that energy. What is available at higher energies are quasi-monoenergetic beams, i.e., beams where a single energy dominates, but always accompanied by a low-energy tail.

At energies of 50 MeV and up, three production reactions give reasonably monoenergetic beams. These are D(p,n), ^{6}Li(p,n) and ^{7}Li(p,n). The rst has a large cross section, but the drawback that the energy resolution of the full-energy neutrons cannot be better than 3 MeV due to the Fermi motion of the neutron inside the deuteron. If a sharper energy de nition is required, one of the two reactions using lithium is selected. They are about equally good, but there is a major practical difference: ^{6}Li is used in hydrogen bombs and is therefore not easily obtained, while ^{7}Li is provided at low cost. As one could expect, ^{7}Li(p,n) is the most common production reaction for monoenergetic neutron beams. At 100 MeV, about 50 % of the neutrons fall within 1 MeV at maximum energy, while the remaining half are distributed about equally from maximum energy down to zero. This is the closest to monoenergetic conditions nature provides.

There is also a completely different approach; instead of trying to get the neutrons as well gathered in energy as possible, all energies are produced simultaneously. A high-energy proton beam hits a thick (in most cases stopping) target and lots of neutrons of all energies are produced, with typically a $1/E_n$ spectrum. If the incident proton beam is bunched and the experiment target is placed at a rather large distance from the neutron production target, time-of- ight (TOF) methods can be used to determine the energy of the incident neutron on an event-by-event basis.

The advantage of such so called white beams is the total intensity, which is larger than for monoenergetic beams, but instead the intensity per energy interval is much lower at high energies. This can partly be compensated for by summing data over limited energy intervals, but still the intensity per such interval is lower. The advantage of being able to measure at many energies simultaneously is not worth much if you get insuf cient statistics everywhere. As a consequence, white beams are restricted to experiments at low energies, where the intensities are large, or to

high-energy reactions with rather large cross sections. Another feature is that white sources require event-by-event measurements. Experiments of effects with an energy dependence where the individual events cannot be distinguished cannot be performed at white beams. For experiments ful lling the requirements above, white sources can, however, provide large quantities of very valuable information. This is especially true when excitation functions, i.e., the energy dependence of a cross section, is of particular interest.

3. Nuclear data status

It is a fairly limited class of reactions that are of interest for the further development of the applications under consideration. The most important are elastic scattering, inelastic neutron emission, light ion production, heavy ion production and ssion.

Elastic scattering has been studied on a range of nuclei up to 96 MeV. At present, ten nuclei have been studied and results are either published or underway [7]. An overall uncertainty of about 5 % has been achieved. A novel normalization method has been established that allows elastic scattering data to be normalized absolutely to about 3 % uncertainty [8]. This method, however, works only for elastic scattering. Feasibility studies have shown that the technique as such works up to about 200 MeV, so these studies can be extended up in energy.

An experimental programme on inelastic neutron emission, i.e., (n,xn') reactions is in progress [9]. Data have been taken on lead and iron, and the method as such seems to work. It is too early to quote a nal uncertainty in the results, but 10 % seems feasible.

Data on light ion production has been acquired on about ten nuclei at 96 MeV, and analysis is in progress [10, 11]. At present, about half the data set has been published. Normalization has been obtained by simultaneous detection of *np* scattering at an angle where the cross section uncertainty can be estimated to about 5 %, which is the dominating uncertatinty in the nal light ion production cross sections. These studies are presently being extended to 180 MeV.

Fission cross sections have been studied at many facilities up to about 200 MeV energy. The energy dependencies of the cross sections agree fairly well in shape, but the absolute scale differs by up to 15 %. It is at present not clear what causes this. One possibility is the normalizations used. Another possible cause is that the sensitivity to low-energy neutrons is not under control for some of the experiments. Dedicated experiments to remedy this situation are underway.

In principle, ssion cross sections can be measured up to several GeV using white beams with a very high initial proton energy, like at the CERN-nTOF facility [12]. The neutron beam intensity is very low, but the cross sections are large and it is possible to detect a major fraction of the ssion fragments, resulting in reasonable statistical precision. A major problem, however, is normalization, since the beam intensity is very dif cult to monitor at these very high energies.

There are only a few examples of other ssion data than cross sections. This means that important ssion parameters, like angular distributions, yields, etc., essentially remain to be investigated at high neutron energies.

4. Possible future facilities

As was discussed in the previous section, the prospects for development in the near future, i.e.,

within ten years, can be summarized to extension to about 200 MeV of ongoing work on elastic scattering, inelastic neutron emission and light ion production at around 100 MeV, and ssion studies of other parameters than the cross section.

If looking a bit further into the future, we can allow ourselves to be more visionary. To my opinion, the single most important problem to solve if we want a signi cant development of the eld is normalization. At present, we inevitably end up with an uncertainty of about 5 %, because we have to normalize to a reference, typically *np* scattering, which is known to - at best - 5%, and it is dif cult to see how this can be radically improved upon in a short term with present techniques.

I consider energy resolution to be the second largest problem, with intensity on third place. These two are, however, to a large degree coupled. If you aim for good neutron-beam energy resolution, you have to pay by poor intensity and vice versa. It is presently close to inconceivable to produce neutrons at high energies with a resolution better than 1 MeV with a reasonable intensity. The limited intensity puts severe constraints on the detection, in such a way that the detection often has to be performed with techniques that sacri ce resolution for ef cienc y, resulting in a nal resolution of a few MeV. This means that only in a few rare cases, nal states can be resolved.

Recently, a way out of this dilemma has been proposed as a by-product of the CERN beta-beam facility [13] under consideration. The background is that neutrino physics has progressed rapidly the last few years, with the discovery of neutrino oscillations as the most visible example. Up to now, essentially all accelerator-produced neutrinos have been muon neutrinos, being the nal product of pion decay. Electron neutrinos are much more dif cult to produce in large amounts, because they require a nuclear beta decay for their creation.

At the proposed CERN beta-beam facility, production of suitable beta-emitting nuclei should be undertaken in an ISOLDE-like facility, and the produced nuclei should be post-accelerated to very high energy and stored in a decay ring of race-track shape. At these very high energies, hundreds of GeV/A, there is a very strong Lorentz boost, which means that the neutrino is emitted very close to the beam direction in the laboratory system, in spite of that the emission is isotropic in its moving reference frame. Thereby, intense neutrino beams can be produced. The idea is to build the decay ring so that one straight section points towards a distant neutrino detector to allow studies of electron neutrino oscillations.

Intense neutron beams could be a spin-off from that facility. It has been proposed to use two production targets, one for nuclei suited for neutrino emission in the decay ring, and one for beta-delayed neutron emitters. Some neutron-rich nuclei beta decay to a nucleus that promptly emits a neutron, which typically has an energy of a few hundred keV in its rest frame. By accelerating the beta-delayed neutron emitters up to a few hundred MeV per nucleon, the Lorentz boost is suf cient to focus the beam to reasonable dimensions. All this can be done in parallel with the primary objective, since the accelerators for the neutrino emitters have a long cycle with a low duty factor.

The resulting neutron beam has an energy in the 100–500 MeV range with an energy resolution of about 1 MeV, and intensities of about 10^{11} n/s are estimated. This should be compared with 10^{6} for present-day technology, i.e., an improvement by a factor 100 000 (!). With such intensities, only imagination sets the limit for what can be achieved.

If we now restrict the discussion to nuclear data for applications and turn to my problem list above, it seems feasible that we can address all of them through one experimental trick: tagging. If we use the neutron beam directly for experiments we have essentially only solved the intensity

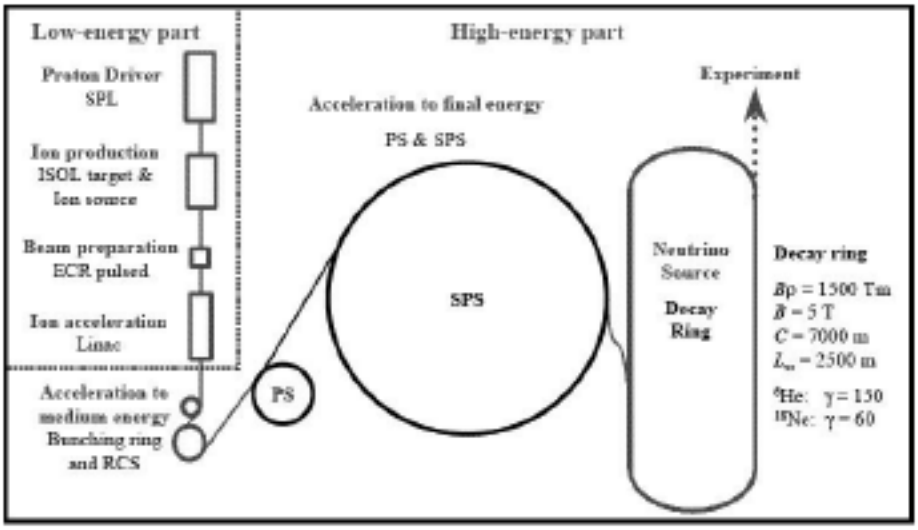

Figure 1: Overview of the proposed CERN beta-beam facility.

problem, but the other two remain; we end up in a 1 MeV resolution due to the inherent energy spread, and we are still plagued by the normalization problem. Tagging means that we produce a secondary neutron beam of less intensity, but with much better known intensity. One candidate reaction is to let neutrons scatter from a hydrogen target, and the recoil proton is detected. Since this is a two-body nal state, detection of the associated proton means that a neutron must have been scattered to the corresponding direction. Thereby, the normalization problem can be circumvented, since we count the neutrons one by one through the associated particle. If high-resolution tagging is performed, we can also know the neutron energy event by event far better than the initial neutron beam energy resolution. If the tagging is performed with a magnetic spectrometer, the tagger can be made rather insensitive to the ambient background, and a proton energy resolution of better than 100 keV can be obtained, resulting in a comparable neutron energy resolution.

With reasonable estimates on tagger parameters, 10^4 tagged neutrons with an energy resolution of 100 keV should be possible to reach, given the beam intensity above. This might sound like a poor intensity, but with such a resolution, nal states can be well resolved, which means that already a small number of events will result in a good precision. Moreover, since the intensity can be determined to about 1 % in a typical tagger system, the accuracy is far better than what can be obtained today. In cases when the demands on energy resolution are not as stringent, a thicker tagger target can be used, resulting in increased intensity. This goes faster than linear, because with a worse resolution, the intensity at the tagger is increased, thicker secondary experimental targets can be used, and the detection limitations are less severe. Therefore, even with resolutions that are on the limit to be possible untagged today, we might have tagged beams of intensities exceeding what is presently available untagged in a not too distant future.

A second technique would be to use a similar production as above (1-2 GeV protons on a combined target-ion source) to produce ^{6}He, which in turn would be accelerated to hit a target. Roughly, ^{6}He can be described as an α particle with two loosely attached neutrons. When hitting a

target, the two neutrons are dissociated with a large probability, and continue along the direction of the incident beam with the incident velocity. The charged particles (the remaining ^{6}He and residual ^{4}He) are bent by a magnet system and a clean neutron beam is produced. This latter technique does not have the potential to produce as intense ux es as the beta-decay in ight, but on the other hand it requires much less advanced accelerators. This technique could possibly be installed at existing CERN facilities after some upgrades. Initial estimates indicate a factor a hundred to a thousand larger neutron ux es than for present facilities to be within reach.

Acknowledgments

The information from Mats Lindroos is gratefully acknowledged. This work was nancially supported by the Swedish Nuclear Fuel and Waste Management Company, the Swedish Nuclear Power Inspectorate, Ringhals AB, Forsmarks Kraftgrupp AB, the Swedish Defense Research Agency, the Swedish Nuclear Safety and Training Centre, and the European Union.

References

[1] A. Koning, *et al.,* J. Nucl. Sci. Tech., Suppl. **2** (2002) 1161.

[2] J. Blomgren, in Proceedings of Workshop on Nuclear Data for Science & Technology: Accelerator Driven Waste Incineration, Trieste, Italy, Sept. 10-21, 2001, eds. M. Herman, N. Paver, A. Stanculescu, ICTP lecture notes **12** (2002) 327.

[3] J. Blomgren, Nuclear data for accelerator-driven systems - Experiments above 20 MeV, in Proceedings of EU enlargement workshop on Neutron Measurements and Evaluations for Applications, Bucharest, Romania, October 20-23, 2004.

[4] J. Blomgren and N. Olsson, Radiat. Prot. Dosim. **103(4)** (2003) 293.

[5] J. Blomgren, B. Granbom, T. Granlund, N. Olsson, Mat. Res. Soc. Bull. **28** (2003) 121.

[6] J. Blomgren, Nuclear Data for Single-Event Effects, in Proceedings of EU enlargement workshop on Neutron Measurements and Evaluations for Applications, Budapest, Hungary, November 5-8, 2003. EUR Report 21100 EN, Luxembourg: Of ce for Of cial Publications of the European Communities, ISBN 92-894-6041-5, European Communities, 2004.

[7] A. Hildebrand, *et al.,* AIP Conference Proceedings **769** (2005) 853.

[8] J. Klug, *et al.,* Phys. Rev. C **68**, 064605 (2003).

[9] F.-R. Lecolley, private communication.

[10] V. Blideanu, *et al.,* Phys. Rev. C **70** (2004) 014607.

[11] U. Tippawan, *et al.,* Phys. Rev. C **69**, 064609 (2004).

[12] L. Tassan-Got, private communication.

[13] The CERN beta-beam working group, http://cern.ch/beta-beam.

Appendix XII

NEUTRON DIAGNOSTICS FOR VOID MONITORING IN BOILING WATER REACTORS

Jan Blomgren*
Department of Neutron Research
Uppsala University
Box 525, S-751 20 Uppsala, Sweden
E-mail: Jan.Blomgren@tsl.uu.se

In present-day Boiling Water Reactors (BWR), the only in-core neutron diagnostics in full-power operation (Power-Range Mode, PRM) is performed with fission-based ionisation chambers loaded with ^{235}U. Since both the neutron flux and the neutron-induced fission cross section on ^{235}U are the highest at thermal energies, the count rate from such PRM detectors is essentially due to the thermal neutrons. It has recently been proposed that adding PRM detectors loaded with ^{238}U, thereby being sensitive only to fast neutrons (above about 1.5 MeV), to the BWR core could facilitate void monitoring.

The neutron energy spectrum in a BWR is very sensitive to the boiling. Since the moderation of neutrons requires the presence of hydrogen, which in reality means water, the moderation gets significantly less efficient in regions of the reactor where the void fraction (the fraction of the water that is in steam phase) is high. Because the density of steam is significantly lower than when water is in liquid phase, increased void results in reduced moderation. Less moderation results in a neutron energy spectrum with a lower fraction of thermal neutrons and a correspondingly larger number of fast neutrons. Thereby, a simultaneous measurement of the fluxes of thermal and fast neutrons may be used to determine the void in a BWR. The potential of this technique will be outlined, as well as applications in realistic technical systems.

International Workshop on Fast Neutron Detectors and Applications
April, 3 - 6, 2006
University of Cape Town, South Africa

*Speaker.

1. Introduction

In Boiling Water Reactors (BWR), the presently second most common reactor design in the world, the uranium fuel is surrounded by water that is brought to boiling within the reactor core by the heat released due to fission. In the lower portion of the core, only liquid water moderator is present. As the water flows through the fuel bundles from the bottom to the top, an increasing fraction of the flowing water is in the form of steam. BWRs depend upon this void fraction in their operation because of two discrete phenomena. Firstly, the heat conductivity from the fuel rods to the steam is optimal if a thin water layer is maintained at the fuel surfaces, because the two-step heat transfer from fuel rod to water and from water to steam is far more efficient than a single-step transfer from rod to steam directly. Thus, if the thin water film is evaporated, the cooling of the fuels is dramatically reduced, and this dry-out phenomenon can rapidly lead to overheating, with severe fuel damages as result.

Secondly, the energy release depends on the moderation. The neutrons emitted in fission display an energy distribution ranging from about 0.1 MeV up to a few MeV, with a maximum typically in the $0.5 - 1.0$ MeV range. After release, these fast neutrons are moderated, i.e., are slowed down, primarily due to collisions with the hydrogen in the water, resulting in thermal neutrons of very low energy, typically 0.025 eV. At any given moment there are both thermal and fast neutrons present, as well as neutrons of intermediate energies. The properties of a BWR depend strongly on the absolute neutron flux, but also on the relative distribution of neutron energies. Since the moderation of neutrons requires the presence of hydrogen, which in reality means water, the moderation gets significantly less efficient in regions of the reactor where the void fraction is high. Less moderation results in a neutron energy spectrum with a lower fraction of thermal neutrons and a correspondingly larger number of fast neutrons. Thereby, a simultaneous measurement of the fluxes of thermal and fast neutrons may be used to determine the void in a BWR.

2. Neutron monitoring for void determination

2.1 Present neutron diagnostics in BWRs

In most BWRs today, the only neutron diagnostics in full-power operation is fission-based ionisation chambers loaded with ^{235}U, so-called Power Range Monitors (PRM). Since neutron-induced fission in ^{235}U is also the main heat production reaction in a BWR, this signal gives a reasonably good measure of the power of the reactor. For an introduction to detector techniques in reactor environments, see, e.g. ref. [1]. A typical PRM detector is based on two cylinders, an inner and an outer one, used as electrodes, with a gas in between, often argon. A bias voltage is applied to the two electrodes. One of the electrodes is coated with ^{235}U. When neutrons induce fission in the ^{235}U coating, fission fragments are released into the gas-filled gap, which cause ionization of the gas. Thereby, an electric current can flow between the electrodes. This current, which is proportional to the neutron flux, is transported out of the reactor in a coaxial cable for further processing. The ionization chamber gas is often under overpressure to ensure that the range of the fission fragments does not exceed the gap dimensions. Typical dimensions of these detectors are up to 10 cm in length, whereof the active volume comprises 2-3 cm length, and about 2 cm in diameter.

In BWRs, the detectors are placed in vertical tubes inside the reactor core. Typically, four detectors are placed in the same tube at different heights (about 1 m separation), and 30-40 tubes are installed, resulting in about 150 detectors in total. In addition, some detectors may be provided with a motorized drive to allow traverses though the reactor core.

2.2 Fast neutron detection

As described above, in present BWRs, fast neutrons are not explicitly monitored. Technically, fast neutron diagnostics can be achieved with various types of devices, for instance ionization chambers. In that case the coating inside, on the inner cylinder, is an element with a neutron energy threshold for fission (like ^{238}U or ^{232}Th). The performance of these fast-neutron detectors is very similar to the presently used thermal-neutron detectors, and essentially identical readout is used. The fission cross section for ^{238}U, the dominating uranium isotope in natural uranium (and in the fuel of a BWR) is very different from the ^{235}U cross section. The cross section for ^{238}U is almost zero below a threshold energy of about 1 MeV, while above that energy the cross section is comparable to that of ^{235}U. This means that a fission monitor loaded with pure ^{238}U would be sensitive essentially only to fast neutrons.

2.3 Determination of the void fraction

The void fraction can be determined from a simultaneous measurement of the thermal and fast neutron flux, since the ratio of these two fluxes depends on the moderation and thereby on the void. Practically, this can be accomplished by measuring the ratio of the currents in two detectors in a detector pair, i.e., where one detector is sensitive to thermal neutrons and the other to fast neutrons.

In a realistic application, the ratio depends on many different technical parameters of the reactor, the fuel and the state of operation. Moreover, they are different in different regions of the reactor, and change over time since the isotopic composition of the fuel changes with burnout. Therefore, the relation between the current ratio and the void fraction has to be computed by large core simulation codes, like POLCA or CASMO, for relevant positions and operational parameters in the reactor.

The results in figure 1 have been obtained in a calculation presuming two detectors, one being the standard neutron-induced fission neutron detector based on ^{235}U, and the other being a similar detector loaded with pure ^{238}U. Hence, figure 1 shows a realistic simulation of the performance of a realistic system illustrating a computer calculation of the void and the ratio of fast-to-thermal neutrons. The calculation refers to a real core that has been run recently in a commercial BWR. Each datum point in the figure refers to a measurement position along a vertical channel in the reactor, going from the bottom (to the left) to the top (to the right) of the BWR. It can be seen that there is essentially no void at the bottom of the reactor, while the void increases when moving up in the reactor, and so does the fast/thermal neutron ratio. At the top end of the reactor, i.e., above the uranium fuel, this relation is no longer valid, but over essentially the entire volume where fission takes place, it is present. (The fast/thermal ratio has an arbitrary scale.) It should be pointed out, however, that this concept is not limited to the two uranium isotopes ^{235}U and ^{238}U. Also other combinations of a fissile nuclide and a nuclide with a fission threshold at a suitable energy could in principle be used.

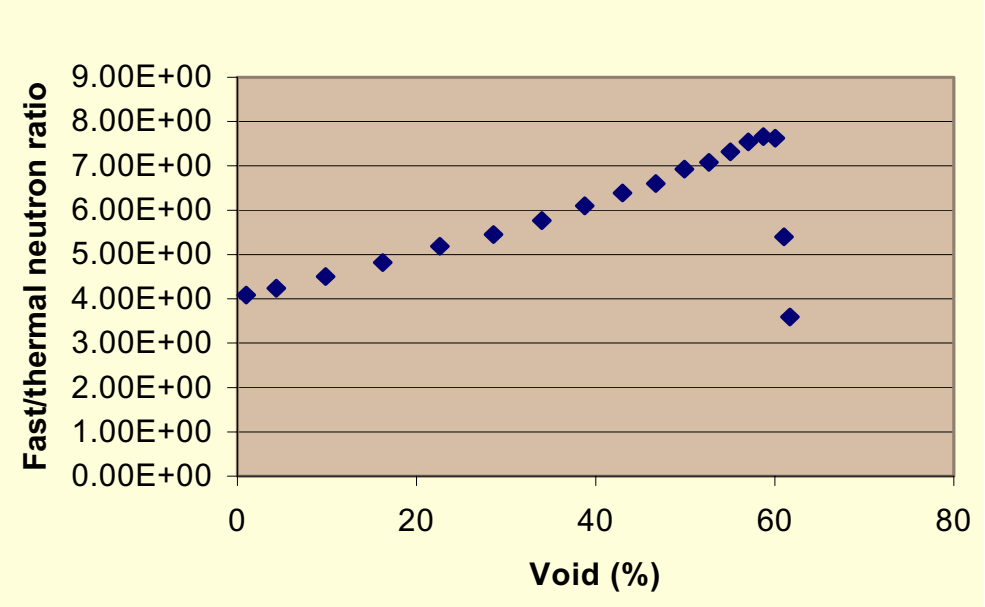

Figure 1: Relation between void and the fast/thermal neutron fraction. The simulation has been performed for a realistic core in a commercially operated reactor. The vertical scale is arbitrary.

3. Previous research on nuclear void measurement techniques

3.1 Why has this not been tried before?

It could seem like a paradox that such a conceptually simple idea – to combine two detectors, whereof one already existing – should be of any news value. Intuitively, one might assume that this should have already been attempted. There are, however, historic reasons. The standard in-core neutron monitors in BWRs are based on ionization chamber techniques. During the design, development and deployment phase of BWR technology (1955-75), many different monitoring schemes were attempted. At that time, however, ionization chambers had not matured to such a level of performance that they could be used for the present application. It was not until BWRs had been established and in regular operation that the ionization chamber technique had reached a sufficiently high level for the present concept to be possible to deploy. At that time, however, the general level of activity on development of genuinely new monitoring concepts had essentially vanished at academic and research institute organizations.

With the recent resurrected interest in academic research on nuclear power applications, there are today possibilities to develop new monitoring concepts for existing LWRs in general and BWRs in particular, as well as Gen-IV type concepts. Below, the present status of knowledge and previous research in nuclear void monitoring techniques for BWRs are outlined.

3.2 Early nuclear void measurement techniques

In the early years of LWR development, a number of various concepts for in-core void monitoring were attempted. Reviews of these early R&D activities can be found in refs. [2, 3, 4, 5]. Below, some of these early investigations are described.

It was early on observed [6] that the thermal neutron flux surrounding an absorbing rod can be modified by the void, insofar that the flux increases with the void fraction. Based on this, two monitoring techniques were tested in the Halden heavy water reactor [7]. In the first test, the flux was measured using activation of a copper foil. It was concluded that the method as such worked (although the precision was far below what we aim for in the present project), but that the technique would not be very useful in a power reactor. The reason for that is that foils need to be transported in and out of the reactor. Besides the practical problems, they are activated also during the transport, and it takes quite some time to achieve the result of the measurement, i.e., an instantaneous result cannot be obtained. In a second test a uranium thermoelement was used. Also in this case it was concluded that the principle worked, but that the precision was insufficient. The authors did, however, speculate about the possibility to use ionization chambers, which at that time had been used for the first time in a reactor [8].

The basis of the present work is that the fast/thermal neutron flux ratio depends on the void. Such a relation, however weaker, is true also for the epithermal/thermal neutron flux ratio. The epithermal/thermal ratio can be measured relatively easily using the fact that cadmium has a very large absorption cross section up to about 0.5 eV, while the cross section drops dramatically above that energy. At Argonne, a system based on this concept was tested in the EBWR reactor [9, 10]. Cobalt wires with and without cadmium wrapping were irradiated in the EBWR core. The induced activity was measured after irradiation, and the activity ratio was used to extract the epithermal/thermal neutron flux ratio, which in turn was used to determine the void. The final result was checked versus computations of the void. There is indeed a correlation between the void and the flux ratio, but the scatter of the data around the calculation is larger than what is acceptable for a practical method. Overall, the method was estimated to have an uncertainty of 15 %, and the technique as such (wire activation with post-irradiation analysis) is not well suited for practical industrial implementation. The authors concluded that the method should be applicable also in power-producing reactors, but no subsequent development in that direction has ever been published.

A test was, however, conducted in a test reactor [11], but it did not produce satisfactory results because the radial variation of the cadmium ratio was too large within a subassembly for accurate measurements of the void fraction distribution. These two development projects are representative for a range of similar activities in the early days of BWR development. A more complete listing can be found in ref. [2]. In conclusion, essentially all these concepts were based on activation, and the measurements did in reality concern thermal and epithermal fluxes. It should be emphasized that the fast/thermal flux ratio is much more sensitive to void changes than the epithermal/thermal ratio is.

Direct detection methods were already identified around 1960 to be of paramount importance to make these techniques practical. At that time, no suitable neutron detectors were available. The first steps towards development of the ionization chambers of today had, however, been taken. Below, the development of ionization chambers for reactor use is outlined.

3.3 Ionization chambers for BWR in-core neutron detection

As was pointed out above, the first use of ionization chambers in a reactor was reported in 1958 [8]. At that time, one of the major limitations was the very short life span of such a detector. The gradual burn-up of the fissile material in the detector resulted in a rapid and significant effi-

ciency decrease. This problem was to a large degree remedied by the introduction of regenerative chambers, in which a fertile material is converted into a fissile element at a rate that is close to the burn-up of the original fissile material. The first such detectors, reported around 1975, used ^{239}Pu as original fissile component and ^{238}U as fertile element [12]. Breeding of ^{238}U into ^{239}Pu resulted in a sensitivity change of less than 5 % for an integrated fluence that would have resulted in a 50 % change using ^{239}Pu alone. Soon thereafter, detectors with mixtures of ^{234}U and ^{235}U were developed, and this is by far the most common design today.

4. Outlook

The principles outlined in the present article constitute the basis for a research project that has recently been initiated. In a first phase, detailed simulations of how the neutron spectrum depends on a large number of conditions, like void, fuel composition, control rods and location in the reactor, will be performed. In a second phase, the results of these simulations will be used to guide the design of a prototype system to be experimentally tested in a research reactor, where the void and neutron spectrum can be controlled, and measured also by other instruments. It has already been established that the principle as such works, but research and technical development is needed to assess the uncertainty to which the void can be determined in a practical implementation.

Acknowledgments

The collaboration with Fredrik Winge is gratefully acknowledged. This work was financially supported by the Swedish Nuclear Fuel and Waste Management Company, the Swedish Nuclear Power Inspectorate, Ringhals AB, Forsmarks Kraftgrupp AB, the Swedish Defense Research Agency, the Swedish Nuclear Safety and Training Centre, and the European Union.

References

[1] G.F. Knoll, Radiation Detection and Measurement, Wiley & Sons, New York, 1979.

[2] J.F. Boland, Nuclear Reactor Instrumentation (In-core), Gordon & Breach, New York, 1970.

[3] J.M. Harrer and J.G. Beckerley, Nuclear Power Reactor Instrumentation Systems Handbook, vol. 1, TID-25952-P1, 1973.

[4] J.M. Harrer and J.G. Beckerley, Nuclear Power Reactor Instrumentation Systems Handbook, vol. 2, TID-25952-P2, 1974.

[5] Proceedings of the Specialists Meeting on In-Core Instrumentation and Reactor Assessment, Nuclear Energy Agency (NEA), OECD, 1984.

[6] J.M. Døderlein, The Influence of Airgaps on the Neutron Flux Around Cylindrical Absorbing Rods in a Moderating Medium, Proceedings of the Second International Conference on the Peaceful Uses of Atomic Energy, Vol. 13, P/570, United Nations, Geneva, 1958.

[7] H. Ager-Hanssen and J.M. Døderlein, A Method for Measuring Steam Voids in Boiling Water Reactors, Proceedings of the Second International Conference on the Peaceful Uses of Atomic Energy, vol. 11, p. 463, United Nations, Geneva, 1958.

[8] A.L. Gray, Nuclear Power, p. 172, 1958.

[9] J.A. Thie, and J. Biedelman, Demonstration of the UTB Voidmeter, Test report no. 72A, in EBWR Test Reports, ed. V.M. Kolba, ANL-6229, 1960.

[10] J.A. Thie, J. Biedelman and B. Hoglund, Void Measurement in a Boiling Reactor, Nucl. Sci. Eng., vol. 11, p. 1, 1961.

[11] BORAX-V Project Staff, Experiments with Central Superheater Core CSH-1, BORAX-V, USAEC Report ANL-6961, Argonne National Laboratory, January 1965, p. 65.

[12] H. Böck and E. Balcar, Nucl. Instr. Meth., vol. 124, p. 563, 1975.

FAST NEUTRON SCATTERING ON CARBON AND OXYGEN

P. Mermod*, J. Blomgren †, M. Hayashi, L. Nilsson, S. Pomp, A. Öhrn, M. Österlund

Department of Neutron Research, Uppsala University, Box 525, S-75120 Uppsala, Sweden

A. Prokofiev

The Svedberg Laboratory, Uppsala University, Uppsala, Sweden

U. Tippawan

Fast Neutron Research Facility, Chiang Mai University, Chiang Mai, Thailand

In fast neutron cancer therapy, more than 10% of the cell damage is expected to be caused by recoil nuclei from elastic and inelastic scattering. There are few data for these reactions in the intermediate energy region.

Using the SCANDAL setup at The Svedberg Laboratory in Uppsala, we have measured differential cross sections for elastic scattering on carbon and oxygen at 95 MeV incident neutron energy, covering the angular range $10-85^{\circ}$ (c.m.). We could also obtain differential cross sections for inelastic scattering reactions up to 12 MeV excitation energy. These data are shown to have a significant impact on the determination of recoil kerma coefficients.

International Workshop on Fast Neutron Detectors and Applications
April, 3 - 6, 2006
University of Cape Town, South Africa

*Speaker.

†Corresponding author, tel. +46 18 471 3788, email address: jan.blomgren@tsl.uu.se

1. Introduction

There are a number of new applications under development where neutrons of higher energies than in the traditional applications (nuclear power and nuclear weapons) play a significant role. The most important are transmutation of nuclear waste [1, 2], medical treatment of tumors with fast neutrons [3], and the mitigation of single-event effects in electronics [4]. Cross-section data for neutron-induced nuclear reactions are needed in the intermediate energy region to improve data evaluations and nuclear models which are to be implemented in Monte-Carlo codes in relation to these applications.

Fast neutrons have a potential for efficient cancer therapy treatment. Among the nuclei of interest for this application, we identify the main components of human tissue and bones, which are hydrogen, carbon, oxygen, nitrogen and calcium. The damage inflicted to the cells depends on cross sections for the neutron-induced reactions on these nuclei as well as the energies and masses of the released ionizing particles. A rough evaluation tells us that about 50% of the cell damage is due to neutron-proton (*np*) scattering, about 10% is due to elastic and inelastic scattering on other nuclei, and the rest is due to neutron-induced emission of light ions [3, 5]. Light-ion production at 96 MeV is discussed in separates article by Pomp *et al.* (the MEDLEY facility) and Tippawan *et al.* (data on oxygen) of this workshop [6, 7]. In the present work, we will focus on the $\sim$10% contribution caused by elastic and inelastic neutron scattering on carbon and oxygen.

Recently, our group has measured differential cross sections for neutron scattering on hydrogen, deuterium, carbon and oxygen at The Svedberg Laboratory in Uppsala, using the SCANDAL multi-detector array (details about SCANDAL can be found in Ref. [8] as well as in a paper by Blomgren *et al.* in these proceedings [9]). The primary aim of the experiments was to investigate three-body force effects in elastic neutron-deuteron (*nd*) scattering. The *nd* data were first published in a short communication [10], and a detailed article has been submitted recently [11]. For normalization purposes, differential cross sections for *np* scattering and ^{12}C(n,n) scattering were also measured, using a water and a graphite target, respectively. The measurement on carbon was an extension of the Klug *et al.* data obtained with the same technique [12], and, in addition, elastic and inelastic scattering on oxygen could be extracted. These new carbon and oxygen data were reported together with the *np* and *nd* data in Ref. [11]. In this publication, we pointed out that the carbon and oxygen data might be relevant for cancer treatment of tumors with fast neutrons, and we identified angular regions where the accuracy of the theoretical calculations were not satisfying. In the present paper, we will discuss further how the uncertainties in the elastic and inelastic differential cross sections on carbon and oxygen may affect the estimation of the nuclear recoil kerma coefficients at intermediate energies.

2. From differential cross sections to kerma coefficients

The partial kerma coefficient k is the average kinetic energy of one type of charged particle produced in matter due to a certain reaction per unit mass divided by the neutron fluence. If the neutrons are propagating inside a living organism, the kerma coefficient is closely related to the probability to cause irreversible DNA damage through the considered reaction. In our case, the reaction is elastic or inelastic scattering at 95 MeV incident neutron energy and the charged

particle is the carbon or oxygen recoil nucleus. Thus, the recoil kerma coefficient is proportional to the integral of the differential cross section multiplied with the solid angle element and the energy of the recoil nucleus:

$$k = N \int E_R \frac{d\sigma}{d\Omega}(\theta) 2\pi \sin\theta d\theta,$$

where N is the inverse nuclear mass of the recoil nucleus, E_R is its kinetic energy in the laboratory system, and $2\pi \sin\theta$ is the solid angle element at the neutron laboratory angle θ.

In Fig. 1, one can follow in a comprehensive way how recoil kerma coefficients are obtained from the differential cross sections. The left panels of the figure correspond to elastic neutron scattering on carbon (here, at 95 MeV), and the right panels correspond to elastic neutron scattering on oxygen. The data are from Mermod *et al.* [11], Klug *et al.* [12], Salmon [13] and Osborne *et al.* [14]. The theoretical curves are predictions from the Koning and Delaroche global potential [15], the Watson global potential [16], Amos *et al.* [17], and Crespo *et al.* [18] (see Refs. [11, 12] for details). In the top panels of the figure, the differential cross sections (in logarithmic scale) are plotted as functions of the neutron scattering angle in the laboratory. The middle panels show the same differential cross sections multiplied with the solid angle element $2\pi \sin\theta$, i.e., they illustrates the angular probability distributions for neutron scattering. As the solid angle vanishes at zero degrees, these distributions are no longer forward-peaked, but rather peak around 10°. In the bottom panels, the distributions have been weighed with the energy of the recoil nuclei E_R, thus illustrating the angular probability distributions for the neutrons to cause cell damage. Back-scattered neutrons transfer more energy to the nuclei than forward-scattered neutrons, and therefore the energy of the recoil nuclei increases with the neutron scattering angle. From these last distributions, which peak at about 16°, we can deduce that most of the damage is caused by neutrons scattered between 10 and 30°, but there is still a significant contribution up to 60°. With this way of plotting, the recoil kerma coefficients are proportional to the area under the distributions.

The data for inelastic scattering on carbon and oxygen at 95 MeV to collective states up to 12 MeV excitation energy (from Ref. [11]) can be treated the same way. The differential cross sections for inelastic scattering multiplied with the solid angle elements and the recoil nuclei energies are plotted in Fig. 2. Here we observe that the main contribution to the kerma from inelastic scattering is between 30 and 60°, and tends to be underestimated by the calculations.

The values of k for different data sets and different theoretical predictions were evaluated in Refs. [11] and [12], and are reported below in Table 1.

3. Concluding comments on the results

Differential cross sections for elastic and inelastic neutron scattering on carbon and oxygen must be well known for a precise evaluation of the damage caused by fast neutrons in human tissue. We have showed that a large angular coverage (up to 60°) was needed, due to the fact that the recoil nucleus energy increases with increasing scattering angle.

There are large variations in the evaluation of the recoil kerma coefficients k obtained with different models. For elastic scattering, the experimental uncertainty in the nuclear recoil kerma coefficients is about 5%, while it is at least 10% for the theoretical calculations or the values from evaluated data. The ICRU value obtained from evaluated data [19] agrees with the experimental

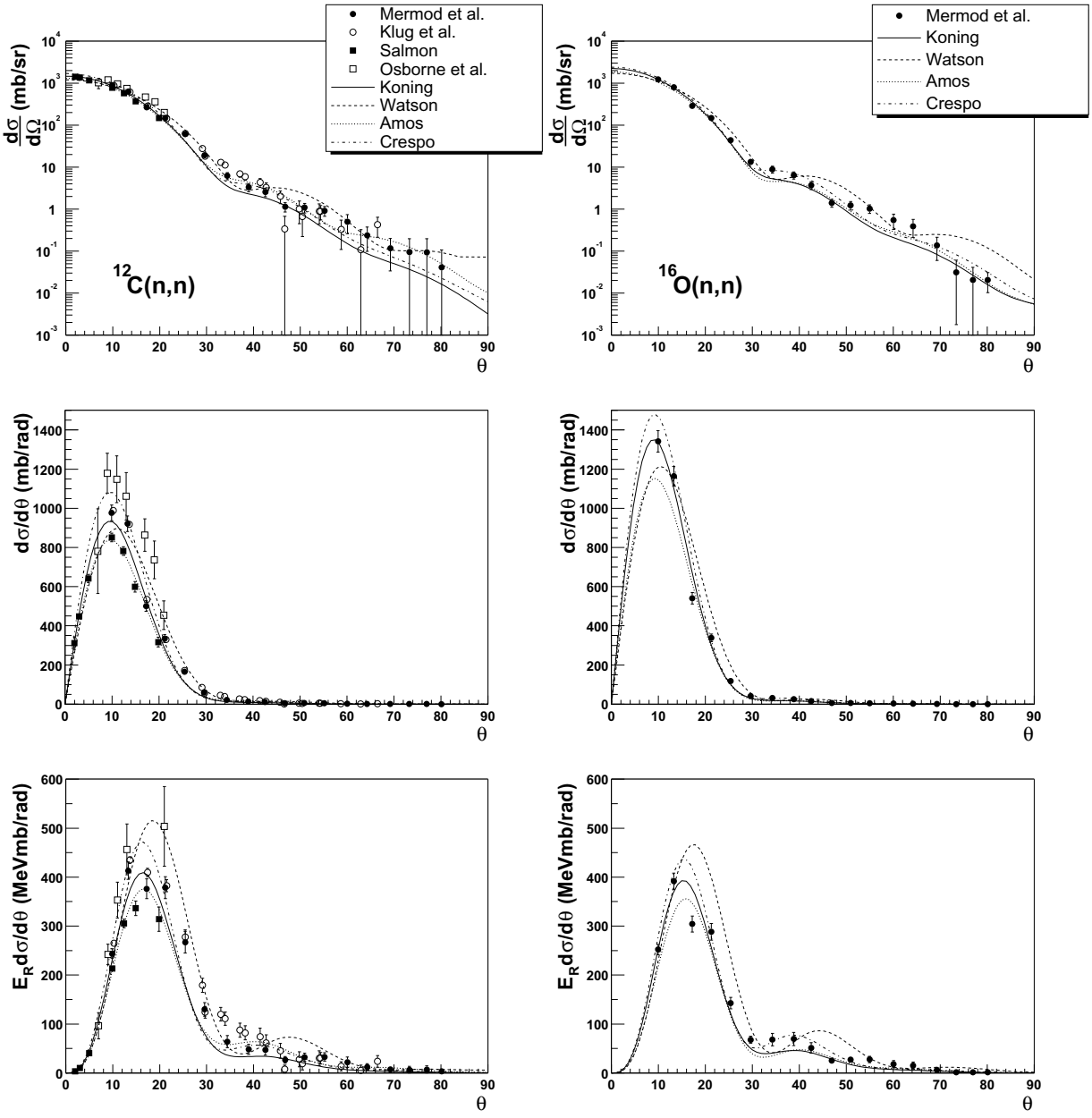

Figure 1: Elastic neutron scattering on carbon (left panels) and oxygen (right panels) at 95 MeV. The angle θ is the neutron scattering angle in the laboratory. The experimental data are from Refs. [11, 12, 13, 14]. Elastic scattering differential cross sections are shown in the top panels; in the middle panels, the differential cross sections were multiplied with the solid angle elements; in the bottom panels, they were further multiplied with the energy of the recoil nuclei. The areas under these last plots are proportional to the nuclear recoil kerma coefficients for elastic scattering.

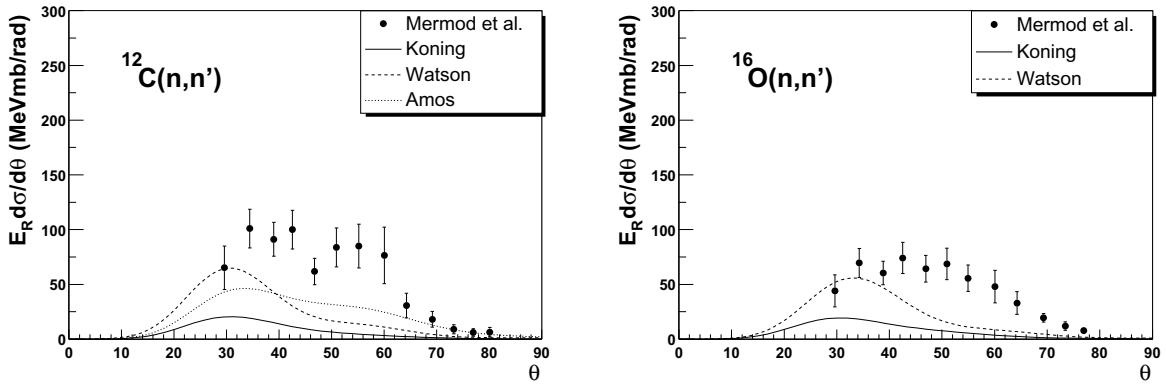

Figure 2: Differential cross sections multiplied with the solid angle elements and the energy of the recoil nuclei for inelastic neutron scattering to collective excited states below 12 MeV on carbon (left panels) and oxygen (right panels) at 95 MeV incident neutron energy. The angle θ is the neutron scattering angle in the laboratory. The experimental data are from Ref. [11]. The areas under these plots are proportional to the nuclear recoil kerma coefficients for inelastic scattering.

k (fGy·m^2)	elastic	inelastic<12 MeV	sum
^{12}C(n,n)			
Mermod *et al.* [11]	0.120±0.007	0.047±0.029	0.167±0.030
Klug *et al.* [12]	0.126±0.009	–	–
ICRU [19]	0.132±0.013	–	–
Koning [15]	0.102	0.007	0.109
Watson [16]	0.145	0.023	0.168
Amos [17]	0.105	0.026	0.131
Crespo [18]	0.118	–	–
^{16}O(n,n)			
Mermod *et al.* [11]	0.073±0.004	0.028±0.006	0.101±0.007
ICRU [19]	0.074±0.007	–	–
Koning [15]	0.071	0.006	0.077
Watson [16]	0.096	0.016	0.112
Amos [17]	0.066	–	–
Crespo [18]	0.082	–	–

Table 1: Kerma coefficients for the recoil carbon (top) and oxygen (bottom) nuclei from elastic and inelastic neutron scattering at 95 MeV. The inelastic scattering data corresponds to collective excited states with excitation energies below 12 MeV.

values from Refs. [11, 12] within these uncertainties. Among the theoretical models, for elastic scattering on carbon, only Crespo *et al.* seems to give a reasonable prediction, and this is due to the fact that most models are inaccurate in the region $25-35^\circ$. For elastic scattering on oxygen, the prediction closest to the data is provided by the Koning and Delaroche potential. For inelastic scattering on both carbon and oxygen, all models underestimate significantly the data above 40°. As a consequence, the contribution to the kerma from inelastic scattering lies above the model predictions by about 50%. This underestimation is responsible for an error in the total recoil kerma coefficient (for elastic and inelastic reactions below 12 MeV excitation energy) of about 8%, which is significant.

We wish to thank the technical staff of the The Svedberg Laboratory for enthusiastic and skillful assistance. We are very grateful to Kenneth Amos, Raquel Crespo, Arjan Koning and Antonio Moro for contributions concerning the theoretical part. This work was supported by the Swedish Nuclear Fuel and Waste Management Company, the Swedish Nuclear Power Inspectorate, Ringhals AB, the Swedish Defence Research Agency and the Swedish Research Council.

References

[1] J. Blomgren, "Experimental Activities at High Energies", Workshop on Nuclear Data for Science & Technology: Accelerator Driven Waste Incineration, Trieste, Italy, Sept. 10-21, 2001, eds. M. Herman, N. Paver and A. Stanculescu, ICTP lecture notes **12**, 327 (2002).

[2] M. Österlund *et al.*, "Elastic neutron scattering studies at 96 MeV for transmutation", these proceedings.

[3] J. Blomgren and N. Olsson, "Beyond Kerma - Neutron Data for Biomedical Applications", Radiat. Prot. Dosim. **103**, 293 (2003).

[4] J. Blomgren, B. Granbom, T. Granlund, and N. Olsson, "Relations Between Basic Nuclear Data and Single-Event Upsets Phenomena", Mat. Res. Soc. Bull. **28**, 121 (2003).

[5] M.B. Chadwick, P.M. DeLuca Jr., and R.C. Haight, "Nuclear data needs for neutron therapy and radiation protection", Radiat. Prot. Dosim. **70**, 1 (1997).

[6] S. Pomp *et al.*, "Light-ion production and fission studies using the MEDLEY facility at TSL", these proceedings.

[7] U. Tippawan *et al.*, "Light charged particle production in 96 MeV neutron induced reactions on oxygen", these proceedings.

[8] J. Klug *et al.*, "SCANDAL−a facility for elastic neutron scattering studies in the 50-130 MeV range", Nucl. Instr. Meth. **A 489**, 282 (2002).

[9] J. Blomgren *et al.*, "SCANDAL−a facility for elastic neutron scattering studies in the 50-130 MeV range", these proceedings.

[10] P. Mermod *et al.*, "Evidence of three-body force effects in neutron-deuteron scattering at 95 MeV", Phys. Rev. C **72**, 061002 (2005).

[11] P. Mermod *et al.*, "95 MeV neutron scattering on hydrogen, deuterium, carbon and oxygen", submitted to Phys. Rev. C (2006).

[12] J. Klug *et al.*, "Elastic neutron scattering at 96 MeV from ^{12}C and ^{208}Pb", Phys. Rev. C **68**, 064605 (2003).

[13] G.L. Salmon, "The elastic scattering of 96 MeV neutrons by nuclei", Nucl. Phys. **21**, 15 (1960).

[14] J.H. Osborne *et al.*, "Measurement of neutron elastic scattering cross sections for ^{12}C, ^{40}Ca, and ^{208}Pb at energies from 65 to 225 MeV", Phys. Rev. C **70**, 054613 (2004).

[15] A.J. Koning and J.P. Delaroche, "Local and global nucleon optical models from 1 keV to 200 MeV", Nucl. Phys. **A713**, 231 (2003);
A.J. Koning, S. Hilaire and M.C. Duijvestijn, "TALYS: Comprehensive Nuclear Reaction Modeling", Proceedings of the International Conference on Nuclear Data for Science and Technology, Santa Fe, USA, Sep. 26 - Oct. 1, 2004, CP769, 1154 (2005).

[16] B.A. Watson, P.P. Singh and R.E. Segel, "Optical-Model Analysis of Nucleon Scattering from 1p-Shell Nuclei between 10 and 50 MeV", Phys. Rev. **182**, 977 (1969).

[17] K. Amos, P.J. Dortmans, H.V. von Geramb, S. Karataglidis, and J. Raynal, "Nucleon-nucleus scatering: a microscopic nonrelativistic approach", Adv. Nucl. Phys. **25**, 275 (2000); S. Karataglidis, P.J. Dortmans, K. Amos, and R. de Swiniarski, "Multi-$\hbar\omega$ shell model analyses of elastic and inelastic proton scattering from ^{14}N and ^{16}O", Phys. Rev. C **53**, 838 (1996).

[18] R. Crespo, R.C. Johnson, and J.A. Tostevin, "Multiple scattering theory of proton elastic scattering at intermediate energies", Phys. Rev. C **46**, 279 (1992).

[19] ICRU Report 63, Nuclear Data for Neutron and Proton Radiotherapy and for Radiation Protection (International Commission on Radiation Units and Measurements, MD, 2000).

A monitor for neutron flux measurements up to 20 MeV

A. Öhrn[1], J. Blomgren[1], H. Park[2], S. Khurana[3], R. Nolte[3], D. Schmidt[3], and K. Wilhelmsen[4]

[1]*Department of Neutron Research, Uppsala University, Sweden*
[2]*Korean Research Institute of Standards and Science, Daejeon, Korea*
[3]*Physikalisch-Technische Bundesanstalt, Braunschweig, Germany*
[4]*Swedish Defense Research Agency, Stockholm, Sweden*
E-mail: angelica.ohrn@tsl.uu.se

A liquid scintillation detector aimed for neutron energy and fluence measurements in the energy region below 20 MeV has been calibrated using monoenergetic and white spectrum neutron fields. Careful measurements of the proton light output function and the response matrix have been performed allowing for the application of unfolding techniques using existing codes. The response matrix is used to characterize monoenergetic neutron fields produced by the T(d,n) at a low-energy deuteron accelerator installed at the Swedish Defense Research Agency (FOI).

International Workshop on Fast Neutron Detectors
University of Cape Town, South Africa
April 3 – 6, 2006

 http://pos.sissa.it

1. Introduction

The strongly expanding importance of fast neutrons in a number of applications requires steps to be taken to improve the technology for neutron fluence and energy measurements in various energy ranges. This requirement was addressed and the current situation summarized at a recent workshop, the International Workshop on Neutron Field Spectroscopy in Science held in Pisa, Italy, June 4 - 8, 2000 [1].

For the application considered in this work - a monitor for fluence and energy measurements in the energy region from a few MeV to about 20 MeV - there are several options possible, but if resolution and detection efficiency are taken into consideration, the most attractive alternatives seem to be the organic scintillator with or without applying time-of-flight techniques. In the present application the neutron source is continuous and therefore the time-of-flight technique is out of question. The obvious choice is therefore to perform pulse-height spectrum measurements and to apply unfolding techniques.

In the present paper a calibration procedure for a liquid scintillator with pulse-shape discrimination possibilities is described. The method is based on the procedures developed at the Physikalisch-Technische Bundesanstalt (PTB), Braunschweig, Germany [2] and involves measure-ments of pulse-height spectra and unfolding of these spectra with existing computer codes using carefully recorded response functions at several energies in the region of interest. The procedure presented in this paper goes beyond the previously applied methods in that both the experimental and calculated response matrices are used with existing unfolding codes to determine the energy and fluence of monoenergetic neutron fields and make comparisons with time-of-flight (TOF) methods.

2. Experimental methods

For neutron energies below 20 MeV, the response matrix of a scintillation detector can be calculated using Monte Carlo codes provided the specific light outputs for protons, deuterons and alpha particles are known for that particular detector. For energies above about 8 MeV, however, no available Monte Carlo code is capable of describing the response of a scintillation detector in full detail, because the required sufficiently detailed multi-differential emission cross sections for alpha particles from the $^{12}C(n,n'3\alpha)$ reaction are not available. Hence, the characterization of scintillation detectors always requires an experimental investigation of the detector response. The standard procedure developed at PTB for the characterization of scintillation detectors uses monoenergetic and breakup neutrons produced with the D(d,n) reaction.

The standard procedure is satisfactory for the application of the TOF method. For the application of unfolding techniques, however, a proper description of the full response matrix is required since any deviation of the response matrix from the 'true' pulse-height response of the detector would cause spurious structures in the unfolded spectral fluence.

For this purpose, a method described by Dekempeneer et al. [3] has been adopted. A white neutron beam measurement is used to obtain a smooth light output function for protons and an experimental response matrix with sufficient resolution in neutron energy. This method has been tested on a liquid scintillator to be used as a neutron monitor for a DT neutron generator, i. e., a commercial cylindrical detector cell of the MAB-1F type filled with BC501 scintillator liquid.

The PTB standard procedure for the determination of the relevant properties of an organic scintillation detector has been described in detail elsewhere [2]. Only the results obtained for the particular detector under study are summarized here.

Five neutron beams were produced by deuterons with energies of 5.01, 7.12, 9.06, 10.30, and 11.27 MeV using a deuterium gas target at the PTB neutron scattering facility. The energies of the monoenergetic neutrons were 7.95, 10.05, 11.93, 13.12, and 14.05 MeV. The maximum energy of the corresponding breakup continua was about 6.5 MeV below that of the monoenergetic neutrons. About 30 narrow TOF windows were placed on the monoenergetic neutrons and the breakup continuum to produce pulse-height spectra which were used to determine the proton light output and the efficiency of the detector.

The Monte Carlo code NRESP7 [4] was used to calculate pulse-height spectra for comparison with experimental spectra obtained at the five energies where monoenergetic neutrons from the $D(d,n)^3He$

reaction were available. By fitting these calculated spectra to the experimental ones, the light output function for protons, i.e., the pulse height corresponding to the recoil proton edge, was determined with an iterative procedure. The pulse height was measured using a calibration with photon sources.

The fluences of the monoenergetic neutrons were measured with the PTB 4"x1" NE213 reference detector. This detector was repeatedly compared with the PTB recoil proton telescope. For a selected pulse-height threshold, the efficiency of the detector is known with an uncertainty of about 1.5 % [5]. The mean ratio of the fluence determined with the present BC501 detector and that measured with the PTB reference detector was 1.018 +/- 0.009, which is within the range of results for other detectors [2].

A white neutron beam was produced at the PTB time-of-flight (TOF) facility by bombarding a thick Be target with a 19 MeV proton beam from the PTB isochronous cyclotron. The maximum energy of the neutron field at an emission angle of 0^o is 17.15 MeV. The neutron field was collimated by one of the collimators of the PTB TOF facility. The scintillation detector was positioned at a distance of 27.39 m from the Be target.

Energy calibration of the pulse-height spectra was established using ^{137}Cs, ^{22}Na and ^{207}Bi photon sources. The calibration of the measured pulse height in electron energies and the electronic offset were determined by fitting pulse-height spectra calculated with the PHRESP code [6] to the experimental spectra.

To establish an experimental response matrix, the PH spectra obtained with the white beam have to be normalized to unit fluence at the centre of the detector. This normalization was carried out by fitting PH spectra calculated with NRESP7 to the experimental ones. The fit was restricted to the region extending from the beginning of the flat plateau to the recoil proton edge. This region is essentially determined by np scattering and can be accurately described by NRESP7.

3. Test of calculated and experimental response matrices in monoenergetic neutron fields

In the present work it was considered important to test the calculated and experimental response matrices in well-defined monoenergetic neutron fields in an energy region of relevance for the actual application. Such a test was regarded as particularly relevant, because of the observed deviations between the experimentally determined response matrix and the calculated one.

The experimental response matrix was tested in monoenergetic neutron fields with energies between 14 MeV and 15.5 MeV. These fields were produced by the T(d,n)^{4}He reaction. Deuteron beams of 242, 412 and 643 keV were produced with the PTB 3.5 MeV van-de-Graaff accelerator. The spectral distributions of the neutron fields were calculated with the TARGET code [7]. The calculated average energies at 0^o were 14.85, 14.99 and 15.60 MeV, respectively, and the corresponding calculated FWHM of the peaks amounted to 451, 699 and 644 keV. For the 412 keV deuteron beam, measurements were also carried out at a neutron emission angle of 98^o. At this angle, the T(d,n)^{4}He reaction shows so-called kinematical focusing, i.e., the energy of the emitted neutrons is almost independent of the energy of the incident deuterons. Hence, broadening of the spectral distribution of the neutrons due to the energy loss of the deuterons in the Ti(T) layer is very small. In this particular case, the neutron field had a peak energy of 13.98 MeV and a FWHM of only 17 keV according to the TARGET calculations which were carried out neglecting the angular straggling of the deuterons in the target.

The pulse-height spectra obtained during the present measurements were unfolded with the MAXED code [8] which is part of the UMG code package [9]. It was known from the TOF measurements that the spectral neutron distribution showed a D(d,n) background peak between 2 MeV and 4 MeV in addition to the dominant T(d,n) peak at energies above 14 MeV. Using this preinformation, the unfolding was carried out in two steps. First, a high PH threshold of 7 MeV corresponding to a neutron energy of a about 11.2 MeV was used to select those events which could not be caused by the low-energy background. The spectral fluence distribution obtained from this restricted unfolding exhibited a prominent peak and some background at intermediate energies. Second, this peak was used as preinformation for the next step of the unfolding procedure that comprised the pulse-height spectrum above a PH threshold of 280 keV.

4. Results and discussion

The experimental and calculated response matrices were applied with unfolding codes available in the literature to determine the energy and fluence of monoenergetic neutron fields. Comparison with results from TOF measurements was performed.

Determination of the neutron energy has been performed from experiments performed with neutron energies of 13.98, 14.85 and 15.60 MeV. The pulse-height spectrum has been unfolded using MAXED as well as GRAVEL, the latter being another unfolding code in the UMG package [10]. Both codes give a good description of the neutron distribution. However, some spurious structures are generated especially in the low-energy region. A small structure around 11 MeV can also be seen (see Fig. 1). There is no significant difference between GRAVEL and MAXED when determining the neutron energy (see Table 1). The result from unfolding with the experimental response matrix is in better agreement with the result from the TOF measurements than the result from the calculated response matrix.

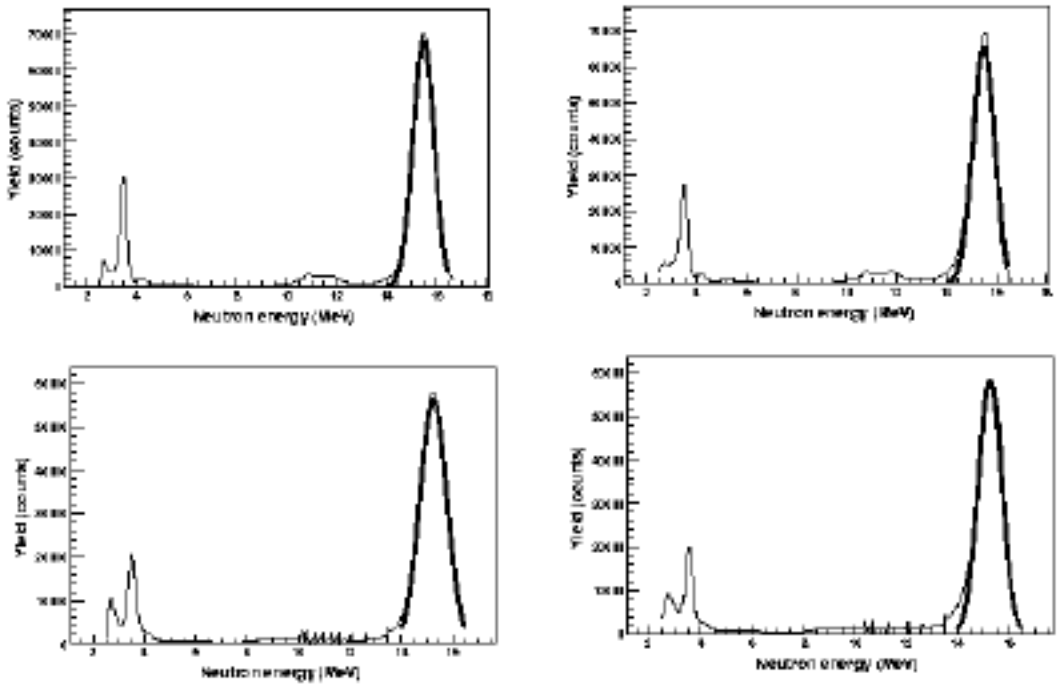

Fig. 1. Results from the 15.60 MeV measurements. The unfolding in the left panels are performed with GRAVEL and those in the right panels with MAXED. In the upper panels the experimental response is used and in the lower panels the calculated one.

The absolute efficiency of the detector has been determined using the PTB proton recoil telescope. These measurements have verified that the efficiency, in terms of total number of counts in the detector above a threshold set at a low pulse height, agrees with what can be expected with the used tagged neutron flux. This has been corroborated using the fact that the pulse height spectrum in the high-energy end is dominated by events due to np scattering, because the np scattering cross section is well known at these energies.

The neutron fluence has been determined by integrating the T(d,n) peak from $E_0 - \Gamma$ to $E_0 + \Gamma$, where E_0 is the centroid and Γ is the FWHM (see Fig. 1). The intrinsic uncertainty of this method has been determined to 0.5 % on the average with a worst case of 1.0 %.

Table 1. Results of the neutron energy measurements. Errors are statistical only.

E_n = 13.98 MeV

Unfolding code	Response matrix	Neutron energy (MeV)
GRAVEL	Experimental	13.91 +/- 0.02
GRAVEL	Calculated	13.67 +/- 0.01
MAXED	Experimental	13.92 +/- 0.03
MAXED	Calculated	13.70 +/- 0.02

E_n = 14.85 MeV

GRAVEL	Experimental	14.69 +/- 0.02
GRAVEL	Calculated	14.43 +/- 0.01
MAXED	Experimental	14.71 +/- 0.03
MAXED	Calculated	14.47 +/- 0.02

E_n = 15.60 MeV

GRAVEL	Experimental	15.48 +/- 0.01
GRAVEL	Calculated	15.26 +/- 0.01
MAXED	Experimental	15.51 +/- 0.03
MAXED	Calculated	15.26 +/- 0.01

The fluence obtained from the time-of-flight spectrum from the 15.60 MeV measurement agrees well with the fluence derived from unfolding with the experimental response matrix. The deviations are 0.7 % (GRAVEL) and 1.9 % (MAXED). The deviations are significantly larger in the unfolding with the calculated response matrix, 1.6 % (GRAVEL) and 5.8 % (MAXED). In all cases, the fluence obtained from unfolding is lower than that from the TOF information. Based on this information, it is concluded that the fluence can be determined with an uncertainty of 2 % using this method.

5. Conclusions

The present work has shown that measurements in white neutrons beams can provide additional information for the specification of scintillation detectors which cannot be obtained with monoenergetic neutron beams alone. In particular, smoother experimental light outputs can be obtained and the deficiencies of the present Monte Carlo codes used for the calculation of response matrices can be circumvented. On the other hand, the application of the TOF method for the determination of experimental response matrices with white neutron beams requires very careful experimental work to avoid artefacts like those observed in the present data for neutron energies above 12 MeV. The application of the unfolding technique with experimentally determined response matrices provides a possibility for spectrometry in neutron beams over a large energy range. The present work has shown that even quite small spectral details can be resolved in the presence of other dominant structures.

6. Acknowledgements

The authors are indebted to A. Zimbal for guiding them through the technical pitfalls of the unfolding codes and for numerous discussions on this subject. The support of K. Tittelmeier, A. Toll and the staff of the PTB accelerator facility is gratefully acknowledged.

References

[1] Proc. of the Int. Workshop on Neutron Field Spectrometry in Science, Technology and Radiation Protection, Pisa, Italy, June 4--8, 2000. Ed.: H. Klein, D. Thomas, H.G. Menzel, G. Curzio, and F. d'Errico, Nucl. Instr. Meth. Phys. Res. A **476**, Issues 1-2, 1 (2002).

[2] D. Schmidt, B. Asselineau, R. B\"ottger, H. Klein, L. Lebreton, S. Neumann, R. Nolte, and G. Pichenot, Nucl. Instr. Meth. Phys. Res. A **476**, 186 (2002).

[3] E. Dekempeneer, H. Liskien, L. Mewissen, and F. Poortmans, Nucl. Instr. Meth. Phys. Res. A **256**, 489 (1987)

[4] G. Dietze and H. Klein, "NRESP4 and NEFF4: Monte Carlo Codes for the Calculation of Neutron Response Functions and Detection Efficiencies for the NE213 ScintillationDetectors", PTB Report PTB-ND-22, Physikalisch-Technische Bundesanstalt Braunschweig,1982, (and an informal supplement describing the changes of version 7, 1991).

[5] D. Schmidt and H. Klein, Precise Time-of-Flight Spectrometry of Fast Neutrons - Principles, Methods and Results. PTB Report PTB-N-35, Physikalisch-Technische Bundesanstalt Braunschweig, 1998.

[6] T. Novotny, "Photon Spectrometry in Mixed Neutron- Photon Fields using NE213 Liquid Scintillation Detectors", PTB Report PTB-N-28, Physikalisch-Technische Bundesanstalt Braunschweig, 1997.

[7] D. Schlegel, "TARGET User´s Manual", PTB Laboratory Report PTB-6.41-98-1, Physikalisch-Technische Bundesanstalt Braunschweig, 1998.

[8] M. Reginatto, P. Goldhagen, and S. Neumann, Nucl. Instr. Meth. Phys. Res. A **476**, 242 (1989).

[9] M. Reginatto, B. Wiegel, and A. Zimbal, UMG-Code Package, available from the Nuclear Energy Agency (NEA) Data Bank, http://www.nea.fr.

Appendix XV

TOMOGRAPHY OF CANISTERS FOR SPENT NUCLEAR FUEL

M. Österlund*[1], J. Blomgren[1], J. Donnard[1,4], A. Flodin[1], J. Gustafsson[1], M. Hayashi[1,5], P. Mermod[1], L. Nilsson[1], S. Pomp[1], L. Wallin[1], A. Öhrn[1], A.V. Prokofiev[2]

[1]*Department of Neutron Research, Uppsala University, Sweden*
[2]*The Svedberg Laboratory, Uppsala University, Sweden*
[3]*Fast Neutron Research Facility, Chiang Mai University, Thailand*
[4]*Ecole des Mines de Nantes, France*
[5]*Department of Advanced Energy Engineering Science, Kyushu University, Japan*
E-mail: Michael.Osterlund@tsl.uu.se

Sweden and Finland are preparing for final deposition of spent nuclear power fuel. The adopted method is to encapsulate spent nuclear fuel in copper canisters filled with iron before deposition in a deep bedrock repository. The canisters will have a diameter of about one metre, which makes examination of the content in sealed canisters virtually impossible with any known technique today.

Two methods for tomography of sealed canisters have been studied, high-energy neutron tomography and cosmic-ray muon tomography. Monte Carlo simulations using MCNPX have shown that it would indeed be possible to produce images of good resolution of thick massive objects, like these canisters, using high-energy neutrons. The cost for installing such a method would, however, be very high. GEANT simulations, supported by experimental tests, indicate that tomography using the natural flux of cosmic-ray muons results in images of lower quality, but to a much more modest cost, acceptable to the application.

International Workshop on Fast Neutron Detectors and Applications
April, 3 - 6, 2006
University of Cape Town, South Africa

*Speaker.

Figure 1: Canisters for spent BWR nuclear fuel. The canister consists of a cylindrical copper shell with a pressure-bearing insert of nodular iron. The outer diameter is 1.05 m and the length 4.83 m [1].

1. Introduction

In Swedish nuclear power plants, a once-through fuel cycle is adopted where it is envisioned that the spent nuclear fuel will be encapsulated in copper canisters with iron inserts as seen in Fig. 1. The canisters will be deposited in bedrock, embedded in clay, at a depth of about 500 m [1]. The rock is expected to isolate and protect the waste and also to provide a stable chemical environment that will not change for the next 100 000 years.

Today, the only known method for investigating the interior of a sealed canister is to open it, which is not a viable proposition. Consequently, verification of the content of canisters would have to be based on documentation and seals, which would have limited reliability. In order to adress this issue, two possible methods for radiograpich imaging of thick massive objects have been investigated, fast-neutron radiography and cosmic-muon radiography.

Research on high-energy ($E_{\mathrm{n}} > 15$ MeV) neutron radiography/tomography has been performed at Los Alamos National Laboratory LANL since 1990 [2]. Unfortunately, no results have been published since 1997 when the project was classified. Because of the high cost associated with the production and the detection of high-energy neutrons, alternative lower cost methods are of particular interest. One such method, cosmic-ray muon radiography [3], that is being developed for the detection of nuclear contraband by LANL may be of used for inspection of canisters for spent nuclear fuel.

2. Neutron tomography

High-energy neutron tomography offers unique possibilities compared to other imaging techniqies, most notable great penetrating power and sensitivity to light elements. In general, the penetration of neutrons increases with energy, opening up the possibility for imaging of large massive objects, which is impossible with the tomographic methods commonly available today. For many nuclides the total cross section, σ_T, exhibits a fairly wide minimum around 300 MeV [4] resulting in maximum penetration. High energy neutrons are usually produced through direct particle-neutron interactions of charged particles against light nuclei or by spallation. This involves the use

of accelerators such as synchrotrons or linacs, the cost of which is a steep function of energy. Also, high energy neutrons are difficult to detect, often involving a conversion process followed by the detection of the resulting charged particles in position sensitive detectors such as drift-chambers. Considering the economical and technical difficulties of generating high-energy neutrons and the availablitity of existing facilities, 100 MeV has been found to be a reasonable good compromise for the present application.

3. Simulations of neutron radiography in MCNPX

In order to investigate the potential of fast-neutron imaging simulations have been performed in MCNPX [5]. The studies have been concentrated on general aspects of fast-neutron tomography, i.e., contrast, the effect of voids inside dense objects and element sensitivity [6].

For the simulations, a simple axial-symmetric geometry consisting of a 100 MeV point neutron source, an object in the shape of a truncated right angle cone and an ideal detector, was used. The center of the 1.0 m thick target was situated 4.5 m from the source and the detector was positioned 5.5 m from the source.

The contrast between a massive object and air was studied using a solid iron object. The observed transmission of neutrons was approx. $2 \cdot 10^{-5}$. When observing the detector signal near the edge of the shadow projected on the detector by the object, it was observed that the signal falls off by a factor 10^{-5} over a distance of less then 1 mm, which is indicative of the resolution.

In order to simulate the effects of voids, a composite iron object consisting of a hollow truncated cone with a wall thickness of 1.0 cm, into which is inserted another solid truncated cone such as to create a uniform 1.0 mm wide void between the cones was used. Simulations were performed with the void extending either along the whole length of the object or being confined to the interior of the object. In the latter case, voids of length 20 cm, 30 cm and 60 cm were simulated.

The viods gave rise to detector signals that in 1D projections are well described by Gaussians. Voids with lengths down to 30 cm could be clearly seen, but for a 20 cm long void the signal was lost in the statistical fluctuations. In all cases the width of the Gaussian was approximately 0.12 cm, implying an intrinsic resolution of $\sigma = 0.04$ cm.

The attenuation of neutrons travelling through any material is caused by nuclear reactions and elastic scattering. Limits on the attenuation can be derived using the total cross section and the reaction cross section, the former giving the maximum limit and the latter giving the minimum limit.

In order to investigate the possibility of distinguishing between different materials, simulations with solid objects made of Fe, U, Pb and liquid H_2 were performed. The transmissions through Fe and U are approximately equal, $2 \cdot 10^{-5}$, whereas for Pb it is $4 \cdot 10^{-5}$. As a comparison, the observed transmission for liquid H_2 was 0.80.

As could be expected the attenuation in liquid H_2, which has a low density and a small total cross section, deviates significantly from the attenuation in the high-Z elements. The only non-elastic process is capture, ^{1}H(n,γ)^{2}H, which has a very small cross section. This means that in liquid H_2 almost all attenuation is due to elastic scattering and because of the fairly isotropic angular distribution of elastic scattering against hydrogen, almost all elastically scattered neutrons are lost.

For the high-Z elements Fe, Pb and U the elastic scattering angular distribution is strongly forward-peaked and a large fraction of the elastically scattered neutrons are detected close to the position of the unscattered neutrons. The attenuation in Pb is a factor of two less than what is the case in Fe and U. This effect is expected because the number of nuclei per volume in Pb is fairly small compared to Fe and U. The simulated attenuations in Fe and U are similar even though the cross section for Fe is much smaller than for U. On the other hand, the number of nuclei per unit volume is larger for Fe. It is possible that these two effects happen to balance each other at this specific energy, resulting in a similar attentuations. The effects of small-angle scattering, which is different for Fe and U, can influence the result. Small-angle scattering can also be expected to change with energy unequally for these two elements. It is therefore conceivable that a combination of neutron tomography at more than one energy could result in element sensitivity. Quantitative assessment of this hypothesis would require repetition of the simulations above at higher energies.

4. Cosmic-ray muon tomography

High-energy muons are created when cosmic rays interact with nuclei in the upper layers of the atmosphere. At the surface of the earth the average energy is $E_\mu = 3-4$ GeV, the flux is approximately 10^4 m^{-2}min^{-1} and the angular distribution with respect to zenith is close to $\cos^2(\theta)$. In contrast to neutrons which only interacts strongly, muons interact through Coulomb and weak forces. At energies typical for cosmic-ray muons, the stopping power is approx. 2.2 MeVcm^{2}g^{-1} giving the muons a range of approx. 1.7 m in Fe and 0.7 m in U [12] which is sufficient for the intended application.

Because of the low flux of muons, the measurement time necessary to obtain sufficient statistics for conventional attenuation measurements [10] is prohibitive. An alternative approach is needed where as much information about an object as possible is inferred from each individual muon. A practical proposition is to measure the scattering that muons are subjected to when traversing an object.

The scattering distribution of muons is approximately Gaussian [11]

$$\frac{dN}{d\theta} = \frac{1}{\sqrt{2\pi}\theta_0} e^{-\frac{\theta^2}{2\theta_0^2}}. \tag{4.1}$$

and the width of the distribution depends on material and muon properties

$$\theta_0 = \frac{13.6MeV}{\beta cp}\sqrt{\frac{L}{L_0}}\left[1+0.038\ln\left(\frac{L}{L_0}\right)\right], \tag{4.2}$$

where p is the momentum of the particle in MeV/c, L_0 is the radiation length and L is the thickness of the target. Generally speaking, the radiation length decreases with the charge density of the material. A high-Z material with high density has a shorter radiation length and therefore muons will be deflected by a larger angle in a high-Z material. For Fe, Pb and U the mean scattering angles are 10.8 mrad, 20.0 mrad and 26.9 mrad respectively. For low-Z materials the average scattering angle is too small to be of any particular use for radiography purposes.

In order to investigate the possibilities of this method a small-scale experiment system has been developed for initial experiments using available equipment [7, 8] and simulations of muon scattering in canisters for spent nuclear fuel have been performed [9].

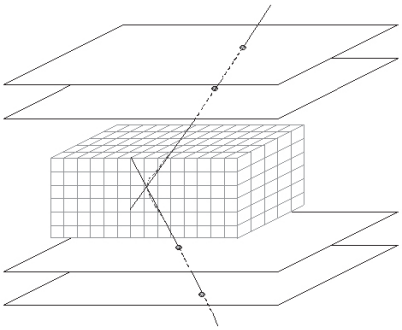

Figure 2: Schematic of a detector system. Two position sensitive detectors above the target area and two below provide muon tracking information. The actual track of the muon through the target is approximated by two straight lines in order to determine a virtual scattering point. The target volume is divided into voxels, i.e., 3D pixels.

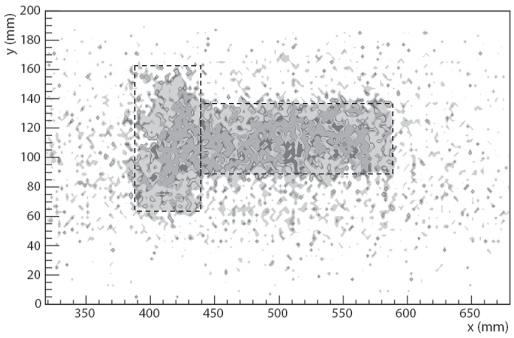

Figure 3: A 2D image of a 50 mm thich T-shaped target reconstructed from approx. 3500 POCAs. The dashed lines indicate the actual outline of the target.

4.1 Experimental measurements

For the small-scale experiment, pairs of drift chambers positioned above and below a target area were used for muon tracking. Plastic scintillators placed at the extreme top and bottom of the setup were used for particle identification and triggering 2. A simple object of lead in the shape of the character T served as target.

Because muons are continuously scattered by the electric charge of atoms in the target material, the actual path of individual muons inside the target volume cannot be determined and assumptions have to be made. One simple assumption is to consider the continous scattering to be taking place in a single point. This virtual scattering point is simply determined by extrapolating entrance and exit tracks reconstructed from drift chamber information and determining the point in space that is closest to both tracks. This point of closest approach (POCA) is considered a good point estimate for where the muon is scattered.

In order to perform the image reconstruction a target volume enclosing the target is divided into voxels, i.e. 3D pixels. For each POCA determined, the corresponding voxel is incremented using the scattering angle squared as a weighting function. The weighting function is motivated

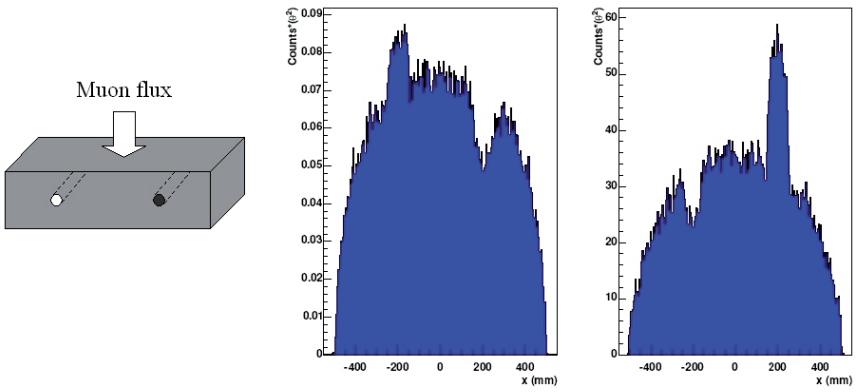

Figure 4: 1D-projections of the image obtained from a rectangular slab of iron $l \times d \times h = 1000 \times 200 \times 250$ mm^3. In the slab there are two cylindrical voids ($d = 50$mm), filled with air and uranium. In the left panel, only POCAs with scattering angles $0 < \theta < 13$ mrad are included, whereas in the right panel only POCAs with scattering angles $\theta > 13$ mrad are included.

by the fact that a large scattering angle indicates the presence of high-Z material and also that the position accuracy of the POCA increases with larger scattering angles.

A typical result of the initial experiments is shown in Fig. 3. In the image the contrast, i.e., the signal to background ratio, is 15.0 $\pm$0.8. The image resolution, determined by fitting a Wood-Saxon function to the edges of the reconstructed image was 2.1 mm.

4.2 Simulation of muon scattering

Geant4 [13] has been used to simulate muon scattering in materials of significance for the long time storage of spent nuclear fuel, e.g., Fe and U. The emphasis was on determining the possibility of detecting the prescence of uranium in an iron environment and on determining whether it is possible to distinguish a single fuel bundle inside a canister for spent nuclear fuel or not.

In Fig. 4 it is shown how muon scattering allow voids, filled with air and uranium, inside an iron slab can be distinguished. By selecting POCAs with different scattering angles it is possible to put the emphasis of the selection towards lighter or heavier elements.

A model of a canister for spent nuclear fuel filled with typical fuel bundles, each containing 8×8 uranium fuel rods, was used to investigate the possibility of detecting if a single fuel bundle is missing as seen in Fig. 5. The resulting histogram was obtained by image subtraction. An image from a reference canister with all fuel bundles present was subtracted from an image of a canister with one fuel bundle missing and the result projected into a histogram. If the contents of the canisters are identical, only statistical fluctuations would remain. Position information from the POCAs has been used to put a geometrical gate that only selects events occuring in the third row of fuel bundle positions. The result was obtained from a flux of $6 \cdot 10^5$ muons, corresponding to a measurement time of 15 minutes.

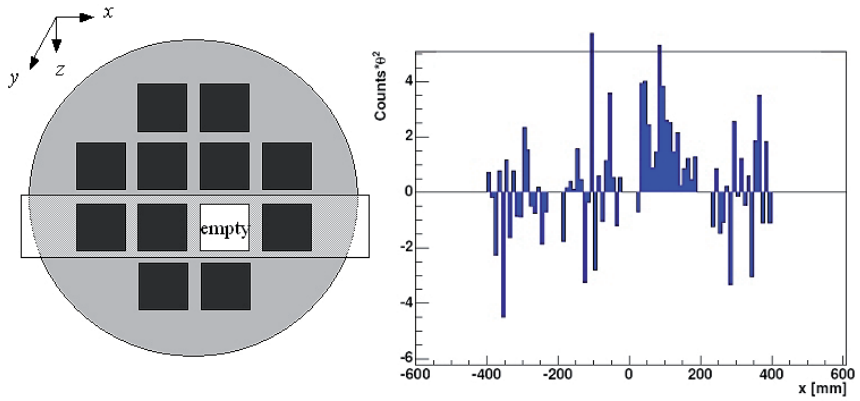

Figure 5: Simulation of a canister for spent nuclear fuel with one fuel bundle missing. The signal is obtained by image subtraction. A position gate, selecting POCAs within the rectangular area, is used to enhance the signal.

5. Conclusion

Fast neutron attenuation measurements and cosmic-ray muon scattering has potential for the imaging of canisters for spent nuclear fuel. High-energy neutron tomography offer the best possibility of high resolution imaging, albeit at high cost and with little possibility to distinguish between different materials. Cosmic-ray muon scattering tomography does not offer the high resolution of neutron tomography, but the method is much less expensive and offers some ability to distinguish between low, medium and high Z-materials. The method can be used to detect missing fuel bundles inside a sealed canister for spent nuclear fuel whithin a reasonable time span, i.e., 15 minutes. The POCA method for reconstruction of images is too simplistic for the intended application. More effort is needed in this area, as conventional tomographic transform-based methods cannot be used, but instead algebraic reconstruction methods must be utilised.

Acknowledgments

This work was financially supported by the Swedish Nuclear Power Inspectorate (SKI).

References

[1] Homepage of the Swedish Nuclear Fuel and Waste Management Co. (SKB), http://www.skb.se/, 2006.

[2] T.N. Taddeucci, C.L. Morris, K.B. Morley, J. Selden, http://lansce.lanl.gov, 1997.

[3] L.J. Schultz, et al., Nucl. Instr. and Meth. **A 519**, 687 (2004).

[4] R.W. Finlay, et al., Phys. Rev. C **47**, 237 (1993).

[5] L.S. Waters, *MCNPX User's Manual*, Los Almos National Laboratory, September, 2002.

[6] L. Wallin, Uppsala University Neutron Physics Report, UU-NF 05#02, February, 2005.

[7] J. Donnard, *Rapport de synthèse*, Uppsala University, Dept. of Neutron Res. Internal Report (2004).

[8] A. Flodin, Uppsala University Master of Science Thesis, UPTEC F05 035 (2005).

[9] J. Gustafsson, Uppsala University Master of Science Thesis, UPTEC F05 077 (2005).

[10] L.W. Alvarez., Science **167**, 832 (1970).

[11] K.N. Borozdin, et al., Nature **422**, 277 (2003).

[12] D.E. Groom, N.V. Mokhov and S.I. Striganov, Atomic Data and Nuclear Data Tables **78**, 183 (2001).

[13] S. Agostinelli, et al., Nucl. Instr. and Meth. **A 506**, 250 (2003).

ELASTIC NEUTRON SCATTERING STUDIES AT 96 MeV ON ELEMENTS OF INTEREST FOR TRANSMUTATION

M. Österlund*[1], J. Blomgren[1], M. Hayashi[1,4], J. Klug[1,5], P. Mermod[1], L. Nilsson[1], S. Pomp[1], A. Öhrn[1], A.V. Prokofiev[2], U. Tippawan[1,3]

[1] *Department of Neutron Research, Uppsala University, Sweden*
[2] *The Svedberg Laboratory, Uppsala University, Sweden*
[3] *Fast Neutron Research Facility, Chiang Mai University, Thailand*
[4] *Department of Advanced Energy Engineering Science, Kyushu University, Japan*
[5] *Forschungszentrum Rossendorf, Dresden, Germany*
E-mail: Michael.Osterlund@stsl.uu.se

Elastic neutron scattering from ^{12}C, ^{14}N, ^{16}O, ^{28}Si, ^{40}Ca, ^{56}Fe, ^{89}Y and ^{208}Pb has been studied at 96 MeV in the $10-70$ degree interval, using the SCANDAL (SCAttered Nucleon Detection AssembLy) facility. The results for ^{12}C and ^{208}Pb have recently been published, while the data on the other nuclei are under analysis. The achieved energy resolution, 3.7 MeV, is about an order of magnitude better than for any previous experiment above 65 MeV incident energy. A novel method for normalization of the absolute scale of the cross section has been used. The estimated normalization uncertainty, 3 %, is unprecedented for a neutron-induced differential cross section measurement on a nuclear target.

Elastic neutron scattering is of utmost importance for a vast number of applications. Besides its fundamental importance as a laboratory for tests of isospin dependence in the nucleon-nucleon, and nucleon-nucleus, interaction, knowledge of the optical potentials derived from elastic scattering come into play in virtually every application where a detailed understanding of nuclear processes are important.

Applications for these measurements are nuclear waste incineration, single event upsets in electronics and fast neutron therapy. The results at light nuclei of medical relevance (^{12}C, ^{14}N and ^{16}O,) are presented separately. In the present contribution, results on the heavier nuclei are presented, among which several are of profound relevance to accelerator-driven systems for transmutation.

International Workshop on Fast Neutron Detectors and Applications
April, 3 - 6, 2006
University of Cape Town, South Africa

*Speaker.

1. Introduction

The interest in high-energy neutron data is rapidly growing, since a number of potential large-scale applications involving fast neutrons are under development, or at least have been identified. These applications primarily fall into three sectors; nuclear energy and waste, nuclear medicine, and effects on electronics. For all these applications, an improved understanding of neutron interactions is needed for calculations of neutron transport and radiation effects. The nuclear data needed for this purpose come almost entirely from nuclear scattering and reaction-model calculations, which all depend heavily on the optical model, which in turn is determined by elastic scattering and total cross-section data.

The nuclear data needs for transmutation of nuclear waste in general and spent nuclear fuel in particular are outlined in refs. [1, 2, 3], while the needs for neutron therapy of cancer tumours are reviewed in ref. [4], and upsets in electronics are discussed in ref. [5, 6]. In the present work, a programme on elastic neutron scattering at 96 MeV is presented, which deals with all these applications.

Neutron-scattering data are also important for a fundamental understanding of the nucleon-nucleus interaction, in particular for determining the the isovector term [7]. Coulomb repulsion of protons creates a neutron excess in all stable nuclei with $A > 40$. Incident protons and neutrons interact differently with this neutron excess. The crucial part in these investigations has been neutron-nucleus elastic scattering data to complement the already existing proton-nucleus data. Above 50 MeV neutron energy, there has been only one previous measurement on neutron elastic scattering with an energy resolution adequate for resolving individual nuclear states, an experiment at UC Davis at 65 MeV on a few nuclei [8]. In addition, a few measurements in the $0-20^\circ$ range are available, all with energy resolution of 20 MeV or more. This is, however, not crucial at such small angles because elastic scattering dominates heavily, but at larger angles such a resolution would make data very difficult to interpret. Recently, results on neutron scattering from ^{12}C, ^{40}Ca and ^{208}Pb in the $65-225$ MeV range from Los Alamos have been published [9]. The energy resolution is comparable to the present work, but the angular range is limited to $7-23^\circ$.

2. Experimental setup

The neutron beam facility at The Svedberg Laboratory, Uppsala, Sweden, has recently been described in detail [10], and therefore only a brief description is given here. The 96 ± 0.5 MeV (1.2 MeV FWHM) neutrons were produced by the ^{7}Li(p,n) reaction by bombarding a 427 mg/cm^2 disc of isotopically enriched (99.98 %) ^{7}Li with protons from the cyclotron. The low-energy tail of the source-neutron spectrum was suppressed by time-of-flight techniques. After the target, the proton beam was bent into a well-shielded beam dump. A system of three collimators defined a 9 cm diameter neutron beam at the scattering target.

Scattered neutrons were detected by the SCANDAL (SCAttered Nucleon Detection AssembLy) setup [10]. It consists of two identical systems, placed to cover $10-50^\circ$ and $30-70^\circ$, respectively. The energy of the scattered neutrons is determined by measuring the energy of proton recoils from a plastic scintillator, and the angle is determined by tracking the recoil proton. In the present experiment, each arm consisted of a 2 mm thick veto scintillator for fast charged-particle

rejection, a 10 mm thick neutron-to-proton converter scintillator, a 2 mm thick plastic scintillator for triggering, two drift chambers for proton tracking, a 2 mm thick ΔE plastic scintillator that was also part of the trigger, and an array of CsI detectors for energy determination of recoil protons produced in the converter by np scattering. The trigger was provided by a coincidence of the two trigger scintillators, vetoed by the front scintillator. The total excitation energy resolution varies with CsI crystal, but is on average 3.7 MeV (FWHM). The angular resolution is in the $1.0 - 1.3^\circ$ (rms) range.

3. Results and discussion

Angular distributions of elastic-neutron scattering from ^{12}C and ^{208}Pb at 96 MeV incident neutron energy are presented in Fig. 1. The data are compared with phenomenological and microscopic optical-model predictions in the left and right panels, respectively. The theoretical curves have all been folded with the experimental angular resolution to facilitate comparisons with data. The data by Salmon at 96 MeV [11] are also shown. The angular distributions presented have been corrected for reaction losses and multiple scattering in the target. The contribution from other isotopes than ^{208}Pb in the lead data has been corrected for, using cross section ratios calculated with the global potential by Koning and Delaroche [12].

The absolute normalization of the data has been obtained from knowledge of the total elastic cross section, which has been determined from the difference between the total cross section (σ_T) [13] and the reaction cross section (σ_R) [14, 15]. This σ_T - σ_R method, which is expected to have an uncertainty of about 3 %, has been used to normalize the ^{12}C data. The ^{208}Pb(n,n) data have been normalized relative to the ^{12}C(n,n) data, knowing the relative neutron fluences, target masses, etc. The total elastic cross section of ^{208}Pb has previously been determined with the σ_T - σ_R method. The accuracy of the present normalization has been tested by comparing the total elastic cross-section ratio (^{208}Pb/^{12}C) obtained with the σ_T - σ_R method above, and with the ratio determination of the present experiment, the latter being insensitive to the absolute scale. These two values differ by about 3 %, i.e., they are in agreement within the expected uncertainty.

A novel technique for normalization, which is based on relative measurements versus the *np* scattering cross section [16], has also been tested and was found to have an uncertainty of about 10 %.

The data are compared with model predictions in Fig. 1, where the left and right panels show phenomenological and microscopic models, respectively. The models are described in detail in refs. [17] and [18].

When comparing these predictions with data, a few striking features are evident. First, all models are in reasonably good agreement with the ^{208}Pb data. It should be pointed out that none of the predictions contain parameters adjusted to the present experiment. In fact, they were all made before data were available. Even the absolute scale seems to be under good control, which is remarkable, given that neutron beam intensities are notoriously difficult to establish. Second, all models fail to describe the ^{12}C data in the $30 - 50^\circ$ range. The models predict a saddle structure, which is not evident from the data.

This mismatch has prompted a re-examination of the ^{12}C(n,n) cross section. Fortunately, this could be accomplished in combination with another experiment. Recently, we have studied *nd*

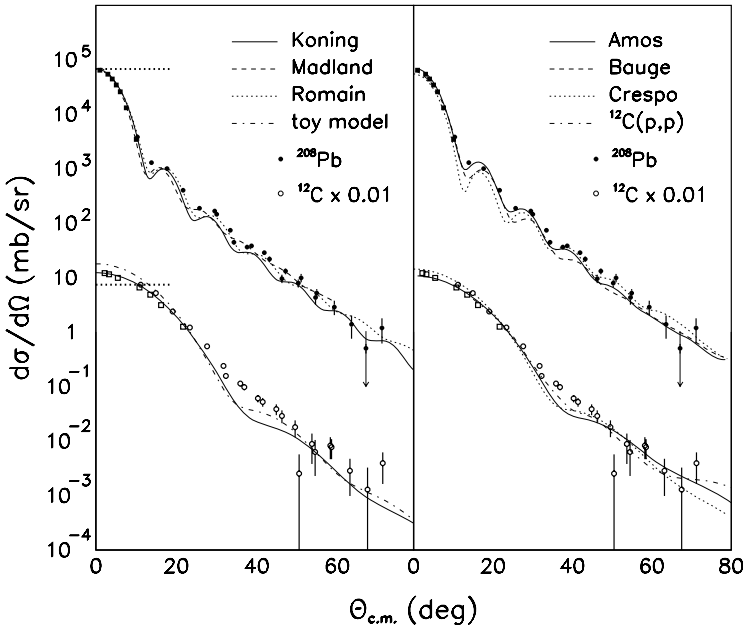

Figure 1: Angular distributions of elastic neutron scattering from ^{12}C (open circles) and ^{208}Pb (solid) at 96 MeV incident neutron energy. The ^{12}C data and calculations have been multiplied by 0.01. The data by Salmon at 96 MeV [11] are shown as squares. Left panel: predictions by phenomenological models. The thick dotted horizontal lines show Wick's limit for the two nuclei. Right panel: predictions by microscopic models, and data on elastic proton scattering from ^{12}C [22]. See the text for details, and refs. [17, 18] and references therein for a description of the theory models.

scattering at the same energy to investigate three-nucleon interaction effects. These results show clear evidence of such 3*N* forces [19, 20, 21]. In these experiments, scattering from carbon was used for normalization, as described above. The size of the target was, however, significantly larger than in the experiments above, resulting in far better statistics. This allowed more stringent analysis procedures to be used, and the results seem to indicate that the ^{12}C elastic scattering cross section is actually in agreement with the theory models. Thus, the main reason for the discrepancy above was probably due to an unbalance between the ground state and the first excited state in the analysis, resulting from the poor statistics for the excited state.

A basic feature of the optical model is that it establishes a lower limit on the differential elastic-scattering cross section at 0° if the total cross section is known, often referred to as Wick's limit [23, 24]. It has been observed in previous experiments at lower energies that for most nuclei, the 0° cross section falls very close to Wick's limit, although there is no a priori reason why the cross section cannot exceed the limit significantly. An interesting observation is that the present ^{208}Pb data are in good agreement with Wick's limit, while the ^{12}C 0° cross section lies about 70 % above the limit. A similar behaviour has previously been observed in neutron-elastic scattering at 65 MeV [8], where the ^{12}C data overshoot Wick's limit by about 30 %, whilst the ^{208}Pb data agree

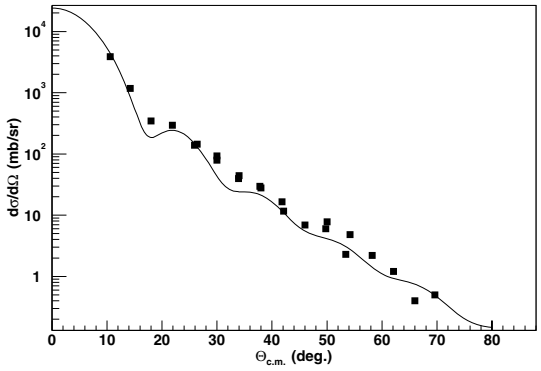

Figure 2: Preliminary angular distribution of elastic neutron scattering from ^{89}Y at 96 MeV incident neutron energy together with a prediction by the Koning-Delaroche potential [12].

with the limit.

It has recently been shown by Dietrich et al. [25] that this makes sense. Using the Koning-Delaroche potential [12], it has been shown that Wick's limit actually deviates less than 5 % from an equality for ^{208}Pb over the entire $5-100$ MeV interval. The lightest nucleus investigated was ^{28}Si, but the systematics imply that large discrepancies for ^{12}C should be expected.

Preliminary data on ^{89}Y are presented in Fig. 2, together with the Koning-Delaroche potential [12]. The data have been normalized to the model and it can be seen that it describes the shape of the data points reasonably well. The measurements on ^{16}O have been analyzed and are presented in another contribution to this workshop. Measurements on ^{14}N, ^{28}Si, ^{40}Ca, and ^{56}Fe have been completed and the data are under analysis.

4. Conclusions and outlook

In short, first results on elastic-neutron scattering from ^{12}C and ^{208}Pb at 96 MeV incident neutron energy are presented, and compared with theory predictions. This experiment represents the highest neutron energy where the ground state has been resolved from the first excited state in neutron scattering. The measured cross sections span more than four orders of magnitude. Thereby, the experiment has met - and surpassed - the design specifications. The overall agreement with theory model predictions, both phenomenological and microscopic, is good. In particular, the agreement in the absolute cross-section scale is impressive.

Performance investigations have revealed that the method as such should work also at higher energies. Recently, the TSL neutron beam facility has been upgraded in intensity, making measurements at the highest energy, 180 MeV, feasible. An experimental campaign at 180 MeV does, however, require an upgrade of the CsI detectors of SCANDAL.

Acknowledgments

This work was financially supported by the Swedish Nuclear Fuel and Waste Management Company, the Swedish Nuclear Power Inspectorate, Ringhals AB, Forsmarks Kraftgrupp AB, the

Swedish Defense Research Agency, the Swedish Nuclear Safety and Training Centre, and the European Union.

References

[1] A. Koning, et al., J. Nucl. Sci. Tech., Suppl. **2** (2002) 1161.

[2] J. Blomgren, in Proceedings of Workshop on Nuclear Data for Science & Technology: Accelerator Driven Waste Incineration, Trieste, Italy, Sept. 10-21, 2001, eds. M. Herman, N. Paver, A. Stanculescu, ICTP lecture notes **12** (2002) 327.

[3] J. Blomgren, Nuclear data for accelerator-driven systems - Experiments above 20 MeV, in Proceedings of EU enlargement workshop on Neutron Measurements and Evaluations for Applications, Bucharest, Romania, October 20-23, 2004.

[4] J. Blomgren and N. Olsson, Radiat. Prot. Dosim. **103(4)** (2003) 293.

[5] J. Blomgren, B. Granbom, T. Granlund, N. Olsson, Mat. Res. Soc. Bull. **28** (2003) 121.

[6] J. Blomgren, Nuclear Data for Single-Event Effects, in Proceedings of EU enlargement workshop on Neutron Measurements and Evaluations for Applications, Budapest, Hungary, November 5-8, 2003. EUR Report 21100 EN, Luxembourg: Office for Official Publications of the European Communities, ISBN 92-894-6041-5, European Communities, 2004.

[7] See, e.g., Neutron-Nucleus Collisions: A probe of Nuclear Structure, AIP Conference Proceedings **124** (AIP, New York, 1985).

[8] E.L. Hjort, et al., Phys. Rev. C **50** (1994) 275.

[9] J.H. Osborne, et al., Phys. Rev. C **70** (2004) 054613.

[10] J. Klug, et al., Nucl. Instr. Meth. **A 489**, 282 (2002).

[11] G.L. Salmon, Nucl. Phys. **21**, 15 (1960).

[12] A.J. Koning, J.P. Delaroche, Nucl. Phys. **A713**, 231 (2003).

[13] R.W. Finlay, et al., Phys. Rev. C **47**, 237 (1993).

[14] J. DeJuren, N. Knable, Phys. Rev. **77**, 606 (1950).

[15] R.G.P. Voss, R. Wilson, Proc. Roy. Soc. **A 236**, 41 (1956).

[16] C. Johansson, et al., Phys. Rev. C **71** (2005) 024002.

[17] J. Klug, et al., Phys. Rev. C. **67** (2003) 031601(R)

[18] J. Klug, et al., Phys. Rev. C **68** (2003) 064605.

[19] P. Mermod, et al., Phys. Lett. **B 597** (2004) 243.

[20] P. Mermod, et al., Phys. Rev. C **72** (2005) 061002(R).

[21] P. Mermod, et al., submitted to Phys. Rev. C.

[22] G. Gerstein, J. Niederer, K. Strauch, Phys. Rev. **108**, 427 (1957).

[23] G.C. Wick, Atti. R. Accad. Naz. Lincei, Mem. Cl. Sci. Fis. Mat. Nat. **13**, 1203 (1943).

[24] G.C. Wick, Phys. Rev. **75**, 1459 (1949).

[25] F.S. Dietrich, J.D. Anderson, R.W. Bauer, S.M. Grimes, Phys. Rev. C **68** (2003) 064608.

Appendix XVII

Neutron-induced light-ion production from Fe, Pb and U at 96 MeV

S. Pomp[1], V. Blideanu[2], J. Blomgren[1], Ph. Eudes[3], A. Guertin[3], F. Haddad[3], C. Johansson[1], J. Klug[1], Ch. Le Brun[4], F.R. Lecolley[2], J.F. Lecolley[2], T. Lefort[2], M. Louvel[2], N. Marie[2], P. Mermod[1], A. Prokofiev[5], U. Tippawan[6], A. Öhrn[1], M. Österlund[1]

[1] *Department of Neutron Research, Uppsala University, Sweden*
[2] *Laboratoire de Physique Corpusculaire, Caen, France*
[3] *SUBATECH, Nantes, France*
[4] *Laboratoire de Physique Subatomique et de Cosmologie, Grenoble, France*
[5] *The Svedberg Laboratory, Uppsala University, Sweden*
[6] *Fast Neutron Research Facility, Chiang Mai University, Thailand*

E-mail: Stephan.Pomp@tsl.uu.se

Double-differential cross sections for light-ion production (up to A=4) induced by 96 MeV neutrons have been measured for ^{nat}Fe, ^{nat}Pb and ^{nat}U. The experiments have been performed at the The Svedberg Laboratory in Uppsala, using two independent devices, MEDLEY and SCANDAL. The recorded data cover a wide angular range (20º - 160º) with low energy thresholds. The work was performed within the HINDAS collaboration studying three of the most important nuclei for incineration of nuclear waste with accelerator-driven systems (ADS). The obtained cross section data are of particular interest for the understanding of the so-called pre-equilibrium stage in a nuclear reaction and are compared with model calculations performed with the GNASH, TALYS and PREEQ codes.

International Workshop on Fast Neutron Detectors
University of Cape Town, South Africa
April 3 – 6, 2006

 http://pos.sissa.it

1. Introduction

To achieve a better understanding of nucleon-induced reactions in the 20-200 MeV range and develop improved models, detailed information on light-ion production in these reactions is needed. The need for such data comes also from a large amount of applications. Incineration of nuclear waste using accelerator-driven systems (ADS) is one example [1]. For this reason, the interest in nucleon-induced reactions has been growing in the last few years. This interest has been manifested in part by extensive experimental campaigns, like the one carried out by several laboratories in Europe within the framework of HINDAS [2]. The results presented here are part of this program and concern double-differential cross sections for light-ion emission (up to A=4) induced by 96 MeV neutrons on ^{nat}Fe, ^{nat}Pb and ^{nat}U [3].

2. Experimental procedure

Experiments have been performed using the neutron beam available at the The Svedberg Laboratory (TSL) in Uppsala, Sweden. The neutron beam characteristics (neutrons are not mono-energetic, large beam spot at the target position, and, compared to proton beams relatively low intensity) lead us to use two independent detection systems in order to obtain satisfactory count rate, keeping at the same time systematical uncertainties within reasonable limits.

The MEDLEY setup [4] is made of eight Si-Si-CsI telescopes, allowing detection of light-ions up to A=4 with a low energy threshold. The statistics accumulated using the MEDLEY setup is relatively poor, due to the thin targets used and to the small solid angles covered by the telescopes. The angular resolution is dictated by the target active area and by the opening angle of the telescopes. It was calculated using Monte Carlo simulations of the experiment, and the typical values found are of the order of 5 degrees (FWHM).

In the case of the SCANDAL setup [5] the angular resolution is significantly improved by reconstructing proton trajectories using drift chambers. This device consists of two identical systems located on either side of the neutron beam. Each system uses two 2 mm thick plastic scintillators for triggering, two drift chambers for particle tracking and an array of 12 CsI detectors for energy determination. The emission angles of the particles are calculated using the trajectories in the drift chambers. The angular resolution achieved is of the order of 0.3 degrees. A multi-target system (MTGT) [6] is used to increase the count rate without impairing the energy resolution. The MTGT allows up to seven targets to be mounted simultaneously, inter-spaced with multi-wire proportional counters. In this way it is possible to study several reactions at the same time since we can determine from which target the particle has been emitted and apply corrections for energy losses in subsequent targets. In contrast to MEDLEY, SCANDAL has been used for proton detection only and with an energy threshold of about 35 MeV, however, with a much higher count rate and better angular resolution.

Due to the difficulties encountered when monitoring neutron beam intensities, the absolute cross section normalisation in neutron-induced reactions is a notorious problem. Therefore, the cross sections are measured relative to the H(n,p) cross section. For this reference cross section, the most recent measurements [7] claim an absolute uncertainty of 2 %. Values given in Ref. [7]

have been used to calculate the absolute cross sections presented in this work. Estimated systematic uncertainties affecting the experimental cross sections reported are below 5%.

3. Results

The light-ion spectra have been measured for ^{nat}Fe, ^{nat}Pb and ^{nat}U over the 20-160 degree angular range. The low-energy threshold was 4 MeV for hydrogen isotopes, 12 MeV for ^{3}He and 8 MeV for alpha particles registered with MEDLEY and 35 MeV for proton detection in SCANDAL. The measurements were done up to the maximum possible energy. The energy bin has been fixed to 4 MeV, governed by the energy resolution of the detectors and the accumulated statistics. Fig. 1a compares double-differential cross sections for proton production from iron at 20 degrees, independently measured by both detection systems. Similar results have been obtained for all measured (n,xp) reactions and over the full angular range. The found good agreement, in the energy range covered by both measurements, shows that systematical uncertainties related to cross-section normalisation are low. Fig. 1b shows the Fe(n,xp) cross-section measured with MEDLEY at 20 degrees together with data from Ref. [8], obtained using the magnetic spectrometer LISA. Also here, good agreement is found between the two measurements in the common energy range. Similar agreement has been found for the Pb(n,xp) reaction.

The experimental double-differential cross sections for the emission of hydrogen isotopes measured with MEDLEY are shown in Ref. [3]. Fig. 2 shows deduced energy-differential cross sections. The errors given in the figures are purely statistical.

Energy distributions are obtained from the double-differential cross sections using the Kalbach systematics [9] to extrapolate the experimentally available angular range over the entire range. Experimental information on the energy-differential cross sections is of great importance, since the agreement between calculations and experimental results for this observable is considered as a minimum condition to validate model predictions.

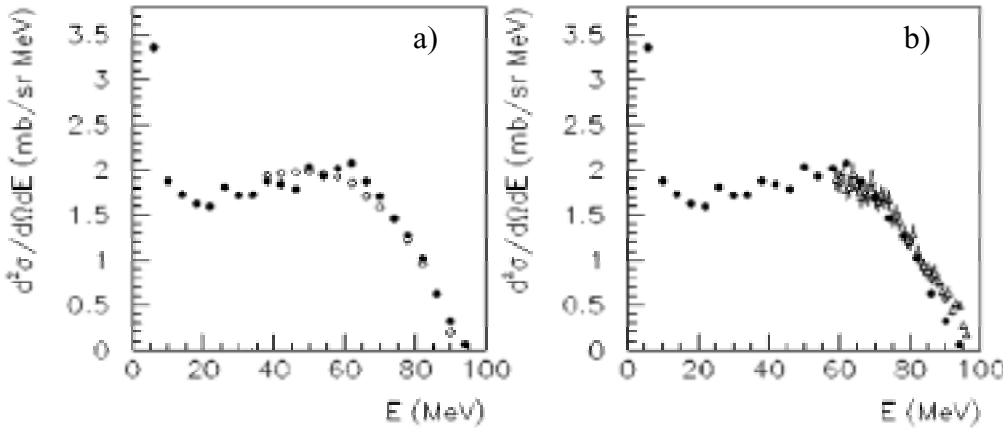

Figure 1. a) Double-differential cross sections for Fe(n,xp) at 20 degrees measured by MEDLEY (filled circles) and SCANDAL (open circles). b) Double-differential cross sections for Fe(n,xp) at 20 degrees measured by MEDLEY (filled circles) and data from Ref. [8] (open triangles).

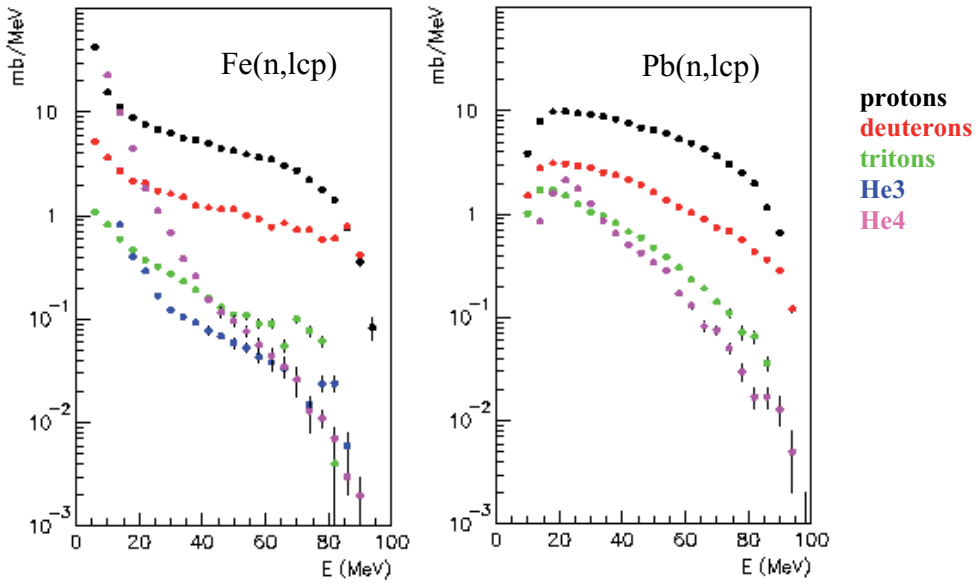

Figure 2: Energy-differential cross sections for the emission of light-ions induced by 96 MeV neutrons on ^{nat}Fe, ^{nat}Pb.

4. Comparison with theoretical calculations

In Fig. 3, the measured energy-differential cross sections for p, d, t and α for 96 MeV neutrons on lead are compared with model calculations. The GNASH code [10] describes the proton production rather well, while a strong underestimation is observed for the case of complex particles. Improvements have recently been done with the TALYS code [11], taking into account the contribution of direct pick-up and knock-out reactions in the complex-particle emission spectra. Even if the agreement in the production rates for complex particles is significantly better, there are still important differences in the shape of the distributions.

A completely different approach takes into account the complex-particle formation probability in the pre-equilibrium stage. This process is treated in the framework of a coalescence model. The code PREEQ [12] uses this approach to calculate energy distributions for particle emission at pre-equilibrium. The results show a good agreement with the data in both shape and amplitude of the distributions.

5. Summary

In this work experimental double-differential cross sections for light-ion production in 96 MeV neutron-induced reactions in iron, lead and uranium are reported. The extracted energy-differential cross sections have been compared with model calculations by the GNASH, TALYS and PREEQ codes. The comparison of these calculations with the experimental data shows clearly that, despite the better agreement obtained with the TALYS code compared to the old version of the exciton model used in the GNASH code, improvements are still needed for a deep understanding of the reaction mechanisms leading to emission of complex-particles. An

alternative is given by the PREEQ code which takes the nucleon coalescence during the pre-equilibrium stage leading to cluster formation into account. This approach seems to give a better description of complex-particle emission in nucleon-induced reactions at intermediate energies.

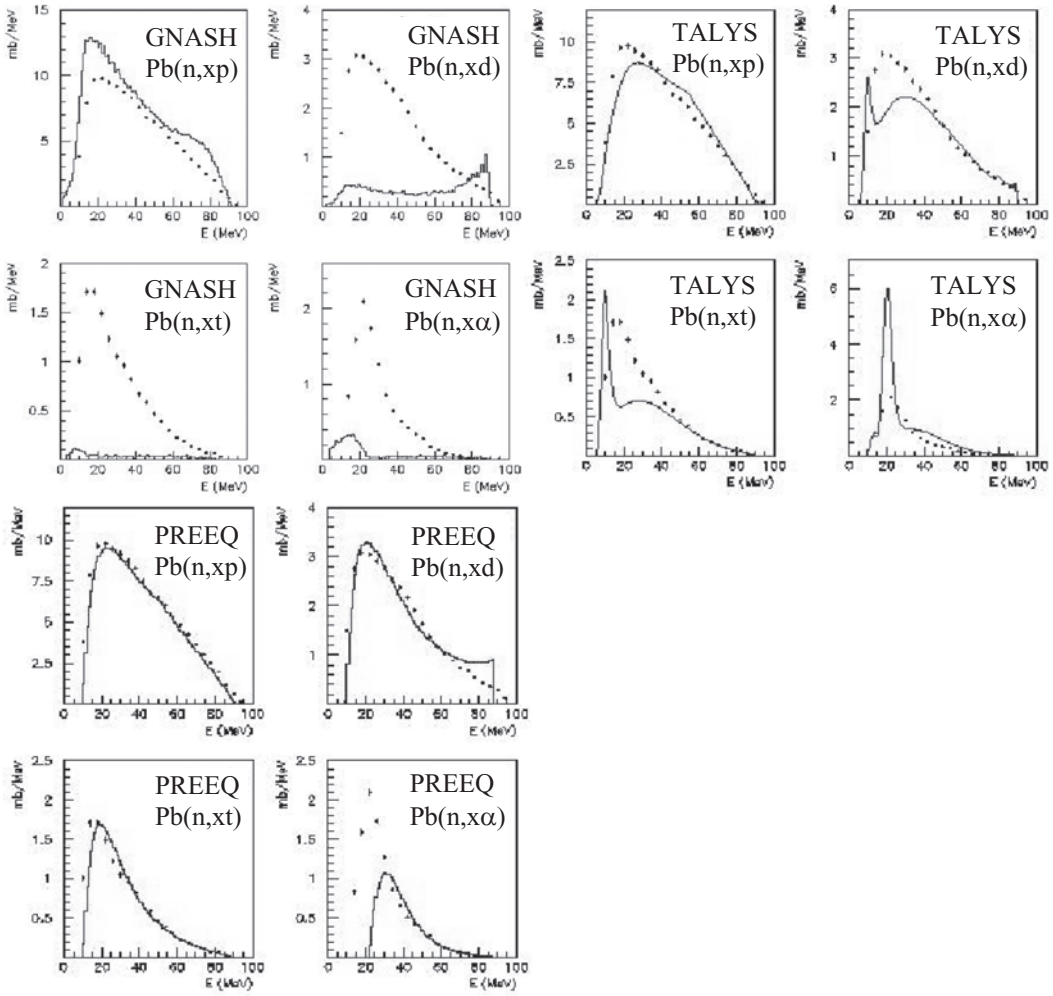

Figure 3: Energy-differential cross sections calculated using the GNASH, TALYS and PREEQ codes. The calculations have been done for 96 MeV neutrons on Pb and are shown as histograms. The experimentally obtained data are shown as points.

Acknowledgments

This work was supported by the European Community under the HINDAS project (Contract No. FIKW-CT-2000-0031), the GDR GEDEON (Research Group CEA-CNRSEDF-FRAMATOME), Vattenfall AB, the Swedish Nuclear Fuel and Waste Management Company, the Swedish Nuclear Power Inspectorate, Barsebäck Power AB, Ringhals AB, the Swedish Defence Research Agency, and the Swedish Research Council. We would like to thank the TSL staff for assistance and quality of the neutron beam. We are also grateful to Dr. E. Betak for

very useful discussions concerning calculations with the PREEQ code. Special thanks to Dr. C. Kalbach for her significant contributions to the progress of theory in nucleon-induced reactions.

References

[1] S. Pomp, et al., *Light-ion production and fission studies using the MEDLEY facility at TSL*, these proceedings.
[2] HINDAS: High and Intermediate energy Nuclear Data for Accelerator-driven Systems, European Community, Contract No. FIKW-CT-2000-00031.
[3] V. Blideanu, et al., *Nucleon-induced reactions at intermediate energies: New data at 96 MeV and theoretical status*, Phys. Rev. C **70** (2004) 014607.
[4] S. Dangtip, et al., *A facility for measurements of nuclear cross sections for fast neutron cancer therapy*, Nucl. Instrum. Methods Phys. Res. A **452** (2000) 484.
[5] J. Klug, et al., *SCANDAL – a facility for elastic neutron scattering studies in the 50-130 MeV range*, Nucl. Instrum. Methods Phys. Res. A **489** (2002) 282.
[6] H. Condé, et al., *A facility for studies of neutron induced reactions in the 50-200 MeV range*, Nucl. Instrum. Methods Phys. Res. A **292** (1990) 121.
[7] J. Rahm, et al., *np scattering measurements at 96 MeV* , Phys. Rev. C **63** (2001) 044001.
[8] A. Ringbom, et al., *The $^{208}Pb(n,p)^{208}Tl$ reaction at E_n = 97 MeV*, Nucl. Phys. A **617** (1997) 316.
[9] C. Kalbach, *Systematics of continuum angular distributions: Extensions to higher energies*, Phys. Rev. C **37** (1988) 2350.
[10] P. G. Young, E. D. Arthur, and M. B. Chadwick, *Comprehensive Nuclear Model Calculations: Introduction to the Theory and Use of the GNASH Code*, Report No. LA-12343-MS, 1992.
[11] A. J. Koning, S. Hilaire, and M.C. Duijvestijn, *TALYS-0.64 User Manual*, December 5, 2004, NRG Report 21297/04.62741/P FAI/AK/AK.
[12] E. Betak, *Program for spectra and cross-section calculations with the pre-equilibrium model of nuclear reactions*, Comp. Phys. Comm. **9** (1975) 92.

Light-ion production and fission studies using the MEDLEY facility at TSL

S. Pomp[*,1], J. Blomgren[1], M. Hayashi[1,2], P. Mermod[1], A. Öhrn[1], N. Olsson[1], M. Österlund[1] , A. Prokofiev[3], U. Tippawan[4]

[1]*Department of Neutron Research, Uppsala University, Sweden*

[2]*Department of Advanced Energy Engineering Science, Kyushu University, Japan*

[3]*The Svedberg Laboratory, Uppsala University, Sweden*

[4]*Fast Neutron Research Facility, Chiang Mai University, Thailand*

E-mail: Stephan.Pomp@tsl.uu.se

The MEDLEY facility at the The Svedberg Laboratory (TSL) in Uppsala has successfully been used in several light-ion production and elastic scattering experiments at 96 MeV. The recent upgrade of the neutron beam facility at TSL now makes the energy range up to 175 MeV accessible. To match the higher energies MEDLEY has been equipped with larger CsI detectors and first tests runs have been performed. The research program at MEDLEY has been extended to include, e.g., studies of neutron-induced fission, especially angular distributions of the fission fragments, over a wide energy range. We present the current status of the facility and the planned research program.

International Workshop on Fast Neutron Detectors
University of Cape Town, South Africa
April 3 – 6, 2006

[*] Speaker

 http://pos.sissa.it

1. Introduction

Understanding how neutrons interact with nuclei is a difficult task since it involves interactions of a large number of nucleons with each other. This is especially true for production of complex particles (A≥2) by neutrons in the energy range of 20-200 MeV. Nevertheless, a wide variety of different applications involving interactions of fast neutrons with nuclei have developed rapidly during the past years. Examples are dosimetry at commercial aircraft altitudes and in space and radiation treatment of cancer within the field of medicine, soft-error effects in computer memory within electronics, and energy production and transmutation of nuclear waste within energy applications. Common for all these applications is the need for high-quality nuclear data for specific nuclei over a wide energy range on the one hand, and the development of reliable nuclear model codes to extrapolate into unmeasured areas on the other hand.

The MEDLEY facility, located at the The Svedberg Laboratory (TSL) in Uppsala, Sweden, has over the past years performed measurements of double-differential cross sections for the production of light ions by 96 MeV neutrons [1-4]. Recently, we have started a program on measuring angular distributions of fission fragments [5]. The facility has also proven to be a valuable tool in the search for three-body force effects [6-7]. All these measurements have been performed at the "old" neutron beam at TSL [8]. At this beam, the neutron fluence above 100 MeV, where the cyclotron has to operate in FM mode, becomes too low to collect good statistics within reasonable time and it was therefore decided to construct a new neutron beamline with shorter distance from the neutron production point to the experimental area, thus delivering higher neutron fluxes. This new beamline is in operation since 2004 [9-10] and opens up the possiblity to extend the experimental program and measure neutron-induced reactions at energies up to 175 MeV.

2. Light-ion production studies with MEDLEY

2.1 Medical applications

It has been established that, due to cosmic-ray neutrons, airflight personnel receive among the largest radiation doses in civil work [11]. Even at space flight altitudes, neutrons give a large contribution to the radiation effects on both human tissue and electronic equipment [12]. Cancer treatment with fast neutrons is performed routinely at several facilities around the world, and represents today one of the largest therapy modalities besides the conventional treatments with photons and electrons. See, e.g., Ref. [13] for a review of this field.

The interaction of neutrons with tissue is very complex, and to a large extent unknown. Neutrons themselves make no damage, but if they induce a nuclear reaction, the emitted charged products interact with the surrounding matter. This interaction between secondary products and tissue is rather well known, but the cross sections for their production are most often poorly known, or even unknown. Due to the absence of high-quality data on neutron-induced nuclear reactions, the concept of kerma (Kinetic Energy Released in MAtter), integrating over a wide

variety of radiation effects, has been used. With microscopic cross section data at hand, the kerma-based dose estimations become obsolete which could revolutionise dosimetry for fast neutrons [14].

In the energy range around 100 MeV, about half the dose delivered to human tissue by neutrons comes from elastic *np* scattering, another 10% from elastic neutron scattering of other nuclei than hydrogen, and the remaining 40% from neutron-induced emission of charged particles. Double-differential cross sections for the production of these charged particles have been and will be measured in tissue relevant material. Carbon data obtained with MEDLEY at 96 MeV at the "old" neutron beam are still under analysis. A paper on double-differential cross sections for light-ion production by 96 MeV neutrons on oxygen has been published recently [3]. Carbon data at 175 MeV have been collected during 50 hours of beamtime in March this year. More data on carbon will be taken in May. It is planned to also collect oxygen data together with silicon data using SiO_2 and Si targets.

2.2 Neutron-induced electronic failures

Cosmic radiation effects in aircraft electronics are well known since more than 20 years. When an electronic circuit is exposed to a charged particle, the latter can, by ionisation inside the sensitive volume, release enough charge to induce a flip in the memory content of a bit. This non-destructive effect is called a single-event upset (SEU). However, a detailed understanding is still lacking (for an overview, see, e.g., Ref. [15] and references therein).

At flight altitudes, as well as at sea level, neutrons and muons dominate the cosmic ray flux. Muons do not interact strongly with nuclei, and therefore neutrons are most important for SEU. Even onboard spacecraft, neutrons produced in the aluminum structure, contribute, on a level comparable to protons, to radiation effects in both electronics and human tissue [12].

Since neutrons have no charge, they can only interact via nuclear reactions, in which charged particles or a heavy recoil are created, that occasionally induce an SEU. Thus, similar to the case of medical applications, detailed knowledge of the nuclear interaction of neutrons with silicon, and even oxygen, are needed. These, together with an adequate description of the electrical and geometrical properties of the decives might lead to a full understanding of the SEU problem [16].

Cross section data on light-ion production in silicon induced by 96 MeV neutrons have already been measured with MEDLEY [2]. SEU cross section data obtained by direct in-beam component testing some years ago [17,18] seemed to indicate that the SEU cross section saturates at a neutron energy of about 100 MeV. However, recent measurements performed at TSL suggest that, for the most recent devices, the SEU cross section might reach a maximum value at a neutron energy of a few tens of MeV and then decrease again with energy [19]. This is supported by a recent study with the nuclear model code TALYS [20]. Since this issue is currently under some debate, there is a further reason to perform a high-quality measurement of double-differential cross sections of neutron-induced light-ion production in silicon and oxygen at 175 MeV.

2.3 Applications in transmutation technologies

The interest in transmutation technologies, especially accelerator-driven systems (ADS), is rapidly growing. They involve neutrons at considerably higher energies than what has been utilised in present reactor applications.

Up to now, extensive data bases exist up to about 20 MeV, which is the relevant energy interval for conventional nuclear power and fusion research. With the proposed technologies, neutron energies up to 2 GeV could become of interest. All ADS proposals deal with spallation-type neutron production methods, which give neutron spectra with an intensity distribution roughly like $1/E_n$. The small number of neutrons at really high energies makes such data not being as important as mid-range data. Above, say, 200 MeV, direct reaction models assuming a single interaction (impulse approximation) works reasonably well, while at lower energies nuclear distortion plays a non-trivial role. This makes the 20 – 200 MeV region the most important for new data [21].

Very little high-quality neutron-induced data exist in this domain. MEDLEY has already served as facility for the measurement of neutron-induced light-ion production on Fe, Pb and U at 96 MeV [4]. Above 100 MeV there are virtually no neutron data that can be used to validate nuclear reaction model codes such as TALYS. From a technical point of few, lead and bismuth (cooling), iron (structure material) and the actinides to be transmuted (uranium, thorium, plutonium, etc.) are the most important. Therefore, we plan measurement of neutron-induced light-ion production on iron, lead, bismuth and uranium at 175 MeV.

3. Fission studies with MEDLEY

Neutron-induced fission reactions of ^{235}U, ^{238}U and ^{209}Bi are internationally recommended standards for monitoring high-energy neutron beams [22]. Fission is also one of the most important processes occuring in the spallation target and the reactor core of an ADS. Furthermore, data on high-energy (n,f) are important for, e.g., developing the theoretical understanding of dynamic effects in the fission process.

Despite the importance of high-energy (n,f) data, few attempts have been made to measure fission cross sections on an absolute scale, i.e., versus the np scattering cross section, which is adopted as the primary neutron standard [22].

The current standard ^{235}U(n,f) and ^{238}U(n,f) cross sections recommended by IAEA [22] are based on the data sets of Lisowski et al. [23]. These data have been revised several times and a thorough description of the experimental technique is still awaited.

We plan to measure the ^{238}U(n,f) cross section and angular distributions of fission fragments in the energy range of 20 to 175 MeV. First results at 20.9 MeV have been published [5]. The strength of the employed experimental technique is the simultaneous measurement of fission fragments and np scattering events in the MEDLEY telescopes. Counting α particles from radioactive decay of the target nuclei gives the effective solid angle.

This can be done either during the beamtime or without beam. Measuring angular distributions thus reduces to counting fragments and α-particles.

4. Experimental considerations

Using MEDLEY at the new Uppsala neutron beam, we plan to measure double-differential cross sections for light-ion production on carbon, oxygen, silicon, iron, lead, bismuth and uranium at 175 MeV. Furthermore we will measure the ^{238}U(n,f) cross section, together with angular distributions of the fission fragments, over the energy region of 20 to 175 MeV. The proposed target nuclei are of highest interest within the applications listed above, and, in addition, of key interest for model development.

4.1 The MEDLEY facility

The charged particles are detected by the MEDLEY setup [2]. It consists of eight three-element telescopes mounted inside a 90 cm diameter evacuated reaction chamber. Each telescope has two fully depleted ΔE silicon surface barrier detectors (the first is 50-60 μm thick, the second 400-550 μm) and one E CsI(Tl) detector. The time-of-flight (TOF) of the neutron and the charged particle triggering the event, obtained from the cyclotron RF and the timing signal from each telescope, is measured for each charged-particle event.

MEDLEY has been equipped with larger CsI detectors to be able to stop protons up to 180 MeV. These new detectors have now been used during several runs and perform according to expectations. The CsI crystals have a total length of 100 mm. The first 70 mm is made cylindrical with a diameter of 50 mm and the remaining 30 mm is tapered to 18 mm diameter to match the size of the readout system. The readout is performed by Hamamatsu S3204-08 photodiodes (PD). The crystals, toghether with the PD, are mounted inside an aluminum tube and have been manufactured by Saint-Gobain, France.

4.2 Background

During the first runs we have found a rather large background probably due to neutrons from the production target penetrating the concrete shielding. While this is no problem for other experiments, it could be for MEDLEY since each individual CsI detector consists of three orders of magnitude more “target” material than the actual target. For acceptance reasons, the registered background is small at the most forward angles but gets large at more backward angles. We anticipate, however, that the particle identification procedure and TOF windows in the offline analysis will filter out most of this background.

4.3 Data-taking and analysis

As mentioned above, we have started to collect data on ^{12}C(n,lcp) in March this year. We will improve the statistics by further runs in May. These data will be analysed by one of us

(MH) at Kyushu University in Japan. For the light-ion production studies from Fe, Pb, Bi and U as well as the fission studies, we will employ two new PhD students in the autumn of this year.

Acknowledgements

We wish to thank the technical staff of the The Svedberg Laboratory for skillful and enthusiastic assistance. The work is supported by the Swedish Nuclear Fuel and Waste Management Company, Swedish Nuclear Power Inspectorate, Ringhals AB, Forsmarks Kraftgrupp AB, Swedish Defence Research Agency, Swedish Nuclear Safety and Training Centre and the European Union.

References

[1] S. Dangtip, et al., *A facility for measurements of nuclear cross sections for fast neutron cancer therapy*, Nucl. Instrum. Methods Phys. Res. A **452** (2000) 484.
[2] U. Tippawan, et al., *Light-ion production in the interaction of 96 MeV neutrons with silicon*, Phys. Rev. C **69** (2004) 064609 and Phys. Rev. C **73** (2006) 039902(E).
[3] U. Tippawan, et al., *Light-ion production in the interaction of 96 MeV neutrons with oxygen*, Phys. Rev. C **73** (2006) 034611 [nucl-ex/0501014].
[4] V. Blideanu, et al., *Nucleon-induced reactions at intermediate energies: New data at 96 MeV and theoretical status*, Phys. Rev. C **70** (2004) 014607.
[5] A. Prokofiev, et al., *A new facility for high-energy neutron-induced fission studies*, Proceedings of the International Conference on Nuclear Data for Science and Industry, AIP Conference Proceedings No. 769 (Melville, New York, 2005), 800.
[6] P. Mermod, et al., *Search for three-body force effects in neutron-deuteron scattering at 95 MeV*, Phys. Lett. B **597** (2004) 243.
[7] P. Mermod, et al., *95 MeV neutron scattering on hydrogen, deuterium, carbon and oxygen*, submitted to Phys. Rev. C.
[8] H. Condé, et al., A facility for studies of neutron induced reactions in the 50-200 MeV range, Nucl. Instrum. Methods Phys. Res. A **292** (1990) 121.
J. Klug, et al., *SCANDAL – a facility for elastic neutron scattering studies in the 50-130 MeV range*, Nucl. Instrum. Methods Phys. Res. A **489** (2002) 282.
[9] S. Pomp, et al., *The new Uppsala neutron beam facility*, Proceedings of the International Conference on Nuclear Data for Science and Industry, AIP Conference Proceedings No. 769 (Melville, New York, 2005), 780.
[10] A. Prokofiev, et al., *A new neutron beam facility at TSL*, these proceedings.
[11] D.T. Bartlett, et al., *The cosmic radiation exposure of aircraft crew*, Radiat. Res. Congress Proceedings **2** (2000) 719.
[12] T.W. Armstrong and B.L. Colborn, *Predictions of secondary neutrons and their importance to radiation effects inside the international space station*, Radiat Meas. **33** (2001) 229.
[13] M. Tubiana, J. Dutreix, and A. Wambersie, *Introduction to Radiobiology*, Taylor & Francis, 1990.
[14] J. Blomgren and N. Olsson, *Beyond kerma – neutron data for biomedical applications*, Radiat. Prot. Dosim. **103** (2003) 293.
[15] Single-Event Upsets in Microelectronics, topical issue, edited by H.H.K. Tang and N. Olsson [*Mater. Res. Soc. Bull.* **28** (2003)].
[16] J. Blomgren, Bo Granborn, T. Granlund, N. Olsson, *Relations Between Basic Nuclear Data and Single-Event Upsets Phenomena*, p. 121 in [15].

[17] K. Johansson, et al., *Energy-resolved neutron SEU measurements from 22 to 160 MeV*, IEEE transactions on Nuclear Science I **45** (1998) 2519.
[18] K. Johansson, et al., *Neutron induced single-word multiple-bit upset in SRAM*, IEEE transactions on Nuclear Science I **46** (1999) 1427.
[19] M. Olmos, A. Prokofiev, and R. Gaillard, *Unfolding procedure for SER measurements using quasi-monoenergetic neutrons*, International Reliability Physics Symposium (IRPS 2005), San Jose, California, April 17-21, 2005.
[20] J.-C. Bourselier, *TALYS Calculations for Evaluation of Neutron-Induced Single-Event Upset Cross Sections*, UU-NF 05#07, ISSN 1401-6269.
[21] J. Blomgren, *Experimental activities at high energies*, invited lecture at Workshop on Nuclear Data for Science & Technology: Accelerator Driven Waste Incineration, Trieste, Italy, Sept. 10-21, 2001.
[22] A. Carlson, et al., *Update to nuclear data standards for nuclear measurements*, Proc. Int. Conf. on Nuclear Data for Science and Technology, Trieste, Italy, May 19-24, 1997, Part II, 1223.
[23] P. Lisowski, et al., *U*, OECD/NEA Report NEANDC-305, 177.

Appendix XIX

A New Neutron Beam Facility at TSL

Alexander V. Prokofiev [*], **Olle Byström, Curt Ekström, Volker Ziemann**
The Svedberg Laboratory, Uppsala University
Box 533, S-751 21 Uppsala, Sweden
E-mail: Alexander.Prokofiev@tsl.uu.se

Jan Blomgren, Stephan Pomp, Michael Österlund
Department of Neutron Research, Uppsala University
Box 525, S-751 20 Uppsala, Sweden
E-mail: Jan.Blomgren@tsl.uu.se

Udomrat Tippawan
Fast Neutron Research Facility, Chiang Mai University
50202 Chiang Mai, Thailand
E-mail: Udomrat@fnrf.science.cmu.ac.th

A new quasi-monoenergetic neutron beam facility has been constructed at The Svedberg Laboratory (TSL) in Uppsala, Sweden. Key features include a neutron energy range of 11 to 175 MeV, high fluxes, user flux control, flexible neutron field size and shape, and spacious and easily accessible user area. The first results of the beam characterization measurements are reported.

International Workshop on Fast Neutron Detectors
University of Cape Town, South Africa
April 3 – 6, 2006

[*] Speaker

1. Introduction

The interest in high-energy neutrons is rapidly growing, since a number of potential large-scale applications involving fast neutrons are under development, or have been identified. These applications primarily fall into four sectors: nuclear energy and waste [1], medicine [2, 3], flight personnel dosimetry [4], and single-event effects (SEE) on electronics [5, 6].

To satisfy the needs of these applications, monoenergetic neutron beams would be most suitable. In the energy region above about 20 MeV, a truly monoenergetic neutron beam is not feasible in a strict sense. For certain nuclear reactions, however, there is a strong dominance of neutrons in a narrow energy range. Therefore, such neutron sources are often called "quasi-monoenergetic". The most popular neutron production reaction above 20 MeV is ^{7}Li(p,n)^{7}Be. It is used, *e.g.*, at quasi-monoenergetic neutron facilities in Cape Town [7], Davis [8], Louvain-la-Neuve [9], Saitama [10], and Takasaki [11].

There is a long-term experience in high-energy neutron production at The Svedberg Laboratory (TSL). The first neutron facility was built at TSL in the late 1980s [12, 13] and remained in operation until 2003. In 2003-2004, a new facility was constructed. Emphasis was put on high neutron beam intensity in combination with flexibility in energy and neutron field shape.

2. Technical specification

The facility uses the ^{7}Li(p,n)^{7}Be reaction to produce a quasi-monoenergetic neutron beam. Two kinds of beams from the Gustaf Werner cyclotron are used for neutron production: 1) proton beam with energy variable in the 25-180 MeV range, and, 2) beam of H_2^+ ions with energy of about 13 MeV/A. The energy of the produced peak neutrons is controllable in the 11-175 MeV range.

A drawing of the neutron beam facility is shown in Fig. 1. The proton or H_2^+ beam is incident on a target of lithium, enriched to 99.99% in ^{7}Li. The available targets are 1, 2, 4, 8.5, and 23.5 mm thick. Proton energy loss in the target amounts to 2-6 MeV depending on the incident beam energy and target thickness. The targets are rectangular in shape, 20x32 mm^2, and are mounted in a remotely controlled

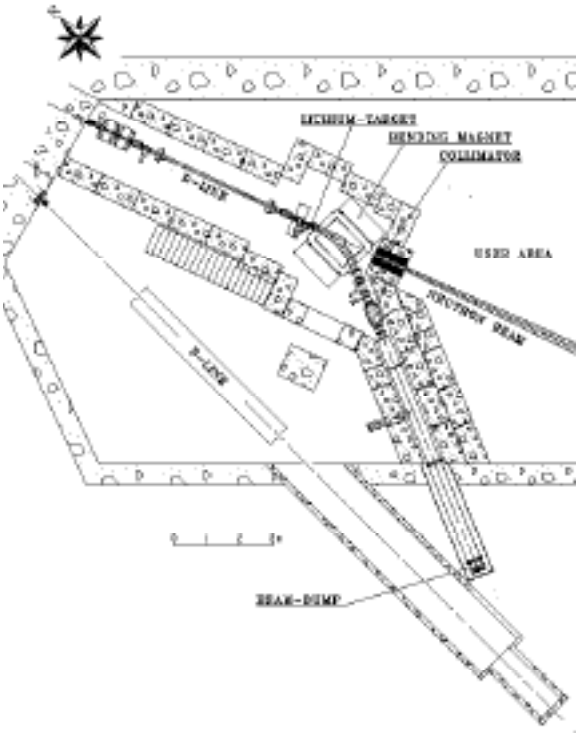

Fig. 1. Drawing of the new neutron beam facility. The neutron beam, produced in the lithium target, continues along the D-line.

water-cooled copper rig. An additional target position contains a fluorescent screen viewed by a TV camera, which is used for beam alignment and focusing. Downstream the target, the proton beam is deflected by a magnet into a 10-m long dumping line, where it is guided onto a heavily shielded water-cooled graphite beam dump.

The neutron beam is formed geometrically by a cylindrically shaped iron collimator block, 50 cm in diameter and 100 cm long, with a hole of variable size and shape. The collimator is surrounded by concrete to form the end wall of the production line towards a user area. Thereby, shielding from the lithium target region is achieved that is sufficient for most experiments. A modular construction of the collimator allows the user to select the size and the shape of the neutron beam. At present, the available collimator openings are 2, 3, 5.5, 10, 15, 20, and 30 cm in diameter. In addition, a quadratically shaped opening of 1 cm^2 is available, which is intended for irradiation of, *e.g.*, a separate electronic component without affecting the rest of an electronic board. Other collimator openings in the 0-30 cm range can be provided upon request. The time needed to change the opening size is typically about 30 min.

The user area extends from 3 to 15 m downstream the lithium target. Positions located closest to the target are used for high-flux irradiation of compact objects, with achievable fluxes about an order of magnitude higher compared to the old TSL neutron facility [12, 13], for the same target thickness, proton energy and current. Remote positions may be used to irradiate large objects, up to 1 m in diameter, e.g., entire computers or aircraft navigation systems. Proton beam currents of up to 10 μA can be used for energies below 100 MeV. Above 100 MeV, the achievable beam current is about a factor of 10 lower. The resulting reduction of the neutron flux can be partly compensated by using thicker lithium targets. The neutron flux can be varied by the user according to the needs of the specific experiment.

The user area, situated at a level of 12 m below the ground, is connected by Ethernet and coaxial cables, about 100 m long, to counting rooms, which are located at the ground level. No time is required for "cooling down" of the user area after irradiation, because the dose rate from residual β- and γ-rays is then only slightly above the natural radiation level.

Two additional irradiation positions, which can be used parasitically with other experiments, are provided closer to the lithium target (see Table I). The increase of the neutron flux at these positions is reached at the expense of limited accessibility, limited size of irradiated objects, lack of standard monitors, and more intense γ-ray background.

Table I. Parasitic irradiation positions.

Position	**Distance from the Li target (m)**	**Angle to the proton beam direction (°)**	**Gain in the peak neutron flux**
PARTY	1.9	1.6	2.5
TUNIS	1.1	7.5	1.7 – 2.2[a)]

[a)] dependent on the peak neutron energy.

3. Characterization of the facility

Neutron spectra at 0° have been obtained by measuring elastic *np*-scattering with the Medley setup [14-16]. The scattered protons are registered at an angle of 20° relative to the neutron beam. The measured neutron spectra are shown in Fig. 2 for peak energies of 21.8 (a), 46.5 (b), 94.7 (c), and 142.7 MeV (d). In all cases, the spectrum is dominated by a peak situated a few MeV below the energy of the primary protons and comprising about 40% of the total number of neutrons.

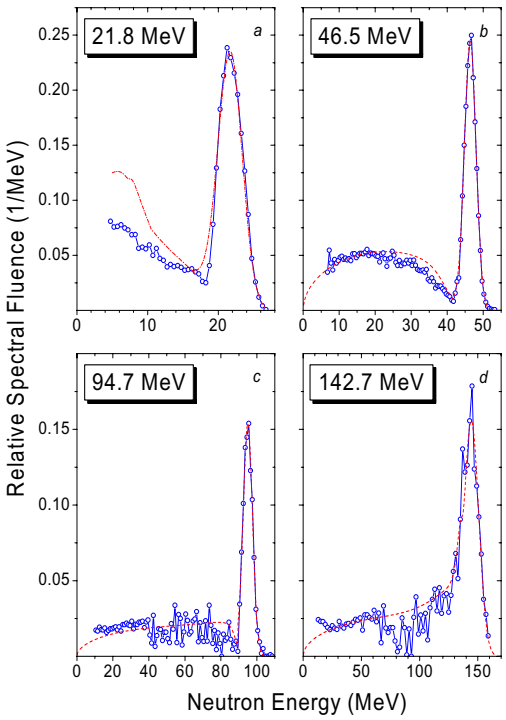

Fig. 2. The neutron spectra at 0° for different peak neutron energies (see Table II for incident proton energies and ^{7}Li target thicknesses). Symbols connected by a solid line represent experimental data obtained in the present work. Predictions are shown as dashed lines (see text).

Fig. 2 includes a comparison of the measurements with model calculations of the neutron spectra folded with the function that describes the energy resolution in the present experiment. For the three higher energies (Fig. 2b-d), the systematics of Prokofiev *et al.* [17] was employed. For the peak neutron energy of 21.8 MeV, the evaluation of Mashnik *et al.* [18] was used (Fig. 2a). The differential cross-section for high-energy peak neutron production at 0° was obtained by multiplication of the angle-integrated cross-section of the ^{7}Li(p,n)^{7}Be reaction [18] to the "index of forwardness" from the systematics of Uwamino *et al.* [19]. The experimental data agree with the calculations except for the low-energy tail region in the 21.8-MeV spectrum where the model overpredicts the yield of neutrons with energies above 5 MeV by about 40%.

Table II summarizes the main features of the measured spectra and the achieved neutron fluxes. The latter have been measured with a monitor based on a thin-film breakdown counter (TFBC) [20]. Another monitoring option is provided by an ionization-chamber monitor (ICM). Both monitors utilize neutron-induced fission of ^{238}U with the cross-section adopted as neutron flux standard [21]. In addition, the neutron flux is indirectly monitored by a Faraday cup, which integrates the current of protons collected at the beam dump. In Table II, γ-ray dose rate in the user area is given as well.

The measured contamination of the neutron beam at the user area, due to interactions of the primary protons with beam transport elements, typically does not exceed 0.05% for peak neutron energies up to 100 MeV and 0.3% for the 174 MeV energy. Such interactions lead to a minor surplus of neutrons in the user area, because charged particles produced near the lithium target and upstream are removed by the deflection magnet. The relative contamination of the

neutron beam by protons with energies above 15 MeV is about 10^{-5} for the peak neutron energy of 95 MeV.

Thermal neutrons were found in the user area, using TFBCs with ^{235}U targets, shielded by a cadmium sheet during a part of the runs. The thermal neutron flux was estimated to be about 1% of the peak neutron flux at 174 MeV energy [22]. This result comes from an ongoing systematic study of the low-energy part of the neutron spectra using TFBCs and different neutron-induced fission reactions.

Figure 3 shows a horizontal beam profile for 142.7-MeV neutrons, measured at a distance of 4.77 m from the lithium target. The measurement was performed by counting neutron-induced SEE in a set of memory chips positioned across the beam [23].

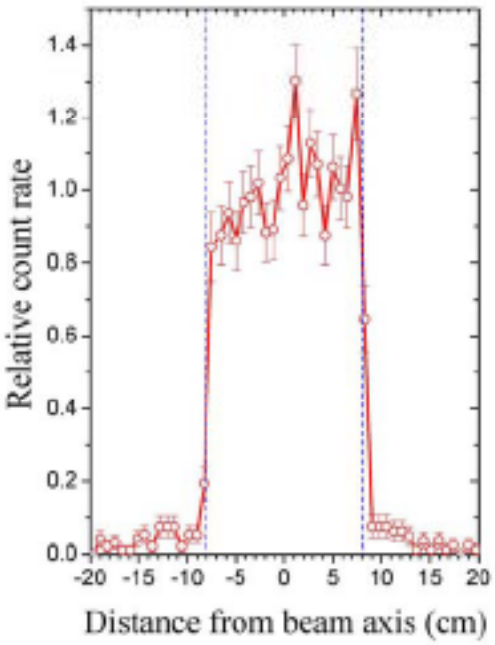

Fig. 3. The horizontal beam profile for 142.7-MeV neutrons, measured at the distance of 4.77 m from the lithium target. Vertical dashed lines represent boundaries of the beam expected from the geometry of the collimator.

4. Summary and outlook

A new neutron beam facility has been constructed at TSL, and it is in frequent operation now (25 weeks during year 2005). The facility is capable of delivering neutrons in the 11-175 MeV range. This makes TSL the only laboratory in the world offering full quasi-monoenergetic neutron testing according to the JESD89 standard [6].

Recently, a neutron field with the peak energy of about 11 MeV has been developed. Processing of neutron spectra at 11 and 174 MeV is in progress. A fast ionization chamber for regular checks of the neutron spectrum is under development [24]. An additional neutron

Table II. Neutron beam parameters.

Proton beam energy (MeV)	^{7}Li target thick-ness (mm)	Proton beam current (μA)	Average energy of peak neutrons (MeV)	Fraction of neutrons in the high-energy peak (%)		Peak neutron flux (10^5 cm^{-2}s^{-1}) [a]	γ-ray dose rate (mSv/h) [b]
				Meas-ured	Calc-ulated		
24.68 ± 0.04	2	10	21.8	~50	--	1.3	0.35
49.5 ± 0.2	4	10	46.5	39	36	2.9	1.7
97.9 ± 0.3	8.5	5	94.7	41	39	4.6	2.4
147.4 ± 0.6	23.5	0.6	142.7	55[c]	40	2.1	-

[a] At the entrance of the beam line to the user area.
[b] At the neutron beam path at the distance of 8 m from the lithium target.
[c] Upper limit due to poor energy resolution.

monitor based on counting of neutron-induced SEE is about to be installed [25]. Independent calibrations of neutron monitors are planned, using measurements of the ^{7}Be activity produced in the ^{7}Li target, following a technique suggested by Uwamino *et al.* [19].

A new upgrade of the facility is being launched in the framework of project ANITA (**A**tmospheric-like **N**eutrons from th**I**ck **TA**rget). The upgrade will allow us to deliver a neutron beam with a continuous "white" spectrum, and thus to reproduce the spectrum of neutrons in the atmosphere. Neutrons will be produced by irradiation of a thick tungsten target by high-energy protons. The possibility to deliver quasi-monoenergetic neutron beams will be kept.

Acknowledgements

We would like to thank all the staff at The Svedberg Laboratory for the excellent work in building this new facility. We are thankful to A.N. Smirnov and M. Olmos for providing us with the thermal neutron data and the beam profile data, respectively.

References

[1] A. Koning, et al., *J. Nucl. Sci. Technol.* **2**, 1161 (2002).
[2] R. Orecchia, et al., *Eur. J. Cancer* **34**, 459 (1998).
[3] D. L. Schwartz, et al., *Int. J. Radiat. Oncol. Biol. Phys.* **50**, 449 (2001).
[4] D. T. Bartlett, et al., *Radiat. Res. Congress Proceedings* **2**, 719–723 (2000).
[5] *Single-Event Upsets in Microelectronics, topical issue,* edited by H. H. K. Tang and N. Olsson [*Mater. Res. Soc. Bull*. **28** (2003)].
[6] *JEDEC Standard. Measurements and Reporting of Alpha Particles and Terrestrial Cosmic Ray-Induced Soft Errors in Semiconductor Devices.* JESD89, August 2001.
[7] R. Nolte, et al., *Nucl. Instrum. Meth. Phys. Res. A* **476**, 369 (2002).
[8] F.P. Brady, *Can. J. Phys.* **65**, 578 (1987).
[9] H. Schuhmacher, et al., *Nucl. Instrum. Meth. Phys. Res. A* **421***,* 284 (1999).
[10] N. Nakao, et al., *Nucl. Instrum. Meth. Phys. Res. A* **420**, 218 (1999).
[11] M. Baba, et al., *Nucl. Instrum. Meth. Phys. Res. A* **428**, 454 (1999).
[12] H. Condé, et al., *Nucl. Instrum. Meth. Phys. Res. A* **292**, 121 (1990).
[13] J. Klug, et al., *Nucl. Instrum. Meth. Phys. Res. A* **489**, 282 (2002).
[14] S. Dangtip, et al., *Nucl. Instrum. Meth. Phys. Res.* **A 452**, 484 (2000).
[15] S. Pomp, et al., *AIP Conf. Proc.* **769**, 780-783 (2005).
[16] S. Pomp, et al., these proceedings
[17] A.V. Prokofiev, et al., *J. Nucl. Sci. Techn., Suppl.* **2**, 112 (2002).
[18] S.G. Mashnik, et al., LANL Report LA-UR-00-1067 (2000).
[19] Y. Uwamino, et al., *Nucl. Instrum. Meth. Phys. Res. A* **389**, 463 (1997).
[20] A.N. Smirnov, et al., *Radiat. Meas.* **25**, 151 (1995).
[21] A.D. Carlson, et al., *Proc. Int. Conf. on Nuclear Data for Science and Technology, Trieste, Italy, May 19-24, 1997,* Part II, p. 1223.
[22] A.N. Smirnov, private communication.
[23] M. Olmos, private communication.
[24] I.V. Ryzhov, private communication.
[25] R. Harboe-Sorensen, private communication.

Light charged particle production in 96 MeV neutron-induced reactions with oxygen

U. Tippawan[1,2*], S. Pomp[1†], A. Ataç[1], B. Bergenwall[1], J. Blomgren[1], S. Dangtip[1,2], A. Hildebrand[1], C. Johansson[1], J. Klug[1], P. Mermod[1], L. Nilsson[1,4], M. Österlund[1], N. Olsson[1,3], A.V. Prokofiev[4], P. Nadel-Turonski[5], V. Corcalciuc[6], and A.J. Koning[7].

[1]*Department of Neutron Research, Uppsala University, Sweden*
[2]*Fast Neutron Research Facility, Chiang Mai University, Thailand*
[3]*Swedish Defence Research Agency (FOI), Stockholm, Sweden*
[4]*The Svedberg Laboratory, Uppsala University, Sweden*
[5]*Department of Radiation Sciences, Uppsala University, Sweden*
[6]*Institute of Atomic Physics, Heavy Ion Department, Bucharest, Romania*
[7]*Nuclear Research and Consultancy Group NRG, Petten, The Netherlands*
E-mail: udomrat@fnrf.science.cmu.ac.th

In recent years, an increasing number of applications involving fast neutrons have been developed or are under consideration, e.g., radiation treatment of cancer, neutron dosimetry at commercial aircraft altitudes, soft-error effects in computer memories, accelerator-driven transmutation of nuclear waste and energy production.

Data on light-ion production in light nuclei such as carbon, nitrogen and oxygen are particularly important in calculations of dose distributions in human tissue for radiation therapy at neutron beams, and for dosimetry of high energy neutrons produced by high-energy cosmic radiation interacting with nuclei (nitrogen and oxygen) in the atmosphere. When studying neutron dose effects in radiation therapy and at high altitude, it is especially important to consider oxygen, because it is the dominant element (65% by weight) in average human tissue.

In this work, we present experimental double-differential cross sections of inclusive light-ion (p, d, t, ^{3}He and α) production in oxygen, induced by 96 MeV neutrons. Spectra were measured at 8 laboratory angles: 20°, 40°, 60°, 80°, 100°, 120°, 140° and 160°. Measurements were performed at The Svedberg Laboratory (TSL), Uppsala, using the dedicated MEDLEY experimental setup. Deduced energy-differential and production cross sections are reported as well. Experimental cross sections are compared to theoretical reaction model calculations and existing experimental data in the literature.

International Workshop on Fast Neutron Detectors
University of Cape Town, South Africa
April 3 – 6, 2006

* Udomrat Tippawan
† Corresponding author, Tel. +46 18 471 6850, Fax. +46 18 471 3853, E-mail: Stephan.Pomp@tsl.uu.se

1. Introduction

Recently, there has been increased attention on various applications where fast neutrons play a significant role, like dose effects due to cosmic-ray neutrons for airplane crew [1], fast-neutron cancer therapy [2,3], studies of electronics failures induced by cosmic-ray neutrons [4], accelerator-driven transmutation of nuclear waste and energy production, and determination of the response of neutron detectors. It has been established during recent years that air flight personnel receive among the largest radiation doses in civil work, due to cosmic-ray neutrons. Cancer treatment with fast neutrons is performed routinely at about a several facilities worldwide, and today it represents the largest therapy modality besides the conventional treatments with photons and electrons. Data on light-ion production in light nuclei such as carbon, nitrogen and oxygen are particularly important in calculations of dose distributions in human tissue for radiation therapy at neutron beams, and for dosimetry of high energy neutrons produced by high energy cosmic radiation interacting with nuclei (nitrogen and oxygen) in the atmosphere. These cosmic-ray neutrons also create a reliability problem in modern electronics. A neutron can cause a nuclear reaction inside or near a chip, thus releasing free charge, which in turn could, e.g., flip the memory content or change the result of a logical operation. For all these applications, improved knowledge of the underlying nuclear physics is of major importance.

In this contribution, experimental double-differential cross sections (inclusive yields) for protons, deuterons, tritons, ^{3}He and alpha particles induced by 96 MeV neutrons incident on oxygen [5] are presented. Measurements have been performed at the cyclotron of The Svedberg Laboratory (TSL), Uppsala, using the dedicated MEDLEY experimental setup [6]. Spectra have been measured at 8 laboratory angles, ranging from 20° to 160° in 20° steps. Extrapolation procedures are used to obtain coverage of the full angular distribution and consequently energy differential and production cross sections are deduced. The experimental data are compared to results of calculations with nuclear reaction codes and to existing experimental data in the literature.

2. Experimental Methods

The neutron beam facility at TSL uses the ^{7}Li(p,n)^{7}Be reaction (Q = –1.64 MeV) to produce a quasi-monoenergetic neutron beam [7]. The 98.5 ± 0.3 MeV protons from the cyclotron impinge on the lithium target, producing a full energy peak of neutrons at 95.6 ± 0.5 MeV with a width of 3 MeV FWHM and containing 40% of the neutrons, and an almost constant low-energy tail containing 60% of the neutrons. The neutron beam is directly monitored by a thin-film breakdown counter (TFBC). Relative monitoring can be obtained by charge integration of the proton beam hitting the Faraday cup in the beam dump. The agreement between the two beam monitors was very good during the measurements.

The charged particles are detected by the MEDLEY setup. It consists of eight three-element telescopes mounted inside a 100 cm diameter evacuated reaction chamber. Each telescope has two fully depleted ΔE silicon surface barrier detectors. The thickness of the first ΔE detector (ΔE_1) is either 50 or 60 μm, while the second one (ΔE_2) is either 400 or 500 μm,

and they are all 23.9 mm in diameter (nominal). In each telescope, a cylindrical CsI(Tl) crystal, 50 mm long and 40 mm in diameter, serves as the *E* detector.

A 22 mm diameter 500 μm thick (cylindrical) disk of SiO_2 is used as the oxygen target. For the subtraction of the silicon contribution, measurements using a silicon wafer having a 32·32 mm^2 quadratic shape and a thickness of 303 μm are performed. For absolute cross section normalization, a 25 mm diameter and 1.0 mm thick polyethylene $(CH_2)_n$ target is used. The *np* cross sections at 20° laboratory angle provides the reference cross section [8].

Background events, collected in target-out runs and analyzed in the same way as target-in events, are subtracted from the corresponding target-in runs, with SiO_2 and silicon targets, after normalization to the same neutron fluence.

The time-of-flight (TOF) obtained from the radio frequency of the cyclotron (stop signal for TDC) and the timing signal from each of the eight telescopes (start signal), is measured for each charged-particle event.

3. Data reduction procedures

The ΔE–E technique is used to identify light charged particles ranging from protons to lithium ions. Good separation of all particles is obtained over their entire energy range and therefore the particle identification procedure is straightforward.

Energy calibration of all detectors is obtained from the data itself [9,10]. Events in the ΔE–E bands are fitted with respect to the energy deposited in the two silicon detectors. This energy is determined from the detector thicknesses and calculations of energy loss in silicon. Supplementary calibration points are provided by transitions to the ground state and low-lying states in the H(n,p) reaction, as well as transitions to the ground state and low-lying states in the $^{12}C(n,d)^{11}B$, $^{16}O(n,d)^{15}N$ and $^{28}Si(n,d)^{27}Al$ reactions. The energy of each particle type is obtained by adding the energy deposited in each element of the telescope.

Low-energy charged particles are stopped in the ΔE_1 detector leading to a low-energy cutoff for particle identification of about 3 MeV for hydrogen isotopes and about 8 MeV for helium isotopes. The helium isotopes stopped in the ΔE_1 detector are nevertheless analyzed and a remarkably low cutoff, about 4 MeV, can be achieved for the experimental alpha-particle spectra. These alpha-particle events could obviously not be separated from ^{3}He events in the same energy region, but the yield of ^{3}He is much smaller than the alpha-particle yield in the region just above 8 MeV, where the particle identification works properly.

Knowing the energy calibration and the flight distances, the TOF for each charged particle from target to detector can be calculated and subtracted from the registered total TOF. The resulting neutron TOF is used for selection of charged-particle events induced by neutrons in the main peak of the incident neutron spectrum.

Absolute double-differential cross sections are obtained by normalizing the oxygen data to the number of recoil protons emerging from the CH_2 target. After selection of events in the main neutron peak and proper subtraction of the target-out and $^{12}C(n,px)$ background contributions, the latter taken from a previous experiment, the cross section can be determined from the recoil

proton peak, using *np* scattering data [8]. All data have been normalized using the *np* scattering peak in the 20° telescope.

Due to the finite target thickness, corrections for energy loss and particle loss are applied to both targets individually. Details of the correction methods are described in Refs. [9,10]. The cross sections for oxygen are obtained after subtraction of the silicon data from the SiO_2 data with proper normalization with respect to the number of silicon nuclei in the two targets.

4. Results and discussion

Double-differential cross sections at laboratory angles of 20°, 40°, 100° and 140° for protons and alpha particles, compared to the calculations based on the GNASH [11] and TALYS [12] models, are shown in Figs. 1-2, respectively. The error bars represent statistical uncertainties only. For protons above 25 MeV, both calculations give a reasonably good description of the spectra, although the calculated 20° cross sections, in particular the TALYS ones, fall below the experimental data. The low-energy statistical peak below 15 MeV in the spectra is considerably overpredicted by the two codes. The overestimate is particularly strong at backward angles for TALYS and at forward angles for GNASH.

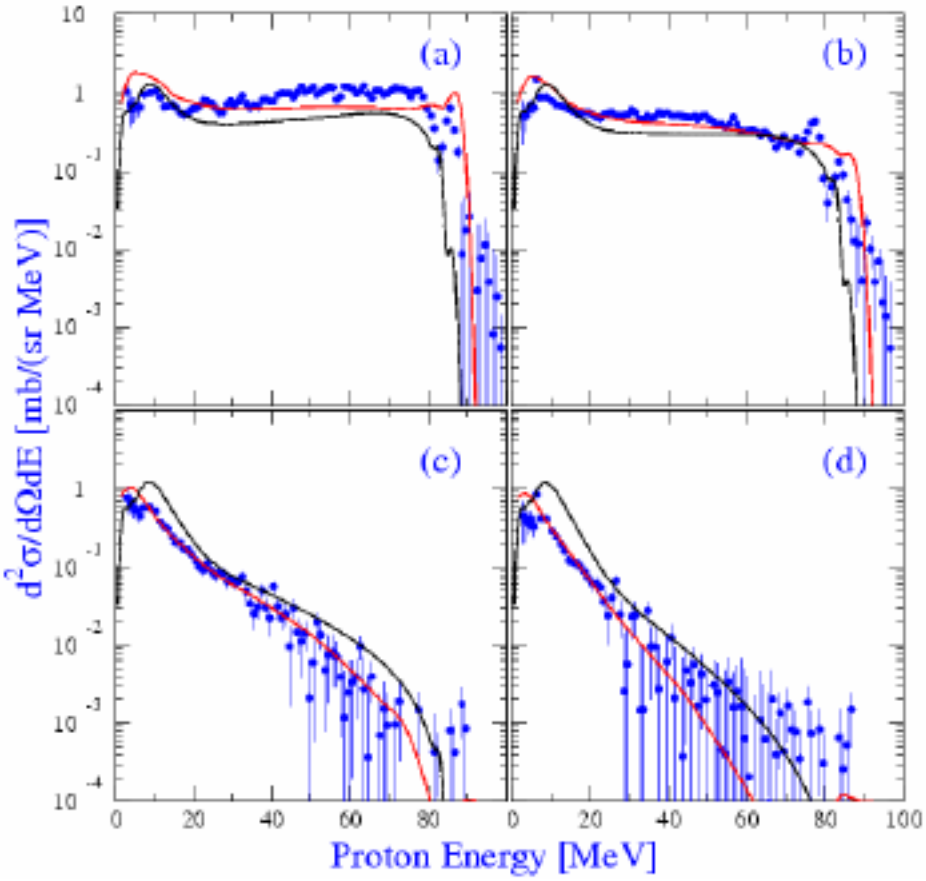

Fig. 1. Experimental double-differential cross sections (filled circles) of the O(n,px) reaction at 96 MeV at a) 20°, b) 40°, c) 100°, and d) 140°. The curves indicate theoretical calculations based on GNASH (red) and TALYS (black).

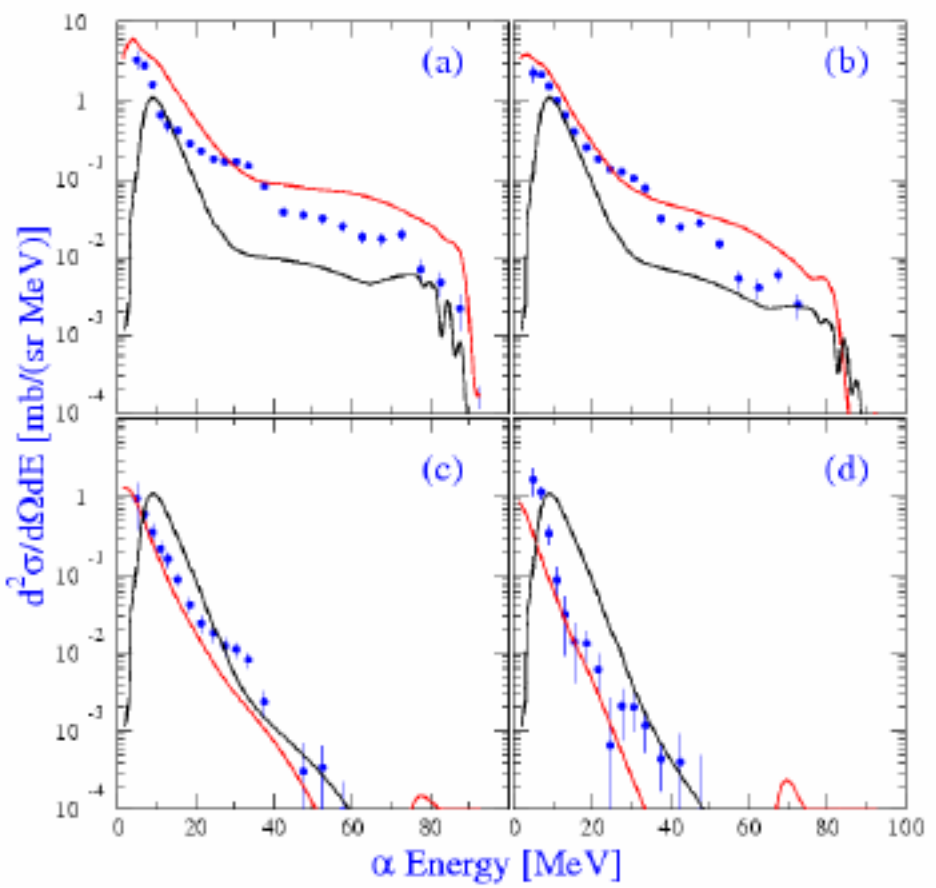

Fig. 2. Same as Fig. 1 for the O(n,αx) reactions.

The overall shapes of the alpha particle spectra (Fig. 2) are reasonably well described by the two models. The GNASH calculations, however, overpredict the cross sections at forward angles and underpredict them at large angles, whereas the TALYS calculations do the opposite, i.e., underpredict at small angles and overpredict at large angles.

By integration of the experimental angular distribution, energy-differential cross sections (dσ/dE) are obtained for each ejectile. These are shown in Fig. 3 together with theoretical calculations. For all ejectiles both calculations give a fair description of the energy dependence. Both calculations are in good agreement with the proton experimental data over the whole energy range, although the calculation for (n,px) reactions to discrete low-lying states underestimates the data. A study of the spectroscopic strengths for these states would be welcome. Concerning the deuteron spectra, the GNASH calculations are in good agreement with the data, whereas the TALYS code gives cross sections a factor of two or more larger than the experimental ones at energies above 30 MeV. In the case of alpha particles, the GNASH calculation tends to overpredict the high-energy part of the spectrum, and the TALYS calculations fall below the data above an alpha particle energy of 25 MeV. The energy dependence of the triton and ^{3}He spectra are well described by the TALYS code, but in both cases the calculation falls below the data above about 20 MeV.

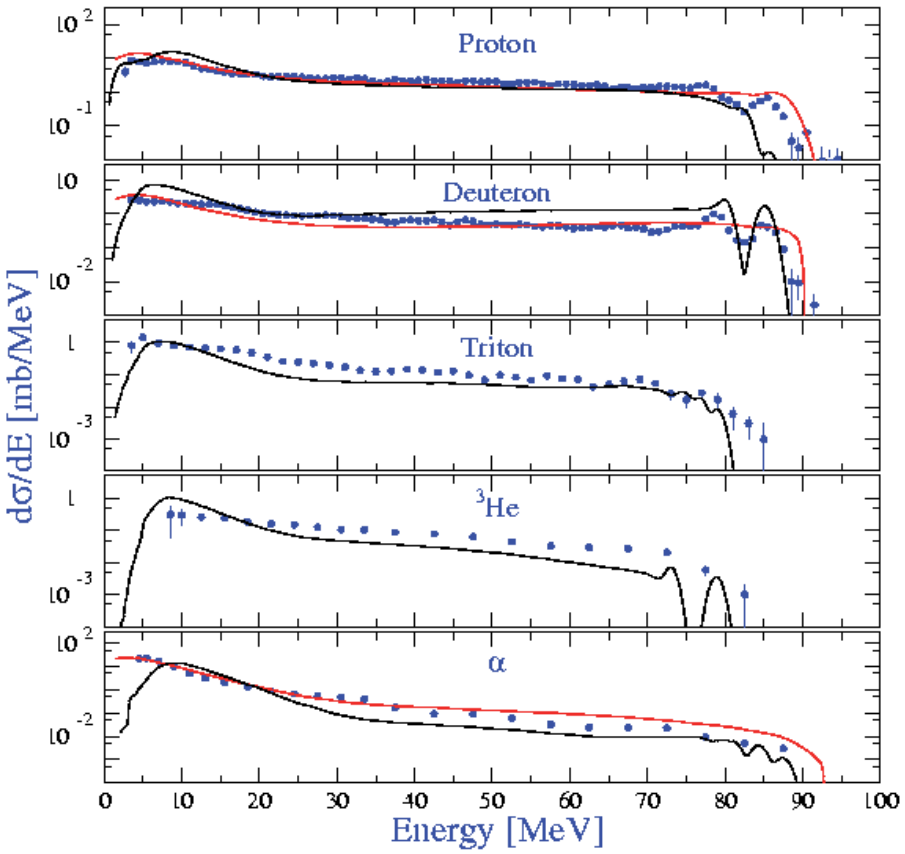

Fig. 3. Experimental energy-differential cross sections (filled circles) for neutron induced p, d, t, ^{3}He and alpha production at 96 MeV. The curves indicate theoretical calculations based on GNASH (red) and TALYS (black).

The production cross sections are deduced by integration of the energy differential spectra (see Table 1). To be compared with the calculated cross sections, the experimental values in Table 1 have to be corrected for the undetected particles below the low-energy cutoff. This is particularly important for ^{3}He because of the high cutoff energy. The corrections obtained with

TABLE 1. Experimental production cross sections for proton, deuteron, triton, ^{3}He and alpha particles from the present work. Theoretical values resulting from GNASH and TALYS calculations are given as well. The experimental data in the second column have been obtained with cutoff energies of 2.5, 3.0, 3.5, 8.0 and 4.0 MeV for p, d, t, ^{3}He and alpha particles, respectively. The third and forth columns show data corrected for these cutoffs, using the GNASH and TALYS calculation, respectively.

σ_{prod}	Experiment (mb)	Cutoff Corrected Experiment		Theoretical calculation	
		GNASH	TALYS	GNASH	TALYS
(n,px)	224 ± 11	248	231	259.9	221.7
(n,dx)	72 ± 4	80	73	73.4	131.3
(n,tx)	20± 1	—	20	—	10.6
(n, ^{3}Hex)	6.9 ± 0.6	—	8.7	—	8.2
(n,αx)	132 ± 7	218	132	224.7	88.4

TALYS seem to be too small in some cases, in particular for the (n,αx) production cross section. This is illustrated in Fig. 3, bottom panel, where the TALYS curve falls well below the experimental dσ/dE data in the 4–7 MeV region.

The proton, deuteron, triton, and alpha particle production cross sections are compared with previous data at lower energies [13] in Fig. 4. There seems to be general agreement between the trends of the previous data and the present data points. The curves in this figure are based on a GNASH calculation.

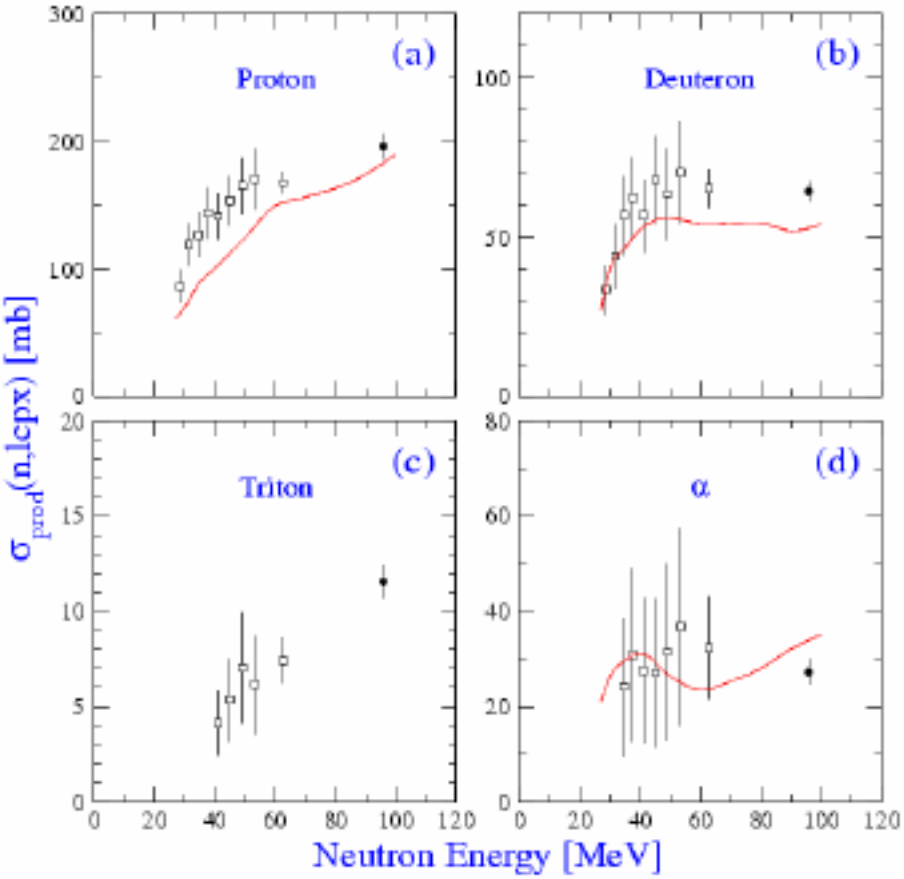

Fig. 4. Neutron-induced a) proton, b) deuteron, c) triton, and d) alpha particle production cross section as a function of neutron energy. The full circles are from the present work, whereas the open squares are from previous work [13]. The curves are based on a GNASH calculation. The data as well as the calculations correspond to cutoff energies of 6 MeV for protons and deuterons and 12 MeV for tritons and alpha particles. Note that the cutoff energies are different from those in Table 1.

5. Conclusion

In the present paper, an experimental data set on light-ion production in oxygen induced by 96 MeV neutrons is reported. Experimental double-differential cross sections are measured at eight angles between 20° and 160°. Energy-differential and production cross sections are obtained for the five types of outgoing particles. Theoretical calculations based on nuclear reaction codes including direct, pre-equilibrium and statistical models give generally a good

account of the magnitude of the experimental cross sections. For proton emission, the shape of the spectra for the double-differential and energy-differential cross sections are well described. The calculated and the experimental alpha-particle spectra are also in fair agreement with the exception of the high-energy part, where the GNASH model predicts higher yield and the TALYS model lower yield than experimentally observed. For the proton evaporation peak, the global TALYS calculation overestimates the data. For the other complex ejectiles, there are important differences between theory and experiment in what concerns the shape of the spectra at various angles.

Acknowledgements

This work was supported by the Swedish Natural Science Research Council, the Swedish Nuclear Fuel and Waste Management Company, the Swedish Nuclear Power Inspectorate, Ringhals AB, and the Swedish Defence Research Agency. The authors wish to thank the The Svedberg Laboratory for excellent support.

References

[1] D. O'Sullivan, D. Zhou and E. Flood, *Investigation of cosmic rays and their secondaries at aircraft altitudes*, Radiat. Meas. 34, 277–280 (2001).

[2] R. Orecchia, A. Zurlo, A. Loasses, M. Krengli, G. Tosi, S. Zurrida, P. Zucali, and U. Veronesi, *Particle Beam Therapy (Hadron therapy): Basis for Interest and Clinical Experience,* Eur. J. Cancer 34, 459 (1998).

[3] D.L. Schwartz, J. Einck, J. Bellon, and G.E. Laramore, *Fast Neutron Radiotherapy For Soft Tissue And Cartilaginous Sarcomas At High Risk For Local Recurrence*, Int. J. Radiat. Oncol. Biol. Phys. 50, 449 (2001).

[4] *Single-Event Upsets in Microelectronics*, topical issue, eds. H.H.K. Tang and N. Olsson, Mat. Res. Soc. Bull. 28 (2003).

[5] U. Tippawan, S. Pomp, A. Ataç, B. Bergenwall, J. Blomgren, S. Dangtip, A. Hildebrand, C. Johansson, J. Klug, P. Mermod, L. Nilsson, M. Österlund, N. Olsson, A.V. Prokofiev, P. Nadel-Turonski, V. Corcalciuc, and A. J. Koning, *Light-ion production in the interaction of 96 MeV neutrons with oxygen*, Phys. Rev. C 73, 034611 (2006).

[6] S. Dangtip, A. Ataç, B. Bergenwall, J. Blomgren, K. Elmgren, C. Johansson, J. Klug, N. Olsson, G. Alm Carlsson, J. Söderberg, O. Jonsson, L. Nilsson, P.-U. Renberg, P. Nadel-Turonski, C. Le Brun, F.R. Lecolley, J.F. Lecolley, C. Varignon, Ph. Eudes, F. Haddad, M. Kerveno, T. Kirchner, and C. Lebrun, *A facility for measurements of nuclear cross sections for fast neutron cancer therapy*, Nucl. Instr. Meth. Phys. Res. A 452, 484 (2000).

[7] J. Klug, J. Blomgren, A. Ataç, B. Bergenwall, S. Dangtip, K. Elmgren, C. Johansson, N. Olsson, S. Pomp, A.V. Prokofiev, J. Rahm, U. Tippawan, O. Jonsson, L. Nilsson, P.-U. Renberg, P. Nadel-Turonski, A. Ringbom, A. Oberstedt, F. Tovesson, V. Blideanu, C. Le Brun, J.F. Lecolley, F.R. Lecolley, M. Louvel, N. Marie, C. Schweitzer, C. Varignon, Ph. Eudes, F. Haddad, M. Kerveno, T. Kirchner, C. Lebrun, L. Stuttgé, I. Slypen, A. Smirnov, R. Michel, S. Neumann, and U. Herpers, *SCANDAL–a facility for elastic neutron scattering studies in the 50–130 MeV range*, Nucl. Instr. Meth. Phys. Res. A 489, 282 (2002).

[8] J. Rahm, J. Blomgren, H. Condé, S. Dangtip, K. Elmgren, N. Olsson, T. Rönnqvist, R. Zorro, O. Jonsson, L. Nilsson, P.-U. Renberg, A. Ringbom, G. Tibell, S.Y. van der Werf, T.E.O. Ericson, and B. Loiseau, *np scattering measurements at 96 MeV*, Phys. Rev. C 63, 044001 (2001).

[9] U. Tippawan, S. Pomp, A. Ataç, B. Bergenwall, J. Blomgren, S. Dangtip, A. Hildebrand, C. Johansson, J. Klug, P. Mermod, L. Nilsson, M. Österlund, N. Olsson, K. Elmgren, O. Jonsson,

A.V. Prokofiev, P.-U. Renberg, P. Nadel-Turonski, V. Corcalciuc, Y. Watanabe, and A. J. Koning, *Light-ion production in the interaction of 96 MeV neutrons with silicon*, Phys. Rev. C 69, 064609 (2004).

[10] U. Tippawan, *Secondary Particle Spectra from Neutron Induced Nuclear Reaction in the 14-100 MeV Region*, Doctoral thesis, Chiang Mai University (2004) (unpublished).

[11] ICRU Report 63, *International Commission on Radiation Units and Measurements*, Bethesda, MD, March 2000.

[12] A.J. Koning, S. Hilaire, and M.C. Duijvestijn, *TALYS-0.64 User Manual*, December 5, 2004, NRG Report 21297/04.62741/P FAI/AK/AK.

[13] S. Benck, I. Slypen, J.P. Meulders, and V. Corcalciuc, *Experimental double-differential cross sections and derived kerma factors for oxygen at incident neutron energies from reaction thresholds to 65 MeV*, Phys. Med. Biol. 43, 3427 (1998).

A Novel Fast Neutron Detector for Nuclear Data Measurements

I. Sagrado Garcia[1], G. Ban[1]*, V. Blideanu[1], J. Blomgren[2], P. Eudes[4], J.M. Fontbonne[1], Y. Foucher[4], A. Guertin[4], F. Hadad[4], L. Hay[1], A. Hildebrand[2], G. Iltis[1], C. Le Brun[3], F.R. Lecolley1, J.F. Lecolley[1], J.L. Lecouey[1], T. Lefort[1], N. Marie[1], N. Olsson[2], S. Pomp[2], M. Österlund[2], A. Prokofiev[5], J-C Steckmeyer[1]

1 Laboratoire de Physique Corpusculaire, IN2P3/CNRS, ENSICAEN, UCBN,
14050 Caen Cedex 04, France
2Department of neutron research, Uppsala University, Box 535, S-75120 Uppsala Sweden
3 Laboratoire de Physique Subatomique et de Cosmologie, IN2P3/CNRS, UJF, INPG,
38026 Grenoble Cedex, France
4 – SUBATECH, 44070 Nantes Cedex 03, France
5 The Svedberg Laboratory, Uppsala University,
Box 533, S-75121 Uppsala, Sweden
E-mail: ban@lpccaen.in2p3.fr

Accelerator driven system will use a heavy element target such as lead. Many calculations are available to simulate high-energy spallation neutron induced reactions, but little data are available for comparison with the simulations.

In order to constrain the simulation tools we have measured (n,Xn) double differential cross section on different targets at The Svedberg Laboratory, Uppsala, Sweden. For neutron energy above 40 MeV, we have developed a novel detector, CLODIA, based on proton recoil and drift chambers to determine neutron energy. CLODIA (Chamber for LOcalization with DrIft and Amplification) is able to track recoil protons with energy up to 90 MeV with spatial resolution of about one millimeter and a detection efficiency of 99% for each drift chamber. Using CLODIA coupled wit*h the SCANDAL set-up, we have been able to measure double differential (n,Xn) cross section on lead and iron for incident neutron energy in the 40-95 MeV energy region.

International Workshop on Fast Neutron Detectors
University of Cape Town, South Africa
April 3 – 6, 2006

* Speaker

 http://pos.sissa.it

1. Introduction

Future accelerator-driven system (ADS) will couple an intense high-energy proton beam (~1 GeV, a few mA) with a spallation target made of heavy element and a subcritical reactor core. The proton beam that is incident on the ADS target will create a large number of secondary particles, mainly neutrons, protons and other light charged particles, with energies covering the full range up to the GeV region. Although a large majority of the neutrons will be below 20 MeV, for safety reasons, as well as for code validation, the relatively small fraction at higher energies still has to be characterized.

Above 200 MeV and under 20 MeV, the nuclear data are well documented [1], but in between (20-200 MeV), the lack of data makes ADS simulations less reliable. For inelastic (n,Xn) cross section in the 20-200 MeV incident neutron energy region, very few measurements are available [2]. In order to obtain accurate data on (n,Xn) reactions, we have measured double differential cross section on different target and at different angles. We have been able to measure inelastic double differential (n,Xn) cross section (E, Ω) on lead and iron for incident neutron energy of 96 MeV. This measurement was made possible by the development of a new detector named CLODIA, Chamber for LOcalization with DrIft and Amplification. This detector tracks the proton emitted after an H(n,p) reaction in a polyethylene (CH_2) converter.

2. Detector system

2.1. Detector requirements

In order to define the incident energy of a neutron that causes the inelastic (n, Xn) reaction, we detect a recoil proton produced in a hydrogenated converter. The proton energy and scattering angle allow us to calculate the initial neutron energy. The detector system has to be able to measure the proton trajectory and energy. Due to the naturally low flux of fast neutron beams (~ 4-5*10^5 n/cm^2/s) [3], the detector has to have high neutron to proton conversion efficiency. The detector has to have a good spatial (angular) resolution and high efficiency for recoil protons. It has to be able to reject charged particles besides of the recoil protons.

2.2. CLODIA

CLODIA is composed of eight 10x10 cm^2 detection modules stacked along the Z-axis, which coincides with the direction of a neutron scattered from the target. Seven converters are placed between modules in order to get neutron to proton conversion. Six of the converters are made of polyethylene (CH_2), and one is made of carbon, in order to subtract the carbon contribution in the inelastic part of the spectra. The thickness is 4 mm for the polyethylene converters and 2 mm for the carbon converter, in order to have equivalent energy losses. Each of the detection modules is an X-Y sensitive gas detector. The proton trajectory is reconstructed using (X,Y) position from each detector. Two different approaches are used to get the (X,Y) position. One is drift time, and the other one is resistive division.

The detection module is made of two Mylar foils, 2.5 μm thick. The gap between the foils is 6.5 mm. On each foil, 200 aluminum strips, each 150 nm thick and 880 μm wide, are

evaporated along the Y axis (Figure 1). The strips produce an electric drift field along the X axis. Voltage difference from one side to the other is about 4500 V. We have chosen to use thin strips instead of wires, so that the protons "see" more homogeneous media along their travel. The charge is collected on a set of Ni wires, 50 µm, at the positive voltage side. The drift time is obtained by the (delayed) charge arrival, and a start is given by an external plastic scintillator located after the CLODIA detector (see Section 3).

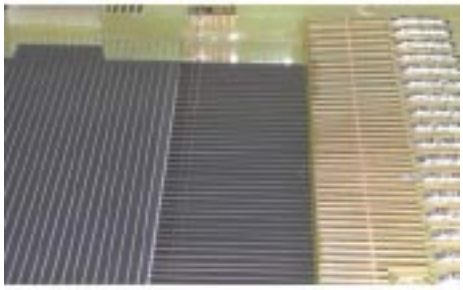

Figure 1. Detail of a CLODIA chamber on the left strips (vertical) for drift field and X localization, Strips (Horizontal) and CMS resistors for Y localization, the wire is seen near the middle of the picture

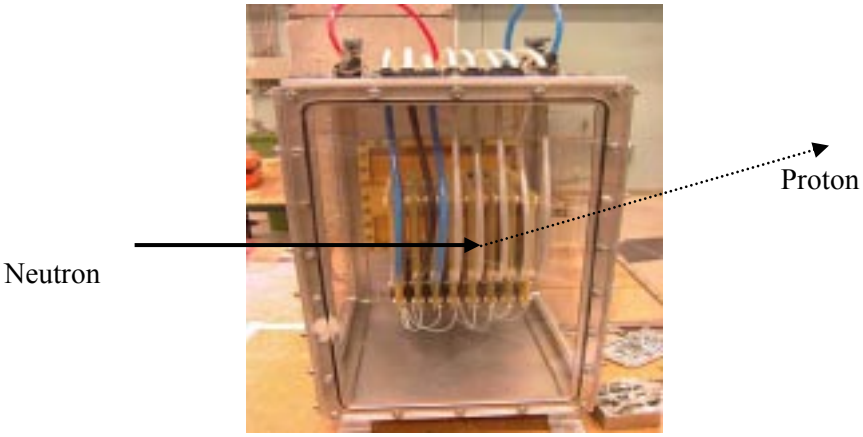

Figure 2. Overall view of CLODIA. Neutron comes from the left. Each module is viewed from the side and is set vertically. The tubes are gas distributor, and the white wires are HV distribution. The converters are not on the picture.

The potential along the electron path is between -3000 V (the first strip) to 2000 V (anode). For Y localization, charge division is used. Around the anode, set at 2000 V, an avalanche takes place. This point has been one of the most critical for CLODIA tuning. High voltage gives a large avalanche, but sparking is also favored by high voltage. A dedicated, very low noise preamplifier, located near the anode, have been developed in order to lower as much as possible the voltage used for the avalanche. From the start of development to the detector we actually use for measurement, the voltage has been lowered from 2000 V to 1500 V. Near the anode, another set of 200 strips parallel to the X axis are evaporated, each of these strips are connected to the next one with a resistor. The charge division obtained with the resistive network gives the Y position. P10 gas (Ar 90%, CH_4 10%) at 1 atm is flowing in each chamber.

All chambers are placed in an aluminum box (Figure 2) with Mylar windows for particle entrance and exit and for detector maintenance.

2.3 CLODIA performance

For commissioning of CLODIA, we used a ^{55}Fe X-ray source. 5.4-keV X-rays produce the same amount of charge as 50-MeV protons, so that we could experimentally simulate the signal produced by such protons. It is crucial to have good spatial resolution in order to track the recoil protons. We have measured the chambers' spatial resolution. The results give standard deviations σ_X= 0.3 mm and σ_Y=0.7 mm along X and Y axes. Since we used at least three chambers, the proton diffusion angle is known with resolution that is sufficient for (n, Xn) measurement.

The CLODIA chamber is very sensitive to charged particles, and its efficiency for protons has been estimated as 99%. Thus, the first detector can be used as a veto for charged particles coming from the target.

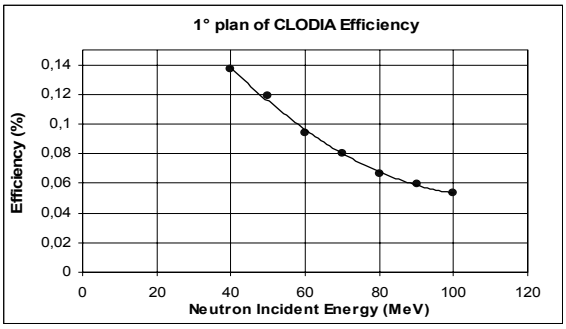

Figure 4. CLODIA efficiency versus incident neutron energy.

The detection principle of CLODIA is based on the elastic H(n,p) reaction. This reaction has a small cross section value (~30 mb), and it was not possible to study it experimentally because of beam time limitations. Nevertheless, this reaction is well known, and simulation codes can be used to calculate the efficiency for the different planes of CLODIA. Figure 4 shows the efficiency of the first plane of CLODIA obtained using the GEANT3 code [4].

3 Measurements

3.1. Set-up

Inelastic (n,Xn) measurements were performed at The Svedberg Laboratory (TSL), where a 96 MeV neutron beam is available. The schematic setup is shown on Figure 5. CLODIA is coupled with the SCANDAL device. The veto for charged particle rejection is obtained from a plastic scintillator, used jointly with the first CLODIA chamber.

The SCANDAL set-up [5] consists of a first trigger, two large wire chambers; and a second trigger followed by an array of CsI detectors. The coincidence between the two triggers gives the start for CLODIA acquisition. SCANDAL gives two additional points of the proton trajectory, and the recoil proton energy. The typical distance between the veto detector and the target is 1.40 m. The solid angle is about 0.00262 sr. Due to all traversed materials, the proton energy measurement threshold in the CsI detectors is 40 MeV.

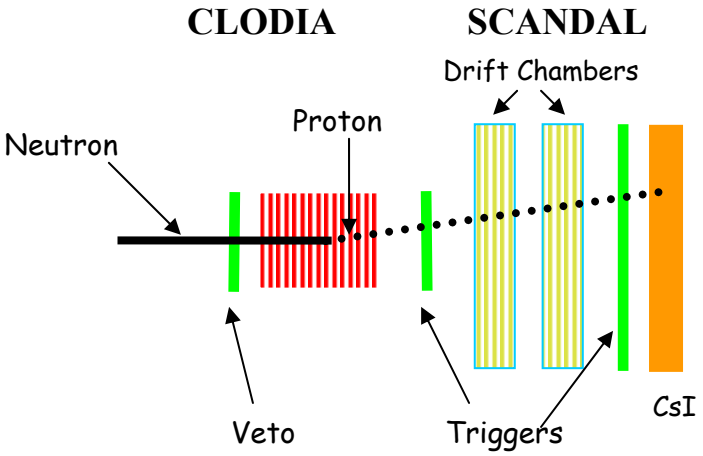

Figure 5. Experimental setup for (n,Xn) measurement at TSL

3.2 Results

Using CLODIA set up at TSL, two different experiments have been performed.

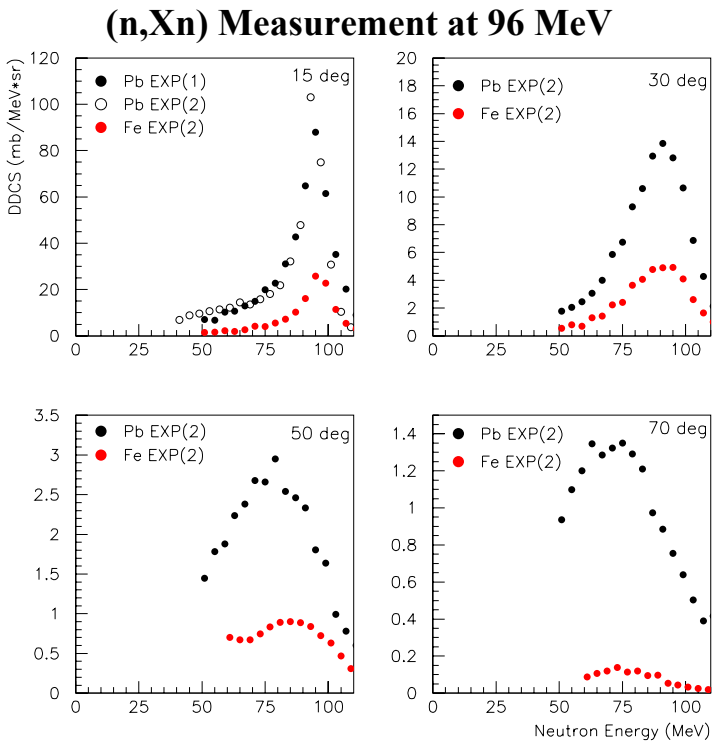

Figure 6 Double differential cross section obtained at different angles on lead and iron targets. Due the low resolution in energy, the energy goes beyond the beam energy.

The first one was a feasibility test. During this test, we have measured the (n,Xn) cross section at 15° for a lead target. After obtaining the first satisfactory results, we have performed

the second experiment. We have been able to measure double differential cross section on lead and iron at 15°, 30°, 50° and 70° angles.
Figure 6 shows preliminary results. There is good agreement between the (n,Xn) cross sections at 15° on lead during the two experiments. In addition, the elastic cross section Pb(n,n) derived from our results is also in good agreement with other experimental measurements [5, 6] and with predictions of theoretical models [7]. The agreement between results of different experiments and calculations can be considered as verification of the whole experimental procedure.

Conclusions

The CLODIA detector coupled with the SCANDAL has allowed us to measure previously unknown (n,Xn) cross section on Pb and Fe for 40-96 MeV incident neutrons. This series of measurement can be extended toward cross sections needed for heavy ion dosimetry where only a few data sets are available.

References

[1] HINDAS, High and Intermediate energy Nuclear Data for Accelerator-driven Systems, European Community, Contract No. FIKW-CT-2000-0031.
[2] E.L Hjort et al, Phys. Rev. C53 (1996) 237.
[3] S. Pomp et al., AIP Conf. Proc. 769, 780-783 (2005).
[4] GEANT3 User's guide.
[5] J. Klug et al, Nucl. Inst. Meth. in Phys. Res. A489 (2002) 282.
[6] G.L. Salmon et al, Nucl. Phys. 21 (1960) 15-20.
[7] A.J Koning, J.P. Delaroche, Nucl. Phys. A713, 231 (2003).

Proceedings of WP-ADS-E&T 2006
Jaipur, India, Jan. 23-25, 2006
Paper No. XXX

Neutron Cross Sections Above 20 MeV for Design and Modeling of ADS

J. Blomgren

Department of Neutron Research, Uppsala University, Box 525, S-751 20 Uppsala, Sweden.

ABSTRACT: One of the outstanding new developments in the field of Partitioning and Transmutation (P&T) concerns Accelerator-Driven Systems (ADS) consists of a combination of a high-power, high-energy accelerator, a spallation target for neutron production and a sub-critical reactor core.

The development of the commercial critical reactors of today motivated a large effort on nuclear data up to about 20 MeV, and presently several million data points can be found in various data libraries. At higher energies, data are scarce or even non-existent. With the development of nuclear techniques based on neutrons at higher energies, there is now a days a need also for higher-energy nuclear data.

To provide alternative to this lack of data is a wide program on neutron-induced data related to ADS for P&T is running at the 20-180 MeV neutron beam facility at the the 'The Svedberg Laboratory' (TSL), Uppsala. The programme encompasses studies of elastic scattering, inelastic neutron production i.e., (n, xn') reactions, light-ion production, fission and production of heavy residues. Recent results are presented and future program of development is outlined.

KEYWORDS: *Neutron, Nuclear data, Elastic Scattering, Light Ion Production, Fission, Residue Production, Accelerator Driven System, Waste Transmutation*

1. INTRODUCTION

One of the outstanding new developments in the field of Partitioning and Transmutation (P&T) concerns Accelerator-Driven Systems (ADS), which consist of a combination of a high-power, high-energy accelerator, a spallation target for neutron production, and a sub-critical reactor core.

The development of the commercial critical reactors of today motivated a large effort on nuclear data up to about 20 MeV, and presently several million data points can be found in various data libraries. At higher energies, data are scarce or even non-existent. With the development of nuclear techniques based on neutrons at higher energies, there is now a days need also for higher-energy nuclear data.

The nuclear data needed for transmutation in an ADS can roughly be divided into two main areas. First, the initial proton beam produces neutrons by spallation reactions. This means that data on proton-induced neutron production are needed. In addition, data on other reactions are needed to assess the residual radioactivity of the target. Second, the produced neutrons can induce a wide range of nuclear reactions, and knowledge of these are useful in the design of ADS. Among these reactions, some cross sections can be used directly. Examples are elastic scattering for neutron transport, proton and alpha production for assessment of the hydrogen and helium gas production in the target window or core, and fission for obvious reasons.

In most cases, however, direct data determination is not the ultimate goal. The global capacity for such measurements is insufficient to obtain complete coverage of important data. It is even impossible in theory to supply all relevant data. In a reactor core, large quantities of short-lived nuclides affect the performance of the core during operation, but measuring cross sections for these nuclides is impossible because experiment targets cannot be made. This means that the experimental work must be focused on providing benchmark data for theory development, making it possible to use theoretical models for unmeasured parameters in a core environment.

An often overlooked aspect is *why* nuclear data should be measured in the first place. Nuclear data are not needed for a demonstration of the principle of driving a sub-critical assembly with an external neutron source. The need for nuclear data becomes imminent when a realistic large-scale facility is the goal. With large uncertainties in the nuclear data, large safety margins have to be used, which results in excessive costs. Thus, the role of nuclear data is to reduce the cost for reaching a certain level of safety.

Another important aspect is the trade-off between general and particular information. Below 20 MeV, a single cross section can be of paramount importance to the entire application. An example is the neutron capture resonance in ^{238}U that provides the Doppler effect so important for the stability of critical reactors. Moreover, some cross sections are fundamentally inaccessible to theory, in particular in the resonance region. As a result, at low energies more or less complete data coverage for major elements is required. Above 20 MeV, the situation is fundamentally different. The cross sections are smooth, and the behaviour of the total technical system is always dictated by the sum of a large number of reactions, neither of which strongly dominates the performance. Therefore, getting a grip on the overall picture is more important than precision data on a single reaction. For a review of nuclear data for ADS at high energies, see, e.g., Blomgren [1].

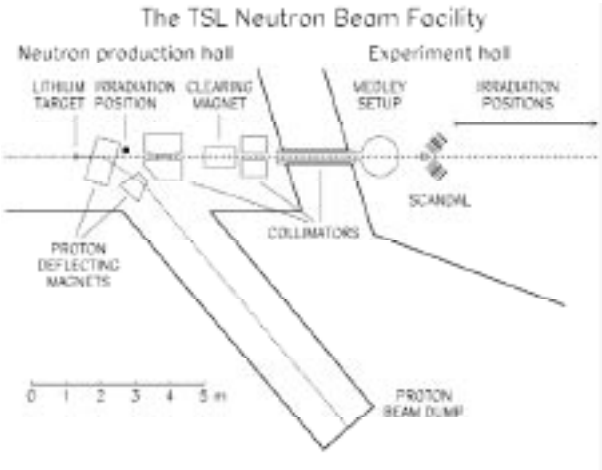

Fig. 1. The old TSL neutron beam facility [3,4]

2. ACTIVITIES AT TSL UPPSALA

To meet the demand described as above, a wide program on measurement of cross sections of neutron-induced nuclear reactions is running at the The Svedberg laboratory (TSL) in Uppsala, Sweden. The results presented here were all obtained at the old neutron beam facility, used in between the years 1990-2003. In the year 2003, a new facility was built and commissioned for joint use in nuclear data measurements and testing of electronics [2].

I. Neutron production

At the old neutron facility (see Fig. 1) [3,4], quasi-mono-energetic neutrons are produced by the reaction ^{7}Li(p, n)^{7}Be in a target of 99.98 % ^{7}Li. After the target, the proton beam is bent by two dipole magnets into an 8 m concrete tunnel, where it is focused and stopped in a well-shielded carbon beam-dump. A narrow neutron beam is formed in the forward direction by a system of three collimators, with a total thickness of more than four metres. The neutron energy spectrum is shown in Fig. 2. About half of all neutrons appear in the high-energy peak, while the rest are roughly equally distributed in energy, from the maximum energy and down to zero. The thermal contribution is small. The low-energy tail of the neutron beam can be reduced by time-of-flight measurements (see Fig. 2).

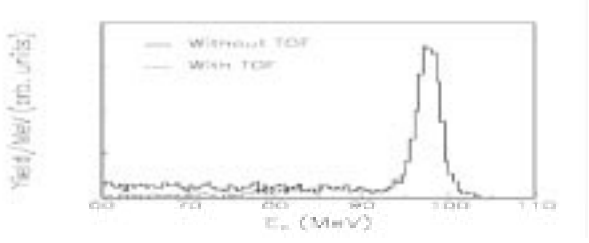

Fig. 2. The neutron energy spectrum with and without TOF rejection of low-energy neutrons [3].

II. Base equipment

Two major experimental setups are semi-permanently installed. The MEDLEY detector telescope array [5] is housed in a scattering chamber and operated in vacuum (see Fig. 3). At the exit of this chamber, a 0.1 mm stainless steel foil terminates the vacuum system, after which the neutrons travel in air. Immediately after MEDLEY follows SCANDAL (SCAttered Nucleon Detection AssembLy), a setup designed for large-acceptance neutron and proton detection [4].

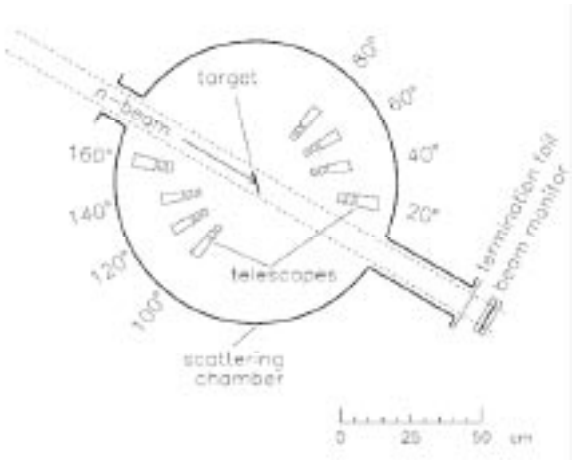

Fig. 3. The MEDLEY setup [5].

The MEDLEY detector array consists of eight particle telescopes, placed at 20-160 degrees with 20 degrees separation. Each telescope is a ΔE-ΔE-E detector combination, with sufficient dynamic range to distinguish all light ions from a few MeV up to maximum energy, i.e., about 100 MeV. The ΔE detection is accomplished by fully depleted silicon surface barrier detectors, and CsI (Tl) crystals are used as E detectors. For some experiments, active collimators are used. These are plastic scintillators with a hole defining the solid angle. All the equipment is housed in a 100 cm diameter scattering chamber, so that the charged particles can be transported in vacuum.

Recently, the facility has been used also for fission studies. In that case, the silicon detectors are used for fission fragment detection.

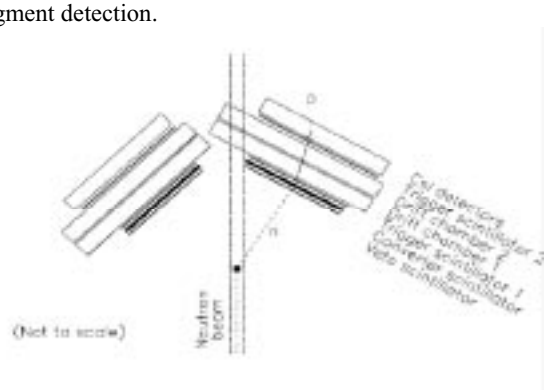

Figure 4. The SCANDAL setup [4].

The SCANDAL (SCAttered Nucleon Detection AssembLy) setup [4] has been designed for elastic neutron scattering studies. It consists of two identical systems, placed to cover 10-50 and 30-70 degrees, respectively (see Fig. 4). The energy of the scattered neutron is determined by measuring the energy of proton recoils from a plastic scintillator and the angle is determined by tracking the recoil proton. In a typical neutron scattering experiment, each arm consists of a 2 mm thick veto scintillator for fast charged-particle rejection, a 10 mm thick neutron-to-proton converter scintillator, a 2 mm thick plastic scintillator for triggering, two drift chambers for proton tracking, a 2 mm thick ΔE-plastic scintillator which is also part of the trigger, and an array of CsI detectors for energy determination of recoil protons produced in the converter by n-p scattering. The trigger is provided by a coincidence of the two trigger scintillators, vetoed by the front scintillator. SCANDAL can also be used as proton or deuteron detector. In those cases, the veto and converter scintillators are removed.

3. RESEARCH PROGRAMME

I. Elastic neutron scattering

Elastic neutron scattering is of utmost importance for a vast number of applications. Besides its fundamental importance as a laboratory for tests of isospin dependence in the nucleon-nucleon and nucleon-nucleus interaction, the optical potentials derived from elastic scattering come into play in virtually every application where a detailed understanding of nuclear processes are important. Elastic neutron scattering is important also for fast-neutron cancer therapy, because the nuclear recoils account for 10-15 % of the dose. Up to now, data on ^{12}C and ^{208}Pb at 96 MeV have been published Klug et al. [6] (see Fig. 5), and five other nuclei are under analysis.

A facility for studies of inelastic neutron scattering has recently been commissioned, and first data have been taken and are under analysis [7].

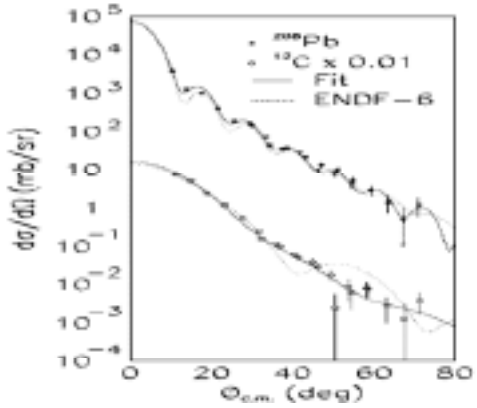

Fig. 5. Elastic neutron scattering at 96 MeV from ^{208}Pb and ^{12}C [6].

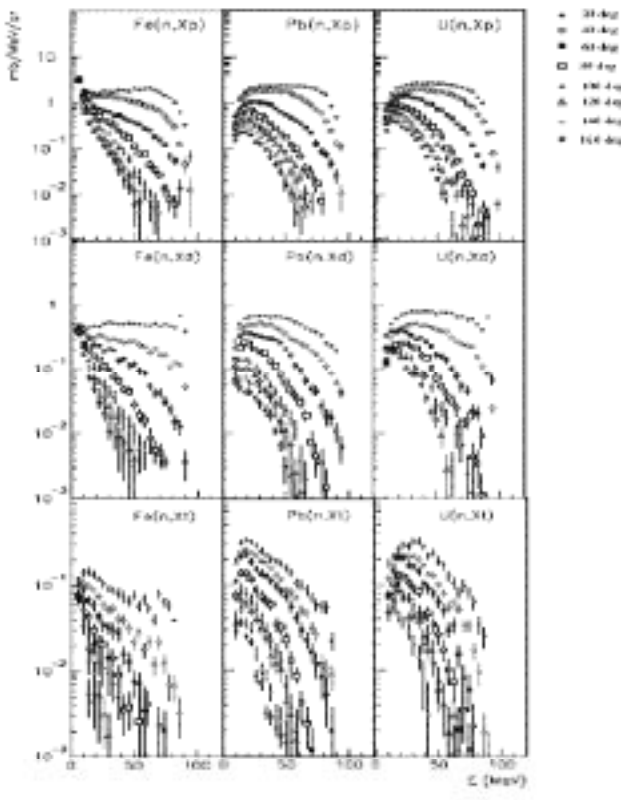

Fig. 6. Neutron- induced light-ion production in iron, lead and uranium at 96 MeV [8].

II. Light-ion production

Although the MEDLEY setup was initially intended for medical purposes, the requirements from these led to a multipurpose detector design, which has turned out to be useful for many different applications. One of these is hydrogen and helium production in ADS, exemplified with measurements on iron, lead and uranium (Blideanu et al. [8], see Fig. 6).

III. Fast-neutron fission

Although the main fission effects in an ADS arise from neutrons at lower energies, the high-energy neutron fission gives significant contributions to the power released. Very little data exist on high-energy fission, but the situation is under rapid improvement. This can be exemplified by the ongoing work at the TSL neutron beam, manifested in a number of recent publications by Smirnov et al. [9] and Ryzhov et al. [10]. In Figs. 7 and 8 some of these measured data of fast neutron fission cross sections are displayed. A new facility for studies also of angular distributions is under commissioning [11].

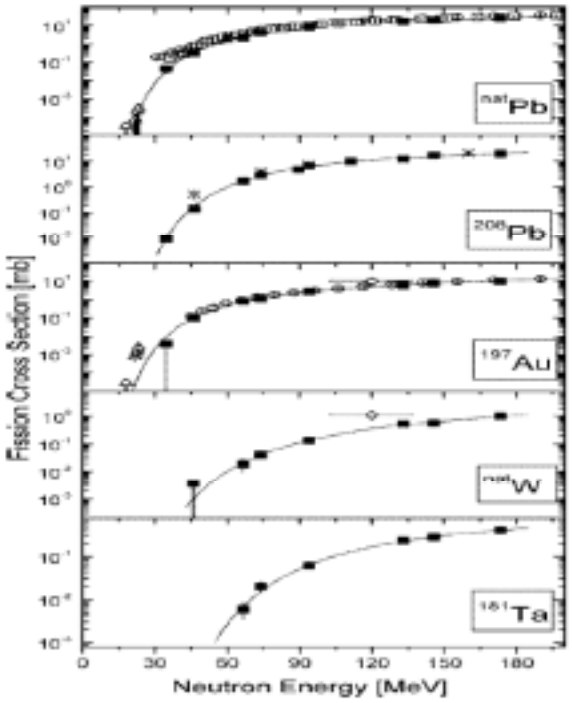

Figure 7. Cross sections for neutron-induced fission [9].

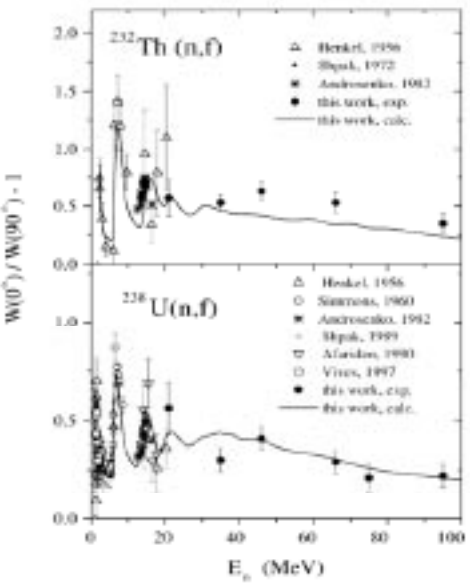

Figure 8. Anisotropies in neutron-induced fission [10].

4. Residue production

A series of studies of residue production has been carried out in parallel with the other experiments mentioned here, at an irradiation facility located just outside the primary neutron beam. For the short-lived residual radio-nuclides, cross sections were determined using activation techniques (see Fig. 9). The production of long-lived radio-nuclides was studied by Accelerator-Mass Spectroscopy (AMS) after chemical separation [12].

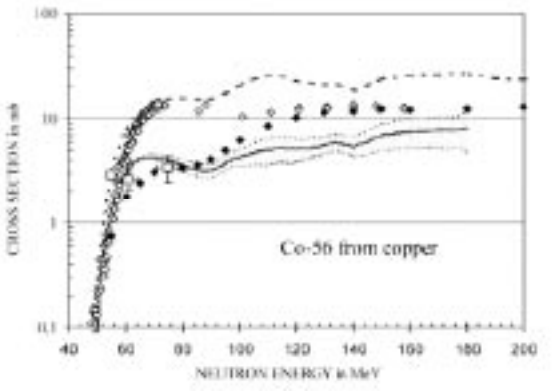

Fig. 9. Excitation function for the production of ^{56}Co from natural copper by neutron-induced reactions [12].

Fig. 10. The new TSL neutron beam facility [2].

IV. CONCLUSIONS

The rapid growth in demand for neutrons has motivated the construction of a new 20-180 MeV neutron beam facility at TSL (see Fig. 10) [2]. The most important features of the new facility are increased intensity by reduction of the distance from neutron production to experiments, availability of much larger beam diameters, increased versatility concerning various beam parameters, like the shape, and reserved space for a future pulse sweeping system.

For nuclear data research, the increased intensity will facilitate a large experimental program at 180 MeV, hitherto excluded by count rate limitations. For testing of electronics,

the increased intensity in combination with a larger beam diameter, which facilitates testing of a large number of components simultaneously, will provide a total failure rate of about a factor 300 larger than for the present facility. This means that the new TSL neutron beam facility can outperform any existing facility in the world. The facility being developed at TSL has wide applications also in the measurement of cross sections of medical relevance [13-14].

ACKNOWLEDGMENTS

This work was financially supported by Vattenfall AB, the Swedish Nuclear Fuel and Waste Management Company, the Swedish Nuclear Power Inspectorate, Ringhals AB, Barsebäck Power AB, Forsmarks Kraftgrupp AB, the Swedish Defense Research Agency, the Swedish Natural Science Research Council, the Swedish International Development Authority, the Swedish Nuclear Safety and Training Centre, and the European Union.

REFERENCES

1. J. Blomgren, "Experimental activities at high energies", Workshop on Nuclear Data for Science & Technology: Accelerator Driven Waste Incineration, Trieste, Italy, Sept. 10-21, 2001, eds. M. Herman, N. Paver and A. Stanculescu, ICTP lecture notes 12 (2002) 327.

2. S. Pomp, et al., "The new Uppsala neutron beam facility", AIP Conference Proceedings 769 (2005) 780.

3. H. Condé, et al., "A facility for studies of neutron induced reactions in the 50-200 MeV range", Nucl. Instr. Meth. A292 (1990) 121.

4. J. Klug, et al., "SCANDAL - A facility for elastic neutron scattering studies in the 50-130 MeV range", Nucl. Instr. Meth. A489 (2002) 282.

5. S. Dangtip, et al., "A facility for measurements of nuclear cross sections for fast neutron cancer therapy", Nucl. Instr. Meth. Phys. Res. A452 (2000) 484.

6. J. Klug, et al., "Elastic neutron scattering at 96 MeV from ^{12}C and ^{208}Pb,", Phys. Rev. C 68 (2003) 064605.

7. J. Blomgren, et al., "SCANDAL – a facility for elastic neutron scattering studies in the 50-130 MeV range", Proceedings of Science (FNDA2006) 052.

8. V. Blideanu, et al., "Nucleon-induced reactions at intermediate energies: New data at 96 MeV and theoretical status," Phys. Rev. C 70 (2004) 014607.

9. A.N. Smirnov, et al., "Measurement of Neutron-induced Fission Cross-sections for ^{nat}Pb, ^{208}Pb, ^{197}Au, ^{nat}W, and ^{181}Ta in the Intermediate Energy Region", Phys. Rev. C70 (2004) 054603.

10. I.V. Ryzhov, et al., "Influence of multichance fission on fragment angular anisotropy in the 232Th(n,f) and 238U(n,f) reactions at intermediate energies", Nucl. Phys. A760 (2005) 19.

11. A. V. Prokofiev, et al., "A new facility for high-energy neutron-induced fission studies", AIP Conference Proceedings 769 (2005) 800.

12. R. Michel, et al., "Residual nuclide production from iron, lead and uranium by neutron induced reactions up to 180 MeV", AIP Conference Proceedings 769 (2005) 861.

13. J. Blomgren and N. Olsson " Beyond KERMA - Neutron data for biomedical applications", Radiat. Prot. Dosim. 103(4) (2003) 293.

14. U. Tippawan, et al., "Light-Ion Production in the Interaction of 96 MeV Neutrons with Oxygen", Phys. Rev. C 73 (2006) 034611.

Radiation Protection Dosimetry (2007), Vol. 0, No. 0, pp. 1–4
DOI: 10.1093/rpd/xxx000

FAST NEUTRON BEAMS - PROSPECTS FOR THE COMING DECADE

J. Blomgren*
Department of Neutron Research, Uppsala University, Box 525, S-751 20 Uppsala, Sweden.

Received on June 12, 2006, revised on June 13, 2006, accepted on June 14, 2006

The present status of neutron beam production techniques above 20 MeV is discussed. Presently, two main methods are used; white beams and quasi-monoenergetic beams. The performances of these two techniques are discussed, as well as the use of such facilities for measurements of nuclear data for fundamental and applied research. Recently, two novel ideas on how to produce extremely intense neuton beams in the 100-500 MeV range have been proposed. Decay in flight of beta-delayed neutron-emitting nuclei could provide beam intensities five orders of magnitudes larger than present facilities. A typical neutron energy spectrum would be essentially mono-energetic, i.e., the energy spread is about 1 MeV with essentially no low-energy tail. A second option would be to produce beams of ^{6}He and dissociate the ^{6}He nuclei into α particles and neutrons. The basic features of these concept are outlined, and the potential for improved nuclear data research is discussed.

INTRODUCTION

The interest in high-energy neutron data is rapidly growing since a number of potential large-scale applications involving fast neutrons are under development, or have been identified. This has motivated nuclear data research for neutron therapy of cancer tumours [4], transmutation of spent nuclear fuel [1, 2, 3], and upsets in electronics [5, 6]. In the present paper, present and future techniques for nuclear data production for these applications are discussed.

PRESENT-DAY FACILITIES FOR NUCLEAR DATA MEASUREMENTS

At low energies (below 20 MeV or so), truly monoenergetic neutron beams can be produced. There are a few light-ion reactions, like D(d,n)^{3}He and T(d,n)^{4}He, which have positive Q-values and sizeable cross sections. Such a beam is strictly monoenergetic up to about 2 MeV incident deuteron energy. Above this energy, there is a possibility that the deuteron breaks up into a proton and a neutron. In reality, this is not a major obstacle until you get up to about 30 MeV neutron energy, because the T(d,n)^{4}He cross section is so large that the breakup neutrons form only a small low-energy tail. At even higher energies though, the T(d,n)^{4}He cross section is smaller, making the total yield too low for most measurements.

The largest neutron separation energy is about 20 MeV, making truly monoenergetic beams impossible to produce above that energy. What is available at higher energies are quasi-monoenergetic beams, i.e., beams where a single energy dominates, but always accompanied by a low-energy tail.

At energies of 50 MeV and up, three production reactions give reasonably monoenergetic beams. These are D(p,n), ^{6}Li(p,n) and ^{7}Li(p,n). The first has a large cross section, but the drawback that the energy resolution of the full-energy neutrons cannot be better than 3 MeV due to the Fermi motion of the neutron inside the deuteron. If a sharper energy definition is required, one of the two reactions using lithium is selected. They are about equally good, but there is a major practical difference: ^{6}Li is used in hydrogen bombs and is therefore not easily obtained, while ^{7}Li is provided at low cost. As one could expect, ^{7}Li(p,n) is the most common production reaction for monoenergetic neutron beams. At 100 MeV, about 50 % of the neutrons fall within 1 MeV at maximum energy, while the remaining half are distributed about equally from maximum energy down to zero. This is the closest to monoenergetic conditions nature provides. Effects due to the low-energy tail can in some cases be remedied on-line by time-of-flight rejection techniques. If that is unavailable, unfolding procedures are often used, in which cross sections at a few nominal energies have to be undertaken.

There is also a completely different approach; instead of trying to get the neutrons as well gathered in energy as possible, all energies are produced simultaneously. A high-energy proton beam hits a thick (in most cases stopping) target and lots of neutrons of all energies are produced, with typically a $1/E_n$ spectrum. If the incident proton beam is bunched and the experiment target is placed at a rather large distance from the neutron production target, time-of-flight (TOF) methods can be used to determine the energy of the incident neutron on an event-by-event basis.

The advantage of such so called white beams is the total intensity, which is larger than for monoenergetic beams, but instead the intensity per energy interval is much lower at high energies. This can partly be compensated for by summing data over limited energy intervals, but still the intensity per such interval

*Corresponding author. E-mail: Jan.Blomgren@tsl.uu.se

is lower. The advantage of being able to measure at many energies simultaneously is not worth much if you get insufficient statistics everywhere. As a consequence, white beams are restricted to experiments at low energies, where the intensities are large, or to high-energy reactions with rather large cross sections. Another feature is that white sources require event-by-event measurements. Experiments of effects with an energy dependence where the individual events cannot be distinguished cannot be performed at white beams. For experiments fulfilling the requirements above, white sources can, however, provide large quantities of very valuable information. This is especially true when excitation functions, i.e., the energy dependence of a cross section, is of particular interest.

NUCLEAR DATA STATUS

It is a fairly limited class of reactions that are of interest for the further development of the applications under consideration. The most important are elastic scattering, inelastic neutron emission, light ion production, heavy ion production and fission. The most recent work in the field has been carried out at the The Svedberg Laboratory, Uppsala, Sweden. Below, an account of the recent research at TSL is given, and this is also a good indication on the present level of the field.

Elastic scattering has been studied at TSL on a range of nuclei up to 96 MeV. At present, ten nuclei have been studied and results are either published or underway [7]. An overall uncertainty of about 5 % has been achieved. A novel normalization method has been established that allows elastic scattering data to be normalized absolutely to about 3 % uncertainty [8]. This method, however, works only for elastic scattering. Feasibility studies have shown that the technique as such works up to about 200 MeV, so these studies can be extended up in energy.

An experimental programme on inelastic neutron emission, i.e., (n,xn') reactions is in progress [9]. Data have been taken on lead and iron, and the method as such seems to work. It is too early to quote a final uncertainty in the results, but 10 % seems feasible.

Data on light ion production has been acquired on about ten nuclei at 96 MeV, and analysis is in progress [10, 11]. At present, about half the data set has been published. Normalization has been obtained by simultaneous detection of np scattering at an angle where the cross section uncertainty can be estimated to about 5 %, which is the dominating uncertatinty in the final light ion production cross sections. These studies are presently being extended to 180 MeV.

Fission cross sections have been studied at many facilities up to about 200 MeV energy. The energy dependencies of the cross sections agree fairly well in shape, but the absolute scale differs by up to 15 %. It is at present not clear what causes this. One possibility is the normalizations used. Another possible cause is that the sensitivity to low-energy neutrons is not under control for some of the experiments. Dedicated experiments to remedy this situation are underway.

In principle, fission cross sections can be measured up to several GeV using white beams with a very high initial proton energy, like at the CERN-nTOF facility [12]. The neutron beam intensity is very low, but the cross sections are large and it is possible to detect a major fraction of the fission fragments, resulting in reasonable statistical precision. A major problem, however, is normalization, since the beam intensity is very difficult to monitor at these very high energies.

There are only a few examples of other fission data than cross sections. This means that important fission parameters, like angular distributions, yields, etc., essentially remain to be investigated at high neutron energies.

POSSIBLE FUTURE FACILITIES

As was discussed in the previous section, the prospects for development in the near future, i.e., within ten years, can be summarized to extension to about 200 MeV of ongoing work on elastic scattering, inelastic neutron emission and light ion production at around 100 MeV, and fission studies of other parameters than the cross section.

If looking a bit further into the future, we can allow ourselves to be more visionary. To my opinion, the single most important problem to solve if we want a significant development of the field is normalization. At present, we inevitably end up with an uncertainty of about 5 %, because we have to normalize to a reference, typically np scattering, which is known to - at best - 5 %, and it is difficult to see how this can be radically improved upon in a short term with present techniques.

I consider energy resolution to be the second largest problem, with intensity on third place. These two are, however, to a large degree coupled. If you aim for good neutron-beam energy resolution, you have to pay by poor intensity and vice versa. It is presently close to inconceivable to produce neutrons at high energies with a resolution better than 1 MeV with a reasonable intensity. The limited intensity puts severe constraints on the detection, in such a way that the detection often has to be performed with techniques that sacrifice resolution for efficiency, resulting in a final resolution of a few MeV. This means that only in a few rare cases, final states can be resolved.

Recently, a way out of this dilemma has been proposed as a by-product of the CERN beta-beam facility [13] under consideration. The background is that neutrino physics has progressed rapidly the last few years, with the discovery of neutrino oscillations as the most visible example. Up to now, essentially all accelerator-produced neutrinos have been muon neutrinos, being the final product of pion decay. Electron neutrinos are much more difficult to produce in large

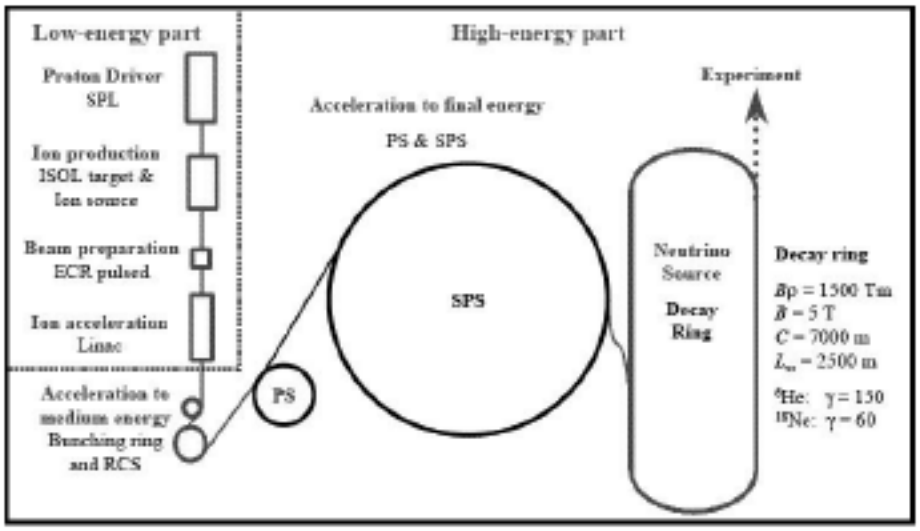

Figure 1. Overview of the proposed CERN beta-beam facility.

amounts, because they require a nuclear beta decay for their creation.

At the proposed CERN beta-beam facility, production of suitable beta-emitting nuclei should be undertaken in an ISOLDE-like facility, and the produced nuclei should be post-accelerated to very high energy and stored in a decay ring of race-track shape. At these very high energies, hundreds of GeV/A, there is a very strong Lorentz boost, which means that the neutrino is emitted very close to the beam direction in the laboratory system, in spite of that the emission is isotropic in its moving reference frame. Thereby, intense neutrino beams can be produced. The idea is to build the decay ring so that one straight section points towards a distant neutrino detector to allow studies of electron neutrino oscillations.

Intense neutron beams could be a spin-off from that facility. It has been proposed to use two production targets, one for nuclei suited for neutrino emission in the decay ring, and one for beta-delayed neutron emitters [14]. Some neutron-rich nuclei beta decay to a nucleus that promptly emits a neutron, which typically has an energy of a few hundred keV in its rest frame. By accelerating the beta-delayed neutron emitters up to a few hundred MeV per nucleon, the Lorentz boost is sufficient to focus the beam to reasonable dimensions. For instance, at 100 MeV per nucleon, with a maximum transverse neutron energy of about 1 MeV (the maximum energy of a beta-delayed neutron), the maximum opening angle is about 6 degrees. The average divergence, however, is much smaller because the average neutron energy is smaller and since the decay is isotropic in the center-of-momentum system, many decays take place close to the beam direction. Typically, a 2 degree divergence can be reached. All this can be done in parallel with the primary objective, since the accelerators for the neutrino emitters have a long cycle with a low duty factor.

The resulting neutron beam has an energy in the 100–500 MeV range with an energy resolution of about 1 MeV, and intensities of about 10^{11} n/s are estimated [14]. One example of a precursor nucleus is ^{137}I, for which the estimated production is $1 \cdot 10^{13}$ s^{-1}, based on an expected fission rate of $1 \cdot 10^{15}$ s^{-1} with high-energy protons impinging on a UC_2 target. If the filling of a storage ring balances the decays, it means that the fraction of decays leading to delayed neutron emission determines the neutron intensity. In the present case, it is 7 %, leading to $7 \cdot 10^{11}$ s^{-1} neutron intensity. Finally, only decays along the straight section of a race-track storage ring would result in a beam. Assuming 15 % of the circumference to act as a useful neutron source, the resulting neutron intensity would be $1 \cdot 10^{11}$ s^{-1}.

This should be compared with 10^{6} for present-day technology, i.e., an improvement by a factor 100 000 (!). With such intensities, only imagination sets the limit for what can be achieved.

If we now restrict the discussion to nuclear data for applications and turn to my problem list above, it seems feasible that we can address all of them through one experimental trick: tagging. If we use the neutron beam directly for experiments we have essentially only solved the intensity problem, but the other two remain; we end up in a 1 MeV resolution due to the inherent energy spread, and we are still plagued by the normalization problem. Tagging means that we produce a secondary neutron beam of less intensity, but with much better known intensity. One candidate

reaction is to let neutrons scatter from a hydrogen target, and the recoil proton is detected. Since this is a two-body final state, detection of the associated proton means that a neutron must have been scattered to the corresponding direction. Thereby, the normalization problem can be circumvented, since we count the neutrons one by one through the associated particle. If high-resolution tagging is performed, we can also know the neutron energy event by event far better than the initial neutron beam energy resolution. If the tagging is performed with a magnetic spectrometer, the tagger can be made rather insensitive to the ambient background, and a proton energy resolution of better than 100 keV can be obtained, resulting in a comparable neutron energy resolution.

With reasonable estimates on tagger parameters, 10^4 tagged neutrons with an energy resolution of 100 keV should be possible to reach, given the beam intensity above. This might sound like a poor intensity, but with such a resolution, final states can be well resolved, which means that already a small number of events will result in a good precision. Moreover, since the intensity can be determined to about 1 % in a typical tagger system, the accuracy is far better than what can be obtained today. In cases when the demands on energy resolution are not as stringent, a thicker tagger target can be used, resulting in increased intensity. This goes faster than linear, because with a worse resolution, the intensity at the tagger is increased, thicker secondary experimental targets can be used, and the detection limitations are less severe. Therefore, even with resolutions that are on the limit to be possible untagged today, we might have tagged beams of intensities exceeding what is presently available untagged in a not too distant future.

A second technique would be to use a similar production as above (1-2 GeV protons on a combined target-ion source) to produce ^{6}He, which in turn would be accelerated to hit a target [15]. Roughly, ^{6}He can be described as an α particle with two loosely attached neutrons. When hitting a target, the two neutrons are dissociated with a large probability, and continue along the direction of the incident beam with the incident velocity. The charged particles (the remaining ^{6}He and residual ^{4}He) are bent by a magnet system and a clean neutron beam is produced, with a divergence similar to that of a beta-delayed neutron beam. This latter technique does not have the potential to produce as intense fluxes as the beta-decay in flight, but on the other hand it requires much less advanced accelerators. This technique could possibly be installed at existing CERN facilities after some upgrades. Initial estimates indicate a factor a hundred to a thousand larger neutron fluxes than for present facilities to be within reach.

Acknowledgments

The information from Mats Lindroos is gratefully acknowledged. This work was financially supported by the Swedish Nuclear Fuel and Waste Management Company, the Swedish Nuclear Power Inspectorate, Ringhals AB, Forsmarks Kraftgrupp AB, the Swedish Defense Research Agency, the Swedish Nuclear Safety and Training Centre, and the European Union.

REFERENCES

1. A. Koning, *et al.*, J. Nucl. Sci. Tech., Suppl. **2** (2002) 1161.
2. J. Blomgren, in Proceedings of Workshop on Nuclear Data for Science & Technology: Accelerator Driven Waste Incineration, Trieste, Italy, Sept. 10-21, 2001, eds. M. Herman, N. Paver, A. Stanculescu, ICTP lecture notes **12** (2002) 327.
3. J. Blomgren, Nuclear data for accelerator-driven systems - Experiments above 20 MeV, in Proceedings of EU enlargement workshop on Neutron Measurements and Evaluations for Applications, Bucharest, Romania, October 20-23, 2004.
4. J. Blomgren and N. Olsson, Radiat. Prot. Dosim. **103(4)** (2003) 293.
5. J. Blomgren, B. Granbom, T. Granlund, N. Olsson, Mat. Res. Soc. Bull. **28** (2003) 121.
6. J. Blomgren, Nuclear Data for Single-Event Effects, in Proceedings of EU enlargement workshop on Neutron Measurements and Evaluations for Applications, Budapest, Hungary, November 5-8, 2003. EUR Report 21100 EN, Luxembourg: Office for Official Publications of the European Communities, ISBN 92-894-6041-5, European Communities, 2004.
7. A. Hildebrand, *et al.*, AIP Conference Proceedings **769** (2005) 853.
8. J. Klug, *et al.*, Phys. Rev. C **68**, 064605 (2003).
9. F.-R. Lecolley, private communication.
10. V. Blideanu, *et al.*, Phys. Rev. C **70** (2004) 014607.
11. U. Tippawan, *et al.*, Phys. Rev. C **69**, 064609 (2004).
12. L. Tassan-Got, private communication.
13. The CERN beta-beam working group, http://cern.ch/beta-beam.
14. M. Lindroos, private communication.
15. I. Tanihata and T. Nilsson, private communication.

Radiation Protection Dosimetry (2004), Vol. 0, No. 0, pp. 1–4
DOI: 10.1093/rpd/xxx000

PRECISION MEASUREMENTS OF THE NP SCATTERING DIFFERENTIAL CROSS SECTION IN THE INTERMEDIATE ENERGY REGION

P. Mermod [a], J. Blomgren [a,*], L. Nilsson [a], S. Pomp [a], A. Öhrn [a], M. Österlund [a], A. Prokofiev [b], and U. Tippawan [c]
[a]Department of Neutron Research, Uppsala University, Box 525, S-75120 Uppsala, Sweden
[b]The Svedberg Laboratory, Uppsala University, Uppsala, Sweden
[c]Fast Neutron Research Facility, Chiang Mai University, Chiang Mai, Thailand

Received on April 2, 2003, revised on November 19, 2003, accepted on December 22, 2003

In fast neutron cancer therapy, about 50% of the cell damage is caused by recoil protons from neutron-proton (*np*) scattering. In the intermediate energy region, there is a need for unambiguous *np* scattering data with good precision in both the shape of the angular distribution and the absolute normalization. We review the normalization techniques for *np* scattering measurements as well as recent experimental results, in particular the data obtained at The Svedberg Laboratory (TSL) at 96 and 162 MeV. In addition, to what extent systematic uncertainties in the *np* differential cross section might affect the determination of proton recoil kerma coefficients is investigated.

INTRODUCTION

Besides its crucial importance as a primary standard in neutron scattering measurements, the neutron-proton (np) differential cross section plays a major role in both fundamental nuclear physics and medical fast neutron applications. Precision measurements in two-nucleon systems allow to test the nucleon-nucleon potential models such as the CD-Bonn potential [1] and the AV18 potential [2], to cite two of the most recent ones. In particular, the np differential cross section at backward angles at intermediate energies can be used to extract the strength of the coupling of the pion to the nucleon in meson-exchange models, the πNN coupling constant.

In the present work, we are interested in fast neutron applications such as dosimetry and cancer treatment. Among the nuclei of interest for this application, we identify the main components of human tissue and bones, which are hydrogen, carbon, oxygen, nitrogen and calcium. The damage inflicted to the cells depends on cross sections for the neutron-induced reactions on these nuclei as well as the energies and masses of the released ionizing particles. A rough evaluation tells us that about 50% of the cell damage is due to recoil protons in np scattering, about 10% is due to elastic and inelastic scattering on other nuclei, and the rest is due to neutron-induced emission of light ions [3, 4]. The contribution from neutron scattering on carbon and oxygen is investigated in a separate paper [5], and light-ion production at 96 MeV is discussed in articles by Tippawan *et al.* and Pomp *et al.* of this workshop [6, 7]. In the present paper, we investigate how the evaluation of the 50% contribution from np scattering is affected by uncertainties in the np differential cross section.

*Corresponding author. E-mail: jan.blomgren@tsl.uu.se

METHODS FOR NP DIFFERENTIAL CROSS SECTION MEASUREMENTS

For the reasons mentioned above, one would like the np differential cross section at intermediate energies (typically between 65 and 250 MeV) to be known as precisely as possible, in both shape and absolute scale.

The np differential cross section at backward neutron angles can be obtained in a rather straightforward manner by detecting the recoil protons, usually from a CH_2 target foil (and a graphite foil for carbon background subtraction), either with detector telescopes placed at different angles or with a magnetic spectrometer (see, e.g., the Rahm *et al.* experiments in Refs. [8, 9]). In the forward angular range, this method becomes impractical because the energy of the protons becomes too low, and the scattered neutrons must be detected instead. This can be done by converting the scattered neutrons into protons by a subsequent np reaction in a plastic scintillator, and tracking the secondary protons through a detector setup (see, e.g., the Johansson *et al.* experiment in Ref. [10]).

A notorious problem is the absolute normalization of the cross section, since the neutron beam fluence, when measured by means of fission-based monitors, is not known to a precision better than 10% in the intermediate energy region. There are two possible unambiguous methods to determine the np scattering cross section absolutely. One method is tagging, i.e., the number of neutrons produced in the neutron production target are counted by detecting associated charged particles, for instance, proton recoils in the reaction $p + d \rightarrow n + 2p$. In that way, one sacrifices beam intensity for its exact knowledge. Recently, this method has been successfully applied at IUCF (see the Sarsour *et al.* experiment at 194 MeV in Ref. [11]). The second method is to normalize the np differential cross section to the total

np cross section, which in turn can be measured without knowledge of the beam intensity (a measurement of the relative beam attenuation in the target is sufficient) to a precision of about 1%. The draw-back of this method is that it requires a large angular distribution coverage. In the Rahm *et al.* experiments at 96 and 162 MeV [8, 9], the lacking forward angular range was filled using nuclear models; it resulted in an absolute normalization uncertainty of about 2%. Later on, data at 96 MeV were obtained in this angular range by Johansson *et al.* [10], which resulted in a renormalization of the Rahm *et al.* data by 0.7%, and allowed to reduce the normalization uncertainty to about 1%.

RECENT DATA AT 96 AND 162 MEV

We consider recent data of the np differential cross section obtained at 96 and 162 MeV, shown in the upper panels of Figs. 1 and 2, respectively. The data shown at 96 MeV were taken at the TSL neutron beam facility in Uppsala, with the LISA (L) magnetic spectrometer (Rahm *et al.* [8]), the SCANDAL (S) setup (Johansson *et al.* [10], Blideanu *et al.* [12], and Mermod *et al.* [13]) and the MEDLEY (M) setup (Mermod *et al.* [14]). The data at 162 MeV are from Rahm *et al.* [9]. The data from Sarsour *et al.* [11], obtained with a tagged neutron beam, were originally taken at 194 MeV. For comparison purposes, they are transformed to 162 MeV by multiplying each data point by the ratio of the differential cross section at 162 MeV to the differential cross section at 194 MeV (at the corresponding angle), using the Nijmegen partial wave analysis PWA93 [15]. The PWA93 calculations and the prediction from the CD-Bonn NN potential (and, in Fig. 1, also the AV18 potential) are plotted for comparison.

In the middle and bottom panels of the figures, one can follow in a comprehensive way how the probability to cause cell damage is obtained from the differential cross sections. The middle panels show the differential cross sections multiplied with the solid angle element $2\pi \sin\theta$ as functions of the neutron scattering angle in the laboratory system, θ: they illustrate the angular probability distributions for neutron scattering. As the solid angle vanishes at zero and 180 degrees, these distributions are no longer forward and backward peaked. In the bottom panels, the distributions have been weighted with the energy of the recoil protons E_R, thus illustrating the angular probability distributions for the neutrons to cause cell damage. Back-scattered neutrons transfer more energy to the protons than forward-scattered neutrons, and therefore the energy of the recoil nuclei increases with the neutron scattering angle. From these distributions, which peak at about 70°, we deduce that most of the damage is caused by neutrons scattered between 50 and 85° (in the laboratory).

Table 1. Proton recoil partial kerma coefficients at 96 MeV and 162 MeV, for the Rahm *et al.* data [9, 8], the ICRU report from evaluated data [16], the Nijmegen partial-wave analysis PWA93 [15], and the CD-Bonn and AV18 NN potentials [1, 2].

k (fGy·m^2)	$E_n = 96$ MeV	$E_n = 162$ MeV
Rahm *et al.*	36.5±0.4	40.6±0.8
ICRU	36.6	–
PWA93	37.2	41.4
CD Bonn	37.0	41.1
AV18	36.9	–

PROTON RECOIL KERMA COEFFICIENTS

The partial kerma coefficient k is the average kinetic energy of one type of charged particle produced in matter due to a certain reaction per unit mass divided by the neutron fluence. If the neutrons are propagating inside a living organism, the kerma coefficient is closely related to the probability to cause irreversible DNA damage through the considered reaction. In the case under consideration, the reaction is np scattering at 96 and 162 MeV incident neutron energy and the charged particle is the recoil proton. Thus, the proton recoil kerma coefficient is proportional to the integral of the differential cross section multiplied with the solid angle element and the energy of the recoil nucleus:

$$k = N \int E_R \frac{d\sigma}{d\Omega}(\theta) 2\pi \sin\theta d\theta,$$

where N is the inverse nuclear mass of the recoil proton, E_R is its kinetic energy in the laboratory system, and $2\pi \sin\theta$ is the solid angle element at the neutron laboratory angle θ. We note that the proton recoil kerma coefficients are proportional to the area under the distributions in the bottom panels of Figs. 1 and 2.

The values of k are obtained for the Rahm *et al.* data at the two energies under consideration [8, 9] as well as for the different theory predictions, and presented in Table 1. For the Rahm *et al.* data, in the forward region (where data are lacking) the curve from PWA93 was used for the extraction of k: this caused a negligible uncertainty since the contribution to k is small in this angular range. At 96 MeV, the ICRU value obtained from evaluated data [16] is also shown in the table.

DISCUSSION AND CONCLUSION

By plotting the angular probability distribution for np scattering weighted with the recoil proton energy, we have identified that the most relevant angular range as far as the deposited dose is concerned is the region $50-85°$. In this angular range, there exist high-precision np data from Uppsala at 96 and 162 MeV (the Rahm *et al.*

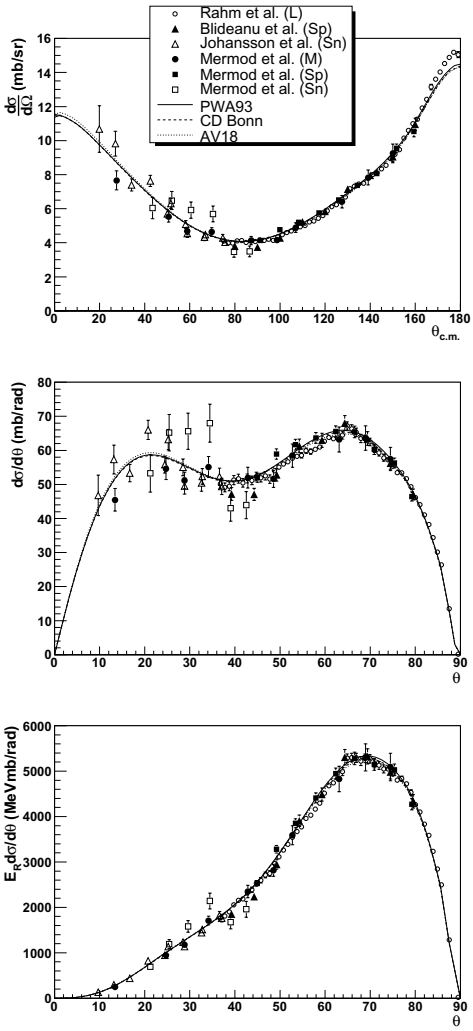

Figure 1. Elastic np scattering at 96 MeV. The angles $\theta_{c.m.}$ and θ are the neutron scattering angles in the c.m. and laboratory systems, respectively. The experimental data are from Uppsala, from Refs. [8, 10, 12, 13, 14]: (L) stands for the LISA magnetic spectrometer, (Sp) and (Sn) for the SCANDAL setup where protons and neutrons are detected, and (M) for the MEDLEY setup. The calculations are from the partial wave analysis PWA93 [15] and the CD-Bonn [1] and AV18 [2] NN potentials. Elastic scattering differential cross sections are shown in the top panels; in the middle panels, the differential cross sections were multiplied with the solid angle elements; in the bottom panels, they were further multiplied with the energy of the recoil protons. The areas under these last plots are proportional to the proton recoil kerma coefficients.

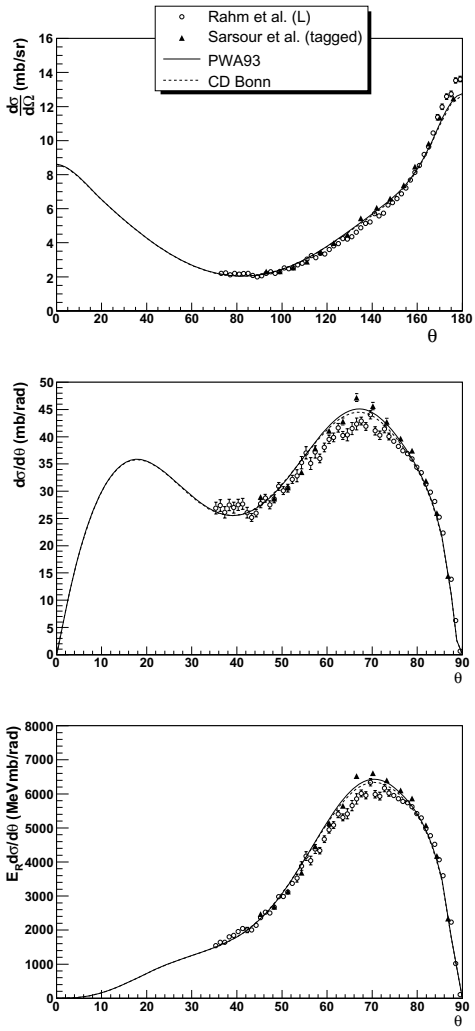

Figure 2. Elastic np scattering at 162 MeV. The angles $\theta_{c.m.}$ and θ are the neutron scattering angles in the c.m. and laboratory systems, respectively. The experimental data are from Rahm *et al.* [9] and Sarsour *et al.* [11]. The Sarsour *et al.* data, originally taken at 194 MeV, were transformed to 162 MeV using the PWA93 calculations. The curves are from PWA93 [15] and the CD-Bonn [1] NN potential. Elastic scattering differential cross sections are shown in the top panels; in the middle panels, the differential cross sections were multiplied with the solid angle elements; in the bottom panels, they were further multiplied with the energy of the recoil protons. The areas under these last plots are proportional to the proton recoil kerma coefficients.

data [8, 9]), which were normalized to the total np cross section with an accuracy of $1-2\%$. The shape of the Rahm *et al.* data, however, do not match exactly the shape of the PWA93 or NN potential calculations: the predictions tend to overestimate very slightly the data in the range $50-80^{\circ}$, which happens to be our sensitive region (and they tend to underestimate the data above 80°, but this has no consequences in the present

discussion). Thus, this little mismatch is responsible for a difference of up to 2% in the proton recoil kerma coefficients between the data and calculations. However, the Sarsour *et al.* data [11], obtained with a tagged neutron beam at 194 MeV, agree very well with the calculations in both the shape and the absolute scale, indicating that the effect might be due to systematic uncertainties in the Rahm *et al.* data affecting the shape of the angular distribution. This interpretation is supported by the observation that the shapes of the other sets of data at 96 MeV, measured with different techniques, tend to be in good agreement with PWA93.

ACKNOWLEDGEMENTS

We wish to thank the technical staff of the The Svedberg Laboratory for enthusiastic and skillful assistance. This work was supported by the Swedish Nuclear Fuel and Waste Management Company, the Swedish Nuclear Power Inspectorate, Ringhals AB, the Swedish Defence Research Agency and the Swedish Research Council.

REFERENCES

1. R. Machleidt, "High-precision, charge-dependent Bonn nucleon-nucleon potential", Phys. Rev. C **63**, 024001 (2001).
2. R.B. Wiringa, V.G.J. Stoks, and R. Schiavilla, "Accurate nucleon-nucleon potential with charge-independence breaking", Phys. Rev. C **51**, 38 (1995).
3. J. Blomgren and N. Olsson, "Beyond Kerma - Neutron Data for Biomedical Applications", Radiat. Prot. Dosim. **103**, 293 (2003).
4. M.B. Chadwick, P.M. DeLuca Jr., and R.C. Haight, "Nuclear data needs for neutron therapy and radiation protection", Radiat. Prot. Dosim. **70**, 1 (1997).
5. P. Mermod *et al.*, "Elastic neutron scattering from light nuclei at 96 MeV", these proceedings.
6. U. Tippawan *et al.*, "Light charged-particle production in 96 MeV neutron-induced reactions on carbon and oxygen", these proceedings.
7. S. Pomp *et al.*, "Neutron-induced light-ion production from Fe, Pb and U at 96 MeV", these proceedings.
8. J. Rahm *et al.*, "np scattering measurements at 96 MeV", Phys. Rev. C **63**, 044001 (2001).
9. J. Rahm *et al.*, "np scattering measurements at 162 MeV and the πNN coupling constant", Phys. Rev. C **57**, 1077 (1998).
10. C. Johansson *et al.*, "Forward-angle neutron-proton scattering at 96 MeV", Phys. Rev. C **71**, 024002 (2005).
11. M. Sarsour *et al.*, "Measurement of the Absolute np Scattering Differential Cross Section at 194 MeV", Phys. Rev. Lett. **94**, 082303 (2005).
12. V. Blideanu *et al.*, "Nucleon-induced reactions at intermediate energies: New data at 96 MeV and theoretical status", Phys. Rev. C **70**, 014607 (2004).
13. P. Mermod *et al.*, "Evidence of three-body force effects in neutron-deuteron scattering at 95 MeV", Phys. Rev. C **72**, 061002(R) (2005); P. Mermod *et al.*, "95 MeV neutron scattering on hydrogen, deuterium, carbon and oxygen", submitted to Phys. Rev. C.
14. P. Mermod *et al.*, "Search for three-body force effects in neutron-deuteron scattering at 95 MeV", Phys. Lett. B **597**, 243 (2004).
15. V.G.J. Stoks, R.A.M. Klomp, M.C.M. Rentmeester, and J.J. de Swart, "Partial-wave analysis of all nucleon-nucleon scattering data below 350 MeV", Phys. Rev. C **48**, 792 (1993).
16. ICRU Report 63, Nuclear Data for Neutron and Proton Radiotherapy and for Radiation Protection (International Commission on Radiation Units and Measurements, MD, 2000).

Radiation Protection Dosimetry (2004), Vol. 0, No. 0, pp. 1–4
DOI: 10.1093/rpd/xxx000

KERMA COEFFICIENTS FOR NEUTRON SCATTERING ON ^{12}C AND ^{16}O AT 96 MEV

P. Mermod [a], J. Blomgren [a] *, L. Nilsson [a], S. Pomp [a], A. Öhrn [a], M. Österlund [a], A. Prokofiev [b], and U. Tippawan [c]
[a] Department of Neutron Research, Uppsala University, Box 525, S-75120 Uppsala, Sweden
[b] The Svedberg Laboratory, Uppsala University, Uppsala, Sweden
[c] Fast Neutron Research Facility, Chiang Mai University, Chiang Mai, Thailand

Received on April 2, 2003, revised on November 19, 2003, accepted on December 22, 2003

Recently, many new applications of fast neutrons are emerging or under development, like dose effects due to cosmic-ray neutrons for airplane crew, fast neutron cancer therapy, studies of electronics failure induced by cosmic-ray neutrons and accelerator-driven incineration of nuclear waste and energy production technologies. In radiation treatment the kerma (Kinetic Energy Release in MAtter) coefficient, which describes the average energy transferred from neutrons to charged particles, is widely used. The kerma coefficient can be calculated from microscopic nuclear data. Nuclear data above 20 MeV are rather scarce and more complete nuclear data libraries are needed in order to improve the understanding of the processes occurring on a cellular level. About half the dose in human tissue due to fast neutrons comes from proton recoils in neutron-proton (np) scattering, $10-15$% from nuclear recoils due to elastic and inelastic neutron scattering and the remaining $35-40$% from neutron-induced emission of light ions. Experimental data on elastic and inelastic neutron scattering at 96 MeV from ^{12}C and ^{16}O have been obtained recently at The Svedberg Laboratory in Uppsala, Sweden. These data are shown to be relevant for the determination of nuclear recoil kerma coefficients from elastic and inelastic neutron scattering at intermediate energies.

INTRODUCTION

Neutron cross sections at intermediate energies are relevant to applications such as transmutation of nuclear waste [1, 9], medical treatment of tumors with fast neutrons [2], and the mitigation of single-event effects in electronics [3]. Experimental data for neutron-induced reactions on a wide range of nuclei are needed to improve data evaluations and nuclear models which are to be implemented in Monte-Carlo codes in relation to these applications.

Fast neutrons have a potential for efficient cancer therapy treatment. Among the nuclei of interest for this application, we identify the main components of human tissue and bones, which are hydrogen, carbon, oxygen, nitrogen and calcium. The damage inflicted to the cells depends on cross sections for the interactions of neutrons with these nuclei as well as the energies and masses of the released ionizing particles. A rough evaluation tells us that about 50% of the cell damage is due to neutron-proton (np) scattering, about 10% is due to elastic and inelastic scattering on other nuclei, and the rest is due to neutron-induced emission of light ions [2, 4]. The contribution from np scattering is investigated in a separate paper [5], and light-ion production at 96 MeV is discussed in articles by Tippawan *et al.* and Pomp *et al.* of this workshop [6, 7]. In the present work, we focus on the $\sim$10% contribution caused by elastic and inelastic neutron scattering on carbon and oxygen.

*Corresponding author. E-mail: jan.blomgren@tsl.uu.se

Using the SCANDAL multi-detector array at The Svedberg Laboratory in Uppsala (details about SCANDAL can be found in Ref. [8]), we performed neutron elastic scattering experiments at 96 MeV on a large variety of nuclei, such as ^{1}H, ^{2}H, ^{12}C, ^{14}N, ^{16}O, ^{28}Si, ^{40}Ca, ^{56}Fe, ^{89}Y, and ^{208}Pb. In the present discussion, we concentrate on carbon and oxygen, and data on heavy nuclei are discussed in a separate contribution to this workshop by Österlund *et al.* [9]. Recently, in the context of a neutron-deuteron scattering experiment whose primary aim was to investigate three-nucleon force effects [10, 11], high-precision differential cross sections were obtained for ^{12}C(n,n) and ^{16}O(n,n) scattering at 96 MeV. The measurement on carbon is an extension of the Klug *et al.* data obtained with the same technique [12]. In addition, inelastic scattering data were extracted. The new data on carbon and oxygen were reported in Ref. [11]. In this publication, we pointed out that these data might be relevant for cancer treatment of tumors with fast neutrons, and we identified angular regions where the accuracy of the theoretical calculations were not satisfying. In the present paper, we discuss further how the uncertainties in the elastic and inelastic differential cross sections on carbon and oxygen affect the estimation of the nuclear recoil kerma coefficients at intermediate energies.

DIFFERENTIAL CROSS SECTIONS AND KERMA COEFFICIENTS

The partial kerma coefficient k is the average kinetic energy of one type of charged particle produced in

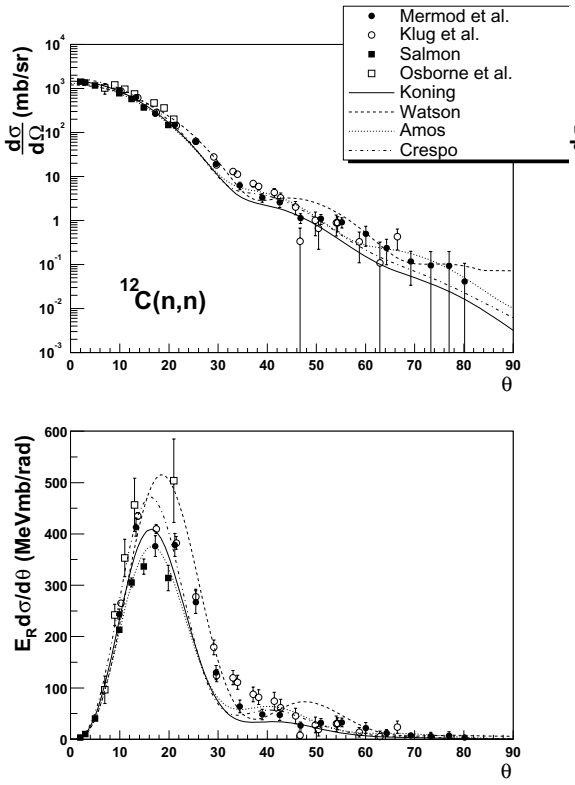

Figure 1. Elastic neutron scattering on carbon at 96 MeV. The angle θ is the neutron scattering angle in the laboratory. The experimental data are from Refs. [11, 12, 13, 14]. The elastic scattering differential cross section is shown in the top panel, and in the bottom panel, the differential cross section was multiplied with the solid angle element and with the energy of the recoil nucleus. The area under this plot is proportional to the nuclear recoil kerma coefficient for elastic scattering.

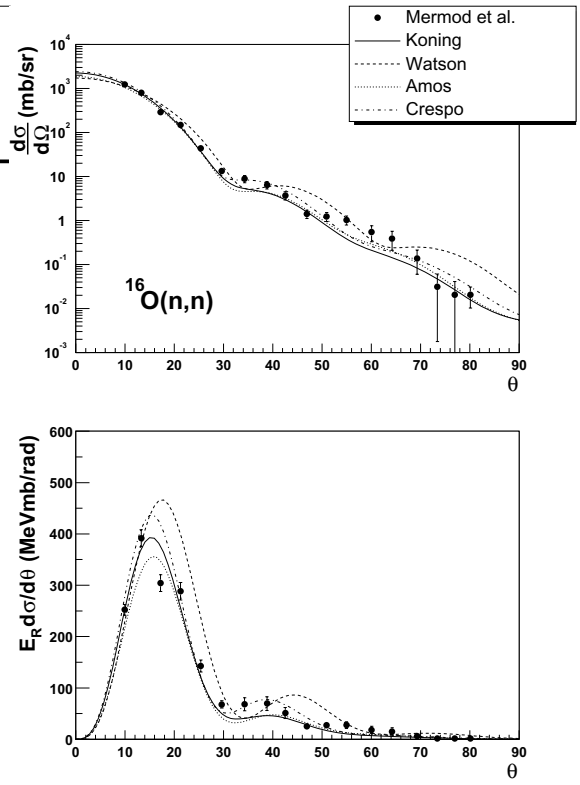

Figure 2. Elastic neutron scattering on oxygen at 96 MeV. The angle θ is the neutron scattering angle in the laboratory. The experimental data are from Ref. [11]. The elastic scattering differential cross section is shown in the top panel, and in the bottom panel, the differential cross section was multiplied with the solid angle element and with the energy of the recoil nucleus. The area under this plot is proportional to the nuclear recoil kerma coefficient for elastic scattering.

matter due to a certain process per unit mass divided by the neutron fluence. If the neutrons are propagating inside a living organism, the kerma coefficient is closely related to the probability to cause irreversible DNA damage through the considered process. In our case, the process is elastic or inelastic scattering at 96 MeV incident neutron energy and the charged particle is the carbon or oxygen recoil nucleus. Thus, the recoil kerma coefficient is proportional to the integral of the differential cross section multiplied with the solid angle element and the energy of the recoil nucleus:

$$k = N \int E_R \frac{d\sigma}{d\Omega}(\theta) 2\pi \sin\theta d\theta,$$

where N is the inverse nuclear mass of the recoil nucleus, E_R is its kinetic energy in the laboratory system, and $2\pi \sin\theta$ is the solid angle element at the neutron laboratory angle θ.

Figs. 1 (carbon) and 2 (oxygen) illustrate how recoil kerma coefficients are obtained from the differential cross sections. The elastic neutron scattering data at 96 MeV are from Mermod *et al.* [11], Klug *et al.* [12], Salmon [13] and Osborne *et al.* [14]. The theoretical curves are predictions from the Koning and Delaroche global potential [15], the Watson global potential [16], Amos *et al.* [17], and Crespo *et al.* [18] (see Refs. [11, 12] for details). In the top panels of the figures, the differential cross sections (in logarithmic scale) are plotted as functions of the neutron scattering angle in the laboratory. In the bottom panels, the distributions have been multiplied with the solid angle element $2\pi \sin\theta$ and weighed with the energy of the recoil nuclei E_R, thus illustrating the angular probability distributions for the neutrons to cause cell damage. As the solid angle vanishes at zero degrees, these distributions are no longer forward-peaked. Back-scattered neutrons

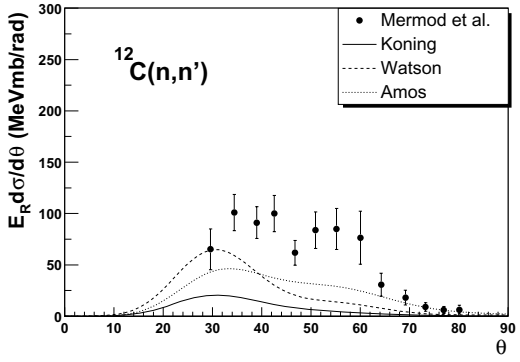

Figure 3. Differential cross section multiplied with the solid angle elements and the energy of the recoil nuclei for inelastic neutron scattering to excited states below 12 MeV on carbon at 96 MeV. The angle θ is the neutron scattering angle in the laboratory. The experimental data are from Ref. [11]. The area under this plot is proportional to the nuclear recoil kerma coefficient for inelastic scattering.

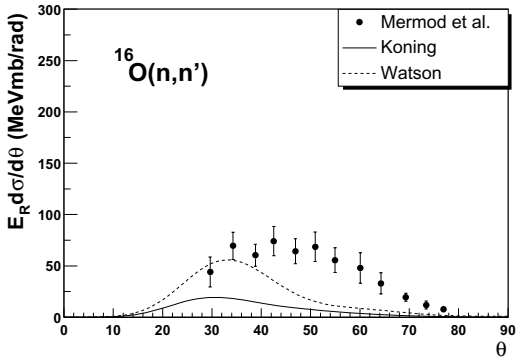

Figure 4. Differential cross section multiplied with the solid angle elements and the energy of the recoil nuclei for inelastic neutron scattering to excited states below 12 MeV on oxygen at 96 MeV. The angle θ is the neutron scattering angle in the laboratory. The experimental data are from Ref. [11]. The area under this plot is proportional to the nuclear recoil kerma coefficient for inelastic scattering.

transfer more energy to the nuclei than forward-scattered neutrons, and therefore the energy of the recoil nuclei increases with the neutron scattering angle. From these distributions, which peak at about 16°, we can deduce that most of the damage is caused by neutrons scattered between 10 and 30°, but there is still a significant contribution up to 60°. With this way of plotting, the recoil kerma coefficients are proportional to the areas under the distributions.

The data for inelastic scattering on carbon and oxygen at 96 MeV to excited states up to 12 MeV excitation energy (from Ref. [11]) were treated the same way. The differential cross sections for inelastic scattering multiplied with the solid angle elements and the recoil nuclei energies are plotted in Figs. 3 (carbon) and 4 (oxygen). Here we observe that the main contribution to the kerma from inelastic scattering is between 30 and 60°, and tends to be significantly underestimated by the calculations.

The values of k for different data sets and different theoretical predictions were evaluated in Refs. [11] and [12], and are reported below in Table 1.

Table 1. Kerma coefficients for the recoil carbon (top) and oxygen (bottom) nuclei from elastic and inelastic neutron scattering at 96 MeV. The inelastic scattering data corresponds to the sum of the excited states with excitation energies below 12 MeV.

k (fGy·m^2)	elastic	inelastic
^{12}C(n,n)		
Mermod *et al.* [11]	0.120±0.007	0.047±0.029
Klug *et al.* [12]	0.126±0.009	–
ICRU [19]	0.132±0.013	–
Koning [15]	0.102	0.007
Watson [16]	0.145	0.023
Amos [17]	0.105	0.026
Crespo [18]	0.118	–
^{16}O(n,n)		
Mermod *et al.* [11]	0.073±0.004	0.028±0.006
ICRU [19]	0.074±0.007	–
Koning [15]	0.071	0.006
Watson [16]	0.096	0.016
Amos [17]	0.066	–
Crespo [18]	0.082	–

RESULTS

Differential cross sections for elastic and inelastic neutron scattering on carbon and oxygen must be well known for a precise evaluation of the damage caused by fast neutrons in human tissue. We have shown that a large angular coverage (up to 60°) was needed, due to the fact that the recoil nucleus energy increases with increasing scattering angle.

There are large variations in the evaluation of the recoil kerma coefficients k obtained with different models. For elastic scattering, the experimental uncertainty in the nuclear recoil kerma coefficients is about 5%, while it is at least 10% for the theoretical calculations or the values from evaluated data. The ICRU value obtained from evaluated data [19] agrees with the experimental values from Refs. [11, 12] within these uncertainties. Among the theoretical models, for elastic scattering on carbon, only Crespo *et al.* seems to give a reasonable prediction, and this is due to the fact that most models are inaccurate in the region 25−35°.

For elastic scattering on oxygen, the prediction closest to the data is provided by the Koning and Delaroche potential. For inelastic scattering on both carbon and oxygen, all models underestimate significantly the data above 40°. As a consequence, the contribution to the kerma from inelastic scattering lies above the model predictions by about 50%. Although the contribution from inelastic scattering is small compared to elastic scattering, the disagreement between calculations and data for inelastic scattering is still responsible for a significant (about 8%) discrepancy in the recoil kerma coefficient for the sum of elastic and inelastic scattering below 12 MeV excitation energy.

ACKNOWLEDGEMENTS

We wish to thank the technical staff of the The Svedberg Laboratory for enthusiastic and skillful assistance. This work was supported by the Swedish Nuclear Fuel and Waste Management Company, the Swedish Nuclear Power Inspectorate, Ringhals AB, the Swedish Defence Research Agency and the Swedish Research Council.

REFERENCES

1. J. Blomgren, "Experimental Activities at High Energies", Workshop on Nuclear Data for Science & Technology: Accelerator Driven Waste Incineration, Trieste, Italy, Sept. 10-21, 2001, eds. M. Herman, N. Paver and A. Stanculescu, ICTP lecture notes **12**, 327 (2002).
2. J. Blomgren and N. Olsson, "Beyond Kerma - Neutron Data for Biomedical Applications", Radiat. Prot. Dosim. **103**, 293 (2003).
3. J. Blomgren, B. Granbom, T. Granlund, and N. Olsson, "Relations Between Basic Nuclear Data and Single-Event Upsets Phenomena", Mat. Res. Soc. Bull. **28**, 121 (2003).
4. M.B. Chadwick, P.M. DeLuca Jr., and R.C. Haight, "Nuclear data needs for neutron therapy and radiation protection", Radiat. Prot. Dosim. **70**, 1 (1997).
5. P. Mermod *et al.*, "Precision measurements of the np scattering differential cross section in the intermediate energy region", these proceedings.
6. U. Tippawan *et al.*, "Light charged-particle production in 96 MeV neutron-induced reactions on carbon and oxygen", these proceedings.
7. S. Pomp *et al.*, "Neutron-induced light-ion production from Fe, Pb and U at 96 MeV", these proceedings.
8. J. Klug *et al.*, "SCANDAL−a facility for elastic neutron scattering studies in the 50-130 MeV range", Nucl. Instr. Meth. **A 489**, 282 (2002).
9. M. Österlund *et al.*, "Elastic neutron scattering studies on heavy nuclei at 96 MeV", these proceedings.
10. P. Mermod *et al.*, "Evidence of three-body force effects in neutron-deuteron scattering at 95 MeV", Phys. Rev. C **72**, 061002 (2005).
11. P. Mermod *et al.*, "95 MeV neutron scattering on hydrogen, deuterium, carbon and oxygen", submitted to Phys. Rev. C.
12. J. Klug *et al.*, "Elastic neutron scattering at 96 MeV from ^{12}C and ^{208}Pb", Phys. Rev. C **68**, 064605 (2003).
13. G.L. Salmon, "The elastic scattering of 96 MeV neutrons by nuclei", Nucl. Phys. **21**, 15 (1960).
14. J.H. Osborne *et al.*, "Measurement of neutron elastic scattering cross sections for ^{12}C, ^{40}Ca, and ^{208}Pb at energies from 65 to 225 MeV", Phys. Rev. C **70**, 054613 (2004).
15. A.J. Koning and J.P. Delaroche, "Local and global nucleon optical models from 1 keV to 200 MeV", Nucl. Phys. **A713**, 231 (2003);
    A.J. Koning, S. Hilaire and M.C. Duijvestijn, "TALYS: Comprehensive Nuclear Reaction Modeling", Proceedings of the International Conference on Nuclear Data for Science and Technology, Santa Fe, USA, Sep. 26 - Oct. 1, 2004, CP769, 1154 (2005).
16. B.A. Watson, P.P. Singh and R.E. Segel, "Optical-Model Analysis of Nucleon Scattering from 1p-Shell Nuclei between 10 and 50 MeV", Phys. Rev. **182**, 977 (1969).
17. K. Amos, P.J. Dortmans, H.V. von Geramb, S. Karataglidis, and J. Raynal, "Nucleon-nucleus scatering: a microscopic nonrelativistic approach", Adv. Nucl. Phys. **25**, 275 (2000); S. Karataglidis, P.J. Dortmans, K. Amos, and R. de Swiniarski, "Multi-$\hbar\omega$ shell model analyses of elastic and inelastic proton scattering from ^{14}N and ^{16}O", Phys. Rev. C **53**, 838 (1996).
18. R. Crespo, R.C. Johnson, and J.A. Tostevin, "Multiple scattering theory of proton elastic scattering at intermediate energies", Phys. Rev. C **46**, 279 (1992).
19. ICRU Report 63, Nuclear Data for Neutron and Proton Radiotherapy and for Radiation Protection (International Commission on Radiation Units and Measurements, MD, 2000).

Radiation Protection Dosimetry (2007), Vol. 0, No. 0, pp. 1–4
DOI: 10.1093/rpd/xxx000

ELASTIC NEUTRON SCATTERING STUDIES AT 96 MEV FOR TRANSMUTATION

M. Österlund[a,*], J. Blomgren [a], M. Hayashi [a,d], P. Mermod [a], L. Nilsson [a], S. Pomp [a], A. Öhrn [a], A.V. Prokofiev [b], U. Tippawan [a,c]
[a]Department of Neutron Research, Uppsala University, Sweden, [b]The Svedberg Laboratory, Uppsala University, Sweden, [c]Fast Neutron Research Facility, Chiang Mai University, Thailand, [d]Department of Advanced Energy Engineering Science, Kyushu University, Japan

Received on June 12, 2006, revised on June 13, 2006, accepted on June 14, 2006

Elastic neutron scattering from ^{12}C, ^{14}N, ^{16}O, ^{28}Si, ^{40}Ca, ^{56}Fe, ^{89}Y and ^{208}Pb has been studied at 96 MeV in the $10-70$ degree interval, using the SCANDAL (SCAttered Nucleon Detection AssembLy) facility. The results for ^{12}C and ^{208}Pb have recently been published, while the data on the other nuclei are under analysis. The achieved energy resolution, 3.7 MeV, is about an order of magnitude better than for any previous experiment above 65 MeV incident energy. A novel method for normalization of the absolute scale of the cross section has been used. The estimated normalization uncertainty, 3 %, is unprecedented for a neutron-induced differential cross section measurement on a nuclear target.

Elastic neutron scattering is of utmost importance for a vast number of applications. Besides its fundamental importance as a laboratory for tests of isospin dependence in the nucleon-nucleon, and nucleon-nucleus, interaction, knowledge of the optical potentials derived from elastic scattering come into play in virtually every application where a detailed understanding of nuclear processes are important.

Applications for these measurements are dose effects due to fast neutrons, including fast neutron therapy, as well as nuclear waste incineration and single event upsets in electronics. The results at light nuclei of medical relevance (^{12}C, ^{14}N and ^{16}O,) are presented separately. In the present contribution, results on the heavier nuclei are presented, among which several are of relevance to shielding of fast neutrons.

INTRODUCTION

The interest in high-energy neutron data is rapidly growing, since a number of potential large-scale applications involving fast neutrons are under development, or at least have been identified. These applications primarily fall into three sectors; nuclear energy and waste, nuclear medicine, and effects on electronics. For all these applications, an improved understanding of neutron interactions is needed for calculations of neutron transport and radiation effects. The nuclear data needed for this purpose come almost entirely from nuclear scattering and reaction-model calculations, which all depend heavily on the optical model, which in turn is determined by elastic scattering and total cross-section data.

The nuclear data needs for transmutation of nuclear waste in general and spent nuclear fuel in particular are outlined in refs. [1, 2, 3], while the needs for neutron therapy of cancer tumours are reviewed in ref. [4], and upsets in electronics are discussed in ref. [5, 6]. In the present work, a programme on elastic neutron scattering at 96 MeV is presented, which deals with all these applications.

Neutron-scattering data are also important for a fundamental understanding of the nucleon-nucleus interaction, in particular for determining the the isovector term [7]. Coulomb repulsion of protons creates a neutron excess in all stable nuclei with $A > 40$. Incident protons and neutrons interact differently with this neutron excess. The crucial part in these investigations has been neutron-nucleus elastic scattering data to complement the already existing proton-nucleus data. Above 50 MeV neutron energy, there has been only one previous measurement on neutron elastic scattering with an energy resolution adequate for resolving individual nuclear states, an experiment at UC Davis at 65 MeV on a few nuclei [8]. In addition, a few measurements in the $0-20^\circ$ range are available, all with energy resolution of 20 MeV or more. This is, however, not crucial at such small angles because elastic scattering dominates heavily, but at larger angles such a resolution would make data very difficult to interpret. Recently, results on neutron scattering from ^{12}C, ^{40}Ca and ^{208}Pb in the $65-225$ MeV range from Los Alamos have been published [9]. The energy resolution is comparable to the present work, but the angular range is limited to $7-23^\circ$.

EXPERIMENTAL SETUP

The neutron beam facility at The Svedberg Laboratory, Uppsala, Sweden, has recently been described in detail [10], and therefore only a brief description is given here. The 96 ± 0.5 MeV (1.2 MeV FWHM) neutrons were produced by the ^{7}Li(p,n) reaction by bombarding a

*Corresponding author. E-mail: Michael.Osterlund@tsl.uu.se

427 mg/cm^2 disc of isotopically enriched (99.98 %) ^{7}Li with protons from the cyclotron. The low-energy tail of the source-neutron spectrum was suppressed by time-of-flight techniques. After the target, the proton beam was bent into a well-shielded beam dump. A system of three collimators defined a 9 cm diameter neutron beam at the scattering target.

Scattered neutrons were detected by the SCANDAL (SCAttered Nucleon Detection AssembLy) setup [10]. It consists of two identical systems, placed to cover $10 - 50^\circ$ and $30 - 70^\circ$, respectively. The energy of the scattered neutrons is determined by measuring the energy of proton recoils from a plastic scintillator, and the angle is determined by tracking the recoil proton. In the present experiment, each arm consisted of a 2 mm thick veto scintillator for fast charged-particle rejection, a 10 mm thick neutron-to-proton converter scintillator, a 2 mm thick plastic scintillator for triggering, two drift chambers for proton tracking, a 2 mm thick ΔE plastic scintillator that was also part of the trigger, and an array of CsI detectors for energy determination of recoil protons produced in the converter by np scattering. The trigger was provided by a coincidence of the two trigger scintillators, vetoed by the front scintillator. The total excitation energy resolution varies with CsI crystal, but is on average 3.7 MeV (FWHM). The angular resolution is in the $1.0 - 1.3^\circ$ (rms) range.

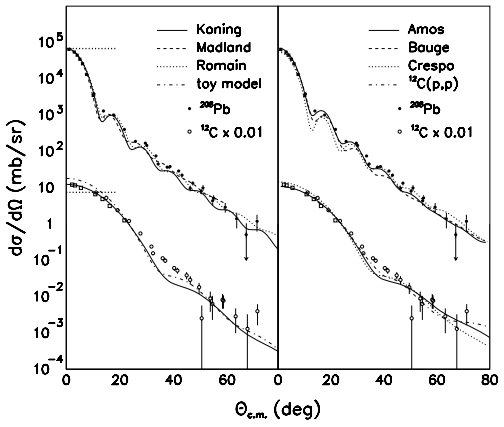

Figure 1. Angular distributions of elastic neutron scattering from ^{12}C (open circles) and ^{208}Pb (solid) at 96 MeV incident neutron energy. The ^{12}C data and calculations have been multiplied by 0.01. The data by Salmon at 96 MeV [11] are shown as squares. Left panel: predictions by phenomenological models. The thick dotted horizontal lines show Wick's limit for the two nuclei. Right panel: predictions by microscopic models, and data on elastic proton scattering from ^{12}C [22]. See the text for details, and refs. [17, 18] and references therein for a description of the theory models.

RESULTS AND DISCUSSION

Angular distributions of elastic-neutron scattering from ^{12}C and ^{208}Pb at 96 MeV incident neutron energy [17, 18] are presented in Fig. 1. The data are compared with phenomenological and microscopic optical-model predictions in the left and right panels, respectively. The theoretical curves have all been folded with the experimental angular resolution to facilitate comparisons with data. The data by Salmon at 96 MeV [11] are also shown. The angular distributions presented have been corrected for reaction losses and multiple scattering in the target. The contribution from other isotopes than ^{208}Pb in the lead data has been corrected for, using cross section ratios calculated with the global potential by Koning and Delaroche [12].

The absolute normalization of the data has been obtained from knowledge of the total elastic cross section, which has been determined from the difference between the total cross section (σ_T) [13] and the reaction cross section (σ_R) [14, 15]. This σ_T - σ_R method, which is expected to have an uncertainty of about 3 %, has been used to normalize the ^{12}C data (see ref. [18] for details). The ^{208}Pb(n,n) data have been normalized relative to the ^{12}C(n,n) data, knowing the relative neutron fluences, target masses, etc. The total elastic cross section of ^{208}Pb has previously been determined with the σ_T - σ_R method. The accuracy of the present normalization has been tested by comparing the total elastic cross-section ratio (^{208}Pb/^{12}C) obtained with the σ_T - σ_R method above, and with the ratio determination of the present experiment, the latter being insensitive to the absolute scale. These two values differ by about 3 %, i.e., they are in agreement within the expected uncertainty.

A novel technique for normalization, which is based on relative measurements versus the np scattering cross section [16], has also been tested and was found to have an uncertainty of about 10 %.

The data are compared with model predictions in Fig. 1, where the left and right panels show phenomenological and microscopic models, respectively. The models are described in detail in refs. [17] and [18].

When comparing these predictions with data, a few striking features are evident. First, all models are in reasonably good agreement with the ^{208}Pb data. It should be pointed out that none of the predictions contain parameters adjusted to the present experiment. In fact, they were all made before data were available. Even the absolute scale seems to be under good control, which is remarkable, given that neutron beam intensities are notoriously difficult to establish. Second, all models fail to describe the ^{12}C data in the $30 - 50^\circ$ range. The models predict a saddle structure, which is not evident from the data.

This mismatch has prompted a re-examination of the ^{12}C(n,n) cross section. Fortunately, this could be

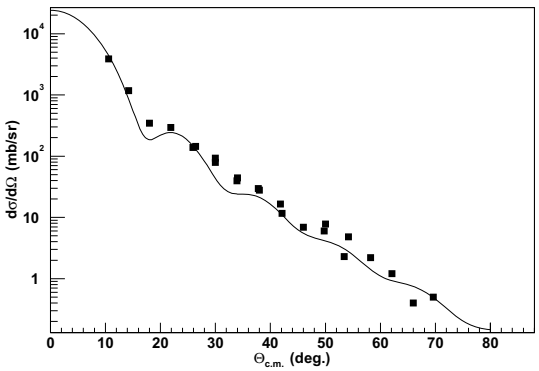

Figure 2. Preliminary angular distribution of elastic neutron scattering from ^{89}Y at 96 MeV incident neutron energy together with a prediction by the Koning-Delaroche potential [12].

accomplished in combination with another experiment. Recently, we have studied nd scattering at the same energy to investigate three-nucleon interaction effects. These results show clear evidence of such $3N$ forces [19, 20, 21]. In these experiments, scattering from carbon was used for normalization, as described above. The size of the target was, however, significantly larger than in the experiments above, resulting in far better statistics. This allowed more stringent analysis procedures to be used, and the results seem to indicate that the ^{12}C elastic scattering cross section is actually in agreement with the theory models. Thus, the main reason for the discrepancy above was probably contamination of the first excited state into the ground state in the analysis.

A basic feature of the optical model is that it establishes a lower limit on the differential elastic-scattering cross section at 0° if the total cross section is known, often referred to as Wick's limit [23, 24]. It has been observed in previous experiments at lower energies that for most nuclei, the 0° cross section falls very close to Wick's limit, although there is no a priori reason why the cross section cannot exceed the limit significantly. An interesting observation is that the present ^{208}Pb data are in good agreement with Wick's limit, while the ^{12}C 0° cross section lies about 70 % above the limit. A similar behaviour has previously been observed in neutron-elastic scattering at 65 MeV [8], where the ^{12}C data overshoot Wick's limit by about 30 %, whilst the ^{208}Pb data agree with the limit.

It has recently been shown by Dietrich et al. [25] that this makes sense. Using the Koning-Delaroche potential [12], it has been shown that Wick's limit actually deviates less than 5 % from an equality for ^{208}Pb over the entire $5 - 100$ MeV interval. The lightest nucleus investigated was ^{28}Si, but the systematics imply that large discrepancies for ^{12}C should be expected.

Preliminary data on ^{89}Y are presented in Fig. 2, together with the Koning-Delaroche potential [12]. The data have been normalized to the model and it can be seen that it describes the shape of the data points reasonably well. The measurements on ^{16}O have been analyzed and are presented in another contribution to this workshop. Measurements on ^{14}N, ^{28}Si, ^{40}Ca, and ^{56}Fe have been completed and the data are under analysis.

CONCLUSIONS AND OUTLOOK

In short, first results on elastic-neutron scattering from ^{12}C and ^{208}Pb at 96 MeV incident neutron energy are presented, and compared with theory predictions. This experiment represents the highest neutron energy where the ground state has been resolved from the first excited state in neutron scattering. The measured cross sections span more than four orders of magnitude. Thereby, the experiment has met - and surpassed - the design specifications. The overall agreement with theory model predictions, both phenomenological and microscopic, is good. In particular, the agreement in the absolute cross-section scale is impressive.

Performance investigations have revealed that the method as such should work also at higher energies. Recently, the TSL neutron beam facility has been upgraded in intensity, making measurements at the highest energy, 180 MeV, feasible. An experimental campaign at 180 MeV does, however, require an upgrade of the CsI detectors of SCANDAL.

Acknowledgments

This work was financially supported by the Swedish Nuclear Fuel and Waste Management Company, the Swedish Nuclear Power Inspectorate, Ringhals AB, Forsmarks Kraftgrupp AB, the Swedish Defense Research Agency, the Swedish Nuclear Safety and Training Centre, and the European Union.

REFERENCES

1. A. Koning, et al., J. Nucl. Sci. Tech., Suppl. **2** (2002) 1161.
2. J. Blomgren, in Proceedings of Workshop on Nuclear Data for Science & Technology: Accelerator Driven Waste Incineration, Trieste, Italy, Sept. 10-21, 2001, eds. M. Herman, N. Paver, A. Stanculescu, ICTP lecture notes **12** (2002) 327.
3. J. Blomgren, Nuclear data for accelerator-driven systems - Experiments above 20 MeV, in Proceedings of EU enlargement workshop on Neutron Measurements

and Evaluations for Applications, Bucharest, Romania, October 20-23, 2004.
4. J. Blomgren and N. Olsson, Radiat. Prot. Dosim. **103(4)** (2003) 293.
5. J. Blomgren, B. Granbom, T. Granlund, N. Olsson, Mat. Res. Soc. Bull. **28** (2003) 121.
6. J. Blomgren, Nuclear Data for Single-Event Effects, in Proceedings of EU enlargement workshop on Neutron Measurements and Evaluations for Applications, Budapest, Hungary, November 5-8, 2003. EUR Report 21100 EN, Luxembourg: Office for Official Publications of the European Communities, ISBN 92-894-6041-5, European Communities, 2004.
7. See, e.g., Neutron-Nucleus Collisions: A probe of Nuclear Structure, AIP Conference Proceedings **124** (AIP, New York, 1985).
8. E.L. Hjort, et al., Phys. Rev. C **50** (1994) 275.
9. J.H. Osborne, et al., Phys. Rev. C **70** (2004) 054613.
10. J. Klug, et al., Nucl. Instr. Meth. **A 489**, 282 (2002).
11. G.L. Salmon, Nucl. Phys. **21**, 15 (1960).
12. A.J. Koning, J.P. Delaroche, Nucl. Phys. **A713**, 231 (2003).
13. R.W. Finlay, et al., Phys. Rev. C **47**, 237 (1993).
14. J. DeJuren, N. Knable, Phys. Rev. **77**, 606 (1950).
15. R.G.P. Voss, R. Wilson, Proc. Roy. Soc. **A 236**, 41 (1956).
16. C. Johansson, et al., Phys. Rev. C **71** (2005) 024002.
17. J. Klug, et al., Phys. Rev. C. **67** (2003) 031601(R)
18. J. Klug, et al., Phys. Rev. C **68** (2003) 064605.
19. P. Mermod, et al., Phys. Lett. **B 597** (2004) 243.
20. P. Mermod, et al., Phys. Rev. C **72** (2005) 061002(R).
21. P. Mermod, et al., submitted to Phys. Rev. C.
22. G. Gerstein, J. Niederer, K. Strauch, Phys. Rev. **108**, 427 (1957).
23. G.C. Wick, Atti. R. Accad. Naz. Lincei, Mem. Cl. Sci. Fis. Mat. Nat. **13**, 1203 (1943).
24. G.C. Wick, Phys. Rev. **75**, 1459 (1949).
25. F.S. Dietrich, J.D. Anderson, R.W. Bauer, S.M. Grimes, Phys. Rev. C **68** (2003) 064608.

DOI: 10.1093/rpd/nc0000

NEUTRON-INDUCED LIGHT-ION PRODUCTION FROM FE, PB AND U AT 96 MEV

S. Pomp[1,*], V. Blideanu[2], J. Blomgren[1], Ph. Eudes[3], A. Guertin[3], F. Haddad[3], C. Johansson[1], J. Klug[1], Ch. Le Brun[4], F.R. Lecolley[2], J.F. Lecolley[2], T. Lefort[2], M. Louvel[2], N. Marie[2], A. Prokofiev[5], U. Tippawan[6], A. Öhrn[1], M. Österlund[1]
[1]Department of Neutron Research, Uppsala University, Sweden
[2] Laboratoire de Physique Corpusculaire, Caen, France
[3] SUBATECH, Nantes, France
[4] Laboratoire de Physique Subatomique et de Cosmologie, Grenoble, France
[5] The Svedberg Laboratory, Uppsala University, Sweden
[6] Fast Neutron Research Facility, Chiang Mai University, Thailand

Received June 30 2006, amended month date year, accepted month date year

Double-differential cross sections for light ion production (up to A=4) induced by 96 MeV neutrons have been measured for Fe, Pb and U. The experiments have been performed at the The Svedberg Laboratory in Uppsala, using two independent devices, MEDLEY and SCANDAL. The recorded data cover a wide angular range (20º - 160º) with low energy thresholds. The data have been normalised to obtain cross sections using np elastic scattering events. The latter have been recorded with the same setup and results for this measurement are reported. The work was performed within the HINDAS collaboration with the primary aim of improving the database for three of the most important nuclei for incineration of nuclear waste with accelerator-driven systems (ADS). The obtained cross section data are of particular interest for the understanding of the so-called pre-equilibrium stage in a nuclear reaction and will be compared with model calculations.

To achieve a better understanding of nucleon-induced reactions in the 20-200 MeV range and develop improved models, detailed information on light-ion production in these reactions is needed. The need for such data comes also from a large amount of applications. Incineration of nuclear waste using accelerator-driven systems (ADS) is one example. For this reason, the interest in nucleon-induced reactions has been growing in the last few years. This interest has been manifested in part by extensive experimental campaigns, like the one carried out by several laboratories in Europe within the framework of HINDAS[(1)]. The results presented here are part of this program and concern double-differential cross sections for light-ion emission (up to A=4) induced by 96 MeV neutrons on ^{nat}Fe, ^{nat}Pb and ^{nat}U[(2)].

EXPERIMENTAL PROCEDURE

Experiments have been performed using the neutron beam available at the The Svedberg Laboratory (TSL) in Uppsala, Sweden. The neutron beam characteristics (neutrons are not mono-energetic, large beam spot at the target position, and, compared to proton beams relatively low intensity) lead us to use two independent detection systems in order to obtain satisfactory count rate, keeping at the same time systematical uncertainties within reasonable limits.

The MEDLEY setup[(3)] is made of eight Si-Si-CsI telescopes, allowing detection of light-ions up to A=4 with a low energy threshold. The statistics accumulated using the MEDLEY setup is relatively poor, due to the thin targets used and to the small solid angles covered by the telescopes. The angular resolution is dictated by the target active area and by the opening angle of the telescopes. It was calculated using Monte Carlo simulations of the experiment, and the typical values found are of the order of 5 degrees (FWHM).

In the case of the SCANDAL setup[(4)] the angular resolution is significantly improved by reconstructing proton trajectories using drift chambers. This device consists of two identical systems located on either side of the neutron beam. Each system uses two 2 mm thick plastic scintillators for triggering, two drift chambers for particle tracking and an array of 12 CsI detectors for energy determination. The emission angles of the particles are calculated using the trajectories in the drift chambers. The angular resolution achieved is of the order of 0.3 degrees. A multi-target system (MTGT) [(5)] is used to increase the count rate without impairing the energy resolution. The MTGT allows up to seven targets to be mounted simultaneously, inter-spaced with multi-wire proportional counters. In this way it is possible to study several reactions at the same time since we can determine from which target the particle has been emitted and apply corrections for energy losses in subsequent targets. In contrast to MEDLEY,

*Corresponding author: Stephan.Pomp@tsl.uu.se

SCANDAL has been used for proton detection only and with an energy threshold of about 35 MeV, however, with a much higher count rate and better angular resolution.

Due to the difficulties encountered when monitoring neutron beam intensities, the absolute cross section normalisation in neutron-induced reactions is a notorious problem. Therefore, the cross sections are measured relative to the H(n,p) cross section. For this reference cross section, the most recent measurements[6] claim an absolute uncertainty of 2 %. Values given in Ref. 6 have been used to calculate the absolute cross sections presented in this work. Estimated systematic uncertainties affecting the experimental cross sections reported are below 5%.

RESULTS

The light-ion spectra have been measured for ^{nat}Fe, ^{nat}Pb and ^{nat}U over the 20-160 degree angular range. The low-energy threshold was 4 MeV for hydrogen isotopes, 12 MeV for ^{3}He and 8 MeV for alpha particles registered with MEDLEY and 35 MeV for proton detection in SCANDAL. The measurements were done up to the maximum possible energy. The energy bin has been fixed to 4 MeV, governed by the energy resolution of the detectors and the accumulated statistics. Fig. 1a compares double-differential cross sections for proton production from iron at 20 degrees, independently measured by both detection systems. Similar results have been obtained for all measured (n,xp) reactions and over the full angular range. The found good agreement, in the energy range covered by both measurements, shows that systematical uncertainties related to cross-section normalisation are low. Fig. 1b shows the Fe(n,xp) cross-section measured with MEDLEY at 20 degrees together with data from Ref. 7, obtained using the magnetic spectrometer LISA. Also here, good agreement is found between the two measurements in the common energy range. Similar agreement has been found for the Pb(n,xp) reaction.

The experimental double-differential cross sections for the emission of hydrogen isotopes measured with MEDLEY are shown in Ref. 2.

Energy distributions are obtained from the double-differential cross sections using the Kalbach systematics[8] to extrapolate the experimentally available angular range over the entire range. Experimental information on the energy-differential cross sections is of great importance, since the agreement between calculations and experimental results for this observable is considered as a minimum condition to validate model predictions.

COMPARISON WITH THEORETICAL CALCULATIONS

In Figs. 2 and 3, the measured energy-differential cross sections for p, d, t and α for 96 MeV neutrons on lead are compared with model calculations performed with the GNASH, TALYS and PREEQ codes. The GNASH code[9] describes the proton production rather well, while a strong underestimation is observed for the case of complex particles. Improvements have recently been done with the TALYS code[10], taking into account the contribution of direct pick-up and knock-out reactions in the complex-particle emission spectra. Even if the agreement in the production rates for complex particles is significantly better, there are still important differences in the shape of the distributions.

A completely different approach takes into account the complex-particle formation probability in the pre-equilibrium stage. This process is treated in the framework of a coalescence model. The code PREEQ[11] uses this approach to calculate energy distributions for particle emission at pre-equilibrium. The results show a good agreement with the data in both shape and amplitude of the distributions.

SUMMARY

In this work experimental double-differential cross sections for light-ion production in 96 MeV neutron-induced reactions in iron, lead and uranium are reported. The extracted energy-differential cross sections have been compared with model calculations by the GNASH, TALYS and PREEQ codes. The comparison of these calculations with the experimental data shows clearly that, despite the better agreement obtained with the TALYS code compared to the old version of the exciton model used in the GNASH code, improvements are still needed for a deep understanding of the reaction mechanisms leading to emission of complex-particles. An alternative is given by the PREEQ code which takes the nucleon coalescence during the pre-equilibrium stage leading to cluster formation into account. This approach seems to give a better description of complex-particle emission in nucleon-induced reactions at intermediate energies.

ACKNOWLEDGEMENTS

This work was supported by the European Community under the HINDAS project (Contract No. FIKW-CT-2000-0031), the GDR GEDEON (Research Group CEA-CNRSEDF-FRAMATOME), Vattenfall AB, the Swedish Nuclear Fuel and Waste Management Company, the Swedish Nuclear Power Inspectorate, Barsebäck Power AB, Ringhals AB, the Swedish Defence Research Agency, and the Swedish Research Council. We would like to thank the TSL staff for assistance and quality of the neutron beam. We are also grateful to Dr. E. Betak for very useful discussions concerning calculations with the PREEQ code. Special thanks to Dr. C. Kalbach for her significant

contributions to the progress of theory in nucleon-induced reactions.

REFERENCES

1. HINDAS: High and Intermediate energy Nuclear Data for Accelerator-driven Systems, European Community, Contract No. FIKW-CT-2000-00031.
2. V. Blideanu, et al., Nucleon-induced reactions at intermediate energies: New data at 96 MeV and theoretical status, Phys. Rev. C 70 (2004) 014607.
3. S. Dangtip, et al., A facility for measurements of nuclear cross sections for fast neutron cancer therapy, Nucl. Instrum. Methods Phys. Res. A 452 (2000) 484.
4. J. Klug, et al., SCANDAL – a facility for elastic neutron scattering studies in the 50-130 MeV range, Nucl. Instrum. Methods Phys. Res. A 489 (2002) 282.
5. H. Condé, et al., A facility for studies of neutron induced reactions in the 50-200 MeV range, Nucl. Instrum. Methods Phys. Res. A 292 (1990) 121.
6. J. Rahm, et al., np scattering measurements at 96 MeV , Phys. Rev. C 63 (2001) 044001.
7. T. Rönnqvist, et al., The ^{54,56}Fe(n,p)^{54,56}Mn reactions at E_n = 97 MeV, Nucl. Phys. A 563 (1993) 225.
8. C. Kalbach, Systematics of continuum angular distributions: Extensions to higher energies, Phys. Rev. C 37 (1988) 2350.
9. P. G. Young, E. D. Arthur, and M. B. Chadwick, Comprehensive Nuclear Model Calculations: Introduction to the Theory and Use of the GNASH Code, Report No. LA-12343-MS, 1992.
10. A. J. Koning, S. Hilaire, and M.C. Duijvestijn, TALYS-0.64 User Manual, December 5, 2004, NRG Report 21297/04.62741/P FAI/AK/AK.
11. E. Betak, Program for spectra and cross-section calculations with the pre-equilibrium model of nuclear reactions, Comp. Phys. Comm. 9 (1975) 92.

Figure 1. a) Double-differential cross sections for Fe(n,xp) at 20 degrees measured by MEDLEY (filled circles) and SCANDAL (open circles). b) Double-differential cross sections for Fe(n,xp) at 20 degrees measured by MEDLEY (filled circles) and data from Ref. 7 (open triangles).

Figure 2. Energy-differential cross sections calculated using the GNASH code (solid line) and the TALYS code (dashed line). The calculations have been done for 96 MeV neutrons on Pb. The experimentally obtained data are shown as points.

Figure 3. Same as Fig. 2, but for PREEQ calculations.

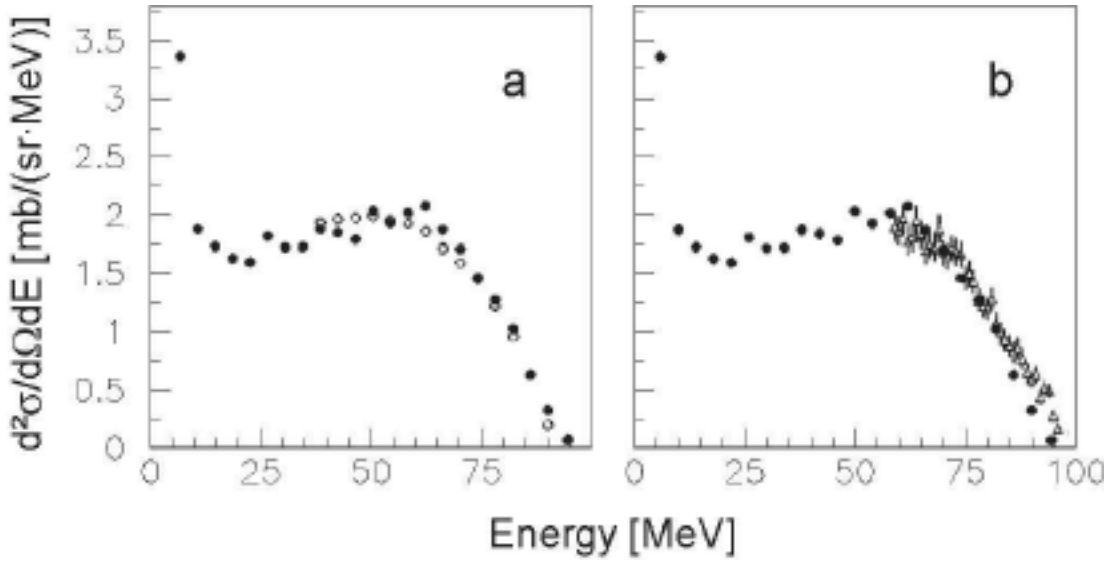
d²σ/dΩdE [mb/(sr·MeV)]
3.5
3
2.5
2
1.5
1
0.5
0
a
b
0
25
50
75
0
25
50
75
100
Energy [MeV]

Figure 1

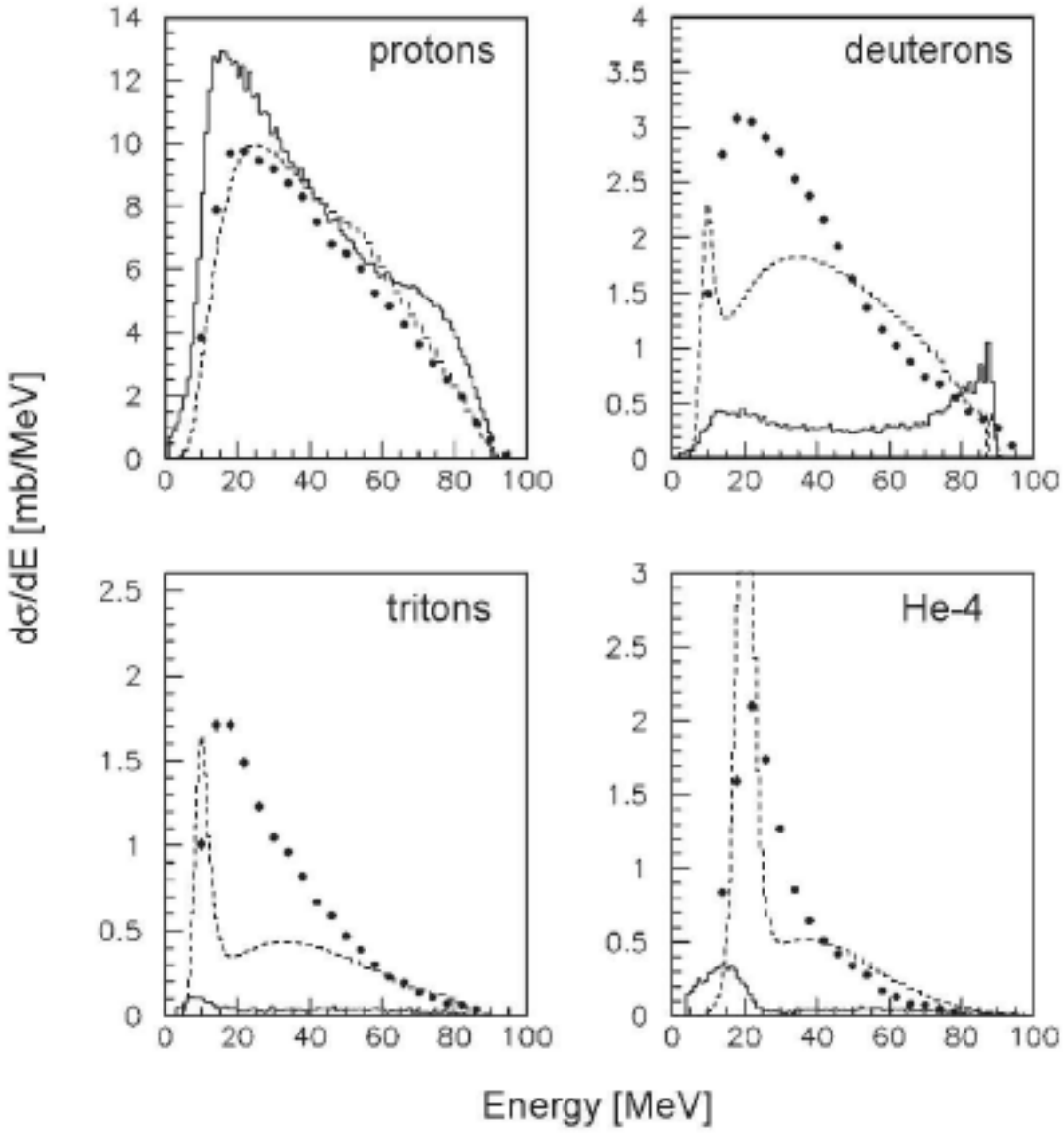

Figure 2

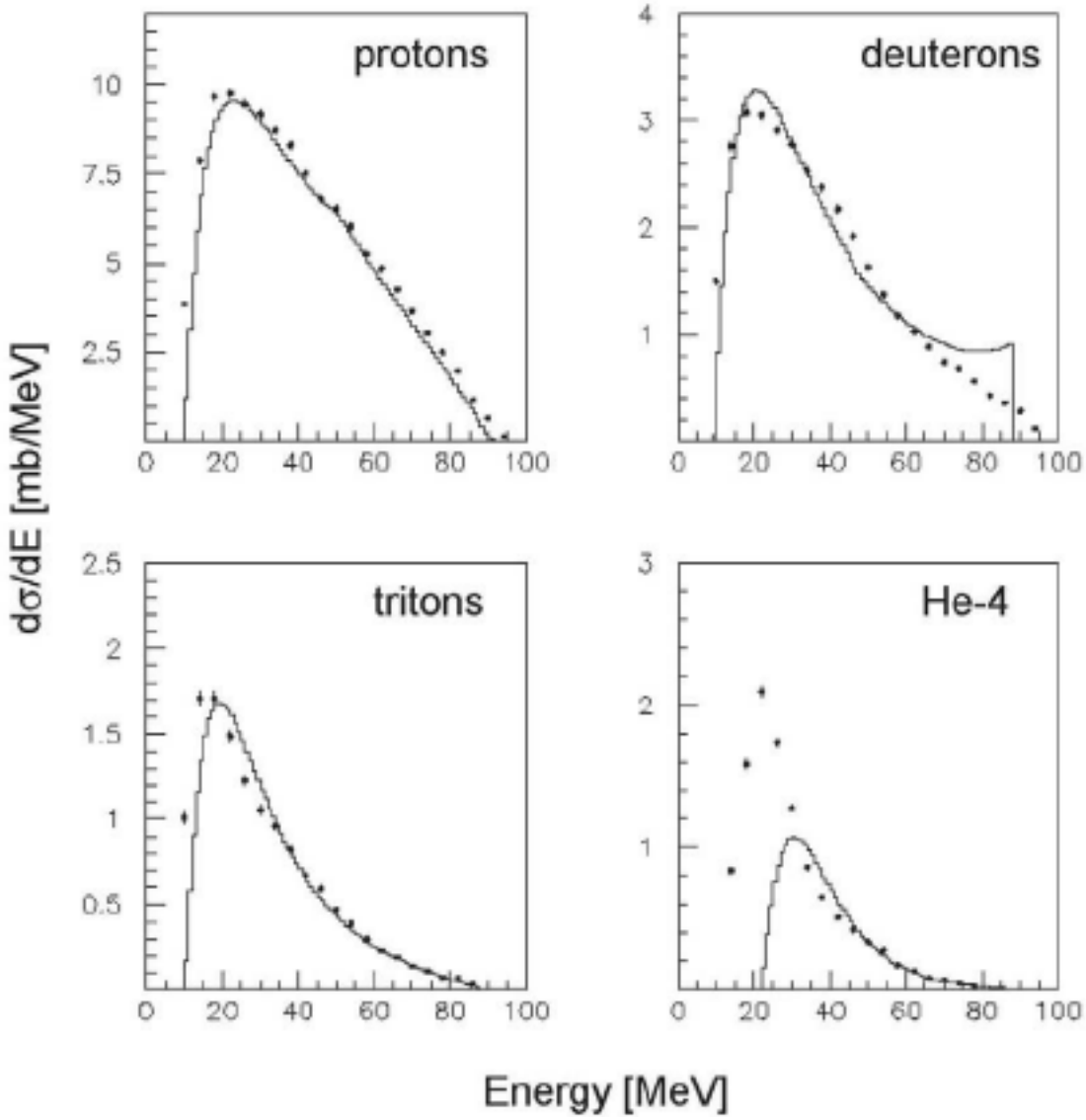

Figure 3

LIGHT CHARGED-PARTICLE PRODUCTION IN 96 MEV NEUTRON-INDUCED REACTIONS ON CARBON AND OXYGEN

U. Tippawan[1,2], S. Pomp[2,*], J. Blomgren[2], S. Dangtip[1,2], C. Johansson[2], J. Klug[2], P. Mermod[2], L. Nilsson[2,4], A. Öhrn[2], M. Österlund[2], N. Olsson[2,3], A.V. Prokofiev[4], P. Nadel-Turonski[5], V. Corcalciuc[6], A.J. Koning[7], and Y. Watanabe[8].

[1]Fast Neutron Research Facility, Department of Physics, Chiang Mai University, Thailand

[2]Department of Neutron Research, Uppsala University, Sweden

[3]Swedish Defence Research Agency (FOI), Stockholm, Sweden

[4]The Svedberg Laboratory, Uppsala University, Sweden

[5]Department of Radiation Sciences, Uppsala University, Sweden

[6]Institute of Atomic Physics, Heavy Ion Department, Bucharest, Romania

[7]Nuclear Research and Consultancy Group NRG, Petten, The Netherlands

[8]Department of Advanced Energy Engineering Science, Kyushu University, Japan

Received month date year, amended month date year, accepted month date year

In recent years, an increasing number of applications involving fast neutrons have been developed or are under consideration, e.g., radiation treatment of cancer, neutron dosimetry at commercial aircraft altitudes, soft-error effects in computer memories, accelerator-driven transmutation of nuclear waste and energy production, and determination of the response of neutron detectors. Data on light-ion production in light nuclei such as carbon, nitrogen and oxygen are particularly important in calculations of dose distributions in human tissue for radiation therapy at neutron beams, and for dosimetry of high energy neutrons produced by high-energy cosmic radiation interacting with nuclei (nitrogen and oxygen) in the atmosphere. When studying neutron dose effects, it is especially important to consider carbon and oxygen, since they are, by weight, the most abundant elements in human tissue. Preliminary experimental double-differential cross sections of inclusive light-ion (p, d, t, ^{3}He and α) production in carbon induced by 96 MeV neutrons are presented. Energy spectra were measured at 8 laboratory angles: 20°, 40°, 60°, 80°, 100°, 120°, 140° and 160°. Measurements were performed at The Svedberg Laboratory (TSL), Uppsala, using the dedicated MEDLEY experimental setup. We have earlier reported experimental double-differential cross sections of inclusive light-ion production in oxygen. Here we present the deduced kerma coefficients for oxygen and compare them with reaction model calculations.

INTRODUCTION

In the past few years, a number of applications involving fast neutrons have been developed or are under consideration, e.g., neutron dosimetry at commercial aircraft altitudes(1), fast-neutron cancer therapy(2,3), soft-error effects in computer memories induced by cosmic-ray neutrons(4), energy applications, and determination of the response of neutron detectors. In fact, airplane personnel are the category, which receives the largest doses in civil work, due to cosmic-ray neutrons. Cancer treatment with fast neutrons is performed routinely at about a several facilities around the world, and today it represents the largest therapy modality besides the conventional treatments with photons and electrons. Data on light-ion production in light nuclei such as carbon, nitrogen and oxygen are particularly significant in calculations of dose distributions in human tissue for radiation therapy at neutron beams, and for dosimetry of high energy neutrons produced by high energy cosmic radiation interacting with nuclei (nitrogen and oxygen) in the upper atmosphere. When studying neutron dose effects in radiation therapy and at high altitude, it is particularly essential to consider carbon and oxygen, because they are the dominant elements (18% and 65% by weight, respectively) in average human tissue.

In this paper, experimental double-differential cross sections (inclusive yields) for protons, deuterons, tritons, ^{3}He and α particles induced by 96 MeV neutrons incident on carbon are presented. Measurements have been performed at the cyclotron of The Svedberg Laboratory (TSL), Uppsala, using the dedicated MEDLEY experimental setup(5). Spectra have been measured at 8 laboratory angles, ranging from 20° to 160° in 20° steps. Partial kerma coefficients for oxygen are obtained directly from the measured microscopic cross sections for the five types of outgoing particles reported in Ref. (6).

EXPERIMENTAL METHODS

The neutron beam facility at TSL uses the ^{7}Li(p,n)^{7}Be reaction (Q = –1.64 MeV) to produce a quasi-

*Corresponding author: stephan.pomp@tsl.uu.se

monoenergetic neutron beam[7]. The 98.5 ± 0.3 MeV protons from the cyclotron impinge on the lithium target, producing a full energy peak of neutrons at 95.6 ± 0.5 MeV with a width of 3 MeV FWHM and containing 40% of the neutrons, and an almost constant low-energy tail containing 60% of the neutrons. The neutron beam is directly monitored by a thin-film breakdown counter (TFBC). Relative monitoring can be obtained by charge integration of the proton beam hitting the Faraday cup in the beam dump. The agreement between the two beam monitors was very good, deviating less than 2%, during the measurements.

The charged particles are detected by the MEDLEY setup. It consists of eight three-element telescopes mounted inside a 100 cm diameter evacuated reaction chamber. Each telescope has two fully depleted ΔE silicon surface barrier detectors. The thickness of the first ΔE detector (ΔE_1) is either 50 or 60 μm, while the second one (ΔE_2) is either 400 or 500 μm, and they are all 23.9 mm in diameter (nominal). In each telescope, a cylindrical CsI(Tl) crystal, 50 mm long and 40 mm in diameter, serves as the E detector.

A 22 mm diameter 500 μm thick (cylindrical) disk of graphite is used as the carbon target and a same dimensional disk of fused quartz SiO_2 is used as the oxygen target. For the subtraction of the silicon contribution, measurements using a silicon wafer having a 32•32 mm^2 quadratic shape and a thickness of 303 μm are performed. For absolute cross section normalization, a 25 mm diameter and 1.0 mm thick polyethylene $(CH_2)_n$ target is used. The *np* cross section at 20° laboratory angle provides the reference cross section[8].

Background events, collected in target-out runs and analyzed in the same way as target-in events, are subtracted from the corresponding target-in runs, with carbon, SiO_2 and silicon targets, after normalization to the same neutron fluence.

The time-of-flight (TOF) obtained from the radio frequency of the cyclotron (stop signal for TDC) and the timing signal from each of the telescopes (start signal), is measured for each charged-particle event.

DATA REDUCTION PROCEDURES

The ΔE–E technique is used to identify light charged particles ranging from protons to lithium ions. Good separation of all particles is obtained over their entire energy range and therefore the particle identification procedure is straightforward.

Energy calibration of all detectors is obtained from the data itself[9,10]. Events in the ΔE–E bands are fitted with respect to the energy deposited in the two silicon detectors. This energy is determined from the detector thicknesses and calculations of energy loss in silicon. Supplementary calibration points are provided by the H(n,p) reaction, as well as transitions to the ground state and low-lying states in the ^{12}C(n,p)^{12}B and ^{12}C(n,d)^{11}B reactions. The energy of each particle type is obtained by adding the energy deposited in each element of the telescope.

Low-energy charged particles are stopped in the ΔE_1 detector leading to a low-energy cutoff for particle identification of about 3 MeV for hydrogen isotopes and about 8 MeV for helium isotopes. The helium isotopes stopped in the ΔE_1 detector are nevertheless analyzed and a remarkably low cutoff, about 4 MeV, can be achieved for the experimental alpha-particle spectra. These alpha-particle events could obviously not be separated from ^{3}He events in the same energy region, but the yield of ^{3}He is much smaller than the alpha-particle yield in the region just above 8 MeV, where the particle identification works properly. That the relative yield of ^{3}He is small is also supported by the theoretical calculations in the evaporation peak region. In conclusion, the ^{3}He yield is within the statistical uncertainties of the alpha-particle yield for alpha energies between 4 and 8 MeV. Knowing the energy calibration and the flight distances, the TOF for each charged particle from target to detector can be calculated and subtracted from the registered total TOF. The resulting neutron TOF is used for selection of charged-particle events induced by neutrons in the main peak of the incident neutron spectrum.

Absolute double-differential cross sections are obtained by normalising the target-in data to the number of recoil protons emerging from the CH_2 target. After selection of events in the main neutron peak and proper subtraction of the target-out and ^{12}C(n,px) background contributions, the cross section can be determined from the recoil proton peak, using *np* scattering data[8]. All data have been normalized using the *np* scattering peak in the 20° telescope.

Due to the finite target thickness, corrections for energy loss and particle loss are applied to all targets individually. Details of the correction methods are described in Refs. (9,10). The cross sections for carbon are obtained directly after the thick target corrections while the cross sections for oxygen are achieved after subtraction of the silicon data from the SiO_2 data with proper normalization with respect to the number of silicon nuclei in the two targets.

RESULTS AND DISCUSSION

Preliminary double-differential cross sections for the ^{12}C(n,px), ^{12}C(n,dx) and ^{12}C(n,αx) reactions at laboratory angles of 20°, 40°, 100° and 140° are shown in Figures 1-3, respectively. The error bars represent statistical uncertainties only and the systematic uncertainty contributions are due to thick target correction (1%–20%), collimator solid angle (5%–9%), beam monitoring (2%–3%), number of carbon nuclei (<5%), CsI(Tl) intrinsic efficiency (1%), particle identification (2%) and dead time (<0.1%).

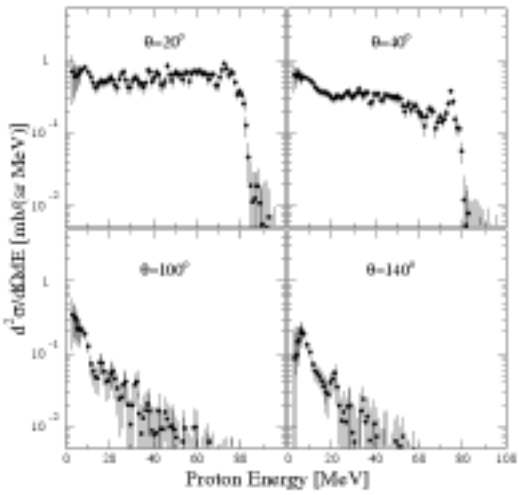

Figure 1. Preliminary double-differential cross sections (filled circles) of the C(*n*,*px*) reaction at 96 MeV at four laboratory angles.

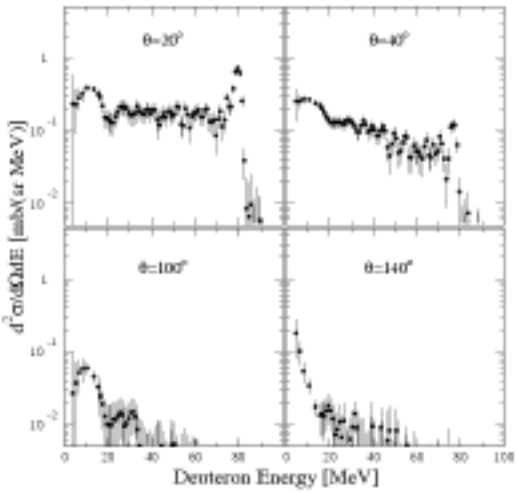

Figure 2. Same as Figure 1 for the C(*n*,*dx*) reactions.

The uncertainty in the absolute cross section normalisation is about 4%, which is due to uncertainties in the contribution from the low-energy continuum of the ^{7}Li(p, n) spectrum to the *np* scattering proton peak (3%), reference np cross sections (2%)[8], statistics in the *np* scattering proton peak (2%), carbon contribution (0.1%).

All the particle spectra at forward angles show relatively large yields at medium-to-high energies. The emission of high-energy particles is strongly forward-peaked and hardly visible in the backward hemisphere. In addition to this broad distribution of emitted particles, the deuteron spectra at forward angles show narrow peaks corresponding to transitions to the ground state and low-lying states in the final nucleus, ^{11}B. These transitions are most likely due to pickup of weakly bound protons in the target nucleus, ^{12}C. A similar but less pronounced effect is observed in the proton spectra at forward angles.

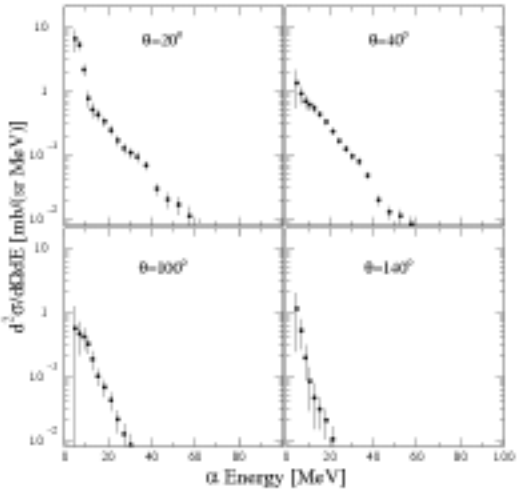

Figure 3. Same as Figure 1 for the C(*n*,*αx*) reactions.

Partial kerma coefficients were calculated from energy-differential cross sections[5] using

$$k_{\phi} = N\sum_{i}\left(\int \frac{d^{2}\sigma}{d\Omega dE}(\theta, E_{i})d\Omega\right)_{i} E_{i}\Delta E_{i} = N\sum_{i}\left(\frac{d\sigma}{dE}(E_{i})\right)_{i} E_{i}\Delta E_{i} \quad (1)$$

where N gives the number of nuclei in the target per unit mass, i denotes the energy bin number and E_i is the centroid of the energy bin with the width ΔE_i. For the oxygen data we have N = 0.603225x10^{-3}. Table I presents the resulting experimental and theoretical partial kerma coefficients for the five types of outgoing particles in oxygen, induced by 96 MeV neutrons. The experimental values have to be corrected for the undetected particles below the low-energy cutoff to be compared with the calculated kerma.

The deduced kerma coefficients for protons, deuterons and α particles agree well with the calculated kerma base on the GNASH[11] model. The TALYS[12] calculations overpredict the measured deuteron kerma coefficient by factor of 2 or more. For the other types of particles, the TALYS calculations greatly underpredict the measured kerma coefficients.

CONCLUSION AND OUTLOOK

In the present paper, experimental data sets on light-ion production in carbon and oxygen induced by 96 MeV neutrons are reported. Experimental double-differential cross sections are measured at eight angles between 20°

and 160°. The partial kerma coefficients for light-ion production for oxygen are presented and compared with the theoretical calculations base on the GNASH and the TALYS models. The carbon data are still preliminary and further minor corrections, such as the wraparound correction described in Refs. (9,10), have to be applied.

Since the use of kerma is widely spread in the dosimetry community we report the derived kerma values. Nevertheless we would like to emphasize the superior amount of information which is contained in microscopic data of the type presented here and which can be used directly in dosimetry applications[13].

TABLE I. Partial kerma coefficients for protons, deuterons, tritons, ^{3}He, and α particles in oxygen, induced by 96 MeV neutrons, from the present work. Theoretical values resulting from GNASH[11] and TALYS[12] calculations are given as well. The experimental data in the second column have been obtained with cutoff energies of 2.5, 3.0, 3.5, 8.0 and 4.0 MeV for p, d, t, ^{3}He and α particles, respectively. The third and forth columns show data corrected for these cutoffs, using the GNASH and the TALYS calculations, respectively.

k_ϕ	Experiment (fGy·m^2)	Cutoff Corrected Experiment		Theoretical calculation	
		GNASH	TALYS	GNASH	TALYS
(n,px)	3.99 ±0.20	4.02	3.99	3.574	3.253
(n,dx)	1.31 ± 0.07	1.32	1.31	1.239	2.971
(n,tx)	0.24± 0.01	—	0.24	—	0.134
(n, ^{3}Hex)	0.11 ± 0.01	—	0.12	—	0.087
(n,αx)	0.80 ±0.04	0.92	0.80	0.985	0.730

ACKNOWLEDGEMENTS

This work was supported by the Swedish Natural Science Research Council, the Swedish Nuclear Fuel and Waste Management Company, the Swedish Nuclear Power Inspectorate, Ringhals AB, and the Swedish Defence Research Agency. The authors wish to thank the The Svedberg Laboratory for excellent support.

REFERENCES

1. D. O'Sullivan, D. Zhou and E. Flood, *Investigation of cosmic rays and their secondaries at aircraft altitudes*, Radiat. Meas. 34, 277–280 (2001).
2. R. Orecchia, A. Zurlo, A. Loasses, M. Krengli, G. Tosi, S. Zurrida, P. Zucali, and U. Veronesi, *Particle Beam Therapy (Hadron therapy): Basis for Interest and Clinical Experience,* Eur. J. Cancer 34, 459 (1998).
3. D.L. Schwartz, J. Einck, J. Bellon, and G.E. Laramore, *Fast Neutron Radiotherapy For Soft Tissue And Cartilaginous Sarcomas At High Risk For Local Recurrence*, Int. J. Radiat. Oncol. Biol. Phys. 50, 449 (2001).
4. *Single-Event Upsets in Microelectronics*, topical issue, eds. H.H.K. Tang and N. Olsson, Mat. Res. Soc. Bull. 28 (2003).
5. S. Dangtip, A. Ataç, B. Bergenwall, J. Blomgren, K. Elmgren, C. Johansson, J. Klug, N. Olsson, G. Alm Carlsson, J. Söderberg, O. Jonsson, L. Nilsson, P.-U. Renberg, P. Nadel-Turonski, C. Le Brun, F.R. Lecolley, J.F. Lecolley, C. Varignon, Ph. Eudes, F. Haddad, M. Kerveno, T. Kirchner, and C. Lebrun, *A facility for measurements of nuclear cross sections for fast neutron cancer therapy*, Nucl. Instr. Meth. Phys. Res. A 452, 484 (2000).
6. U. Tippawan, S. Pomp, A. Ataç, B. Bergenwall, J. Blomgren, S. Dangtip, A. Hildebrand, C. Johansson, J. Klug, P. Mermod, L. Nilsson, M. Österlund, N. Olsson, A.V. Prokofiev, P. Nadel-Turonski, V. Corcalciuc, and A. J. Koning, *Light-ion production in the interaction of 96 MeV neutrons with oxygen*, Phys. Rev. C 73, 034611 (2006).
7. J. Klug, J. Blomgren, A. Ataç, B. Bergenwall, S. Dangtip, K. Elmgren, C. Johansson, N. Olsson, S. Pomp, A.V. Prokofiev, J. Rahm, U. Tippawan, O. Jonsson, L. Nilsson, P.-U. Renberg, P. Nadel-Turonski, A. Ringbom, A. Oberstedt, F. Tovesson, V. Blideanu, C. Le Brun, J.F. Lecolley, F.R. Lecolley, M. Louvel, N. Marie, C. Schweitzer, C. Varignon, Ph. Eudes, F. Haddad, M. Kerveno, T. Kirchner, C. Lebrun, L. Stuttgé, I. Slypen, A. Smirnov, R. Michel, S. Neumann, and U. Herpers, *SCANDAL–a facility for elastic neutron scattering studies in the 50–130 MeV range*, Nucl. Instr. Meth. Phys. Res. A 489, 282 (2002).
8. J. Rahm, J. Blomgren, H. Condé, S. Dangtip, K. Elmgren, N. Olsson, T. Rönnqvist, R. Zorro, O. Jonsson, L. Nilsson, P.-U. Renberg, A. Ringbom, G. Tibell, S.Y. van der Werf, T.E.O. Ericson, and B. Loiseau, *np scattering measurements at 96 MeV*, Phys. Rev. C 63, 044001 (2001).
9. U. Tippawan, S. Pomp, A. Ataç, B. Bergenwall, J. Blomgren, S. Dangtip, A. Hildebrand, C. Johansson, J. Klug, P. Mermod, L. Nilsson, M. Österlund, N. Olsson, K. Elmgren, O. Jonsson, A.V. Prokofiev, P.-U. Renberg, P. Nadel-Turonski, V. Corcalciuc, Y. Watanabe, and A. J. Koning, *Light-ion production in the interaction of 96 MeV neutrons with silicon*, Phys. Rev. C 69, 064609 (2004).
10. U. Tippawan, Secondary Particle Spectra from Neutron Induced Nuclear Reaction in the 14-100 MeV Region, Doctoral thesis, Chiang Mai University (2004) (unpublished).
11. ICRU Report 63, International Commission on Radiation Units and Measurements, Bethesda, MD, March 2000.
12. A.J. Koning, S. Hilaire, and M.C. Duijvestijn, *TALYS-0.64 User Manual*, December 5, 2004, NRG Report 21297/04.62741/P FAI/AK/AK.
13. J. Blomgren and N. Olsson, *Beyond kerma – neutron data for biomedical applications*, Radiat. Prot. Dosim. 103, 293-304 (2003).

A MONITOR FOR NEUTRON FLUX MEASUREMENTS UP TO 20 MEV

A. Öhrn[1,*], J. Blomgren[1], H. Park[2], S. Khurana[3], R. Nolte[3], D. Schmidt[3], and K. Wilhelmsen[4]
[1]Department of Neutron Research, Uppsala University, Sweden
[2]Korean Research Institute of Standards and Science, Daejeon, Korea
[3]Physikalisch-Technische Bundesanstalt, Braunschweig, Germany
[4]Swedish Defense Research Agency, Stockholm, Sweden

Received June 12 2006, amended June 13 2006, accepted June 14 2006

A liquid scintillation detector aimed for neutron energy and fluence measurements in the energy region below 20 MeV has been calibrated using monoenergetic and white spectrum neutron fields. Careful measurements of the proton light output function and the response matrix have been performed allowing for the application of unfolding techniques using existing codes. The response matrix is used to characterize monoenergetic neutron fields produced by the T(d,n) at a low-energy deuteron accelerator installed at the Swedish Defense Research Agency (FOI).

INTRODUCTION

The strongly expanding importance of fast neutrons in a number of applications requires steps to be taken to improve the technology for neutron fluence and energy measurements in various energy ranges. This requirement has been addressed and the current situation summarized at recent workshops [1,2].

For the application considered in this work - a monitor for fluence and energy measurements in the energy region from a few MeV to about 20 MeV - there are several options possible, but if resolution and detection efficiency are taken into consideration, the most attractive alternatives seem to be the organic scintillator with or without applying time-of-flight techniques. In the present application the neutron source is continuous and therefore the time-of-flight technique is out of question. The obvious choice is therefore to perform pulse-height spectrum measurements and to apply unfolding techniques.

In the present paper a calibration procedure for a liquid scintillator with pulse-shape discrimination possibilities is described. The method is based on the procedures developed at the Physikalisch-Technische Bundesanstalt (PTB), Braunschweig, Germany [3] and involves measurements of pulse-height spectra and unfolding of these spectra with existing computer codes using carefully recorded response functions at several energies in the region of interest. The procedure presented in this paper goes beyond the previously applied methods in that both the experimental and calculated response matrices are used with existing unfolding codes to determine the energy and fluence of monoenergetic neutron fields and make comparisons with time-of-flight (TOF) methods.

EXPERIMENTAL METHODS

For neutron energies below 20 MeV, the response matrix of a scintillation detector can be calculated using Monte Carlo codes provided the specific light outputs for protons, deuterons and alpha particles are known for that particular detector. For energies above about 8 MeV, however, no available Monte Carlo code is capable of describing the response of a scintillation detector in full detail, because the required sufficiently detailed multi-differential emission cross sections for alpha particles from the $^{12}C(n,n'3\alpha)$ reaction are not available. Hence, the characterization of scintillation detectors always requires an experimental investigation of the detector response. The standard procedure developed at PTB for the characterization of scintillation detectors uses monoenergetic and breakup neutrons produced with the D(d,n) reaction.

The standard procedure is satisfactory for the application of the TOF method. For the application of unfolding techniques, however, a proper description of the full response matrix is required since any deviation of the response matrix from the 'true' pulse-height response of the detector would cause spurious structures in the unfolded spectral fluence.

For this purpose, a method described by Dekempeneer et al. [4] has been adopted. A white neutron beam measurement is used to obtain a smooth light output function for protons and an experimental response matrix with sufficient resolution in neutron energy. This method has been tested on a liquid scintillator to be used as a neutron monitor for a DT neutron generator, i.e., a commercial cylindrical

*Corresponding author: angelica.ohrn@tsl.uu.se

Radiation Protection Dosimetry Vol. 0, No. 0 © Oxford University Press 2003; all rights reserved

detector cell of the MAB-1F type filled with BC501 scintillator liquid.

The PTB standard procedure for the determination of the relevant properties of an organic scintillation detector has been described in detail elsewhere [3]. Only the results obtained for the particular detector under study are summarized here.

Five neutron beams were produced by deuterons with energies of 5.01, 7.12, 9.06, 10.30, and 11.27 MeV using a deuterium gas target at the PTB neutron scattering facility. The energies of the monoenergetic neutrons were 7.95, 10.05, 11.93, 13.12, and 14.05 MeV. The maximum energy of the corresponding breakup continua was about 6.5 MeV below that of the monoenergetic neutrons. About 30 narrow TOF windows were placed on the monoenergetic neutrons and the breakup continuum to produce pulse-height spectra which were used to determine the proton light output and the efficiency of the detector.

The Monte Carlo code NRESP7 [5] was used to calculate pulse-height spectra for comparison with experimental spectra obtained at the five energies where monoenergetic neutrons from the $D(d,n)^3He$ reaction were available. By fitting these calculated spectra to the experimental ones, the light output function for protons, i.e., the pulse height corresponding to the recoil proton edge, was determined with an iterative procedure. The pulse height was measured using a calibration with photon sources.

The fluences of the monoenergetic neutrons were measured with the PTB 4"x1" NE213 reference detector. This detector was repeatedly compared with the PTB recoil proton telescope. For a selected pulse-height threshold, the efficiency of the detector is known with an uncertainty of about 1.5 % [6]. The mean ratio of the fluence determined with the present BC501 detector and that measured with the PTB reference detector was 1.018 +/- 0.009, which is within the range of results for other detectors [3].

A white neutron beam was produced at the PTB time-of-flight (TOF) facility by bombarding a thick Be target with a 19 MeV proton beam from the PTB isochronous cyclotron. The maximum energy of the neutron field at an emission angle of 0^o is 17.15 MeV. The neutron field was collimated by one of the collimators of the PTB TOF facility. The scintillation detector was positioned at a distance of 27.39 m from the Be target.

Energy calibration of the pulse-height spectra was established using ^{137}Cs, ^{22}Na and ^{207}Bi photon sources. The calibration of the measured pulse height in electron energies and the electronic offset were determined by fitting pulse-height spectra calculated with the PHRESP code [7] to the experimental spectra.

To establish an experimental response matrix, the PH spectra obtained with the white beam have to be normalized to unit fluence at the centre of the detector. This normalization was carried out by fitting PH spectra calculated with NRESP7 to the experimental ones. The fit was restricted to the region extending from the beginning of the flat plateau to the recoil proton edge. This region is essentially determined by np scattering and can be accurately described by NRESP7.

TESTS OF RESPONSE MATRICES IN MONOENERGETIC NEUTRON FIELDS

In the present work it was considered important to test the calculated and experimental response matrices in well-defined monoenergetic neutron fields in an energy region of relevance for the actual application. Such a test was regarded as particularly relevant, because of the observed deviations between the experimentally determined response matrix and the calculated one.

The experimental response matrix was tested in monoenergetic neutron fields with energies between 14 MeV and 15.5 MeV. These fields were produced by the $T(d,n)^4He$ reaction. Deuteron beams of 242, 412 and 643 keV were produced with the PTB 3.5 MeV van-de-Graaff accelerator. The spectral distributions of the neutron fields were calculated with the TARGET code [8]. The calculated average energies at 0^o were 14.85, 14.99 and 15.60 MeV, respectively, and the corresponding calculated FWHM of the peaks amounted to 451, 699 and 644 keV. For the 412 keV deuteron beam, measurements were also carried out at a neutron emission angle of 98^o. At this angle, the $T(d,n)^4He$ reaction shows so-called kinematical focusing, i.e., the energy of the emitted neutrons is almost independent of the energy of the incident deuterons. Hence, broadening of the spectral distribution of the neutrons due to the energy loss of the deuterons in the Ti(T) layer is very small. In this particular case, the neutron field had a peak energy of 13.98 MeV and a FWHM of only 17 keV according to the TARGET calculations which were carried out neglecting the angular straggling of the deuterons in the target.

The pulse-height spectra obtained during the present measurements were unfolded with the MAXED code [9] which is part of the UMG code package [10]. It was known from the TOF measurements that the spectral neutron distribution showed a D(d,n) background peak between 2 MeV and 4 MeV in addition to the dominant T(d,n) peak at energies above 14 MeV. Using this preinformation, the unfolding was carried out in two steps. First, a high PH threshold of 7 MeV corresponding to a neutron energy of a about 11.2 MeV was used to select those events which could not be caused by the low-energy background. The spectral fluence distribution obtained from this restricted unfolding exhibited a prominent peak and some background at intermediate energies. Second, this peak was used as preinformation for the next step of the

unfolding procedure that comprised the pulse-height spectrum above a PH threshold of 280 keV.

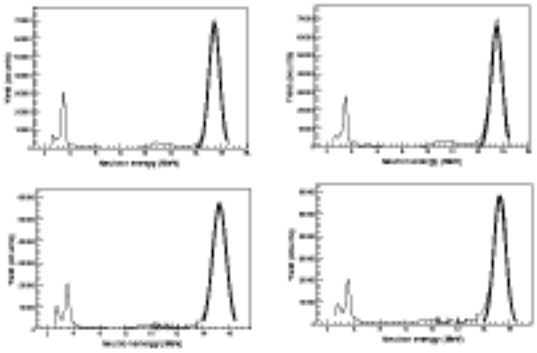

Fig. 1. Results from the 15.60 MeV measurements. The unfolding in the left panels are performed with GRAVEL and those in the right panels with MAXED. In the upper panels the experimental response is used and in the lower panels the calculated one.

RESULTS AND DISCUSSION

The experimental and calculated response matrices were applied with unfolding codes available in the literature to determine the energy and fluence of monoenergetic neutron fields. Comparison with results from TOF measurements was performed.

Determination of the neutron energy has been performed from experiments performed with neutron energies of 13.98, 14.85 and 15.60 MeV. The pulse-height spectrum has been unfolded using MAXED as well as GRAVEL, the latter being another unfolding code in the UMG package [10]. Both codes give a good description of the neutron distribution. However, some spurious structures are generated especially in the low-energy region. A small structure around 11 MeV can also be seen (see Fig. 1). There is no significant difference between GRAVEL and MAXED when determining the neutron energy (see Table 1). The result from unfolding with the experimental response matrix is in better agreement with the result from the TOF measurements than the result from the calculated response matrix.

The absolute efficiency of the detector has been determined using the PTB proton recoil telescope. These measurements have verified that the efficiency, in terms of total number of counts in the detector above a threshold set at a low pulse height, agrees with what can be expected with the used tagged neutron flux. This has been corroborated using the fact that the pulse height spectrum in the high-energy end is dominated by events due to np scattering, because the np scattering cross section is well known at these energies.

Table 1. Results of the neutron energy measurements. Errors are statistical only.

E_n = 13.98 MeV		
Unfolding code	Response matrix	Neutron energy (MeV)
GRAVEL	Experimental	13.91 +/- 0.02
GRAVEL	Calculated	13.67 +/- 0.01
MAXED	Experimental	13.92 +/- 0.03
MAXED	Calculated	13.70 +/- 0.02
E_n = 14.85 MeV		
Unfolding code	Response matrix	Neutron energy (MeV)
GRAVEL	Experimental	14.69 +/- 0.02
GRAVEL	Calculated	14.43 +/- 0.01
MAXED	Experimental	14.71 +/- 0.03
MAXED	Calculated	14.47 +/- 0.02
E_n = 15.60 MeV		
Unfolding code	Response matrix	Neutron energy (MeV)
GRAVEL	Experimental	15.48 +/- 0.01
GRAVEL	Calculated	15.26 +/- 0.01
MAXED	Experimental	15.51 +/- 0.03
MAXED	Calculated	15.26 +/- 0.01

The neutron fluence has been determined by integrating the T(d,n) peak from $E_0 - \Gamma$ to $E_0 + \Gamma$, where E_0 is the centroid and Γ is the FWHM (see Fig. 1). The intrinsic uncertainty of this method has been determined to 0.5 % on the average with a worst case of 1.0 %.

The fluence obtained from the time-of-flight spectrum from the 15.60 MeV measurement agrees well with the fluence derived from unfolding with the experimental response matrix. The deviations are 0.7 % (GRAVEL) and 1.9 % (MAXED). The deviations are significantly larger in the unfolding with the calculated response matrix, 1.6 % (GRAVEL) and 5.8 % (MAXED). In all cases, the fluence obtained from unfolding is lower than that from the TOF information. Based on this information, it is concluded that the fluence can be determined with an uncertainty of 2 % using this method.

CONCLUSIONS

The present work has shown that measurements in white neutrons beams can provide additional information for the specification of scintillation detectors which cannot be obtained with monoenergetic neutron beams alone. In particular, smoother experimental light outputs can be obtained and the deficiencies of the present Monte Carlo codes used for the calculation of response matrices can be circumvented. On the other hand, the application of the TOF method for the determination of experimental response matrices with white neutron beams requires very careful experimental work to avoid artefacts like those observed in the present data for neutron energies above 12 MeV. The application of the unfolding technique with experimentally determined response matrices provides a possibility for spectrometry in neutron beams over a large energy range. The present work has shown that even quite small spectral details can be resolved in the presence of other dominant structures.

ACKNOWLEDGMENTS

The authors are indebted to A. Zimbal for guiding them through the technical pitfalls of the unfolding codes and for numerous discussions on this subject. The support of K. Tittelmeier, A. Toll and the staff of the PTB accelerator facility is gratefully acknowledged.

REFERENCES

1. Proc. of the Int. Workshop on Neutron Field Spectrometry in Science, Technology and Radiation Protection, Pisa, Italy, June 4-8, 2000. Ed.: H. Klein, D. Thomas, H.G. Menzel, G. Curzio, and F. d'Errico, Nucl. Instr. Meth. Phys. Res. A 476, Issues 1-2, 1 (2002).
2. Proceedings of Fast Neutron Detection and Applications, Cape Town, South Africa, April 3-6, 2006. To be published in Proceedings of Science.
3. D. Schmidt, B. Asselineau, R. Böttger, H. Klein, L. Lebreton, S. Neumann, R. Nolte, and G. Pichenot, Nucl. Instr. Meth. Phys. Res. A 476, 186 (2002).
4. E. Dekempeneer, H. Liskien, L. Mewissen, and F. Poortmans, Nucl. Instr. Meth. Phys. Res. A 256, 489 (1987)
5. G. Dietze and H. Klein, "NRESP4 and NEFF4: Monte Carlo Codes for the Calculation of Neutron Response Functions and Detection Efficiencies for the NE213 Scintillation Detectors", PTB Report PTB-ND-22, Braunschweig,1982, (and an informal supplement describing the changes of version 7, 1991).
6. D. Schmidt and H. Klein, Precise Time-of-Flight Spectrometry of Fast Neutrons - Principles, Methods and Results. PTB Report PTB-N-35, Braunschweig, 1998.
7. T. Novotny, "Photon Spectrometry in Mixed Neutron-Photon Fields using NE213 Liquid Scintillation Detectors", PTB Report PTB-N-28, Braunschweig, 1997.
8. D. Schlegel, "TARGET User´s Manual", PTB Laboratory Report PTB-6.41-98-1, Braunschweig, 1998.
9. M. Reginatto, P. Goldhagen, and S. Neumann, Nucl. Instr. Meth. Phys. Res. A 476, 242 (1989).
10. M. Reginatto, B. Wiegel, and A. Zimbal, UMG-Code Package, available from the Nuclear Energy Agency (NEA) Data Bank, http://www.nea.fr.

Appendix XXX

The problems associated to the monitoring of complex workplace radiation fields at European high-energy accelerators and thermonuclear fusion facilities

P. Bilski [(1)], J. Blomgren [(2)], F. d'Errico [(3)], A. Esposito [(4)], G. Fehrenbacher [(5)], F. Fernàndez [(6)], A. Fuchs [(7)], N. Golnik [(8)], V. Lacoste [(9)], A. Leuschner [(10)], S. Sandri [(11)], M. Silari [(12)], F. Spurny [(13)], B. Wiegel [(14)], P. Wright [(15)]

[(1)] IFJ, Krakow, Poland, [(2)] TSL/INF, Uppsala University, Sweden, [(3)] DIMNP, Pisa, Italy, [(4)] INFN, Frascati, Italy, [(5)] GSI, Darmstadt, Germany, [(6)] UAB, Barcelona, Spain, [(7)] PSI, Villigen, Switzerland, [(8)] IAE, Swierk, Poland, [(9)] IRSN, Cadarache, France, [(10)] DESY, Hamburg, Germany, [(11)] ENEA, Frascati, Italy, [(12)] CERN, Geneva, Switzerland, [(13)] NPI ASCR, Prague, Czech Republic, [(14)] PTB, Braunschweig, Germany, [(15)] RAL, Didcot, UK

Corresponding author:
Marco Silari
CERN
1211 Geneva 23
Switzerland
Phone: +41 22 7673937
Fax: +41 22 7679360
E-mail: marco.silari@cern.ch

Running title: Monitoring of complex radiation fields at workplaces

The problems associated to the monitoring of complex workplace radiation fields at European high-energy accelerators and thermonuclear fusion facilities

P. Bilski [1], J. Blomgren [2], F. d'Errico [3], A. Esposito [4], G. Fehrenbacher [5], F. Fernàndez [6], A. Fuchs [7], N. Golnik [8], V. Lacoste [9], A. Leuschner [10], S. Sandri [11], M. Silari [12], F. Spurny [13], B. Wiegel [14], P. Wright [15]

[1] IFJ, Krakow, Poland, [2] TSL/INF, Uppsala University, Sweden, [3] DIMNP, Pisa, Italy, [4] INFN, Frascati, Italy, [5] GSI, Darmstadt, Germany, [6] UAB, Barcelona, Spain, [7] PSI, Villigen, Switzerland, [8] IAE, Swierk, Poland, [9] IRSN, Cadarache, France, [10] DESY, Hamburg, Germany, [11] ENEA, Frascati, Italy, [12] CERN, Geneva, Switzerland, [13] NPI ASCR, Prague, Czech Republic, [14] PTB, Braunschweig, Germany, [15] RAL, Didcot, UK

Abstract

The European Commission is funding within its 6th Framework Programme a three-year project (2005-2007) called CONRAD, *COordinated Network for RAdiation Dosimetry*. The organisational framework for this project is provided by the European radiation Dosimetry Group EURADOS. One task within the CONRAD project, Work Package 6 (WP6) was to provide a report outlining research needs and research activities within Europe to develop new and improved methods and techniques for the characterization of complex radiation fields at workplaces around high-energy accelerators, but also at the next generation of thermonuclear fusion facilities. The paper provides an overview of the report, which will be availabe as CERN Yellow Report.

INTRODUCTION

Monitoring of ionising radiation around high-energy particle accelerators is a difficult task due to the complexity of the radiation field. The capability to distinguish between the high-LET (mostly neutrons) and the low-LET components of the radiation field at workplaces, and to correctly measure them, is of primary importance to evaluate the exposure of personnel. At proton machines the dose equivalent outside a thick shield is mainly due to neutrons, with some contribution from photons and, to a minor extent, charged particles. At certain locations the radiation field may contain neutrons with energies exceeding tens of MeV, which contribute 30% to 50% of the ambient dose equivalent outside the shielding. At high-energy electron accelerators the dominant secondary radiations are high-energy neutrons, the shielding being thick enough to absorb most of the bremsstrahlung photons.

Similar high-LET and low-LET radiation components are present at experimental nuclear fusion facilities. The nuclear reactions employed – the deuterium-deuterium (D-D) and the deuterium-tritium (D-T) – produce high flux of fast neutrons. The plasma current in the toroidal vessels (tokamak) of fusion experiments based on magnetic confinement, the most practised fusion technology in Europe, generates bremsstrahlung X-rays. Special system components of some fusion facilities, like neutral beam injectors, have their own radiation environment due to neutron and photon fields. Neutron activation for D-T based systems like JET is elevated in the in-vessel components and sometimes it is important also in the material of some associated devices, like in the water cooling system of the ITER project. The resulting radiation fields at workplaces, out of the concrete shielding that encase the main fusion facilities, are dominated by thermal neutrons but fast neutrons and photons are also present.

Neutron and photon dosimetry and spectrometry are thus essential tools in radiation protection dosimetry around both high-energy particle accelerators and nuclear fusion facilities. There are some similarities between these radiation fields and those encountered at flight altitudes, and it is actually possible to partly "simulate" the radiation field in the atmosphere with accelerator-produced radiation [(1)]. However, one important difference is that accelerators can operate in pulsed mode so that the radiation fields at workplaces can be pulsed. This is an important aspect to be taken into account for instrument response, and measurements of average dose equivalent rates for radiation protection purposes in these fields present a challenge for instrumentation.

The European Commission is funding within its 6th Framework Programme a three-year project (2005-2007) called CONRAD, *COordinated Network for RAdiation Dosimetry*. The organisational framework for this project is provided by the European radiation Dosimetry Group EURADOS. One task within the CONRAD project, Work Package 6 (WP6) was to provide a report outlining research needs and research activities within Europe to develop new and improved methods and techniques for the characterization of complex radiation fields at workplaces around high-energy accelerators, but also at the next generation of thermonuclear fusion facilities.

The CONRAD WP6 report [(2)] reviews the relevant techniques and instrumentation employed for monitoring neutron and photon fields around high-energy accelerators and fusion facilities (mainly JET and ITER), both in terms of dosimetry and spectrometry, emphasizing some recent developments to improve the response of neutron measuring devices beyond 20 MeV. The report also reviews the major high-energy European accelerator facilities – both research accelerators and hospital-based hadron therapy centres – and the way workplace monitoring is organized at each of them. On-going research in radiation dosimetry and development work in passive dosimetry and active counting and spectrometric instrumentation at several European laboratories are discussed. Calibration problems are addressed and the neutron calibration facilities available in Europe are listed. This paper provides a brief overview of the report, focussing in particular on some of the most important issues, such as the influence of the

pulsed nature of the radiation field on the instrument and the calibration problems. For the review of the instrumentation and of the European facilities the reader should refer to ref. [2].

MONITORING OF MIXED RADIATION FIELDS

Two types of dose quantities exist for radiological protection: body-related "protection quantities" defined by the International Commission on Radiological Protection (ICRP) [3] and "operational quantities" defined by the International Commission on Radiation Units and Measurements (ICRU) [4]. While protection quantities serve to define dose limits but are not directly measurable, the exposure can be monitored by calculations or by measuring the operational quantities. Calculations of protection quantities require comprehensive knowledge of the energy and directional distribution of the particles in the radiation field and of their interaction with tissue.

One operational dose quantity suited to demonstrate compliance with limits of the effective dose at workplaces is the ambient dose equivalent, $H^*(10)$, which is the dose equivalent, H, at a reference point at 10 mm depth in the ICRU sphere under defined irradiation conditions. Many radiation protection instruments used to measure $H^*(10)$ follow measurement principles other than those used in the definition and therefore require calibration with respect to this quantity. An alternative and in general more accurate procedure is to measure the spectral neutron fluence and fold this information with an appropriate set of fluence to dose equivalent conversion coefficients. In practice monitoring instruments usually have a response function which approximately follows $H^*(10)$ for a given type of radiation and over a given energy range. The approaches to the determination of ambient dose equivalent for neutrons are discussed in detail in ICRU Report 66 [5].

Starting from the beam parameters of the accelerator important to radiation monitoring (type, energy, intensity and time structure of the accelerated particles) or from the characteristics of the radiation produced at nuclear fusion facilities, one can make predictions of the composition of the radiation field outside the shielding and then decide the type of area monitors to be employed (active and/or passive) and how to calibrate them.

PULSED FIELDS AND INSTRUMENT RESPONSE

Most accelerators operate in pulsed mode. Usually such sources deliver their output pulses in time intervals from nanoseconds to tens of microseconds spaced by at least a few milliseconds. This also concerns most of conventional electron linacs used in radiotherapy, which are operated at 100 – 400 Hz with pulse widths of about 1 – 10 μs. In some accelerators the microsecond output pulses consist of a series of separate "bunches" each of duration of a few picoseconds, while the interval between bunches is generally less than one nanosecond. This time structure within the microsecond pulse can usually be ignored for radiation field spectrometry and dosimetry.

Radiation protection at workplaces deals with stray radiation fields outside shielding. At high-energy accelerators, such radiation fields comprise neutrons, photons and charged particles, with pulses which are usually shorter than 10 μs with high instantaneous fluence rates and dose rates. Measurements of average dose equivalent (rate) for radiation protection purpose in these fields present a challenge for instrumentation and may become even more difficult at workplaces in the vicinity of new facilities with increasing particle energy.

At present, the time structure of the stray radiation fields is usually deduced from the design of the accelerator. Little or no experimental work has yet been reported concerning the pulsed structure of the radiation field modified by transport through the shield. It can be expected that thick shields of high-energy accelerators may seriously disturb the initial pulse structure because of e.g. different time of flight of secondary particles through the material of the shield.

The information about the real time structure behind the shields can be important in order to decide whether a particular radiation field must be considered to be pulsed, for a particular dosemeter. An important problem can also be represented by the time structure of high-energy neutron leakage from spallation targets.

The influence of pulsed radiation on the response of radiation detectors is considered in the literature first of all for dosimetry of the primary beam. The guidelines from such studies can be applied in radiation protection at workplaces but lower dose rates at workplaces comparing to the beam conditions should be taken into account.

The most comprehensive source of information on the dosimetry of pulsed X-ray or electron beams is ICRU Report 34 [6]. Measurements using ionization chambers, chemical dosemeters, calorimeters and solid state devices are discussed. The report provides information on certain precautions to be taken and on the selection of calibration constants needed for dosimetry of pulsed low-LET radiation. High-LET radiation, mainly heavy charged particles and neutrons, is only shortly mentioned in ICRU 34, because there was not enough information about the influence of radiation pulsing on dosimetry in complex radiation fields at the time the report was issued (1982). Some up-to-date information and operational guidelines for radiation protection at particle accelerator facilities with energies from about 5 MeV up to the highest energies available can be found in NCRP Report No 144 [7], where the special problems of measurements in pulsed radiation fields are also addressed.

Workplace monitoring in complex radiation fields usually involves instruments based on the use of ionization chambers, particle counting devices or solid state detectors. The last two types of detectors are also often used in neutron and charge particle spectrometers. Tissue equivalent proportional counters (TEPC) and recombination ionization chambers are used for microdosimetry and LET-spectrometry. The influence of the pulsed structure of the particle beam on the instrument response is different for the three classes of detectors.

RADIATION PROTECTION AND MONITORING AT EUROPEAN THERMONUCLEAR FUSION FACILITIES

Many radiation protection issues at experimental thermonuclear fusion machines and at associated facilities are similar to those arising around medium and low-energy accelerators. Radiation fields around these facilities are complex and mainly consist of neutrons and photons. Pulsed fields, short operation periods, complex operation scenarios, variable radiation energy spectrum are common situations at nuclear fusion facilities. The main difference to the radiation fields at particle accelerators is the lower maximum neutron energy: about 2.5 MeV for D-D plasmas and 14 MeV for D-T plasmas.

A specific radiation monitoring problem is related to the short time during which the so called “plasma burning” (or “shot” or “pulse”) takes place. In this time period, that ranges from about 1 s to some tenths of seconds, plasma heating systems are activated and the thermonuclear conditions make the fusion reactions possible. Usually an intense, mixed neutron/photon radiation field is generated during the burning phase and to collect the needed dosimetric information the monitoring response during this interval has to be recorded. This is usually accomplished with active monitors and associated electronic devices suitable to activate the measurement for the time needed and to record the related dosimetric information. A discussion on the radiation monitoring system in use at JET and that planned for ITER is given in ref. [2].

CALIBRATION

Calibration is the process in which the calibration factor (quotient of the conventional true value by the value indicated) of a measuring device is determined in a reference radiation field of well-known ambient dose equivalent under well specified calibration conditions [5].

Radioactive sources are frequently used, e. g. ^{60}Co or ^{137}Cs sources for photon dosemeters and ^{252}Cf or ^{241}Am(Be) sources for neutron dosemeters, since they can provide stable and reproducible calibration conditions. National standard laboratories, for example, provide such reference fields. Then, if used under conditions identical to the calibration conditions, a calibrated instrument will measure $H^*(10)$ correctly. However, under different irradiation conditions, for example in fields of other particle compositions or with other particle energy distributions, deviations will occur since dosemeters used in radiation protection practice usually do not have ideal response characteristics (e. g. the same energy dependence as the fluence-to-dose equivalent conversion function). In practical applications, these deviations are either small enough for the desired degree of accuracy, or the user must apply field-specific correction factors to take the differences between calibration conditions and the conditions actually prevailing into account.

Since the radiation fields at workplaces around high-energy accelerators (but similar considerations apply for the cosmic radiation field in aircrafts responsible for aircrew exposure) differ strongly from those applied in standard calibration, the correction factors required can be large. In addition, since the field characteristics and the response of the instrument to all particles in the field are usually not well known, correction factors cannot be calculated with the desired precision. The reliability and accuracy in personnel exposure monitoring can therefore be improved by performing the calibration in the field of interest or in a calibration field with similar characteristics. The direct *field calibration* of instruments in a given workplace requires a reference instrument which should be able to measure the (true value of) ambient dose equivalent (nearly) correctly for all radiation components and energies. The use of *reference fields* ("simulated workplace fields") produced under laboratory conditions requires particle compositions and spectral fluences similar to those in the workplace of interest. Those fields offer a good opportunity of investigating the dosemeter characteristics and of intercomparing different dosemeters under identical and reproducible conditions.

Photon dosemeters are conventionally calibrated with ^{137}Cs radionuclide sources emitting monoenergetic photon radiation with energy of 0.661 MeV. The reference quantity for the calibration is primarily the air kerma, K_a, which can be converted to $H^*(10)$ by applying appropriate conversion coefficients. Photon dosimetry is mostly understood for pure photon fields as well as low-energy photon spectrometry. In mixed fields the situation is more complex, as is often not easy to take into account the response of a photon spectrometer or dosemeter to neutrons. On the other hand, photon spectrometry in the high-energy region still needs a lot of development work.

Reference neutron fields can be produced by radionuclide sources, by nuclear reactors and by nuclear reactions with charged particles from accelerators. A recent review of the subject can be found in ref. [8]. Recommendation for producing reference neutron radiation fields are given by the International Organization for Standardization (ISO) [9-11]. The calibration of neutron instrumentation is discussed in more detail below.

NEUTRON CALIBRATION FIELDS

The calibration of instruments used for routine neutron monitoring, e.g. rem counters or personal dosemeters, is carried out using reference neutron fields with broad spectral distributions like those produced by radionuclide sources. The spectra encountered at workplaces, however, are usually significantly different from those used for the calibration. Hence the fluence response $R_\Phi(E)$ of the instrument has to be determined as a function of the neutron energy E to enable the calculation of so-called "field correction factors" which account for the dependence of the response on the neutron spectrum. The experimental determination of the response is carried out using reference fields in which the neutron fluence is concentrated at a single energy (monenergetic fields) or, at least, the majority of the fluence is at a single energy with only a smaller contribution at other energies (quasi-monoenergetic fields). The basic quantity for the

specification of reference fields is the spectral neutron fluence Φ_E. The neutron ambient dose equivalent *H*(10)* is obtained from Φ_E by folding the spectral distribution with recommended energy dependent fluence-to-dose-equivalent conversion coefficients $h_{\Phi}(E)$.

Monoenergetic or quasi-monoenergetic reference fields are produced by bombarding low-Z targets (D, T, ^{7}Li) with light ions (protons or deuterons) accelerated with Van-de-Graaff accelerators or cyclotrons. In most cases monoenergetic neutrons can be obtained only under ideal conditions. In reality, however, the effects of finite target thickness, neutron scattering in the target surroundings and the finite detector size as well as break-up reactions at higher projectile energies cause deviations from the ideal situation, i.e. the fields are only quasi-monoenergetic with a high-energy peak of finite width and a low-energy continuum.

The response of a detector to high-energy neutrons ($E_n > 20$ MeV) is quite difficult to determine experimentally because of the low-energy tail in the spectrum provided by the available quasi-monoenergetic neutron facilities. Moreover, when measuring in unshielded radiation fields the contribution of high-energy hadrons also has to be taken into account (see, for example, ref. [12]).

If both the energy and angular response characteristics of an instrument and the energy and direction distribution of the radiation field to be determined are well known – either experimentally or theoretically – the response data can be folded with the field data to obtain a field correction factor. An alternative approach is to determine the response of the device either in the radiation field of interest (a "field calibration") or in an experimental radiation field of sufficiently similar characteristics (a "simulated workplace field"). Modern Monte Carlo codes can help a lot in designing instrumentation and in understanding their performances and their response functions to various types of radiation. It is nonetheless important that the simulations are validated with calibration measurements in reference fields. A list of available calibration facilities providing monoenergetic or quasi-monoenergetic beams is given in ref. [2].

SIMULATED WORKPLACE FIELDS

When selecting a workplace neutron field (designed for calibrating and testing either personal dosemeters or area monitors) one has to consider the characteristics of the field to be simulated (such as its energy and direction distributions) and the response of the instruments or dosemeters used to determine the neutron distributions. Workplace neutron fields can be simulated using three types of irradiation facilities: radionuclide sources, nuclear reactors and particle accelerators [13]. Since we are here interested in workplace fields around high-energy accelerators, the latter of the three methods is the only practicable one. Essentially only two facilities of this type are available in Europe: the CERF facility at CERN [1] and CANEL at Cadarache [14].

CONCLUSIONS

The CONRAD WP6 report has reviewed the principal techniques, based both on active detectors and passive dosemeters, employed to monitor mixed radiation fields around high-energy particle accelerators and experimental thermonuclear fusion reactors. Neutron measuring devices include rem counters, Bonner sphere spectrometers, bubble detectors and track etched detectors. Techniques discussed for photon dosimetry and spectrometry are scintillation detectors, ionization chambers, Geiger Müller counters, TLDs and EPR dosemeters. Instruments capable to distinguish between the low-LET and high-LET components of a field like TEPCs and recombination chambers are also discussed. Secondary (stray) radiation often keeps "memory" of the original time structure of the primary beam, and if the beam is made up of very short bursts, the influence of such structure on active instruments has to be properly taken into account when selecting or designing a monitoring system. The characterization of the neutron field produced at

high-energy proton accelerators is quite a challenging task: developments occurred over the past few years to improve the response of neutron counters and spectrometers beyond 20 MeV are discussed.

Instruments and dosemeters used for workplace monitoring usually do not have ideal response characteristics, i.e. the same energy dependence as the fluence-to-dose equivalent conversion function. They are normally employed under irradiation conditions that are different from those in which they were calibrated. Thus deviations will occur and proper correction factors have to be applied.

The response of a device to the various components of a mixed radiation field can nowadays be determined quite precisely by means of Monte Carlo codes. It is nonetheless important that the simulations are validated with calibration measurements in monoenergetic or quasi-monoenergetic reference fields. It is also important to be able to calibrate a dosemeter in a simulated workplace field produced under laboratory conditions with particle compositions and spectral fluences similar to those encountered at the workplace of interest. Such a field offers the opportunity of investigating the dosemeter characteristics and of intercomparing different dosemeters under identical and reproducible conditions.

There are a number of issues that still need to be better understood, such as the problems arising from calibration for high-energy devices, for instance rem counters with a lead insert which are also sensitive to low-energy neutrons. For neutrons above 20 MeV only "quasi-monoenergetic" fields are available, i.e. fields with a major component at one energy, but with an additional broad energy component, usually at lower energies, for which corrections have to be made. In addition, the quasi-monoenergetic neutron fields above 20 MeV are not regularly available for "routine" calibrations. There is also a certain need of better estimating uncertainties in conversion coefficients.

The basic protection quantity is the effective dose E, but for purposes of radiation protection metrology the operational quantity ambient dose equivalent, $H^*(10)$, is used, which is meant to be a conservative approximation of E. Recent studies [15-17] have shown that in some circumstances the operational quantities may not always provide an overestimate of protection quantities, so that future developments in instrumentation will have to take this fact into account

ACKNOWLEDGEMENTS

This work is funded in part by the European Commission under the auspices of the Euratom 6th Framework Programme for research and training in nuclear energy, Contract No FI6R-012684.

REFERENCES

1 Mitaroff A. and Silari M. The CERN–EU high-energy reference field (CERF) facility for dosimetry at commercial flight altitudes and in space, Radiat. Prot. Dosim. 102**,** 7-22 (2002).

2. Bilski, P., Blomgren, J., d'Errico, F., Esposito, A., Fehrenbacher, G., Fernàndez, F. Fuchs, A., Golnik, N., Lacoste, V., Leuschner, A., Sandri, S., Silari, M., Spurny, F., Wiegel, B. and Wright, P. Complex workplace radiation fields at European high-energy accelerators and thermonuclear fusion facilities, Yellow Report CERN-2006-007, M. Silari, editor (2006).

3. International Commission on Radiological Protection (ICRP), 1990 Recommendations of the International Commission on Radiological Protection, Publication 60 (Pergamon Press, Oxford, 1991).

4. International Commission on Radiation Units and Measurements (ICRU), Quantities and units in radiation protection dosimetry, Report 51 (Bethesda, MD, USA, 1993).

5. International Commission on Radiation Units and Measurements (ICRU), Determination of operational dose equivalent quantities for neutrons, Report 66 (Bethesda, MD, USA, 2001).

6. International Commission on Radiation Units and Measurements (ICRU), The dosimetry of pulsed radiation, Report 34 (Bethesda, MD, USA, 1983).

7. National Council on Radiation Protection and Measurements (NCRP), Radiation protection for particle accelerator facilities, Report 144 (Bethesda, MD, USA, 2003).

8. Schuhmacher, H. Neutron calibration facilities, Radiat. Prot. Dosim. 110, 33-42 (2004).

9. International Organization for Standardization (ISO), Reference neutron radiations – Part 1: characteristics and methods of production, ISO Standard 8529-1 (ISO, Geneva, 2001).

10. International Organization for Standardization (ISO), Reference neutron radiations – Part 2: calibration fundamentals of radiation protection devices related to the basic quantities characterizing the radiation field, ISO Standard 8529-2 (ISO, Geneva, 2000).

11. International Organization for Standardization (ISO), Reference neutron radiations – Part 3: calibration of area and personal dosimeters and determination of their response as a function of neutron energy and angle of incidence, ISO Standard 8529-3 (ISO, Geneva, 1998).

12. Agosteo, S., Dimovasili, E., Fassò, A. and Silari, M. The response of a Bonner sphere spectrometer to charged hadrons, Radiat. Prot. Dosim. 110, 161-168 (2004).

13. International Organization for Standardization (ISO), Reference neutron radiation – Characteristics and method of production of simulated workplace neutron fields, ISO standard 12789-1 (ISO, Geneva, 2000).

14. Gressier, V. Les installations de l'IRSN dédiées à la métrologie des neutrons, IRSN Report DRPH/SDE 2005-012 (2005).

15. ICRP/ICRU Joint Publication. Conversion coefficients for use in radiological protection against external radiation, ICRP Publication 74 (Oxford, Pergamon, 1997) and ICRU Report 57 (Bethesda, MD, USA, 1998).

16. Ferrari, A., Pelliccioni, M. and Pillon, M. Fluence to effective dose conversion coefficients for neutrons up to 10 TeV, Radiat. Prot. Dosim. 71, 165-173 (1997).

17. Bartlett, D.T., Drake, P., d'Errico, F., Luszik-Bhadra, M., Matzke, M. and Tanner, R.J. The importance of the direction distribution of neutron fluence and methods of determination, Nucl. Instrum. Meth. A476, 386-394 (2002).

Appendix XXXI

E HERE

THE TSL NEUTRON BEAM FACILITY

A.V. Prokofiev[1,*], J. Blomgren[2], O. Byström[1], C. Ekström[1], S. Pomp[2], U. Tippawan[3], V. Ziemann[1], and M. Österlund[2]
[1]The Svedberg Laboratory, Uppsala University, Box 533, S-751 21 Uppsala, Sweden
[2]Department of Neutron Research, Uppsala University, Box 525, S-751 20 Uppsala, Sweden
[3]Fast Neutron Research Facility, Chiang Mai University, 50202 Chiang Mai, Thailand

Received July 6 2006

A new quasi-monoenergetic neutron beam facility has been constructed at The Svedberg Laboratory (TSL) in Uppsala, Sweden. Key features include a neutron energy range of 11 to 175 MeV, high fluxes, user flux control, flexible neutron field size and shape, and spacious and easily accessible user area. The first results of the beam characterization measurements are reported.

INTRODUCTION

The interest in high-energy neutrons is rapidly growing, since a number of potential large-scale applications involving fast neutrons are under development, or have been identified. These applications primarily fall into four sectors: nuclear energy and waste[(1)], medicine[(2,3)], personnel dosimetry in aircraft[(4)] and spacecraft[(5)], and single-event effects (SEE) on electronics[(6,7)].

To satisfy the needs of these applications, monoenergetic neutron beams would be most suitable. In the energy region above about 20 MeV, a truly monoenergetic neutron beam is not feasible in a strict sense. For certain nuclear reactions, however, there is a strong dominance of neutrons in a narrow energy range. Therefore, such neutron sources are often called "quasi-monoenergetic". The most popular neutron production reaction above 20 MeV is ^{7}Li(p,n)^{7}Be. It is used, *e.g.*, at quasi-monoenergetic neutron facilities in Cape Town[(8)], Davis[(9)], Louvain-la-Neuve[(10)], Saitama[(11)], and Takasaki[(12)].

There is a long-term experience in high-energy neutron production at The Svedberg Laboratory (TSL). The first neutron facility was built at TSL in the late 1980s[(13,14)] and remained in operation until 2003. In 2003-2004, a new facility was constructed. Emphasis was put on high neutron beam intensity in combination with flexibility in energy and neutron field shape.

TECHNICAL SPECIFICATION

The facility uses the ^{7}Li(p,n)^{7}Be reaction to produce a quasi-monoenergetic neutron beam. Two kinds of beams from the Gustaf Werner cyclotron are used for neutron production: 1) proton beam with energy variable in the 25-180 MeV range, and, 2) beam of H_2^+ ions with energy of about 13 MeV/A. The energy of the produced peak neutrons is controllable in the 11-175 MeV range.

A schematic plan view of the neutron beam facility is shown in Fig. 1. The proton or H_2^+ beam is incident on a target of lithium, enriched to 99.99% in ^{7}Li. The available targets are 1, 2, 4, 8.5, and 23.5 mm thick. Proton energy loss in the target amounts to 2-6 MeV depending on the incident beam energy and target thickness. The targets are rectangular in shape, 20x32 mm^2, and are mounted in a remotely controlled water-cooled copper rig. An additional target position contains a fluorescent screen viewed by a TV camera, which is used for beam alignment and focusing. Downstream the target, the proton beam is deflected by a magnet into a 10-m long dumping line, where it is guided onto a heavily shielded water-cooled graphite beam dump.

The neutron beam is formed geometrically by a cylindrically shaped iron collimator block, 50 cm in diameter and 100 cm long, with an aperture of variable size and shape. The collimator is surrounded by concrete to form the end wall of the production line towards a user area. Thereby, shielding from the lithium target region is achieved that is sufficient for most experiments. A modular construction of the collimator allows the user to select the size and the shape of the neutron beam. At present, the available collimator apertures are 2, 3, 5.5, 10, 15, 20, and 30 cm in diameter. In addition, a quadratically shaped aperture of 1 cm^2 is available, which is intended for irradiation of, *e.g.*, a separate electronic component without affecting the rest of an electronic board. Other collimator apertures in the 0-30 cm range can be provided upon request. The time needed to change the aperture is typically about 30 min.

The user area extends from 3 to 15 m downstream the lithium target. Positions located closest to the target are used for high-flux irradiation of compact objects, with achievable fluxes about an order of magnitude

*Corresponding author. Phone: +46 (0)18 471 38 50, Fax +46(0)18 471 38 33, E-mail: Alexander.Prokofiev@tsl.uu.se

Radiation Protection Dosimetry Vol. 0, No. 0

higher compared to the old TSL neutron facility[13,14], for the same target thickness, proton energy and current. Remote positions may be used to irradiate large objects, up to 1 m in diameter, *e.g.*, entire computers or aircraft navigation systems. Proton beam currents of up to 10 μA can be used for energies below 100 MeV. Above 100 MeV, the achievable beam current is about a factor of 10 lower. The resulting reduction of the neutron flux can be partly compensated by using thicker lithium targets. The neutron flux can be varied by the user according to the needs of the specific experiment.

The time structure of the neutron beam (see Table 1) is defined by the time structure of the proton beam incident on the lithium target.

The user area, situated at a level of 12 m below the ground, is connected by Ethernet and coaxial cables, about 100 m long, to counting rooms, which are located at the ground level. No time is required for "cooling down" of the user area after irradiation, because the dose rate from residual β- and γ-rays is then only slightly above the natural radiation level.

Two additional irradiation positions, which can be used parasitically with other experiments, are provided closer to the lithium target (see Table 2). The increase of the neutron flux at these positions is reached at the expense of limited accessibility, limited size of irradiated objects, lack of standard monitors, and more intense γ-ray background.

CHARACTERIZATION OF THE FACILITY

Neutron spectra at 0° have been obtained by measuring elastic *np*-scattering with the Medley setup[15-17]. The scattered protons are registered at an angle of 20° relative to the neutron beam. The measured neutron spectra are shown in Fig. 2 for peak energies of 21.8 (a), 46.5 (b), 94.7 (c), and 142.7 MeV (d). In all cases, the spectrum is dominated by a peak situated a few MeV below the energy of the primary protons and comprising about 40% of the total number of neutrons.

Fig. 2 includes a comparison of the measurements with model calculations of the neutron spectra folded with the function that describes the energy resolution in the present experiment. For the three higher energies (Fig. 2b-d), the systematics of Prokofiev *et al.*[18] was employed. For the peak neutron energy of 21.8 MeV, the evaluation of Mashnik *et al*.[19] was used (Fig. 2a). The differential cross-section for high-energy peak neutron production at 0° was obtained by multiplication of the angle-integrated cross-section of the ^{7}Li(p,n)^{7}Be reaction[19] to the "index of forwardness" from the systematics of Uwamino *et al*.[20]. The experimental data agree with the calculations except for the low-energy tail region in the 21.8-MeV spectrum where the model overpredicts the yield of neutrons with energies above 5 MeV by about 40%.

Table 3 summarizes the main features of the measured spectra and the achieved neutron fluxes. The latter have been measured with a monitor based on a thin-film breakdown counter (TFBC)[21]. Another monitoring option is provided by an ionization-chamber monitor (ICM). Both monitors utilize neutron-induced fission of ^{238}U with the cross-section adopted as neutron flux standard[22]. In addition, the neutron flux is indirectly monitored by a Faraday cup, which integrates the current of protons collected at the beam dump. In Table 3, γ-ray dose rate in the user area is given as well.

The measured contamination of the neutron beam at the user area, due to interactions of the primary protons with beam transport elements, typically does not exceed 0.05% for peak neutron energies up to 100 MeV and 0.3% for the 174 MeV energy. Such interactions lead to a minor surplus of neutrons in the user area, because charged particles produced near the lithium target and upstream are removed by the deflection magnet. The relative contamination of the neutron beam by protons with energies above 15 MeV is about 10^{-5} for the peak neutron energy of 95 MeV.

Thermal neutrons were observed in the user area, using TFBCs with ^{235}U targets, shielded by a cadmium sheet during a part of the runs. Measurements of the relative thermal neutron flux were performed at the distance of about 11 m from the lithium target, for peak neutron energies from 22 to 174 MeV. The thermal neutron flux was estimated to be about 0.5-2% of the peak neutron flux, decreasing with the peak neutron energy. No statistically significant difference was found between the thermal neutron flux measured in-beam and out-of-beam. Thus, a rather isotropic thermal neutron field was observed in the user area. These results come from an ongoing study of the low-energy part of the neutron spectra using TFBCs and different neutron-induced fission reactions[23].

Figure 3 shows a horizontal beam profile for 142.7-MeV neutrons, measured at a distance of 4.77 m from the lithium target. The measurement was performed by counting neutron-induced SEE in a set of memory chips positioned across the beam[24].

SUMMARY AND OUTLOOK

A new neutron beam facility has been constructed at TSL, and it is in frequent operation now (25 weeks during year 2005). The facility is capable of delivering neutrons in the 11-175 MeV range. This makes TSL the only laboratory in the world offering full quasi-monoenergetic neutron testing according to the JESD89 standard[7].

Recently, a neutron field with the peak energy of about 11 MeV has been developed. Processing of neutron spectra at 11 and 174 MeV is in progress. A fast ionization chamber for regular checks of the neutron spectrum is under development[25]. An

additional neutron monitor based on counting of neutron-induced SEE is about to be installed[26]. Independent calibrations of neutron monitors are planned, using measurements of the ^{7}Be activity produced in the ^{7}Li target, following a technique suggested by Uwamino *et al.*[20]. It is planned to rebuild the shielding wall around the collimator in order to diminish the flux of stray high-energy neutrons that lack through the wall and create unwanted background in *e.g.* experiments with the Medley setup[17].

A new upgrade of the facility is being launched in the framework of project ANITA (**A**tmospheric-like **N**eutrons from th**I**ck **TA**rget). The upgrade will allow us to deliver a neutron beam with a continuous "white" spectrum, and thus to reproduce the spectrum of neutrons in the atmosphere. Neutrons will be produced by irradiation of a thick tungsten target by high-energy protons. The possibility to deliver quasi-monoenergetic neutron beams will be kept.

ACKNOWLEDGEMENTS

We would like to thank the staff at The Svedberg Laboratory for the excellent work in building this new facility. We are thankful to A.N. Smirnov and M. Olmos for providing us with the thermal neutron data and the beam profile data, respectively.

REFERENCES

1. F.-R. Lecolley, G. Ban, V. Blideanu, J. Blomgren, P. Eudes, Y. Foucher, A. Guertin, F. Hadad, A. Hildebrand, J.-F. Lecolley, T. Lefort, N. Marie, P. Mermod, N. Olsson, M. Österlund, S. Pomp, A.V. Prokofiev, and C. Lebrun. Neutron and light charged particle production in neutron or proton-induced reaction on iron, lead and uranium at intermediate energy (20 to 200 MeV) – the HINDAS collaboration. Proc. Int. Conf. on Nuclear Data for Science and Technology, Santa Fe, NM, September 26 - October 1, 2004; AIP Conf. Proc. 769, 61-66 (2005).
2. R. Orecchia, A. Zurlo, A. Loasses, M. Krengli, G. Tosi, S. Zurrida, P. Zucali and U. Veronesi. Particle beam therapy (hadrontherapy): basis for interest and clinical experience. Eur. J. Cancer 34, 459-468 (1998).
3. D.L. Schwartz, J. Einck, J. Bellon, and G.E. Laramore. Fast neutron radiotherapy for soft tissue and cartilaginous sarcomas at high risk for local recurrence. Int. J. Radiat. Oncol. Biol. Phys. 50, 449-456 (2001).
4. D.T. Bartlett, L.G. Hager, R.J. Tanner, and J.D. Steele. Measurements of the high energy neutron component of cosmic radiation fields in aircraft using etched track dosemeters. Radiation Measurements 33, 243-253 (2001).
5. D.T. Bartlett, L.G. Hager, and R.J. Tanner. Results of measurements on shuttle missions to the ISS of the neutron component of the radiation field. Advances in Space Research 37, 1668-1671 (2006).
6. Single-Event Upsets in Microelectronics, topical issue, edited by H.H.K. Tang and N. Olsson. Mater. Res. Soc. Bull. 28 (2003).
7. JEDEC Standard. Measurements and Reporting of Alpha Particles and Terrestrial Cosmic Ray-Induced Soft Errors in Semiconductor Devices. JESD89, 2001.
8. R. Nolte, M.S. Allie, P.J. Binns, F. Brooks, A. Buffler, V. Dangendorf, J.P. Meulders, F. Roos, H. Schuhmacher, and B. Wiegel. High-energy neutron reference fields for the calibration of detectors used in neutron spectrometry. Nucl. Instrum. Meth. Phys. Res. A 476, 369-373 (2002).
9. F.P. Brady. (n,p) studies at the University of California at Davis. Can. J. Phys. 65, 578-587 (1987).
10. H. Schuhmacher, H.J. Brede, V. Dangendorf, M. Kuhfuss, J.P. Meulders, W.D. Newhauser, R. Nolte. Quasi-monoenergetic neutron beams with energies from 25 to 70 MeV. Nucl. Instrum. Meth. Phys. Res. A 421, 284-295 (1999).
11. N. Nakao, Y. Uwamino, T. Nakamura, T. Shibata, N. Nakanishi, M. Takada, E. Kim, T. Kurosawa. Development of a quasi-monoenergetic neutron field using the ^{7}Li(p, n)^{7}Be reaction in the 70-210 MeV energy range at RIKEN. Nucl. Instrum. Meth. Phys. Res. A 420, 218-231 (1999).
12. M. Baba, Y. Nauchi, T. Iwasaki, T. Kiyosumi, M. Yoshioka, S. Matsuyama, N. Hirakawa, T. Nakamura, Su. Tanaka, S. Meigo, H. Nakashima, Sh. Tanaka, N. Nakao. Characterization of a 40-90 MeV ^{7}Li(p,n) neutron source at TIARA using a proton recoil telescope and a TOF method. Nucl. Instrum. Meth. Phys. Res. A 428, 454-465 (1999).
13. H. Condé, S. Hultqvist, N. Olsson, T. Rönnqvist, R. Zorro, J. Blomgren, G. Tibell, A. Håkansson, O. Jonsson, A. Lindholm, L. Nilsson, P.-U. Renberg, A. Brockstedt, P. Ekström, M. Österlund, F.P. Brady, and Z. Szeflinski. A facility for studies of neutron-induced reactions in the 50-200 MeV range. Nucl. Instrum. Meth. Phys. Res. A 292, 121-128 (1990).
14. J. Klug, J. Blomgren, A. Atac, B. Bergenwall, S. Dangtip, K. Elmgren, C. Johansson, N. Olsson, S. Pomp, A.V. Prokofiev, J. Rahm, U. Tippawan, O. Jonsson, L. Nilsson, P.-U. Renberg, P. Nadel-Turonski, A. Ringbom, A. Oberstedt, F. Tovesson, V. Blideanu, C. Le Brun, J.F. Lecolley, F.R. Lecolley, M. Louvel, N. Marie, C. Schweitzer, C. Varignon, Ph. Eudes, F. Haddad, M. Kerveno, T. Kirchner, C. Lebrun, L. Stuttge, I. Slypen, A.N. Smirnov, R. Michel, S. Neumann, U. Herpers. SCANDAL - a facility for elastic neutron scattering studies in the 50–130 MeV range. Nucl. Instrum. Meth. Phys. Res. A 489, 282-303 (2002).
15. S. Dangtip, A. Atac, B. Bergenwall, J. Blomgren, K. Elmgren, C. Johansson, J. Klug, N. Olsson, G. Alm Carlsson, J. Söderberg, O. Jonsson, L. Nilsson, P.-U. Renberg, P. Nadel-Turonski, C. Le Brun, F.-R. Lecolley, J.-F. Lecolley, C. Varignon, Ph. Eudes, F. Haddad, M. Kerveno, T. Kirchner, C. Lebrun. A facility for measurements of nuclear cross sections for fast neutron cancer therapy. Nucl. Instrum. Meth. Phys. Res. A 452, 484-504 (2000).
16. S. Pomp, A.V. Prokofiev, J. Blomgren, O. Byström, C. Ekström, N. Haag, A. Hildebrand, C. Johansson, O. Jonsson, P. Mermod, L. Nilsson, D. Reistad, N. Olsson, P.-U. Renberg, M. Österlund, U. Tippawan, D. Wessman, V. Ziemann. The New Uppsala Neutron Beam Facility. Proc. Int. Conf. on Nuclear Data for Science and Technology, Santa Fe, NM, September 26 - October 1, 2004; AIP Conf. Proc. 769, 780-783 (2005).

17. U. Tippawan, S. Dangtip, S. Pomp, A. Ataç, B. Bergenwall, J. Blomgren, C. Johansson, J. Klug, P. Mermod, L. Nilsson, N. Olsson, A. Öhrn, M. Österlund, A.V. Prokofiev, P. Nadel-Turonski, V. Corcalciuc, A.J. Koning. Light charged-particle production in 96 MeV neutron-induced reactions on carbon and oxygen. These proceedings.
18. A.V. Prokofiev, M.B. Chadwick, S.G. Mashnik, N. Olsson, and L.S. Waters. Development and validation of the ^{7}Li(p,n) nuclear data library and its application in monitoring of intermediate energy neutrons. Journal of Nuclear Science and Technology, Supplement 2, 112-115 (2002).
19. S.G. Mashnik, M.B. Chadwick, P.G. Young, R.E. MacFarlane, and L.S. Waters. ^{7}Li(p,n) nuclear data library for incident proton energies to 150 MeV. LANL Report LA-UR-00-1067 (2000).
20. Y. Uwamino, T.S. Soewarsono, H. Sugita, Y. Uno, T. Nakamura, T. Shibata, M. Imamura, S. Shibata. High-energy p-Li neutron field for activation experiment. Nucl. Instrum. Meth. Phys. Res. **A** 389, 463-473 (1997).
21. V.P. Eismont, A.V. Prokofiev, and A.N. Smirnov. Thin film breakdown counters and their applications (review). Radiation Measurements 25, 151-156 (1995).
22. A.D. Carlson, S. Chiba, F.-J. Hambsch, N. Olsson, and A.N. Smirnov. Update to "Nuclear Data Standards for Nuclear Measurements". Proc. Int. Conf. on Nuclear Data for Science and Technology, Trieste, Italy, May 19-24, 1997, Part II, 1223-1229, Italian Physical Society (1997).
23. A.N. Smirnov, private communication; A.N. Smirnov, et al., to be published.
24. M. Olmos, private communication.
25. I.V. Ryzhov, private communication.
26. R. Harboe-Sorensen, private communication.

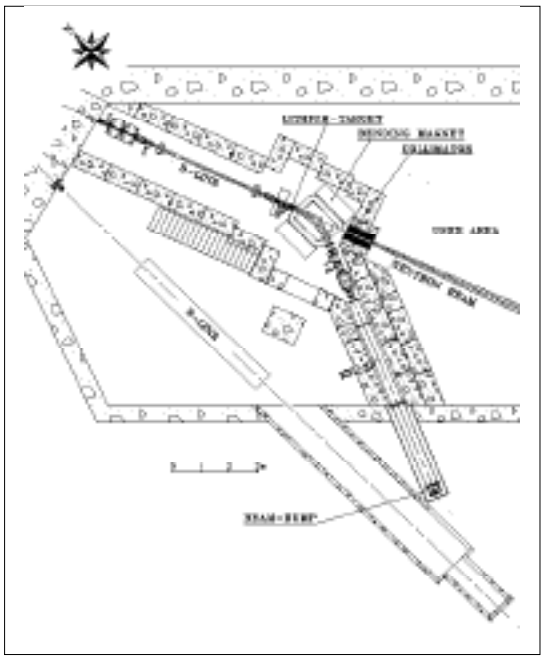

Figure 1. The schematic plan view of the neutron beam facility. The neutron beam, produced in the lithium target, continues along the D-line.

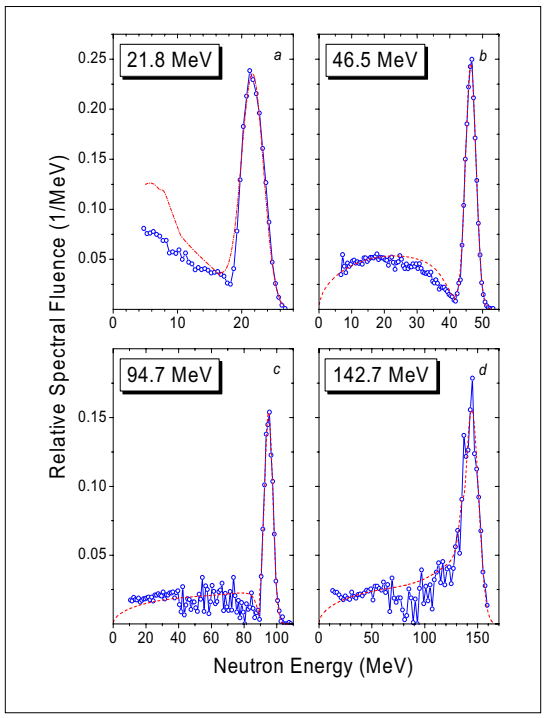

Figure 2. The neutron spectra at 0º for different peak neutron energies (see Table 3 for incident proton energies and ^{7}Li target thicknesses). Symbols connected by a solid line represent experimental data obtained in the present work. Predictions are shown as dashed lines (see text).

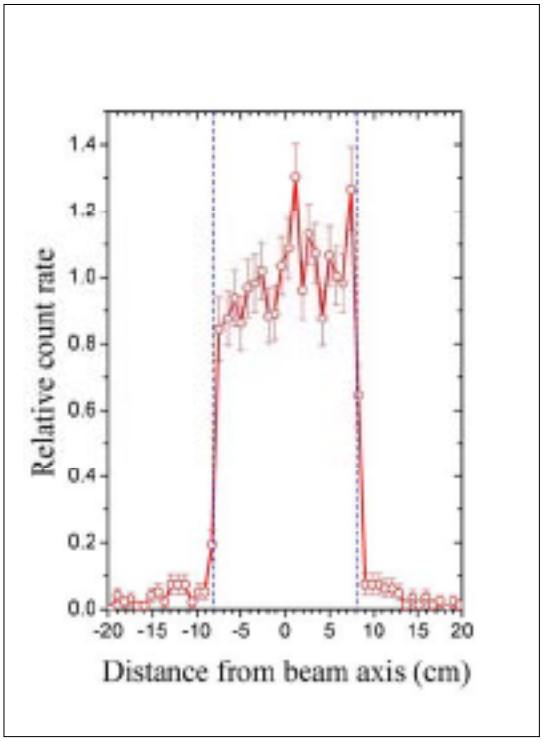

Figure 3. The horizontal beam profile for 142.7-MeV neutrons, measured at the distance of 4.77 m from the lithium target. Vertical dashed lines represent boundaries of the beam expected from the geometry of the collimator.

Table 1. Parameters of the time structure of the beam.

Type of the time structure	Repetition period	Beam pulse duration	Peak neutron energy (MeV)
Microstructure	45 - 80 ns[1]	~4 ns (FWHM)[2]	11 – 174
Macrostructure	≥5 ms[3]	~ 0.7 ms (FWHM)[2]	>100
Beam sharing structure[4]	~40 min[2]	~30 min[2]	174

[1]Dependent on the peak neutron energy
[2]Typical value
[3]May be increased up to 1 s upon user's request
[4]This structure is present only if the accelerator beamtime is shared between the neutron beam facility and the proton cancer therapy facility.

Table 2. Parasitic irradiation positions.

Position	Distance from the Li target (m)	Angle to the proton beam direction (°)	Gain in the peak neutron flux
PARTY	1.9	1.6	2.5
TUNIS	1.1	7.5	1.7 – 2.2[1]

[1]Dependent on the peak neutron energy

Table 3. Parameters of the available neutron beams.

Proton beam energy (MeV)	^{7}Li target thickness (mm)	Proton beam current (μA)	Average energy of peak neutrons (MeV)	Fraction of neutrons in the high-energy peak (%)		Peak neutron flux (10^5 cm^{-2}s^{-1})[1]	γ-ray dose rate (mSv/h)[2]
				Measured	Calculated		
24.68 ± 0.04	2	10	21.8	~50	--	1.3	0.35
49.5 ± 0.2	4	10	46.5	39	36	2.9	1.7
97.9 ± 0.3	8.5	5	94.7	41	39	4.6	2.4
147.4 ± 0.6	23.5	0.6	142.7	55[3]	40	2.1	-

[1]At the entrance of the beam line to the user area.
[2]At the neutron beam path at the distance of 8 m from the lithium target.
[3]Upper limit due to poor energy resolution.

Laboratory work – Not just a necessary evil?

J. Blomgren[1], S. Pomp[1] and M. Weiszflog[1]

[1]Department of Neutron Research, Uppsala University, Box 525, S – 751 20 Uppsala, Sweden (Jan.Blomgren@tsl.uu.se)

Abstract
It is not uncommon that undergraduate engineering students at Uppsala University do not appreciate laboratory work. Often instructions are of a type leaving little room for initiative by the students. Moreover, laboratory work is often considered of minor importance, reflected in that they rarely are given a large weight in the final examination.

We have developed a new strategy for laboratory work in electric engineering on bachelor's level. The methodology can be summarized as follows:

1. Minimum instruction. Only the problem is described, not how to reach the goal.
2. Open problem. The problem should be possible to solve in many different ways, and it should not be obvious how.
3. Mandatory preparation. Students should prepare the work themselves and have a strategy before starting practical work.
4. Plenty of time. It should be possible to try many strategies within the allocated time.
5. Free use of equipment. The laboratory should be equipped with plenty of equipment of so many types that there are many ways to solve the problem, and no approach should be obvious.

Last but not least, this methodology has also been established in the examination of the course, where a practical examination provides about half the weight in the final grade.

Keywords: Laboratory, student creativity, practical examination.

1. INTRODUCTION

1.1 Why develop new methods in laboratory teaching?

Many undergraduate studies at Uppsala University (UU) testify that they consider laboratory exercises a necessary evil, and this situation is not unique to UU. To a large degree, the instructions follow a "cook-book" structure, with detailed instructions how to proceed, leaving little room for student initiatives. Moreover, laboratory work is given low status by the fact that they rarely are part of the examination.

Examination in physics at UU is by tradition essentially always carried out by written exams with theory problems to solve. This is true also for bachelor's level engineering programs, in spite of the fact that they are intended to be more practically oriented.

This has motivated the development of a new methodology in the laboratory tutorials, and to include practical moments in the examination.

1.2 Student background

The present development work has been carried out as part of the bachelor's programme in mechanical engineering. There are two types of engineering education. The largest one is the masters' program that comprises four and a half years full-time studies. This program is on a high theoretical level, while the

bachelors program is rather different. This education is three years full-time studies and it originally emanates from an extension of high school. The student profile is very different. We estimate that a majority of the students should not have even tried to get into the masters program if the bachelors program was unavailable. Our experience is that about 10 % of the bachelors students could follow the pace at the masters program. The very different nature of these two educations is also evident from the fact that you cannot continue from the bachelors program to get a masters degree by adding extra courses. Another testimony is that students not being able to follow the masters program switch to the bachelors program.

Taking the risk to become unpopular, we claim that the bachelors program students do not belong to the elite in theory studies. Instead, they represent a category of students that hardly would have studied on an academic level at all if the bachelors program had not existed. Thereby, this education fulfils a large societal need, and it represents a challenge for teachers. How do you motivate students that are not very talented and often not very interested in academic studies as such, and how do you inspire them to reach demanding goals, preferably at a much higher level than their own expectations?

This challenged is accentuated further by that the course of the present work, electric technology, is not a natural favourite source. There is an education in electric engineering that is the natural choice for students with an interest in electricity. Among the students, there is a popular quote that "if you hate electricity, you study mechanical engineering". With a slight exaggeration you can say that our course is for students that are neither very talented nor like the subject as such…

This has motivated a more practically oriented teaching to be developed [1]. Improved laboratory work has become a natural part of this process.

2. LABORATORY WORK WITHOUT INSTRUCTIONS: IS THAT REALLY TEACHING?

2.1 Background

Laboratory work in undergraduate education at UU is often undertaken with very detailed instructions. Every step in the procedure is described, and sometimes there are even ready-made forms to fill out. Often these exercises are carried out under stress, i.e., the time allocated is very limited. As a result, there is often no alternative for the students than to follow the instructions in detail.

One of the authors (J.B.) had an interesting experience during his undergraduate studies at UU. At one occasion, the dedicated equipment was broken. As a consequence, he had to find other pieces of equipment, but there were no spare parts, so instead he visited research labs, talked with people and was allowed to borrow equipment from them. The fact that the new equipment was not intended for that particular use resulted in that the entire layout of the experiment had to be changed. As a consequence, the formal precision in the measurement suffered significantly, but instead the learning process gained so much more. This experience has been an important source of inspiration behind the present work.

2.2 Realization

Based on these experiences, an approach different from the UU standard described above has been attempted. The instructions have been shortened to a minimum. The instructions only describe a general problem, but do not indicate how to solve it.

The students are presumed to have thought about how to solve the problem beforehand. They are obliged to arrive to the laboratory with a plan. They present the plan to the assistants. The plan has to be reasonably elaborated, but it does not have to be "correct". In fact, the assistants do not comment on the feasibility of it, they only check that they have studied the problem in some detail.

Plenty of time is a very important aspect. In this course, the total number of laboratory exercises has been reduced dramatically, and the time allocated to each task has been increased. This provides sufficient time to try an approach, realize that it does not work, analyze why it failed, establish a new

strategy, try it out and succeed. The most important role for the laboratory assistants is to be discussion partner in the analysis of failed attempts. Our experience is that this suits students with limited practical training in handling technical equipment well. These exercises are carried out relatively early in the education, and a fairly large fraction of the students have little or no experience in handling measurement devices and similar equipment. Plenty of time to get used to the equipment is therefore very valuable in the creation of a good teaching environment.

Another important aspect is plenty of equipment and free use of it. There should be much more equipment in the laboratory than needed to solve the problems. If there is only one way of solving the problem with existing equipment, the learning will suffer.

Also this can be illustrated with an episode from the student years of one of the authors (J.B.). There was actually a laboratory examination in electronics. In that examination, the problem was to build a signal transformer that can shape a sinusoidal wave into a square wave. At the beginning of the examination, there were two standard electric components (a resistor and a capacitor), both possible to vary in five fixed steps, and a few cables (the number needed for the "right" solution). The fact that only a minimal amount of equipment was available made it possible to try all possible combinations in a few minutes, and he passed the test without having learned much, neither earlier in the course nor during the examination itself.

In this particular case, this was unnecessary. If only a few extra components had been supplied, systematic testing of all possible combinations would have been impossible. Moreover, the type of filter asked for in the problem description can be built in more than one way, using different components. With plenty of equipment available, a much more creative environment could have been obtained, and a range of working solutions could have emanated.

This last point is not just a detail. Our experience is that in teaching often on single "correct" solution is presented, even in situations when many different solutions are possible. This was certainly the case in the examination described above. The students left the laboratory and thought they had found *the solution*, instead of having realized that they had found *one of the solutions*.

The methodology can be summarized as follows:

1. Minimum instruction. Only the problem is described, not how to reach the goal.
2. Open problem. The problem should be possible to solve in many different ways, and it should not be obvious how.
3. Mandatory preparation. Students should prepare the work themselves and have a strategy before starting practical work.
4. Plenty of time. It should be possible to try many strategies within the allocated time.
5. Free use of equipment. The laboratory should be equipped with plenty of equipment of so many types that there are many ways to solve the problem, and no approach should be obvious.

It has to be stressed that the combination of factors is very important. Each of these items is insufficient to create a stimulating and creative environment. If you give a minimal instruction, but limit the equipment so that only one way of addressing the problem is possible, little is gained concerning student creativity. Even if all other aspects are there, if too limited time is available, the students can try just one solution, and the learning process by analyzing their failures is missed.

2.3 Feedback in physics

Another area where – to our opinion – present teaching often fails is the coupling between various parts of the education. Often the education is composed of courses in various sub-fields with little or no contact between the courses. Often we find an attitude that in the course on energy engineering, only energy is important. The students study energy engineering before the electricity class. Why not teach electric engineering in such a way that the students have to use their supposedly obtained skills in energy to solve problems in the electricity laborations?

We have tried this approach. In the course on energy engineering, pumps are an important part. We have developed a laboratory exercise in the electric engineering course, in which the students have to work with a pump driven by an electric motor. When the students arrive to the laboratory, they get a non-functioning motor. Their first exercise is to repair the motor. When it works, they should use it to pump water. This part of the exercise cannot be solved unless they use knowledge from the energy engineering course.

Another special aspect is that we give them a problem that cannot be solved unless they have two pumps. This means that half-way through the process, they have to find another student group and start cooperating with them. Thus, they get social training and learn how to collaborate. Moreover, they have to discuss how to solve the problem, which develops their analysis skills.

Finally, they get a last exercise. They are requested to destroy the motor so that next student group can start their work with a non-functional one, but it should be possible to repair it with reasonable efforts. It has become a sport among the students to figure out the most intriguing dysfunction…

We believe that subject feedback is important for more than one reason. It can increase the interest in electricity (which is not their favourite subject) by pointing at its importance for their primary interest (mechanical engineering). In addition, it shows that what was perceived as dry theory in a previous course becomes practically useful later on. Last but not least, it is well known in cognitive science that repeated learning is superior to learning at just one occasion.

Another important aspect is preparation for working life. In a real situation at a normal job, the problems are normally formulated in a much less stringent way than in education. Most often, there is no correct result to check out afterwards, and in many cases there simply is no objectively correct answer. Giving instructions without details is therefore a conscious strategy to create a more realistic situation, hopefully preparing the students for the life to come after the exam.

2.4 Experiences from similar studies

We have performed a literature search on similar projects. It seems as our experiences are in line with a number of international studies. Traditional laboratory work is often hampered by limited possibilities for the students to experiment freely [2], while freedom to try various approaches has been identified as maybe the most important single aspect concerning the learning process [3]. Of the projects that have been attempted, many have failed due to unsuitable structure in the realization [4] and on lack of time for the students [5].

In all studies we have found on student-driven laboratory work is that the teacher has first given lectures on what is supposed to be done, and subsequently left the students to carry out the task, often with written instructions. This has resulted in a number of negative experiences [6]. It might therefore seem surprising – or even contradicting – that our students in general are pleased with the approach. We think that the difference is due to the fact that we force the students to be prepared when they arrive to the laboratory, which was not the case in the studies mentioned above. Students that have not reflected about the work beforehand have limited possibilities to carry out creative learning. Instead the students become frustrated (a common theme in the studies above), and they look for quick fixes, not seldomly by simply copying somebody elses work.

3. LABORATORY EXAMINATION

3.1 Background

After having worked on making laboratory work a larger and more important part of the course, it felt unsatisfying to have a purely theoretical examination, especially as the overall goal of the entire education is that it should be more practically oriented than traditional academic education.

Many courses in physics at UU have mandatory laboratory exercises. To pass the course, the students need to have performed all the exercises, but they rarely play an important role in the actual grading. In most cases, the grade is entirely based on the result on the written theory exam. In some cases, well

performed laboratory work can result in bonus points, but not of major importance for the final outcome. This attitude seems to be common also in other disciplines, like chemistry and biology.

3.2 Realization

Admittedly, we have adopted a rather conventional approach. The students get “black boxes”, i.e., a closed box with an unknown electric circuit inside. To solve the task to figure out the circuit solution inside, both theory knowledge and practical skills are required.

This approach has some advantages. It is fairly easy to keep the exact task secret, but still let the students know what it is about. We tell the students early in the course what the examination is about, and some of them practice, i.e., they construct unknown circuits to each other and let their fellow students try to solve the problem. Almost needless to say, both the student that constructs the problem and the one who solves it benefit a lot, and the students that undertake such training almost inevitably pass the course.

We use a few different circuit solutions and distribute them to the students by lottery. Some information about the interior is given on a separate fact sheet. This has the advantage that the level of difficulty can be changed, simply by changing the fact sheet. Thus, the boxes can be used in different courses. This also allows solutions to another problem. It is difficult to make various circuits that are about equally difficult to work with. This can be balanced by giving more information on the fact sheets for the more complex circuits. Each student gets two or three exercises to solve. The first one requires only practical skill to solve, while the second also requires theory understanding.

We discussed early on to use only a practical examination and skip the theory tests completely. We finally adopted a model in which the practical examination comes first, and it gives 40 % of the total weight in the examination. It is followed up a few days later with a theory test. In total 50 % of the combined practical and theory tests are required to pass. Thus, in reality you cannot pass without the a good result on the practical exam, and you cannot get pass with distinction without mastering both theory and practical skills.

3.3 Results

Does laboratory-based examination test other types of knowledge than a theory test? Do some student categories win or lose on this methodology? These were some questions that have been investigated in follow-up studies of the present project.

As described above, the practical test was followed up with a theory test a few days later. The first two years have been evaluated by in-depth interviews and with inspection of correlations between the results on the practical and theory parts of the examination.

The only significant result we have identified is that female students got lower scores on both theory and experiment. We believe, however, that this difference is to a large degree due to different knowledge beforehand. Among the male students, some had quite some experience already when the course started, which was not the case among the female students.

3.4 Evaluation

Eight students out of 42 were selected for in-depth interviews about the experiences of the course. The selection was not random, since this was not intended to be scientific research, but to be a basis for improvement of the course next year. Therefore, students of different age, sex and societal background were selected. Moreover, we purposely selected students with different level of success in the studies.

A majority viewed the course as useful, and they thought they would benefit from it also in the future. The laboratory exercises were considered valuable, but demanding. None of the students thought the course as such was among the easiest, and a few said it was the toughest they have had so far, still being pleased with it.

No student had any previous experience of practical examination. All of them thought the idea as such is good, irrespective of their own level of success. Essentially all of them also thought the relative weight in the grade (40 %) was suitable. In general, the students testified that the practical examination was good from a learning perspective. About half of the students thought they had learned new things during the practical examination, while only one said that the theory test had resulted in new knowledge.

The least positive student was also the only one that herself indicated insufficient knowledge beforehand, and her results were not very good.

Essentially all students would prefer continuous examination, i.e., all laboratory work should be graded and part of the examination. (It can be commented that we had discussed this option beforehand, but come to the conclusion that it would be better to let students practice in the laboratory and develop skills before being examined.)

All students expressed satisfaction with the grading, i.e., they thought that the grades given were fair and honest, and gave a correct picture of their abilities. It was a common view that the laboratory examination was easier than the theory one, and that it was therefore difficult to use the theory exam to recover from a poor practical examination.

At UU, you are allowed to take a test as many times as you like. Most courses offer a test at the end of the course, and at two more occasions per year. The first year we practiced practical examination, there was just one practical examination, and if you failed the follow-up examinations later on the same year were theoretical. The students pointed out that there ought to be practical re-examinations as well. We thought this was a reasonable attitude, and changed the system next year.

The evaluation after the second season was less ambitious. The reason for this was that the student group was far more homogeneous, making studies of differences due to different background difficult. In short, the main picture from the first season was corroborated. The course as such was positively viewed. The idea as such with practical examination was well perceived, and the minor dissatisfaction expressed was highly correlated to details in the performance (my test box was more difficult than the others…)

3. DISCUSSION, CONCLUSIONS AND OUTLOOK

We have investigated a number of similar projects in Sweden. For an extensive discussion, see our full project report (in Swedish) [7]. We have noted that all but one similar project in physics is from electricity. We believe this is no coincidence. It is relatively easy and inexpensive to allow free use of equipment in electricity, while in other areas of physics, cost is a large obstacle. (Free use of equipment in laboratory exercises in particle physics might be difficult…). There is, however, an example of a similar approach in optics [8], which we find encouraging, since it shows that the methodology described in the present work can be applied also outside electricity.

Outside physics, we have found a number of examples of practical examination, e.g., in pharmacy education.

We believe that the teaching methods presented here are useful in many areas of physics. We find no strong reasons why they should not be applicable in mechanics and thermodynamics, besides electricity and optics already identified as viable areas. We do not, however, want to market these methods as general prescriptions for success. In some areas, like particle physics mentioned above, the practical obstacles are insurmountable.

We have discussed to have practical examination only. Although we find it possible, we find no real reason. Some moments in the course are better examined in written tests. For instance electric safety is difficult (and possibly dangerous!) to examine practically. We do not think it is wise to try to compensate the strong preference for written theory tests is most other courses by a fully practical examination in one particular course. Rather, we find it more important to have a balance in many courses, with both theory and experiment in the examination.

Acknowledgements
Many persons have participated in various parts of the practical implementation of the present work. The contributions by Hans Henriksson, Anders Hjalmarsson, Cecilia Johansson, Joakim Klug, Philippe Mermod, Henrik Sjöstrand, Marco Tardocchi and Angelica Öhrn are gratefully acknowledged. We would like to thank the office for engineering education at Uppsala University for valuable support. Thanks are due to Cedric Linder for very useful suggestions on literature. The project has been financially supported by the Swedish National Agency for Higher Education through the Council for the Renewal of Higher Education

References

[1] J. Blomgren, The car approach to electromagnetism, Physics Education vol. 33:4, s. 224, 1998.
[2] K.P. Raghubir, The laboratory-investigative approach to science instruction. Journal of Research in Science Teaching **16**, vol. 1 (1979) 13.
[3] J. Bliss, J. Ogborn, Students' reaction to undergraduate science: Laboratory and project work. Heinemann Educational Books, London (1977).
[4] J. Bliss, Students' reaction to undergraduate science: Laboratory and project work. In E. Hegarty-Hazel (ed.), The student laboratory and the science curriculum, Routledge, London and New York (1990).
[5] P. Gardner, C. Gauld, Labwork and student attitudes. In E. Hegarty-Hazel (ed.), The student laboratory and the science curriculum, Routledge, London and New York (1990).
[6] C.R. Brew, R.F. Gunstone, Students' perceptions of an innovative university laboratory program, Research in Science Education **22** (1992) 55.
[7] J. Blomgren, Laborationer – inte bara nödvändigt ont? (Laboratory work – not just a necessary evil?), Enheten för utveckling och utvärdering, Uppsala universitet, Arbetsrapport nr 8, 2001.
[8] D. Hanstorp, J. Enger, B.-E. Mellander, K. Stiller, Examination by laboratory work, Swedish National Agency for Higher Education conference on quality in higher education, Luleå, Sweden, 10-11 June 1998. Published at http://www.hsv.se/.

Curricula

Jan Blomgren obtained his PhD in nuclear physics from Uppsala University, Sweden in 1991. He was a Research Associate at Indiana University, USA, 1992–1993 and Assistant Professor at Stockholm University, Sweden, 1993–1994. Since 1994, he has been at the Department of Neutron Research at Uppsala University, as Assistant Professor 1994–1998, Associate Professor 1998–2003 and Full Professor since 2003. His research areas are neutron-induced nuclear reactions and their applications within energy technology, nuclear waste incineration, cancer therapy and reliability of electronics. His CV contains 170 publications in international journals or papers presented at international conferences, and he is a referee for four international journals. Being the Director of Studies of the Swedish Nuclear Technology Center, he has responsibilities for national coordination of education related to nuclear power.

Stephan Pomp obtained his PhD in nuclear physics from Uppsala University, Sweden in 1999. He was Senior Research Engineer at the The Svedberg Laboratory, Uppsala, Sweden, 1999-2000. Since 2000, he has been at the Department of Neutron Research at Uppsala University, as Research Physicist 2000-2002 and as Assistant Professor since 2002. His research areas are neutron-induced nuclear reactions and their applications within energy technology, nuclear waste incineration, cancer therapy and reliability of electronics. His CV contains 60 publications in international journals or papers presented at international conferences.

Matthias Weiszflog obtained his PhD in nuclear physics from University of Göttingen, Germany in 1995. He was research associate at the The Svedberg Laboratory, Uppsala, Sweden, 1995-99. Since 2000, he has been at the Department of Neutron Research at Uppsala University, as Research Physicist. His research areas are nuclear structure and neutron diagnostics for fusion. His CV contains 30 publications in international journals, as well as a number of papers presented at international conferences.

Appendix XXXIII

European Nuclear Education Network

J. Blomgren[1], F. Moons[2], P. De Regge[3] and J. Safieh[4]
on behalf of the
European Nuclear Education Network

[1]Swedish Nuclear Technology Center and Department of Neutron Research, Uppsala University, Box 525, S – 751 20 Uppsala, Sweden (Jan.Blomgren@tsl.uu.se)

[2]Studiecentrum voor Kernenergie•Centre d'étude de l'Energie Nucléaire, SCK•CEN, Boeretang 200, B – 2400 Mol, Belgium

[3]ENEN Association, Institut Nationales des Sciences et Techniques Nucléaires, Saclay, Bât. 395, F – 91 191 Gif sur Yvette Cedex, France

[4]Commissariat à l'Energie Atomique, Institut Nationales des Sciences et Techniques Nucléaires, Saclay, Bât. 395, F – 91 191 Gif sur Yvette Cedex, France

Abstract
In most countries within the European Union that relies to a significant extent on nuclear power, neither the undergraduate nor the PhD education is producing a sufficient number of engineers and doctors to fill the needs of the industry. Moreover, in many countries reactor physics and technology are being reduced or even removed from the academic curriculum. This has motivated EU-supported projects, aiming at finding means for raising the interest in nuclear technology among university students.

As a result of this process, a new education organisation, European Nuclear Education Network (ENEN), has recently been established. This is an organisation that will issue a special certificate in nuclear engineering. Students will be registered at various universities and get their exams from their respective alma mater, just as today. If the student fulfills some criteria on the total amount and type of courses, ENEN will issue an additional certificate stating that the student meets the standards for a European master of nuclear engineering. Thus, accreditation of courses for mutual recognition is an important aspect of the work of ENEN.

Keywords: nuclear engineering, European network

1. INTRODUCTION

The need to preserve, enhance or strengthen nuclear knowledge is worldwide recognised since a couple of years. Among others, "networking to maintain nuclear competence through education and training", was recommended in 2001 by an expert panel to the European Commission [1]. It appears that within the European university education and training framework, nuclear engineering is presently still sufficiently covered, although somewhat fragmented. However, it has been observed that several areas are at risk in the very near future including safety-relevant fields such as reactor physics and nuclear thermal-hydraulics. Furthermore, in some countries deficiencies have been identified in areas such as the back-end of the nuclear fuel cycle, waste management and decommissioning.

To overcome these risks and deficiencies, it is of very high importance that the European countries work more closely together. Harmonization and improvement of the nuclear education and training have to take place at an international level in order to maintain the knowledge properly and to transfer it throughout Europe for the safe and economic design, operation and dismantling of present and future nuclear systems. To take up the challenges of offering top quality, new, attractive and relevant curricula, higher education institutions should cooperate with industry, regulatory bodies and research centres, and more appropriate funding from public and private sources. In addition, European nuclear education and training should benefit from links with international organizations like IAEA, OECD-NEA and others, and should include world-wide cooperation with academic institutions and research centres.

The first and central issue is to establish a European Master of Science in Nuclear Engineering. The concept envisaged is compatible with the projected harmonized European architecture for higher education defining Bachelors and Masters degrees. The basic goal is to guarantee a high quality nuclear education in Europe by means of stimulating student and instructor exchange, through mutual checks of the quality of the programmes offered, by close collaboration with renowned nuclear-research groups at universities and laboratories. The concept for a nuclear master programme consists of a solid basket of recommended basic nuclear science and engineering courses, but also contains advanced courses as well as practical training. Some of the advanced courses also serve as part of the curricula for doctoral programmes.

A second important issue identified is Continued Professional Development. The design of corresponding training courses has to respond to the needs of industry and regulatory bodies, and a specific organization has to be set up to manage the quality assessment and accreditation of the Continued Professional Development programmes.

In order to achieve the important objectives and practical goals described above, the ENEN Association, a non-profit association under French law, has been formed. This international association can be considered as a step towards the creation of a virtual European Nuclear University symbolising the active collaboration between various national institutions pursuing nuclear education.

Based on the concepts and strategy explained above, and with the full co-operation of the participating institutions, it may be possible that the intellectual erosion in the nuclear field can be reversed, and that high quality European education in nuclear sciences and technology can be guaranteed.

2. ENEN – EUROPEAN NUCLEAR EDUCATION NETWORK

Within the 5th Euratom research and training programme on nuclear energy (1998-2002), the European Commission supported a project on European nuclear engineering education. 22 academic institutions and research laboratories participated [2].

Within the project, the major elements for a European master of science in nuclear engineering have been defined, pilot sessions on nuclear engineering education have been performed, the ENEN-association has been established and a process of re-vitalization of nuclear education and training in Europe has been initiated. The project contributed towards farther reaching objectives, e.g., the conservation of nuclear knowledge and expertise, the creation of a European higher education area and the implementation of the Bologna declaration and the enlargement of the European Union.

It should be emphasized that ENEN was created based on a bottom-up approach. It has been formed without governmental or other types of high-level initiatives. Instead, the starting point was a number of active professors in nuclear engineering and related areas that saw a necessity – and possibility – of taking action. The absence of a strong leadership imposed from above has meant that the major properties of the project had to be agreed upon by a majority of its members. This has obviously made decision sometimes somewhat time-consuming, but on the other hand, when a decision has finally been reached, the implementation of it has been relatively straight-forward.

Since ENEN is not an organisation with power to overrule universities, the strategy adopted to promote nuclear engineering had to be based on a voluntary basis. This has resulted in the following approach. The basic organization of the university studies is unchanged. Like today, students are enrolled at their respective university, and they get their degrees from it, like before. If the exam of the student fulfils the ENEN criteria, an additional certificate is issued, stating that the student is also awarded a European master of nuclear engineering.

There are presently major changes of the educational systems in many European countries motivated by the Bologna process. There is an ongoing process to harmonize essentially all the university education system in the EU countries into a 3+2+3 year education system. In this system, three years should be mandatory to obtain a bachelor's degree. A two-year addition would then result in a master's degree, followed by three years of research to get a PhD.

To diminish some confusion on the meaning of ENEN, it has to be mentioned already here that the acronym ENEN historically has referred to two different meanings. The EU project ENEN (European Nuclear Engineering Network) was active during 2002-2003. This project resulted in the establishment of the association European Nuclear Education Network, also abbreviated ENEN. Although all the partners of the ENEN project are now members of the ENEN network, the latter has attracted more members. The change of the name, from "nuclear engineering" to "nuclear education", was suggested by the EU commission, with the motivation that this would facilitate a future expansion into activities related to nuclear engineering, like radiation protection. Below, the major components of the ENEN project are outlined.

3. EUROPEAN MASTER OF SCIENCE IN NUCLEAR ENGINEERING

Based upon a year-long exchange of views between the partners of ENEN, consisting of a representative cross section of nuclear academic institutions and research laboratories of the EU-25, a coherent and practicable concept for a European Master of Science in Nuclear Engineering has emerged. The concept is compatible with the Bologna philosophy of higher education for academic engineers in Europe (a Bachelor of Science after 6 full-time semesters, and a Master of Science after further 4 full-time semesters). In addition, the approach to the European Master of Science in Nuclear Engineering, can accommodate the presently existing variety of educational systems in the EU-25 members and candidate-member states, as well as the Bologna implementation in some countries, where Master degrees will be granted after a 2-semester program beyond the Bachelor.

The full curriculum leading to the degree of Master of Science in Nuclear Engineering is composed of course units formally recognized by ENEN. A Master of Science in Nuclear Engineering can only be granted after having obtained a full-time load of ten semesters beyond secondary level or in other words 300 credits engineering academic level studies. One credit amounts to a student load of about 30 hours and a full semester corresponds to 30 credits or about 900 load hours [3].

A minimum of two semesters equivalent or 60 credits must be obtained in strictly nuclear subjects composed of a set of core-curriculum courses complemented with nuclear electives and a project work/thesis in a nuclear domain (see figure 1).

Students register in one ENEN-accredited "home" institution and acquire the required credits in ENEN-institutions of their choice. The home institution grants the formal degree of Master of Science in Nuclear Engineering, based upon the formal recognition of credits, very much similar to the ERASMUS philosophy. ENEN, on behalf of its members, grants the quality label European Master of Science in Nuclear Engineering if a substantial amount (some 20 or 30) of credits have been followed at an ENEN-member institution other than the home institution. Typically these credits might be obtained by performing "abroad" the project work or master thesis, and taking there also some related advanced courses.

Because of the different meaning of the words "undergraduate, graduate and post-graduate" in UK and US contexts, these terms are preferentially not used in the ENEN terminology. It is advised to talk about

Bachelor, first Master, additional Master always with the number of credits or full-time semesters required, mentioned.

European Master of Science in Nuclear Engineering

Minimal Requirements for EMSNE:

- At least 300 ECTS university-level study
- At least 60 ECTS purely nuclear engineering (NE) oriented
- At least 30 ECTS in other ENEN institution than "home institution"

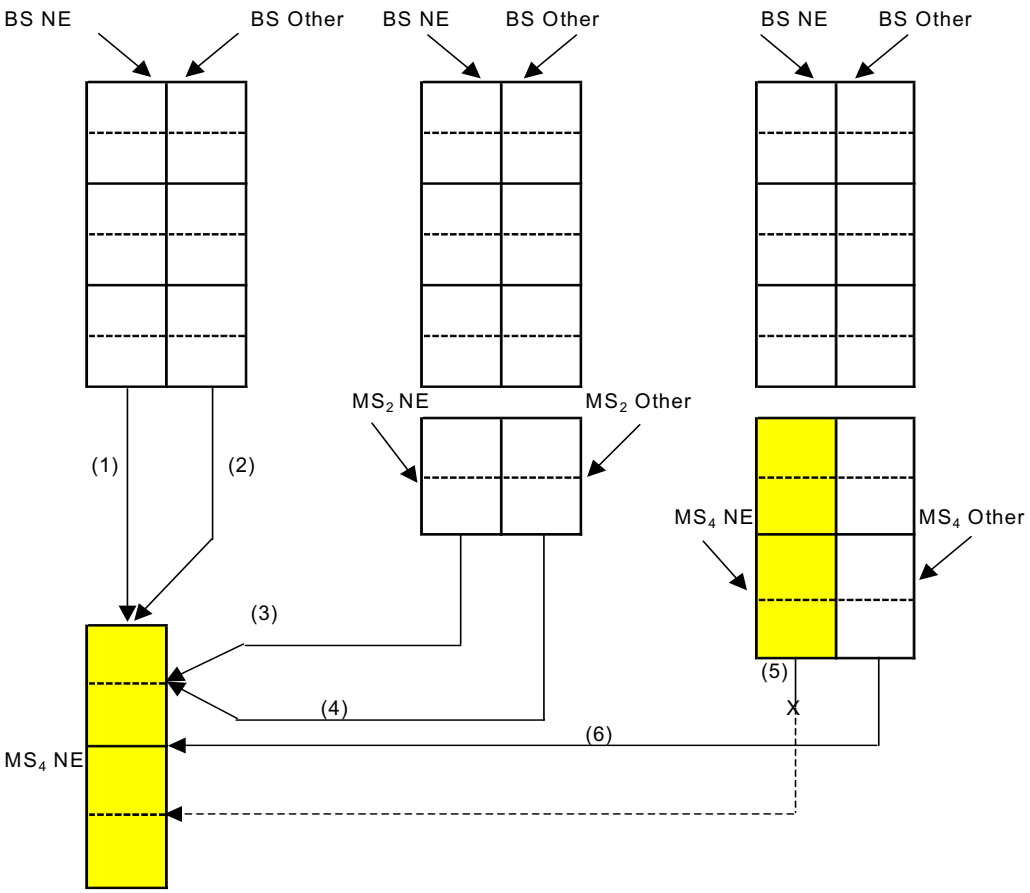

(1) 48-60 ECTS non NE; 48-60 ECTS NE (partly tradeable); 12-24 ECTS Thesis (NE)
(2) 48-60 ECTS non NE; 48-60 ECTS NE; 12-24 ECTS Thesis (NE)
(3) 24-30 ECTS non NE; 48-54 ECTS NE (partly tradeable); 12-18 ECTS Thesis (NE)
(4) 24-30 ECTS non NE; 48-54 ECTS NE; 12-18 ECTS Thesis (NE)
(5) only for "European" quality label; extra 30 ECTS "abroad"
(6) 42-48 ECTS NE; 12-18 ECTS Thesis

Figure 1. Typical full program variations.

4. PILOT SESSIONS ON NUCLEAR ENGINEERING EDUCATION

To demonstrate the feasibility of European nuclear education schemes, a three weeks course, called "Eugene Wigner" course for nuclear reactor physics experiments, was successfully organized from April 28 to May 16, 2003. The main organiser is the Institute of Nuclear Techniques at the Budapest University of Technology and Economics [4]. Some 20 postgraduate students from about 10 different European, including accession countries, participated in nuclear reactor physics experiments, organized jointly by four universities. Students performed reactor physics experiments on research and training reactors in respectively Vienna, Prague and Budapest. One week of theoretical lecturing at Bratislava University introduced or refreshed the knowledge to perform the nuclear reactor physics experiments. The ENEN partners rated the course between 6 to 8 credits or an equivalent student load of some 180 to 240 hours. Students got a certificate of participation. Individual marks are transmitted to the home professors. Because of the success of the first edition, the course has been repeated every year, and other courses with similar organization are now underway [5].

This course has fulfilled many of the ENEN underlying principles. It has a European dimension, since it involves four countries in the organization. Moreover, by joining forces among these partners, an added value is produced that could not have been provided by a single partner. At the time when the course was conceived, one country was already an EU member, while three were candidate countries, all of which are now EU members. Thus, this course also had a moment of integration of candidate countries. Finally, it has to be mentioned that clever use of existing infrastructure is a cornerstone in the EU research and education policy, a policy that was obviously adhered to.

5. THE ENEN ASSOCIATION

The temporary network described above, established through the European 5th Framework Programme project ENEN, was given a permanent character by the foundation in 2003 of the European Nuclear Education Network Association, a non-profit-making association pursuing a pedagogic and scientific aim. Its objective is the preservation and development of higher nuclear education and expertise. It is realized through the co-operation between European universities, involved in education and research in nuclear disciplines, nuclear research centres and nuclear industry. The current membership consists of 35 universities and 6 research centres. Supported by the 5th and 6th Framework Programme of the European Community, the ENEN Association established the delivery of the European Master of Science in Nuclear Engineering certificate. Education and training courses have been developed and delivered to materialise the core curricula and optional fields of study in a European exchange structure. Pilot course editions and try-outs of training programmes have been organised with support of nuclear industries and international organisations. The ENEN Association contributes to the management of nuclear knowledge within the European Union as well as on a world-wide level. It cooperates with regional Networks in Asia, Canada and the USA and participates to activities of the World Nuclear University.

5.1 The ENEN Association objectives

The general goals of the ENEN Association are defined with respect to the academia as follows:

- To develop a more harmonized approach for education in the nuclear sciences and nuclear engineering in Europe;
- To integrate European education and training in nuclear safety and radiation protection;
- To achieve a better cooperation and sharing of academic resources and capabilities at the national and international level; and with respect to the end users, such as nuclear industries, regulatory bodies, nuclear applications, etc.
- To create a secure basis of skills and knowledge of value to the European Union;
- To maintain an adequate supply of qualified human resources for design, construction, operation and maintenance of nuclear infrastructures, industries and power plants;

- To maintain the necessary competence and expertise for the continued safe use of nuclear energy and applications of radiation in industry and medicine.

The objectives and structure of the ENEN Association are formulated in the Statutes, following the conclusions and recommendations of 5th Framework ENEN Project, with the Mission of the ENEN Association being the "Preservation and the Further Development of Higher Nuclear Education and Expertise". A first series of objectives is formulated as follows:

- To deliver a European Master of Science degree in Nuclear Engineering;
- To encourage and support PhD studies;
- To promote exchange of students and teachers participating in the European Nuclear Education Network;
- To establish a framework for mutual recognition;
- To foster and strengthen relations between universities, nuclear research laboratories, industries and regulatory bodies;
- To ensure the quality of nuclear engineering academic education, training and research;
- To create incentives and increase career attractiveness for the enrolment of students and young academics in nuclear disciplines.

5.2 Scope and Framework of the ENEN Association Activities

In order to achieve the objectives, the ENEN Association facilitates exchanges and cooperation among the academia themselves and strengthen their interactions with research centers, thereby assisting them to attract brilliant students by identifying, developing and disseminating new and challenging subjects for research work. Confronted with a lack of interest from students, universities also need to be convinced to recruit new academic members for teaching and research in nuclear disciplines and for maintaining expertise in key nuclear areas. The ENEN Association is therefore developing, promoting and supporting ENEN exchange courses in nuclear disciplines, further by disseminating and supporting the concept of life long learning in the nuclear field, and by facilitating and coordinating the participation of universities to European research projects. The ENEN Association thereby relies on the European Union to promote international cooperation and to support the mobility of teachers, students and researchers, including as well central and Eastern Europe. The European Union provides the architecture for a nuclear "European Research Area" and sets favorable conditions for the creation of added value through university-industry collaborations.

To the benefit of the End-Users, the ENEN Association conserves nuclear knowledge and improves access to expertise by developing and establishing databases, web sites and distance learning tools. In this multinational framework it is mandatory to define the goals and set up the criteria for mutual professional recognition and recruitment throughout the EU. The ENEN Association further provides resources and lecturers for advanced training courses, for professional upgrades and continual training programmes. It has a role as an interface between academia and industries to identify, disseminate and support interesting projects and research topics for internships, master theses and PhDs. With respect to training, the role of the European Union is to provide a framework for quality assurance of advanced courses and professional training programmes through accreditation and ranking. It is expected to construct a nuclear "European Education and Training Area" under competitive conditions of quality and cost and to develop a framework for mutual recognition of professional training, licensing and professional recruitment throughout the European Union.

5.3 Structure and Membership of the ENEN Association

The ENEN Association has two kinds of members. The Effective Members, essentially academia, have a legal status in an EU member or candidate country, provide high level scientific education in the nuclear field in combination with research work, and use selective admission criteria; the Associated Members have a legal status in an EU member or candidate country, have a long term tradition of relations with

effective members in the field of research, training or education and commit themselves to support the ENEN Association.

The ENEN association is managed by a Board of Governors, elected by the General Assembly and the work is organised through a Management Committee. The Management committee is constituted by the Secretary General, appointed by the Board of Governors, and the Chairpersons of the five working committees, which are dedicated to specific tasks, as shown in Table 1. Currently the ENEN Association has 41 members, consisting of 35 universities and 6 research centres, of which 28 are Effective Members and 13 are Associated Members. Without members from the industry and with an overwhelming membership of universities, the ENEN Association seems currently mainly oriented to academic activities. Still, as shown below, the training programmes and courses are well attended by young professionals from nuclear industries.

Advisory Committee	General Assembly Board of Governors			Honorary Members Committee
Management Committee				
		Secretary General		
Chairperson Committee 1	Chairperson Committee 2	Chairperson Committee 3	Chairperson Committee 4	Chairperson Committee 5
Teaching & Academic Affairs Committee 4*+2**	Advanced Courses & Research Committee 3*+2**	Training and Industrial Projects Committee 2*+3**	Quality Assurance Committee 3*+2**	Knowledge Management Committee 3*+2**

* Effective Member ** Associated Member

Table 1. Structure of the ENEN Association

5.4 The ENEN Committees

The work within ENEN is performed by the ENEN Committees. The core of the committees is formed by five to six Effective and Associated members nominated by the Board of Governors. The core calls on any other ENEN member for carrying out specific tasks and producing specific deliverables in the framework of EC supported projects or to fulfil obligations resulting from commitments made by the ENEN Association. The following paragraphs describe the composition, the tasks and some recent achievements of the ENEN Committees.

Teaching and Academic Affairs Committee (TAAC)
TAAC has established and continues to monitor the equivalence and to promote the harmonisation of nuclear engineering education curricula at the ENEN member universities. A reference curriculum consisting of a core package of courses and optional substitute courses in nuclear disciplines has been designed and mutually recognised by the ENEN members. TAAC has designed an information leaflet to attract applications for the ENEN certificate of European Master of Science in Nuclear Engineering (EMSNE). It has developed and implements the bylaws and procedures for receiving and selecting applications and for awarding the EMSNE certificate. TAAC also has the task to promote student and faculty exchanges by encouraging and supporting the organization of international exchange courses and high-quality nuclear engineering courses by the ENEN members. In this framework TAAC produced an information package on 10 established ENEN exchange courses, 23 proposed exchange courses and 5 master thesis projects at ENEN member institutions. In cooperation with the ENEN Quality Assurance Committee, TAAC awards an International ENEN Course Quality label. All information is posted on the ENEN Web site http://www.enen-assoc.org. Other products of TAAC are available on the web site of the 6th Framework project NEPTUNO http://www.sckcen.be/neptuno and include guidelines, best practices and

do-it-yourself kits for the organization of international ENEN exchange courses with examples of flyers and application forms.

Advanced Courses and Research Committee (AC&RC)
The Advanced Courses and Research Committee ensures the link between ENEN members and research laboratories in the European Community. It establishes exchanges with other networks and, through maintaining tight relations with research centres, universities and industry, it identifies and disseminates topics for internships, master theses and PhDs. AC&RC also encourages and supports student mobility. It defines, designs and organizes advanced courses for students, PhD candidates and young professionals. On the basis of a questionnaire, interests for advanced courses have been identified as listed in Table 2.

The AC&RC is also in charge of the organization of 10 advanced training courses for PhD students in the framework of the participation of the ENEN Association to the EU 6th Framework Integrated Project EUROTRANS. This project aims at the design and feasibility assessment of an industrial prototype Accelerator Driven System dedicated to the transmutation of long–lived radioisotopes, mainly actinides, after their partitioning from high level waste streams. Seventeen universities from eight countries are represented by the ENEN Association in this project. The training courses will cover the large variety of research topics addressed by the project. In cooperation with TAAC, AC&RC produced recommendations for the organization of advanced courses, for mentoring PhD students and for continued academic education on an international basis. They are available from http://www.sckcen.be/neptuno.

Training and Industrial Projects Committee (T&IPC)
The Training and Industrial Projects Committee identifies the industrial needs for continued professional development and organizes continuous training sessions and courses on different subjects of common interest for ENEN Associated members, regulator bodies and nuclear industries. T&IPC maintains and disseminates a database on third cycle advanced courses and continued professional development sessions. It facilitates and supports professional training, the mobility of professionals and lecturers, assists in accessing large nuclear infrastructures and integrates European industrial and national projects.

The training courses organised in the framework of the NEPTUNO project are listed in Table 3. Open to students as well as to professionals, they were mainly attended by young professionals from a variety of nuclear industries and regulatory bodies inside and outside the European Union.

Quality Assurance Committee (QAC)
The Quality Assurance Committee develops and implements QA processes to be applied in the design and delivery of education and training courses by the ENEN members. It collects information about rules and practices such as selection, training and certification of teachers and proposes a scheme for their harmonisation. The QAC evaluates and monitors the quality of current and newly proposed members of the ENEN Association according to set of agreed criteria. Following the recommendations issued by the QAC, the Board of Governors proposes new membership applications to the General Assembly. The QAC further evaluates courses and awards the International ENEN Course label, in collaboration with the ENEN TAAC.

Knowledge Management Committee (KMC)
The Knowledge Management Committee identifies and monitors deficiencies in scientific knowledge relevant to nuclear technology and safety. It prepares, maintains and implements an action plan by academia in order to preserve valuable scientific knowledge. The KMC ensures efficient use of ICT for the dissemination of knowledge, for supporting teaching and learning, and for accessing and maintaining databases. It provides access to simulators and specialized software. It further publishes books, and produces CDs and DVDs of interest to ENEN members. The KMC has the task to integrate the current different web sites and to operate them as a single ENEN web site and communication system.

An important achievement made within the 6th Framework NEPTUNO project is the NEPTUNO communication system currently operated by the University of Stuttgart under http://www.neptuno-cs.de. It is in full operation since August 2004 and provides the platform for a common knowledge base for nuclear fission. It merges classical database driven information systems with role-based research and

education functionalities to a common knowledge system.The system is constructed on a framework that uses a LEGO like approach to build web-based knowledge and communication systems for research and training using basic system components. The basic system components are currently customized to the NEPTUNO needs. Each component can be programmed to have access to other components, for example an on-line course can be supported by a simulation package. The system should also provide basic support for communication in the nuclear community like addresses, data bases, technologies, E-learning platforms, etc.

One of the components is a well-documented database on nuclear courses and training sessions. In total more than 700 courses collected from various sources and datasheets are arranged in 4 groups - education, training, education and training, others – and in 14 categories covering different nuclear disciplines. In a restricted area of the system, the courses are submitted for confirmation to the organizing institutions, after which they will be released to the public pages of the system as approved courses. Until now about 200 courses have been approved in this way. The access to the communication system is designed to allow for different users a role- dependent view on a common data base. Views on the database are optimized to respond to the needs of the role, which can be a teacher, a student, a scientist, etc. In this way the knowledge can be more easily managed, preserved and updated. The information is kept in one place with different access methods depending on the goal to be achieved and presented to different users in their different roles in a consistent way.

The communication system intends to support different aspects of Knowledge Management and in particular:

Production of Knowledge

- Provide forms for information input e.g. related to nuclear courses, experimental facilities, knowledge centers, etc.
- Provide tools to store, update, select and visualize documents, reports, tables, presentations, videos, media, etc.
- Accept existing databases for reformatting and reuse of data

Dissemination of Knowledge

- Provide basic tools to support net-based seminars and master theses
- Provide commented hyperlinks to pages in nuclear education and training
- Provide role-based views and access to the content of the system
- Provide reports on selected nuclear applications and fields (e.g. nuclear safety)

Exploitation of Knowledge

- Provide optimized role-based view on the content of the system
- Provide methods to analyze the stored information
- Provide access to consistent and updated information
- Put information into context of specific roles and applications
- Allows to combine information from different sources

5.5 Perspectives for the ENEN Association

Two years after being founded, the ENEN Association has completed a variety of tasks and delivered appreciated products to the European Higher Education and the European Research Areas, as described in the previous paragraphs. The financial support from the EC provided through the NEPTUNO project has been a substantial contribution to reach those achievements. Although the present working field of the ENEN Association started with, and was limited to academic nuclear engineering education, the Association intends to expand and integrate its activities into nuclear disciplines outside nuclear engineering, such as radioprotection, radiochemistry and waste management. The Association also wishes to expand its activities from the academic and research environment into the industrial and regulatory fields and attract the membership of industrial partners and regulatory bodies. Moving out from basic and advanced academic education, the Association intends to define and harmonize for professional training programmes directed to key functions in nuclear industries, regulatory bodies and nuclear applications, and

promote their international mutual recognition. The ENEN association further intends to continue its participation to EC framework projects, in particular in the European Higher Education and European Research Areas. Finally, the ENEN Association will strengthen its cooperation with the World Nuclear University and the regional nuclear education networks in Asia, North America and elsewhere, and continue to promote and support their activities. It will be up to the ENEN Association, its structural bodies, committees and their members to take up this challenging programme, which will significantly contribute to the management of nuclear knowledge within the European Union as well as on a world-wide level.

6. FOLLOW-UP PROJECTS

6.1 NEPTUNO

Within the 6th Euratom research and training programme on nuclear energy (2002-2006), the European Commission supports the project: "Nuclear European Platform of Training and University Organisations, NEPTUNO". 35 partners from industry, training centres, academic institutions and research laboratories participate in it [6].

The ENEN project objective, "to preserve, enhance and strengthen nuclear knowledge", is continued and developed in the NEPTUNO project. However, as the former concentrated on higher education, the latter strives for education and training in the perspective of Continued Professional Development. The rationale is based on internationalisation and globalisation of the nuclear industry and nuclear energy production requesting for mobility, accreditation and recognition of qualified licensed staff. Within NEPTUNO, proposals are formulated for best practices for mobility, accreditation and recognition of qualified licensed staff and in general all staff needing some form of education, schooling or training before operating in the nuclear industry. The ongoing trends towards co-operation between training organisations, research institutes and academia are facilitated. Amongst others, attention is also given to the re-training of trainers and to the modular schemes for staff not requiring the full academic education program, in other words contributing to life-long learning schemes. "Training" is the terminology used in the NEPTUNO initiative to describe the schooling activities other than the regular academic education schemes. The NEPTUNO project strives for training (technicians, engineers) and education (master, PhD, post-doctoral) on equal terms of quality.

6.2 CENETNOM

Recently another project in the 6th Euratom research and training programme on nuclear energy (2002-2006) has been approved, “Consolidation of European Nuclear Education, Training and Knowledge Management, CENETNOM”. The project basically is a follow-up project of the previous ENEN and NEPTUNO, aiming at further implementation of the schemes developed in the two previous projects. At present, the project is in contract negotiation phase. What is notable is that the project received more funding than requested (!), because the European commission consideres the ENEN strategy a reference model for competence management, and has therefore requested the project to be enlarged in order to merge with parallel proposals on education and training in radiation protection and radwaste geological disposal.

7. CONCLUSIONS

In the late nineties, the need to preserve, enhance or strengthen nuclear knowledge was widely recognised. The ENEN association is a bottom-up attempt to remedy these problems. It is a non-profit-making legal association with as main objective to foster high-level nuclear education. It originated as an effort concentrated on higher education in nuclear engineering, but has developed to include also training in the

perspective of Continued Professional Development, and is now extending into other disciplines, i.e., radiation protection.

The present-day reflections on nuclear knowledge management and the different initiatives taken definitely catalyse networking in the nuclear education and training domain. However, the key question still remains: Do we attract more of the better students? Although the process is still in a premature stage to allow solid conclusions to be drawn, preliminary observations indicate a positive evolution, in quantity as well as in quality of students.

Acknowledgements
The contributions to the achievements, as described in this paper, as well as the documents produced by the ENEN Association members and by the other partners of the NEPTUNO project, are gratefully acknowledged. The financial support provided by the EC through the 6th Framework programme, the guidance given and the continuing motivation and confidence expressed by the EC representatives towards the ENEN Association is particularly appreciated.

The ENEN project work was sponsored by the European Commission through contract n° FIR1-CT-2001-80127-ENEN. The NEPTUNO project work was sponsored by the European Commission through contract n° FI6O-CT-2003-508849.

References

[1] EUR 19150 EN, "Strategic issues related to a 6th Euratom Framework Programme (2002-2006)". Scientific and Technical Committee Euratom. p. 14.
[2] ENEN. http://www.sckcen.be/ENEN
[3] ECTS. http://europa.eu.int/comm/education/programmes/socrates/ects_en.html
[4] Eugene Wigner. http://www.reak.bme.hu
[5] The EXTEND school of the CANDIDE EU project (coordinator J. Blomgren).
[6] NEPTUNO. http://www.sckcen.be/NEPTUNO

Curricula

Jan Blomgren obtained his PhD in nuclear physics from Uppsala University, Sweden in 1991. He was a Research Associate at Indiana University, USA, 1992–1993 and Assistant Professor at Stockholm University, Sweden, 1993–1994. Since 1994, he has been at the Department of Neutron Research at Uppsala University, as Assistant Professor 1994–1998, Associate Professor 1998–2003 and Full Professor since 2003. His research areas are neutron-induced nuclear reactions and their applications within energy technology, nuclear waste incineration, cancer therapy and reliability of electronics. His CV contains 170 publications in international journals or papers presented at international conferences, and he is a referee for four international journals. Being the Director of Studies of the Swedish Nuclear Technology Center, he has responsibilities for national coordination of education related to nuclear power.

Frans Moons obtained his electromechanical engineering degree from the Katholieke Universiteit of Leuven in 1973. He started working at the Belgian Nuclear Research Centre as Design Engineer at the BR2 materials testing reactor. From 1983 until 1989, he was seconded to the design team of the Next European Torus (thermonuclear fusion) at Garching, near Munich, Germany. From 1989 until 1998, he worked as a senior scientist on candidate materials for next step fusion machines, co-ordinated the Belgian thermonuclear technology programme, started and built the SCK•CEN corrosion lab, was a member of the EU Fusion Technology Steering Committee and of the OECD Halden Project Program Group (chairman in 1995) and he is still Scientific Secretary to SCK•CEN's external scientific advisory board. Since 1998, he is the research co-ordinator, directly reporting to the general manager. In this
capacity, amongst others, he is responsible for some 20 young researchers preparing doctoral theses at SCK•CEN and co-ordinator of the inter-university programme for Master of Science in Nuclear Engineering.

Peter Paul De Regge obtained a PhD at the State University of Gent, Belgium with a Doctoral Thesis on the Study of (n,p), (n, α) en (n, 2n) reactions in a fission neutron flux spectrum in 1970. He has been in charge for more than 20 years of planning, managing, co-ordinating and supervising scientific services and research activities at the Nuclear Research Centre SCK·CEN in Mol, Belgium. The department of Nuclear Chemistry and Services, which he has been leading for more than 10 years, has long-term commitments to provide analytical and radiochemical services to the Belgian nuclear industry, to the power plant operators and to the Belgian authorities. From 1997 to 2004, he joined the International Atomic Energy Agency in the capacity of Head of the Agency's Physics, Chemistry and Instrumentation Laboratory in Seibersdorf. Starting in May 2004, Peter Paul De Regge is serving the European Nuclear Education Network Association in the capacity of Secretary General.

Joseph Safieh obtained his Master's degree in Nuclear Engineering from the National Institute for Nuclear Sciences and Technology (INSTN) Saclay in 1977. His PhD thesis was devoted to the design, for research reactors, of hot and cold neutron sources facilities. The research work was held in the CEA Saclay centre. From 1983 until 1991, he was in charge of the operation of Ulysse reactor and its education and training activities. From 1991 until 1998, he was the General manager of Ulysse reactor and its training and research activities. Since 1998, as head of the Nuclear Engineering Department he is responsible of the Nuclear Engineering Masters Course of the INSTN (Saclay, Cadarache and Cherbourg). He is also the coordinator of the Nuclear European Platform of Training and University Organisations (NEPTUNO) project within the sixth Euratom research and training programme on nuclear energy.

Appendix XXXIV

Education for the nuclear power industry – Swedish perspective

J. Blomgren[1]

[1]Swedish Nuclear Technology Center and Department of Neutron Research, Uppsala University, Box 525, S – 751 20 Uppsala, Sweden (Jan.Blomgren@tsl.uu.se)

Abstract
In Sweden, about 50 % of the electricity is produced by nuclear power. The nuclear power industry hires about 50 people per year on a masters or PhD level, and engineers on a bachelor's level are hired as reactor operators. Of these, essentially all have their background in other areas than nuclear engineering.

To educate the staff, the nuclear power industry has formed a joint education company, Nuclear Training and Safety Center (KSU). KSU provides education and training programs for all levels of professional skills. Reactor operators undergo an extended training program over many years, where training in simulators constitutes an important part. In addition, courses aiming at a deeper theoretical understanding of reactor physics and thermohydraulics are provided. The latter types of courses are given in collaboration with Uppsala University.

To ensure that nuclear competence will be available also in a long-term perspective, the Swedish nuclear power industry and the Swedish Nuclear Power Inspectorate (SKI) have formed a joint center for support of universities, the Swedish Nuclear Technology Center (SKC). SKC has established collaboration with three Swedish universities, where undergraduate and PhD education is undertaken. Below, the activities of these organizations will be outlined.

Keywords: Nuclear engineering, competence management

1. SWEDISH NUCLEAR POWER – AN INTRODUCTION

About 50 percent of the Swedish electricity is produced by nuclear power. This puts Sweden among the top five countries when it comes to percentage of nuclear power in the electricity production. Counted by installed power per capita, Sweden is the number one nuclear power country in the world.

Twelve light-water reactors were connected to the power grid between 1972 and 1985. Of these, nine boiling water reactors (BWRs) were produced in Sweden and the remaining three reactors are pressurised water reactors (PWRs) originating from the USA.

Nuclear power has had a political dimension in many countries, but Sweden has in some aspects an especially complicated relation between politics and nuclear power. In 1978, a three-party coalition government resigned from office because of disagreement on nuclear power. To my knowledge, this is the only event anytime, anywhere where a government has resigned because of nuclear power.

In 1980, an advisory referendum was held on the future of nuclear power in Sweden, a referendum that can be described as an aftermath of the Three Mile Island (TMI) accident the year before. In this referendum, three alternatives were on the ballot, neither of which indicated operation of nuclear power indefinitely. One alternative was closure within ten years, and the other two, which were to a large degree identical, suggested operation of the already built or planned reactors, i.e., the twelve finally taken into operation, to be run "for their technical lifetime", after which no new reactors should be built. The votes for latter two alternatives were considered merged by the Swedish parliament. The technical lifetime was assumed to be 25 years by the parliament. Since the last reactor should go

critical in 1985, this meant that nuclear power should be phased out by 2010, which was thereby set to be the final date of Swedish nuclear power.

Over time, the perception of nuclear power by the general public has become dramatically more positive. All recent polls indicate that a large majority, 60-80 % of the population, would like to continue running the existing reactors as long as they fulfil the safety criteria. About 20-30 % of the population would prefer new reactors to be built in favour of deployment of fossil fuel-based electricity generation, and only about 20 % would like to see a rapid phase-out of nuclear power [1].

By now, it is clear that the technical life span of these reactors is more than 40 years, and operation for 60 years is seriously considered. With the preset closure in 2010 approaching, it became increasingly clear that a nuclear power phase-out would be very expensive, and it would be detrimental to the environment. This resulted in a new parliamentary decision in 1997 to withdraw 2010 as closing date. Instead, it was decided to close two reactors within two years, not because of safety reasons but to prove that the government was serious in its strive to phase out nuclear power. The remaining ten reactors should be "phased out with even time intervals", but the exact time interval was never defined. In spite of the decision to close two reactors quickly, only one has actually been taken out of operation, although it is kept in such a shape that it can easily be re-started. The other one has been identified, but a condition that the replacement power should not be more costly or cause increased environmental problems has so far lead to repeated postponements of the closure. At present, no date has been fixed.

Recently, the liberal political party has suggested the entire ban on new nuclear power to be lifted, and it has been suggested that installation of new reactors should be investigated. Restart of the already closed reactor was also suggested.

All these political maneuvers have resulted in a situation where nuclear power has for a long time been considered a no-future industry. Not surprisingly, it has not been a prime career choice for young people. As a consequence, the enrolment in nuclear engineering studies has dwindled to very small numbers, and a few years ago, less than ten students in the whole country graduated in nuclear engineering from the technical institutes. This perception has, however, changed dramatically in a rather short time lately. Nuclear power is no longer politically incorrect among young people. On the contrary, it is generally seen as environmentally friendly and economically sound. Moreover, the collapse of the information technology boom in year 2000 has resulted in massive lay-offs from the computer and telecom businesses, which in turn has resulted in that many engineers look for more stable industry jobs. The general perception is that nuclear power is such a safe haven, in spite of the political talk about closure in an undefined future.

These backgrounds are necessary to understand the current situation. For the last twenty years, investments in the reactor park have been hampered by the decision to close them, and the lack of attraction among young people has led to that nuclear engineering has almost vanished from the curriculum of Swedish universities. Because of this, the industry had a difficult time getting its personnel needs satisfied by the universities. Instead, the industry had to hire other types of engineers, often relatively mature in age, and to educate them at work.

2. TRAINING AND EDUCATION IN THE INDUSTRY

The Swedish nuclear power industry employs 30-50 new people per year for duties where knowledge of nuclear physics and engineering is required. Of these, only a minor fraction (less than 10 %) has reactor physics or engineering in their curriculum. The vast majority have engineering degrees with specialization in other fields, with electrical engineering, machine technology and engineering physics being the most common.

This category can roughly be divided into two subgroups, operators and others. A majority of the reactor operators today have high-school education only. There is, however, a strong trend that the newly employed operation staff typically has a three-year engineering education beyond high school, i.e., corresponding to a bachelor's level degree. There is a many-year career track to become an operator. A period of at least three but typically five years as general technical support at the power plant is required before education to become an operator is initiated. During this first phase, the staff undergoes an education programme of typically two years. For promotion to operator, an additional

education programme of one year is mandatory. There are, however, two categories of operators, turbine and reactor operators. These fulfil different duties in the control room during regular operation, and are recognized as different positions. The turbine operator education always comes first and some continue to the second step to become reactor operator. Each of these two levels requires one year full-time education.

This education is composed of regular teaching as well as training in simulators. For all reactors, there are corresponding simulators. Until a few years ago, the simulators were located at the Studsvik site south of Stockholm, which then served as a central hub in the education. Recently, most of the simulators have been moved to the power production sites to increase the accessibility for the personnel.

Finally, there is an educational programme to become operative leader of the production (shift manager), which comprises about half a year. This programme is mostly focused on leadership aspects, organization, etc., but it also involves some technical education.

It is required by the nuclear power inspectorate that an operator undergoes education and training of at least ten days per year, whereof simulator training for at least five days per year. It is not uncommon that a person has dual competence, e.g., both as reactor and turbine operator, and therefore has to spend twice this time per year in simulator training. In reality, personnel with only a single competence, i.e., as turbine operator, nevertheless spends ten days on training.

In addition to the simulator training and the education targeting direct aspects of daily operation, there is teaching on more fundamental understanding of the underlying physics of reactors. The TMI accident in 1979 was the starting point for this type of education. It was a general conclusion that part of the reason for the TMI accident was inadequate education of the staff. They lacked a general understanding of the physics of reactors, which made them poorly suited to handle a situation far from the standard drift scenarios. The Chernobyl accident seven years later further stressed the need for education of the operational personnel, beyond training.

Besides reactor operators, there is a large category working with tasks that require advanced knowledge of reactors for purposes then direct operation. Good examples are core and drift planning, i.e., core simulations to optimise the use of fuel, and staff involved in reactor instrumentation. They do not undergo simulator training, but need general reactor physics and technology, often beyond the needs of operators. In contrast to the operators, which have many years of employment and significant practical experience before going to general reactor physics, the latter category need this education at the beginning of their employment.

To meet the educational demands, the power utilities have jointly formed a dedicated education company, called Nuclear Safety and Training Centre (KärnkraftSäkerhet och Utbildning AB in Swedish, abbreviated KSU) [2]. KSU is owned by the utilities with proportions roughly corresponding the share of the total nuclear electricity production. The company is non-profit in the sense that the employers are charged for the course participation of their staff, such that KSU neither makes profit nor loss when integrated over a few years. Due to this construction, the KSU courses are open to participants also from non-owner organizations, because the fees are set to cover the full costs for the education.

KSU owns and operates the simulators, and provides the regular teaching near practical operation. The courses on general understanding of reactor-relevant physics, from hereby referred to as higher education, is provided by the Department of Neutron Research (Institutionen för neutronforskning, INF) of Uppsala University [3]. This cooperation is based on a six-year contract, where KSU grants a fixed support to INF, and in return KSU can demand a specified teaching volume.

3. EDUCATION AT UNIVERSITIES

Until only a few years ago, nuclear engineering education and research were undertaken at two universities only, the Chalmers Institute of Technology (CTH) in Gothenburg [4] and the Royal Institute of Technology (KTH) in Stockholm [5]. Chalmers has two chairs, one in reactor physics and one in nuclear chemistry directed towards partitioning (separation of spent fuel). KTH had four chairs,

in reactor physics, nuclear chemistry directed towards geological repositories, nuclear engineering and nuclear power safety. All these professors were scheduled for retirement at about the same time a few years ago, and the prospects of replacement were not very positive.

To promote long-term sustainability of reactor-relevant research and education at Swedish universities, the Swedish Centre for Nuclear Technology (Svenskt Kärntekniskt Centrum, SKC) has recently been established [6]. The center is financed by the power plants in proportion to installed power, with added contributions from Westinghouse (Nuclear Fuel production in Västerås) and the Swedish Nuclear Power Inspectorate (Statens KärnkraftInspektion, SKI), i.e., the governmental regulatory body [7].

The fact that the inspectorate contributes might call for an explanation. There is a long-term tradition in Sweden that the inspectorate primarily acts proactively. Thus, instead of just inspecting and handling the judicial aspects after possible incidents, the inspectorate involves itself in a continuing discussion with industry with the aim to guarantee or even raise the security. The inspectorate has a mission issued by the political sphere to promote nuclear security. This has been interpreted to also encompass support to education and research, because such activities are viewed as crucial to uphold a high security standard. Thus, SKI finances about one third of SKC.

SKC has long-term collaboration agreements with three universities, the Royal Institute of Technology (Kungliga Tekniska Högskolan, KTH) in Stockholm, Chalmers Institute of Technology (Chalmers Tekniska Högskola, CTH) and Uppsala University (UU). As part of these agreements, the universities have committed themselves to open reactor-relevant positions, which are then financially supported by SKC. In addition, SKC supports research projects where scientists of any university can apply. Besides projects on reactor technology in traditional sense, SKC also supports reactor-relevant research in areas like materials science (properties of zircalloy, quantum mechanical modelling of neutron-induced materials damage), chemistry (iodine chemistry in severe accidents) and man-machine-organization interface problems.

These long-term collaboration agreements have resulted in that the chairs above will all continue. Without this support, it is likely that very little activities – if any – would have prevailed. Moreover, nuclear power relevant education and research has recently been established at Uppsala University, which has very little previous tradition in the field.

Recently, SKC has initiated a graduate school on nuclear power technology. The background is that the limited enrolment in PhD studies at Swedish universities makes it difficult to uphold a large volume of courses for the PhD students at each university. Instead, courses are re-organized in such a way that students from all universities can attend them. This means in reality that courses have to be concentrated in time, like summer schools. A typical course is therefore organized with full-time teaching for about a week. For a longer course, there could be several separate study weeks.

This type of organization makes the courses suited also for foreign participants. Since the studies are concentrated in time, essentially any student in Europe can attend them. It is notable that at about the time SKC initiated the new organization of its PhD courses, a similar activity began in the entire EU. A large number of European universities have recently formed the European Nuclear Education Network, ENEN [8]. The driving force behind ENEN has been to re-organize nuclear engineering education in Europe to increase the attraction in nuclear engineering careers. Part of the work has been spent on providing courses with a structure similar to the SKC courses, i.e., concentrated in time to allow participation from more than the local students. With the fairly short travel time and modest travel costs in Europe, such an organization can facilitate a significantly increased total education volume, combined with an improved quality. The ENEN initiative is described in detail in a separate contribution to these proceedings, and is therefore not described further here.

One particular aspect needed to understand the structure of the research and education is the absence of research institutes. Besides the Swedish Defence Research Agency, there are essentially no research institutes in Sweden. Instead, industry-oriented research is either carried out in industry itself or at the universities.

A consequence of this strategy is that only a minor fraction of the industry-oriented research at Swedish universities is financed by government grants. Instead, the large majority is financed by external industry grants to the universities, and nuclear engineering is no exception from this rule. In

fact, essentially all the research and PhD education is financed via industry grants. Only the undergraduate education is to a significant degree government-funded, but this is also a truth with qualification. There is a system to finance teaching that barely covers the costs for the actual teaching, but if no other funding was at hand, the teacher would have to work full time on teaching only just to cover the own salary costs. In reality, this would be impossible because it is out of question to fill the agenda so efficiently. Therefore, some additional funding must be present just to have the teaching capability available, and this is possible thanks to the industry support.

4. SYNERGY EFFECTS

With the organization outlined above, it has been possible to achieve a fairly efficient utilization of limited resources, especially when two organizations collaborate.

As has been described above, the KSU courses for industry personnel have been designed for newly employed personnel. A pre-requisite for such courses to be useful for the industry is that they are concentrated in time. This requirement, however, also makes them well suited for PhD students. Accordingly, an agreement has been reached between KSU and SKC that whenever there are free seats available during a KSU course, PhD students from any Swedish university can participate. This has resulted in a marked increase in the total course volume. Moreover, the fact that course participants come from different backgrounds have resulted in increased student activity in the courses, simply because of the need to explain various concepts across professional barriers, and because questions are being asked from a wider range of perspectives.

Up to now, this collaboration has been established in general courses on nuclear power technology for newly employed industry personnel. The content of these courses is essentially basic reactor physics and thermo-hydraulics, with moments of nuclear power safety. Thus, these courses are giving a broad introduction to nuclear power, but they do not go deeply into the subject. Thereby, they are useful to PhD students working in areas related to nuclear power, but where the focus is not on reactor technology. A good example is nuclear chemists working with partitioning. For them, a broad view of nuclear power is useful to put their work into a larger perspective, but their cutting edge knowledge has to be in chemistry. Other examples are nuclear physicists, PhD students working with reactor applications like neutron scattering for materials investigations, boron-neutron capture therapy (BNCT), etc.

This student category is fairly large. In loose terms, it comprises about 50 PhD students in Sweden. For the students in more reactor-oriented research, however, these courses are not sufficiently deep. Therefore, more specialized courses have to be taught. Recently, an example of synergy effects also in more specialized education has materialized. A two-week course on probabilistic safety analysis (PSA) will take place during autumn 2004, where about half the participants come from academia and half from industry and the regulatory body. The course is provided by a commercial company that performs PSA studies on demand. Neither participant category is sufficiently large to carry the costs for such a course, but by joining forces, the total number of participants is sufficiently large to make the cost per participant realistic.

Recently, the cross-disciplinary collaboration has been taken a step further. As described above, in the introductory KSU industry-oriented courses above, PhD students have been accepted as participants for a few years. Since these courses are nowadays taught at a university, they are now available also to undergraduate students. For simple geographic reasons, up to now mostly local students have taken the chance to follow the course whenever there are available seats. This has resulted in a number of new aspects of this teaching. First and foremost, this has allowed an expansion of the total volume of nuclear power education at a university hitherto not involved in the field. Because of this teaching, a faculty staff of five young professors has emanated, and suitable teaching material has been developed. This has opened new opportunities for other courses, targeting undergraduate education on nuclear engineering. Second, it has rapidly become popular among undergraduate students to follow these courses because of the unusual format. The students strongly appreciate the presence of industry personnel, because they benefit from their knowledge, and it makes the education feel more realistic. A common student complaint on undergraduate education is that it is poorly linked to industrial reality. Therefore, taking a course originally intended and designed for industry and where half the participants work in industry is perceived as an utterly positive experience.

5. OUTLOOK

Sweden is a country with a small population on a relatively large area. This has to a considerable degree prompted the solution that courses within a relatively small subject, like advanced nuclear engineering, are organized in such a way that students and teachers meet full time during a relatively short period (one or a few study periods of 1-2 weeks each). With such an organisation, the education is already well suited for integration into a larger European perspective. The time and cost to travel is not dramatically different within Sweden and within Europe. Belgium has already re-organized its nuclear engineering education with a similar course structure, however for other reasons [9]. Moreover, in Belgium this has also been done for undergraduate education. Within ENEN, similar organisational changes are underway in many European countries. Recently, a similar harmonisation process has been initiated on industrial training via the NEPTUNO project [10].

We are presently facing a major change of the educational system in many European countries through the Bologna process. There is an ongoing process to harmonize essentially all European university education system into a 3+2+3 year education system. In this system, three years should be mandatory to obtain a bachelor's degree. A two-year addition would then result in a master's degree, followed by three years of research to get a PhD. In this report, I have distinguished undergraduate engineering courses and PhD student studies, but in a few years, this will no longer be a valid distinction. Instead, we are entering a situation where what today is last-year specialization undergraduate courses and PhD courses will become the same, i.e., part of the master's programmes. Referring to the discussion above, this means that ENEN can have a large impact on the master's education level.

I believe it is possible that nuclear engineering education can increase both in popularity and quality, even in a short time perspective. Even if that happens, however, I do not foresee that this will lead to that industry can fill even half their vacant employment positions with well-educated nuclear engineers or doctors. Nuclear power is nowadays a mature technology, and in all mature technologies the required competence is primarily built by hiring people with general technology skills, and then educate them for their particular duties through training programs. This has long been the situation in the paper and pulp industry, in forestry, mining, etc., i.e., mature industries. Because of this, training and education in industry is not likely to diminish even if the undergraduate education situation improves.

Sweden is such a small country that we simply cannot afford duplication in the long run. In this report, I have given a few examples of how synergy effects have been possible to achieve through cross-disciplinary activities during the last few years. I do not believe that all possibilities of collaboration for clever use of resources have been exhausted. On the contrary, I foresee increased synergetic activities. Last but not least, it should be stressed that efficient use of resources is not the only benefit that can be obtained through cross-disciplinary initiatives. Such approaches are also important because they have a potential to improve the quality. When people from various environments meet, new challenges and opportunities emanate, and this provides – more or less intrinsically – quality assurance.

References

[1] See, e.g., http://www.analys.se/engsite/engopin.html
[2] KSU. www.ksu.se
[3] Department of neutron research, Uppsala University. www.inf.uu.se
[4] Department of reactor physics, Chalmers Institute of Technology, Gothenburg. www.nephy.chalmers.se
[5] Department of nuclear and reactor physics, Royal Institute of Technology, Stockholm. www.neutron.kth.se
[6] Swedish Centre for Nuclear Technology, www.nuclear-tech-centre.org
[7] Swedish Nuclear Power Inspectorate, www.ski.se
[8] ENEN. http://www.sckcen.be/ENEN
[9] BNEN. http://www.sckcen.be/BNEN
[10] NEPTUNO. http://www.sckcen.be/NEPTUNO

Curriculum

Jan Blomgren obtained his PhD in nuclear physics from Uppsala University, Sweden in 1991. He was a Research Associate at Indiana University, USA, 1992–1993 and Assistant Professor at Stockholm University, Sweden, 1993–1994. Since 1994, he has been at the Department of Neutron Research at Uppsala University, as Assistant Professor 1994–1998, Associate Professor 1998–2003 and Full Professor since 2003. His research areas are neutron-induced nuclear reactions and their applications within energy technology, nuclear waste incineration, cancer therapy and reliability of electronics. His CV contains 170 publications in international journals or papers presented at international conferences, and he is a referee for four international journals. Being the Director of Studies of the Swedish Nuclear Technology Center, he has responsibilities for national coordination of education related to nuclear power.

Using spreadsheets to promote student understanding of dynamic systems.

Michael Österlund

Department of Neutron Research, Uppsala University, Box 525, SE-75120 Uppsala, Sweden (michael.osterlund@tsl.uu.se)

Abstract
There is a universal need for engineers to understand dynamic physical systems and being able to determine the outcome of such systems. In order to overcome the limitations sometimes imposed by the mathematical skills of undergraduate students, different softwares for simulation of dynamical systems are available. One often-overlooked alternative is to use commonly available spreadsheet programs.

A specific example is provided from the training of nuclear reactor staff. The training involves the use of multi-million dollar simulators with very accurate models of the nuclear reactor process. However, it is not feasible to use such simulators to study the underlying fundamental processes. In order to help students to obtain an understanding of the basic principles, simple spreadsheet simulations that illustrate different aspects of the nuclear reactor process are very useful.

Using examples from courses in mechanics, electricity and reactor physics, it is shown how Excel can be used as a tool for the solution of dynamic problems. On the lowest level of complexity, calculations can be performed using worksheet functions only. On a slightly higher level of complexity, it is shown how VBA (Visual Basic for Applications) components can be incorporated into spreadsheets in order to enhance their functionality and capability.

Keywords: dynamic simulation, Excel, spreadsheets, reactor physics

1. INTRODUCTION

Simulations and simulators are commonly used for the training of personnel required to operate complicated dynamic systems such as aircraft, ships and nuclear power plants. It is recognized that simulations allows the student of such a system to acquire an accurate mental model of the system and to become proficient in its operation. Simulators also provide a safe environment where accidents can be simulated and emergency procedures practiced.

For students of physics and engineering there is a universal need to understand the basic principles governing dynamic, i.e., time-dependent physical systems and being able to determine the outcome of such systems. For this purpose, simulations on a much smaller scale can provide a useful means of promoting the understanding of basic physical principles. It is important to emphasize that in most cases, these simulations cannot stand on their own. The simulations need to be accompanied by introductory presentations of the concepts.

Given the constraints sometimes imposed by the mathematical skills of students, different softwares that facilitate the modeling and simulation of dynamical systems have been developed. One often-overlooked alternative to these softwares is to use commonly available spreadsheet programs, e.g., Microsoft Excel. The first spreadsheet program, VisiCalc by Dan Bricklin and Bob Frankston, was released to the public in 1979. The concept of a computerized accountant's grid where one could change the content of any cell, and the entire spreadsheet would be automatically recalculated, quickly caught on and spreadsheet programs such as VisiCalc, Multiplan, Lotus 1-2-3 and Microsoft Excel became the most commonly used tools for accounting and financial calculations. Today Microsoft Excel, which remains true to the original concept of the accountant's grid, has evolved into a powerful mathematical software that is of use in almost all field of science and technology. Most physics teachers have probably at times used a spreadsheet program in order to make tables and graphs of data

points. The power of spreadsheet programs, however, extends far beyond these simple tasks. Although spreadsheet programs are probably not the ideal solution for any given problem, they have advantages that in many cases far outweighs the limitations:

- Spreadsheet programs do not have the steep learning curve of other more complex, and possibly more capable, software for mathematical calculations. Once the concepts of the grid and formulas have been grasped, students are ready to use the spreadsheet program.
- Modern spreadsheet programs combine powerful calculation capabilities with a very useful graphing feature, which is extremely important for visualization of mathematical and physical relationships.
- A spreadsheet program is almost always included in software bundles installed on personal computers making it easily accessible to students everywhere.

From a science education point of view spreadsheet programs can be used for many different purposes such as calculations, visualizations and also simulations of dynamic systems. Drawing from undergraduate courses in electricity, mechanics [1] and nuclear engineering, examples of the use of spreadsheets are given below.

2 CALCULATION AND VISUALISATION

2.1 AC-circuits and phasors

Spreadsheet programs are well suited for the visualization of different concepts. As an example, when dealing with AC circuits in basic electrical engineering courses, the concept of phasors is introduced in order to visualize the phase difference between voltages and currents. Often the phasors are presented in a *static* figure next to a graph displaying sinusoidal voltages or currents with a phase shift with respect to each other. As an alternative the same figure can be made dynamically displayed using Microsoft Excel, see figure 1.

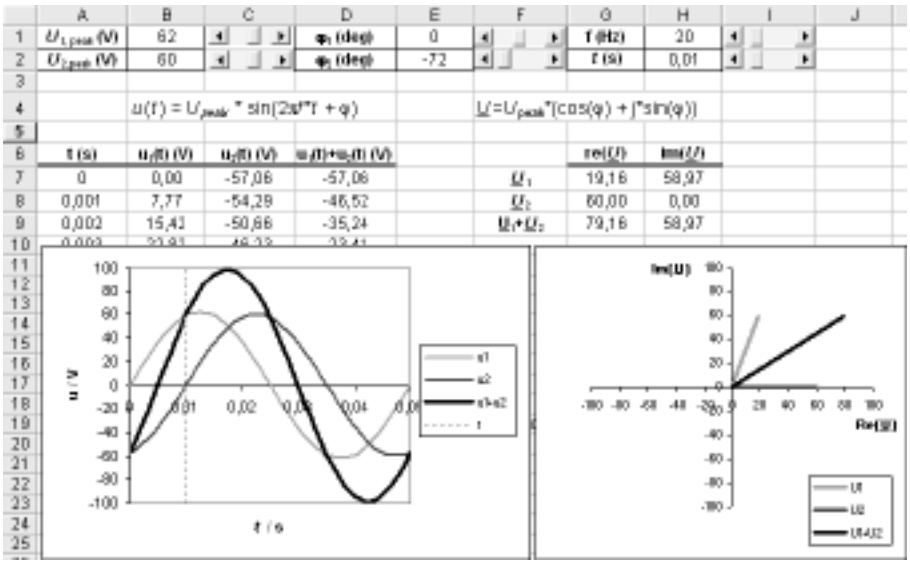

Figure 1. Example of visualization of phasors in AC circuits applications.

In the first two rows of the spreadsheet, parameters for two sinusoidal voltages are set. Columns B, C and D are used to calculate the instantaneous voltages and their sum as a function of time. The voltages are displayed in the leftmost graph in figure 1. In the rightmost graph of figure 1, the corresponding phasors are plotted in a "scatter graph" where each phasor is defined by two points, the origin (0,0) and (Re(U),Im(U)). The latter values are calculated in cells G7:H9, e.g,

=B3*COS(2*PI()*H3*H4+E3*PI()/180) and
=B3*SIN(2*PI()*H3*H4+E3*PI()/180) in cells G7 and H7 respectively.

In order to visualize the concept of phasors it is important that the spreadsheet is made interactive and that students can vary parameter values easily. In cell H2 in figure 1, the time for which the phasors are plotted can be adjusted at will in order to see the effect it has on the phasors. The time at which the phasors are plotted are

displayed in the leftmost diagram in figure 1 as a dashed vertical line. This is in contrast to the static view depicted in most textbooks where only the situation at $t = 0$ is displayed. By varying the time t students can get an understanding for what phasors represents, i.e., a snapshot in time with the length of the phasors representing amplitudes, the relative angles representing phase differences and the projection of phasors on the imaginary axis representing instantaneous voltages.

2.2 The use of scrollbars to adjust parameter values.

Preferably visualizations should involve instant updates of calculated values and diagrams. This is easily accomplished by the use of scrollbars, which are a feature of Excel. The scrollbar tool is available in the [View] [Toolbars] [Control Toolbar] menu, figure 2. In order to define the range of the scrollbar and which cell it should be linked to, the Visual Basic for Applications (VBA) editor must be invoked by double-clicking on the scrollbar itself. The range of the scrollbar is limited to integer values, but this limitation can be overcome by defining the methods _Scroll() and _Change() in the VBA editor, figure 3. It is worth noting that in order to make the spreadsheet respond immediately to movements of the scrollbar slider only the _Scroll() method need to be defined. The _Change() method allows incremental adjustments by clicking on the arrows of the scrollbar.

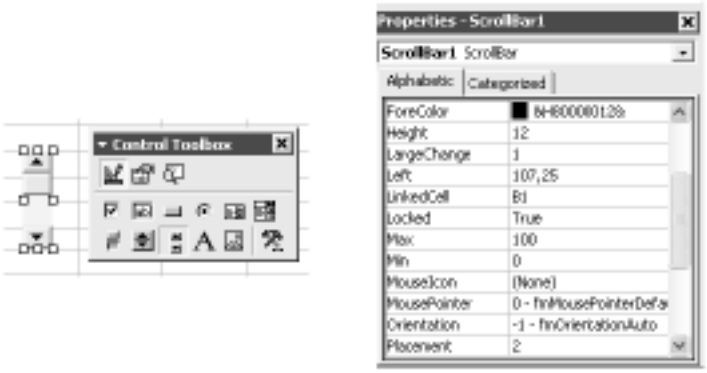

Figure 2. Scrollbars are created using the scrollbar tool in the Control Toolbox. The properties of the scrollbar are set in a properties window available in the Excel VBA editor. The editor is invoked simply by double-clicking on the scrollbar or by pressing [Alt]+[F11]. In the figure the linked cell is B3 and the range is 0 – 100.

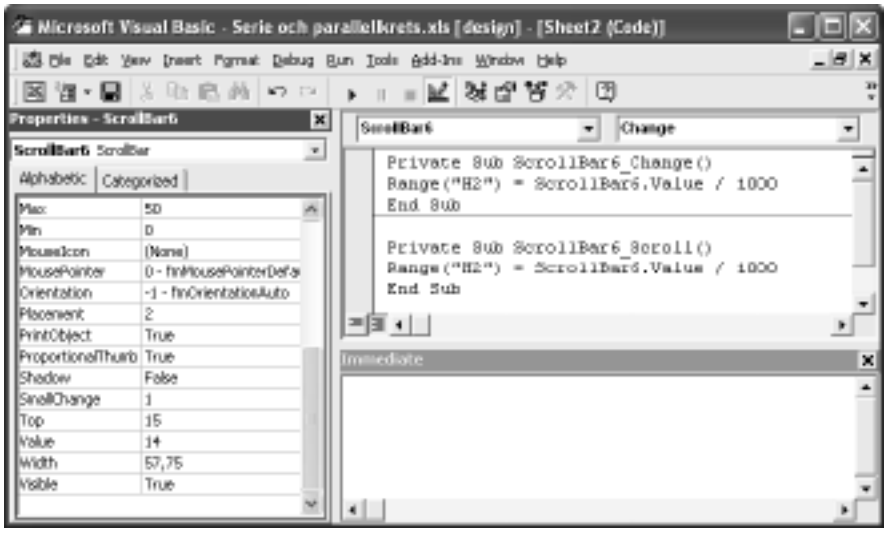

Figure 3. The range of a scrollbar is limited to integer numbers. In order to overcome this limitation the _Scroll and _Change methods can be used to define the action of a scrollbar. In the figure the range of the scrollbar is 0 – 50 and this value divided by 1000 is transferred to cell H2.

3 COMPLEX NUMBERS

Excel provides a number of functions that are useful for students of physics and science in general, e.g., functions to handle complex numbers, matrix calculations and fast Fourier transforms. As an example of the use of complex numbers, a calculation of the impedance and current of a series AC-circuit with a resistance, an inductor and a capacitor is displayed in figure 4.

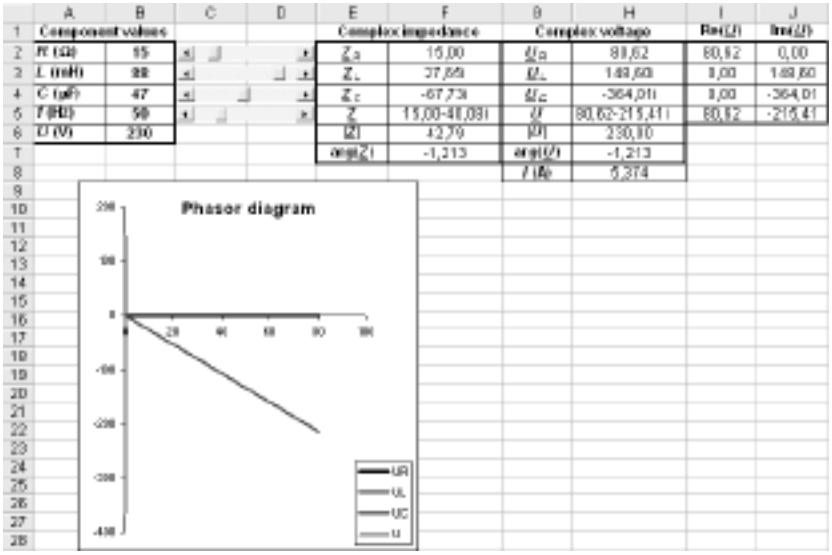

Figure 4. Calculation of impedances and voltages and current in a simple series AC circuit by means of complex numbers. The calculated voltages are displayed in a phasor diagram with the current aligned along the positive real axis.

In the example scrollbars are again used to simplify adjustments of parameter values. Calculations are performed using the complex functions available in Excel, e.g. the complex impedance and voltage of the capacitor are calculated in cells F4 and H4 using the formulas = COMPLEX(0;1/(-2*PI()*B5*B4/1000000)) and = IMPRODUCT(H8;F4) respectively.

4 DYNAMIC SIMULATIONS

The simulation of a dynamic system involves the solution of differential equations. Spreadsheet programs are well suited for the purpose of solving various problems involving ordinary differential equations by means of the Euler method

$$y_{n+1} \approx y_n + h \cdot f(x_n, y_n), \tag{1}$$

which advances the stepwise solution of an ordinary differential equation from x_n to $x_{n+1} = x_n + h$ [2]. At the expense of simplicity it is of course possible to use other solutions methods such as Runge-Kutta.

4.1 Projectile motion with air resistance and Magnus force

Projectile motion is part of the curriculum of most basic physics courses. In most cases the treatment is limited to an idealized case where the influence of air resistance is neglected. Students are, however, aware that air resistance plays an important role and thus, in order to make the connection between the physical model and real world situations, the drag force should be included in the model. Also, in many cases, e.g., golf and baseball, the rotational motion of the object gives rise to the Magnus force that tends to deviate the flight path.

It can be assumed that the Magnus force is proportional to the angular velocity ω and the speed of the projectile v,

$$F_{Magnus} = k|v|\omega. \tag{2}$$

The air resistance of the projectile is considered to be proportional to v^2 [3]

$$F_D = \frac{1}{2}\rho v^2 S C_D, \tag{3}$$

where ρ is the density of the medium and S the cross-section area of the projectile.

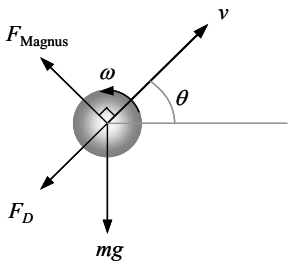

Figure 5. Forces acting on a projectile moving with speed v through a medium, while rotating with an angular speed ω.

With reference to figure 5 and Equations (2) and (3), the motion of a projectile of mass m and drag coefficient C_D, ejected at an elevation angle θ is thus described by

$$\begin{cases} m\dfrac{dv_x}{dt} = -F_D\cos\theta - F_{Magnus}\sin\theta \\ m\dfrac{dv_y}{dt} = -mg - F_D\sin\theta + F_{Magnus}\cos\theta. \end{cases} \tag{4}$$

Using finite differences the equations can be approximated by

$$\begin{cases} \Delta v_x \approx \left(-\dfrac{1}{m}\cdot F_D\cos\theta - F_{Magnus}\sin\theta\right)\cdot\Delta t \\ \Delta v_y \approx \left(-g - \dfrac{1}{m}\cdot F_D\sin\theta + F_{Magnus}\cos\theta\right)\cdot\Delta t. \end{cases} \tag{5}$$

Using Euler's method, Equation (1), the velocity components of the projectile can be calculated in a spreadsheet with each row representing one step forward in time in order to simulate the projectile motion, figure 6.

	A	B	C	D	E	F	G	H	I	J
1	t (s)	x (m)	y (m)	θ (rad)	F_{drag} (N)	F_{Magnus} (N)	v_x (m/s)	v_y (m/s)	a_x (m/s²)	a_y (m/s²)
2	0,000	0,000	0,000	0,6106	0,427	0,389	32,77	22,93	-12,66	-8,18
3	0,025	0,819	0,573	0,6109	0,419	0,386	32,46	22,73	-12,47	-8,15
4	0,050	1,631	1,142	0,6112	0,411	0,382	32,15	22,52	-12,28	-8,12
5	0,075	2,434	1,705	0,6115	0,403	0,378	31,84	22,32	-12,10	-8,09
6	0,100	3,230	2,263	0,6117	0,396	0,374	31,54	22,12	-11,91	-8,06
7	0,125	4,019	2,816	0,6119	0,389	0,371	31,24	21,92	-11,74	-8,03

Figure 6. Spreadsheet for the simulation of projectile motion with air resistance.

The result of the simulation is displayed in a separate worksheet where scrollbars are used to vary projectile parameters, figure 7. One commonly occurring task is to determine the outcome of the simulation, e.g., the time-of-flight and range of the projectile. In the spreadsheet the simulation is continued well beyond the point where the projectile has returned to its original height above ground. In order to look up at which time the projectile returns to ground, i.e., the time of flight until $y = y_{\text{initial}}$, an array formula must be used in Excel. An array formula is like an ordinary formula except that it operates on a range of cells instead of individual cells. It is entered by pressing [Ctrl]+[Shift]+[Enter]. With reference to figure 6, the array formula to determine the time-of-flight is {=INDEX(A3:A402;MATCH(MIN(ABS(C3:C402-0));C3:C402;-1);0)}. Similarly the formula for determining the range is {=INDEX(B3:B402;MATCH(MIN(ABS(C3:C402-0));C3:C402;-1);0)}.

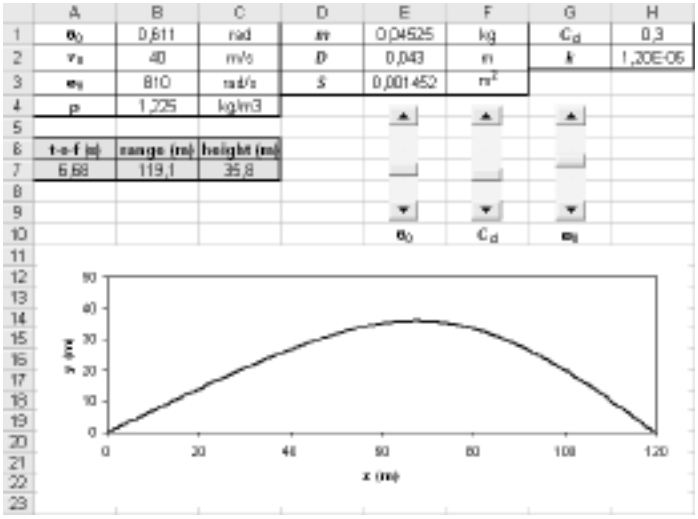

Figure 7. Worksheet displaying the result of the simulation of the motion of a golf ball. Scrollbars are used to vary the elevation angle θ, the drag coeffiecient C_D and the angular velocity of the ball ω_0.

4.2 Natural circulation cooldown in a PWR-type reactor

In pressurized water nuclear reactors (PWR) the coolant water is circulated in a primary-coolant circuit consisting of the reactor core (hot leg) and steam generators (cold leg) by means of recirculation pumps. In the steam generator heat is transferred from the primary coolant to a secondary system involving a steam cycle, usually a steam turbine and a condenser.

In the event of a recirculation pump failure, an emergency stop (scram) is initiated to stop the fission process. Even after the scram, decaying fission products in the nuclear fuel will release significant amounts of decay heat to the coolant. If a temperature difference is maintained between the hot and cold legs of the primary coolant circuit, the resulting difference in density between the two areas will give rise to a thermal driving pressure causing a natural circulation flow to be established. The thermal driving pressure is balanced against the total pressure drops associated with the fluid flow in the primary coolants system.

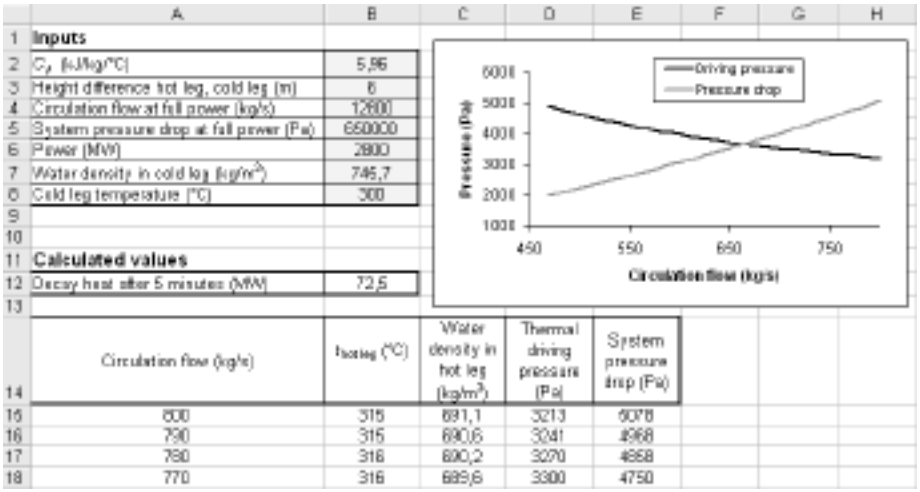

Figure 8. Worksheet for the simulation of natural circulation flow in a PWR nuclear reactor following a pump failure. In this case, using typical PWR data, the natural circulation flow 5 minutes after a scram will be $\dot{m} = 660$ kg/s.

In order to determine the resulting natural circulation flow rate with the thermal driving pressure balancing the total pressure drop of the primary coolant system an iterative approach is used, figure 8:

1. Calculate the decay heat.
2. Choose an initial value for the mass flow rate $\dot{m}$.
3. Calculate the temperature of the water exiting the reactor core using

$$T_{\text{hot leg}} = T_{\text{cold leg}} + \frac{\dot{Q}}{\dot{m} \cdot c_p}. \tag{6}$$

4. Calculate the density of the water exiting the reactor core, $\rho = f(p,T)$ [4].
5. Calculate the thermal driving pressure

$$\Delta p_{\text{driving}} = \left(\rho_{\text{hot leg}} - \rho_{\text{cold leg}}\right) g h \,. \tag{7}$$

6. Using the Darcy-Weisbach equation for fluid flow it can be shown that the total pressure drop due to friction is proportional to $\dot{m}^{1.75}$,

$$\Delta p_{\text{total}}(\dot{m}) \approx \Delta p_{\text{total}}(\dot{m}_0) \cdot \left(\frac{\dot{m}}{\dot{m}_0}\right)^{1.75}. \tag{8}$$

7. If $\Delta p_{\text{driving}} > \Delta p_{\text{total}}$ increment the mass flow rate $\dot{m}$ and repeat from step 3, otherwise stop.

4.2 Xenon poisoning in a nuclear reactor

When the first reactor with higher power, the "Pile B" in Hanford, WA, was started on September 26, 1944, the researchers came across a phenomenon that is today known as xenon poisoning. A few hours after the first start-up, the reactor stopped unexpectedly. The following day it started without any external intervention but after a few hours it stopped again. It turned out that the isotope Xe-135, which has the highest neutron absorbing ability of all the known nuclides, was created when running the reactor. When the concentration of Xe-135 became high enough, the resulting reduction in neutron flux caused the reactor to become subcritical.

In modern reactors xenon poisoning is a well-known effect that plays an important role from an operational point-of-view. All changes in reactor power and neutron flux will have an influence on the concentration and rate-of-change of Xe-135. The negative contribution to the total reactivity of the reactor from Xe-135 must be constantly predicted and corrected for when making reactivity changes to the reactor. For example, after a power increase, the Xe-135 concentration will initially decrease. If this is not taken into account, the power increase will become bigger than anticipated. The concentration will reach a minimum some hours after the power increase and then increase to a new, higher equilibrium value.

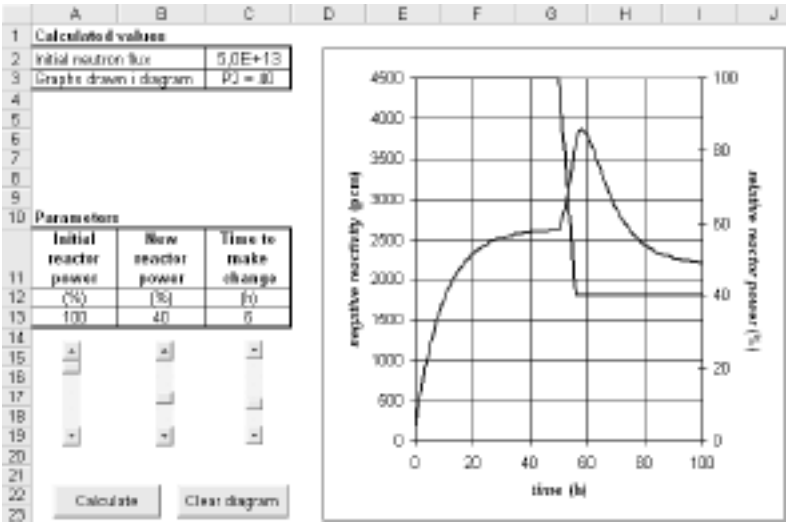

Figure 9. Simulation of Xe-135 concentration, expressed in terms of negative reactivity, in a typical reactor core. Approximately 2 days after the start of the reactor the Xe-135 concentration has reached an equilibrium level. A decrease in reactor power from 100% to 40% over a period of 6 hours creates a peak in the Xe-135 concentration that occurs approximately 8 h after the change was initiated. Approximately 2 days after the change a new, lower equilibrium level is reached

In the operation of a nuclear reactor an equilibrium concentration of both Xe-135 and I-135 is reached as a result of competing processes. Xe-135 is produced directly as a fission product and indirectly following the β-decay of another fission product, I-135, that has a half-life of 6.7 h. The production rate of xenon is proportional to the neutron flux and also the amount of I-135 present in the fuel. Xe-135 is removed from the reactor core by two processes, radioactive decay and neutron capture. The radioactive decay rate is proportional to the amount of Xe-135 present. Neutron capture converts Xe-135 to Xe-136, which has a low absorption cross-section. In this way Xe-135 can be "burned away" at a rate proportional to the neutron flux in the reactor. The rate of change of xenon concentration is expressed by the following equations,

$$\begin{cases} \dfrac{dN_{Xe}}{dt} = \lambda_I \cdot N_I + \gamma_{Xe} \cdot \Sigma_f \cdot \phi - \lambda_{Xe} \cdot N_{Xe} - N_{Xe} \cdot \sigma_{a,Xe} \cdot \phi \\ \dfrac{dN_I}{dt} = \gamma_I \cdot \Sigma_f \cdot \phi - \lambda_I \cdot N_I, \end{cases} \tag{9}$$

where λ is the decay constant, γ the fission yield, Σ_f the macroscopic fission cross-section for U-235 and ϕ the neutron flux in the reactor core. The equations can be solved using Euler's method in a spreadsheet, figure 9.

Although the calculations can be done directly in the spreadsheet grid, in this case the calculations are performed in VBA, figure 10. The advantage of using VBA for this purpose is that the resulting spreadsheet can be kept clean, only the data of interest for the students are shown. Compared to in-line formulas in worksheet cells, the VBA-code can be made much more complex while maintaining readability.

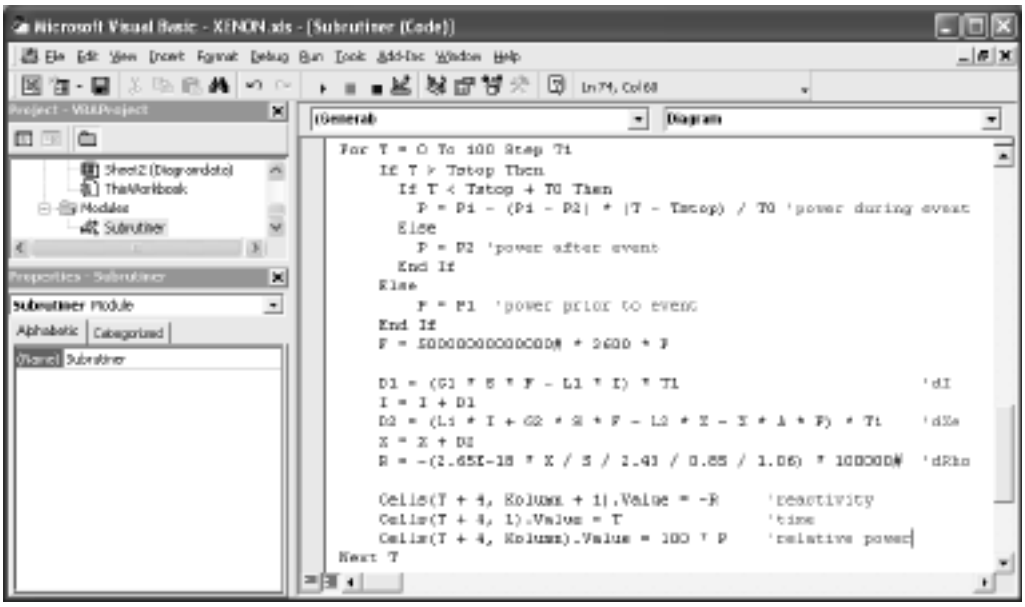

Figure 10. Part of the VBA-code used for the simulation of xenon poisoning in a nuclear reactor. The results of the calculation are transferred to a worksheet using the function Cells(Row #, Column #).Value.

4.3 Visual Basic for Applications (VBA)

VBA is Microsoft's common application scripting language that is fully integrated with Excel [5]. It is a rich programming language that offer many possibilities, but at the expense of a much steeper learning curve than for Excel itself. In addition to defining the actions of scrollbars, from a science teaching point-of-view, VBA is best used to simplify the work of students by automating spreadsheet tasks and also for creating user-defined functions (UDFs) that can be used in spreadsheet formulas in order make them more readable and easier to work with.

By recording actions using Excel's macro recorder repetitive tasks, such as making graphs, can be automated. The macro recorder is invoked from the menu [Tools] [Macro] [Record new macro...]. The actions are stored as VBA code in a Sub procedure that can be examined and modified using the VBA editor. Previously recorded macros can are executed by selecting [Tools] [Macro] [Macros...].

Creating an UDF is fairly simple task, it is done by invoking the VBA editor and selecting [Insert] [Procedure] [Function]. The UDF handles one ore more arguments, perform calculations and returns a single value to the spreadsheet, e.g., figure 11.

```
Public Function Fahrenheit(Celsius As Double) As Double
    Fahrenheit = (32 + (9 * Celsius / 5))
End Function
```

Figure 11. An example of a simple UDF that converts a temperature given in degrees Celsius to the corresponding value in Fahrenheit. In the worksheet the formula =Fahrenheit(100) will return the value 212.

References

[1] Ö. Nilsson, M. Österlund, "Fysik med Excel", Studentlitteratur AB, Lund, Sweden, 1999
[2] W. H. Press; B. P. Flannery, S. A. Teukolsky, and W. T. Vetterling, "Numerical Recipes in FORTRAN: The Art of Scientific Computing", 2nd ed. Cambridge, England: Cambridge University Press, p. 710, 1992.
[3] H. Erlichson, "Maximum projectile range with drag and lift, with particular application to golf", Am. J. Phys., Vol 51, No 4, 1983.
[4] W. Wagner, A. Kruse, "Properties of Water and Steam", Springer-Verlag, Berlin, 1998.
[5] J. Walkenbach "Excel 2003 Power programming with VBA", Wiley Publ. Inc., Indianapolis, 2004.

Curricula

Assoc. Prof. Michael Österlund is employed at the Department of Neutron Research, Uppsala University. Research is focused on neutron physics with applications within nuclear power, electronics and medicine. Since 1996, Michael Österlund has been involved in developing physics courses for B.Sc. engineering education with particular emphasis on the use of tools for simulation of dynamic systems and classroom data acquisition systems. Michael Osterlund is co-author of two textbooks on the use of Excel in physics education and on the simulation of dynamical systems in engineering education.

Appendix XXXVI

NEA/SEN/NSC/EG(2006)4

Organisation de Coopération et de Développement Economiques
Organisation for Economic Co-operation and Development

12-Jun-2006

NUCLEAR ENERGY AGENCY
NUCLEAR SCIENCE COMMITTEE

Executive Group

SUMMARY RECORD

FIFTEENTH MEETING OF THE EXECUTIVE GROUP OF THE NUCLEAR SCIENCE COMMITTEE

31st May 2006

JT03210430

SUMMARY RECORD OF THE FIFTEENTH MEETING OF THE EXECUTIVE GROUP OF THE NUCLEAR SCIENCE COMMITTEE

NEA Headquarters, Issy-les-Moulineaux
31st May 2006

In the absence of the chair, **Pierre D'Hondt**, the vice-chair, **Alain Zaetta**, opened the meeting and welcomed the delegates. Twelve delegates from nine member countries attended the meeting, including two delegates from the EC. Three new members, **Jan Blomgren** (Sweden), **Andy Pearce** (UK), and **Jean Coadou** (EC), participated for the first time as did the observer from Slovenia, **Tomaz Zagar**. **Cassiano de Oliveira**, **Pedro de Oliveira** and **Charles Boyle** were invited to present the status of the GERALD project.

Apologies for absence had been received from **Helmut Leeb** (Austria), **Pierre D'Hondt** (Belgium), **Rostislav Mach** (Czech Republic), **Syed Qaim** (Germany), **Young-Jin Kim** (Korea), **Pedro Vaz** (Portugal), as well as from **Tomas Botella** and **Georges van Goethem**, both from the EC. A list of participants is given in the Annex.

Adoption of the Agenda **[NEA/SEN/NSC/EG(2006)1]**

The proposed agenda for the fifteenth meeting of the Executive Group was adopted with the following modifications: point 6a would be taken just after point 5c and point 6b would be dealt with just after point 5a ii.

Introduction of the Deputy Director

The NEA Deputy Director, **T. Dujardin**, informed the Executive Group that **the arrangement between the NEA and the US DOE to exchange nuclear data and computer programs had been signed** on 10 April 2006. The new arrangement runs for five years and will be automatically renewed through tacit approval. **T. Dujardin** also notified the Group that **Akira Hasegawa**, Japan, had been appointed new head of the NEA Data Bank. Other new Data Bank staff members were **Yoon-Jong Choi**, replacing **Byung-Chan Na** and **Nicolas Soppera**, replacing **Tuncay Ergun**.

Approval of the Summary Record of the Fourteenth Meeting of the Executive Group **[NEA/SEN/NSC/EG(2005)4]**

The Summary Record of the fourteenth meeting of the Executive Group was approved without modifications.

Progress Report for 2005, Work in hand in 2006 and Programme of Work for 2007/2008 **[NEA/SEN/NSC/EG(2006)2]**

Computer program services

E. Sartori gave an overview of the computer program and integral data services. It was noted that the acquisition of new computer codes had been declining in the last few years. The number of requests for the services had been rather stable in recent years. Close to 1 850 computer codes and slightly more than 2 200 integral data sets had been distributed in 2005. A survey had shown that universities mainly requested computer codes related to non-nuclear power applications, whereas industry, as well as engineering and consultancy companies, requested more nuclear power related codes. It was proposed to extend the services to include compilations of benchmark data and reports from past NSC studies with a

Web-based guide to facilitate access to authorised users. The Data Bank training courses on the use of selected computer programs continue to attract many participants.

A. Koning asked about the possibility to provide a secure computer program services directly via Internet. **E. Sartori** answered that 11% of the requests were distributed over Internet via the File Transfer Protocol (FTP) on demand. He also noted that it would be complex to maintain an automatic distribution system, considering the changing distribution constraints associated with the services.

A. Hasegawa welcomed the news about the signing of the NEA – US DOE exchange arrangement and expressed Japan's contentment with the outcome of the negotiations.

As an introduction to the discussion of the declining trend in computer program acquisition, **E. Sartori** recalled the rules for the program distribution, including the tasks and duties of the liaison officers, which had been adopted at the Executive Group meeting on 11 June 2001. It was noted that the services were presently provided to 678 nominated establishments.

The Executive Group discussed the declining trend in the acquisition of new computer codes and recognised that the quality and value of the future Data Bank computer program service will depend on a change in this declining trend, and **agreed that delegates**, with the assistance of the NEA secretariat, **shall contact liaison officers in their respective countries, with the aim of encouraging these liaison officers to release more computer codes to the Data Bank**.

Services to non-OECD countries

I. Kodeli presented the Data Bank computer program services to non-OECD countries. In 2005, close to 600 packages out of a total of about 4 000 were distributed to 29 non-OECD countries and to the IAEA.

Status of the SUSD3D and GERALD projects

The development of the sensitivity and uncertainty code system SUSD3D was presented by **I. Kodeli** and was followed by a presentation of the status of the GERALD project by **J. Galan**, **C. de Oliveira**, **P. de Oliveira** and **C. Boyle**. The aim of the GERALD project is to create a unified software environment to facilitate the definition, solution and analysis of nuclear radiation transport problems.

Following a question from **A. Hasegawa**, **C. de Oliveira** confirmed that the GERALD would be an open source code.

The Executive Group agreed to continue its support to the GERALD project.

Nuclear Data Services

H. Henriksson presented the nuclear data services. He informed the Executive Group that the compilation of experimental data into the EXFOR database had progressed as planned and that the CINDA database, containing bibliographic information, had been updated and would be published in autumn 2006. The high priority request list for nuclear data had also been updated with new requests. Processed data, based on the JEFF-3.1 evaluated data library, for use with the MCNP code had been produced and would be distributed via the Data Bank computer program services.

A. Koning asked if the international data centres network had discussed the possibility of adopting a more modern data format, such as XML. **H. Henriksson** replied that some discussions had been held, but no concrete proposals had so far been presented. He also explained that the format used to exchange data between the centres was quite different from the public format.

A. Hasegawa enquired about the new CINDA format and asked if the US had stopped compiling data for the CINDA database. **H. Henriksson** reported that the last, and hopefully final, version of the new CINDA format had been communicated to the data centres on 18 May 2006 and that the US continued to compile CINDA entries, but only for experimental data entered into the EXFOR database.

The JEFF project

A. Koning outlined the organisation of the JEFF project and described more in detail the content of JEFF-3.1 library, which had been released in May 2005. He pointed out the good results obtained from the benchmark testing of the library, while emphasising that there were scope for further improvements. With the goal of having a new improved version of the library (JEFF-3.2) ready by 2008-2009, **A. Koning** proposed a 3-year prolongation of the JEFF mandate and summarized the planned deliverables.

E. Sartori mentioned that there was a need for cryogenic temperature data for solid state physics applications and proposed that these data could be incorporated in the thermal scattering law file of the next version of the library. **A. Zaetta** stressed the importance of including more covariance data in future versions of the library.

The Executive Group approved the proposed new JEFF mandate for the period October 2006 – October 2009.

The Thermochemical (TDB) database project

In the absence of **F. Mompean**, **C. Nordborg** gave an overview of the status of the Thermochemical Database (TDB) project. Four volumes of the TDB books had been issued in 2005. The work on the four on-going reviews on iron, tin, thorium and solid solutions was advancing well. It was planned to have the thorium review published in early 2007 and the other three volumes later in 2007.

The current phase of the TDB project will come to an end in February 2007, but it is envisaged to prolong the phase by one year to finalise the reviews and to have a thorough discussion on the future of the project. A few new ideas for future work have been collected, but **the NEA secretariat is interested in receiving additional ideas and suggestions from members of the Executive Group before the end of September 2006**.

Provision of expertise to other parts of NEA

The Data Bank provision of expertise to the NEA main secretariat was presented by **C. Nordborg**. The request for Data Bank expertise, especially in the areas of database development and preservation of information, is increasing. In order to remain within the Executive Group's old recommendation, to use less than 25% of the Data Bank resources in support of the NEA main secretariat, some of the requests had to be deferred. However, the newly established cooperation agreement between CSNI, NSC and the Data Bank called for an increase in the support to the NEA safety programme.

The Executive Group reviewed the allocation of Data Bank expertise to other parts of the NEA in 2007. **The proposed increase from 1 to 2 staff-months/year in support of the nuclear safety division, offset by a decrease from 14 to 13 staff-months/year in support of the radioactive waste management and radiation protection division was approved**.

In-house Computer System

P. Nagel presented recent and on-going software and database development activities undertaken by the Data Bank computing staff. He also highlighted the recent hardware upgrades to the Data Bank computer system.

Proposed budget for 2007/2008 **[NEA/SEN/NSC/EG(2006)3]**

The Data Bank budget document was introduced by **C. Nordborg**. It was noted that the 2005 budget had been balanced with carry over funds from 2004 and that the finally approved 2006 budget was identical to the one proposed at the last Executive Group meeting. The only proposed change in the 2007-2008 budgets was a small (~5%) increase in the allocation of resources for "Official travel" to compensate for increasing air fares. The proposed increase was offset by an equivalent saving in "Publications, Printing and Interpretation" in order to have a zero growth budget. The proposal did not take into account the nominal and statutory adjustments, which would be decided by the OECD Council later in 2006.

The Executive Group approved the proposed Data Bank budget and programme of work for 2007/2008 and recommends the Nuclear Science Committee to endorse the approval.

Points for Presentation to the Nuclear Science Committee

The Chair would, in close cooperation with the NEA secretariat, prepare a short summary of the meeting for presentation to the Nuclear Science Committee meeting, covering the following points:

- the signature of the NEA Data Bank – US DOE exchange arrangement;
- stimulation efforts to obtain additional computer programs;
- continued support to the GERALD project;
- extension of the JEFF mandate;
- demand for additional ideas for the future of the TDB project;
- approval of the programme of work and budget.

ANNEX

LIST OF PARTICIPANTS

DENMARK

NONBOEL, Erik
Radiation Research
Risoe National Laboratory
Postbox 49
DK-4000 Roskilde

Tel: +45 4677 4923
Fax: +45 4677 4977
Eml: erik.nonboel@risoe.dk

FINLAND

ANTTILA, Markku
VTT Processes
P.O. Box 1604
FIN-02044 VTT

Tel: +358 9 456 5012
Fax: +358 9 456 5000
Eml: Markku.Anttila@vtt.fi

FRANCE

ZAETTA, Alain
CEA Cadarache
DEN/DER - Bat 707
F-13108 St.-Paul-lez-Durance

Tel: +33 4 4225 27 61
Fax: +33 4 4225 76 27
Eml: alain.zaetta@cea.fr

GERMANY

TROMM, Th. Walter
Programme Manager
Nuclear Safety Research Program (NUKLEAR)
Forschungszentrum Karlsruhe GmbH
P.O Box 3640
D-76344 Eggenstein-Leopoldshafen

Tel: +49 7247 82 55 09
Fax: +49 7247 82 55 08
Eml: walter.tromm@nuklear.fzk.de

JAPAN

HASEGAWA, Akira
Deputy Director
Department of Nuclear Energy System
Japan Atomic Energy Research Institute
2-4 Shirakata, Tokai-mura, Naka-gun
Ibaraki-ken 319-1195

Tel: +81 29 282 6929
Fax: +81 29 282 6122
Eml: hasegawa@ndc.tokai.jaeri.go.jp

MORI, Takamasa
Research Group for Reactor Physics
Department of Nuclear Energy System
Japan Atomic Energy Research Institute
Shirakta-shirane, Tokai-mura, Naka-gun
Ibaraki-ken, 319-1195

Tel: +81 29 282 5360
Fax: +81 29 282 6122
Eml: mori@mike.tokai.jaeri.go.jp

NETHERLANDS

KONING, Arjan
NRG Nuclear Research and
Consultancy Group
Building 34.213
Westerduinweg 3, P.O. Box 25
NL-1755 ZG PETTEN

Tel: +31 (224) 56 4051
Fax: +31 (224) 56 8490
Eml: koning@nrg-nl.com

SPAIN

PENA GUTIERREZ, Jorge
Desarrollo de Aplicaciones
Computing Centre
Consejo de Seguridad Nuclear
C/ Justo Dorado, 11
28040 MADRID

Tel: +34 91 346 0123
Fax: +34 91 346 0275
Eml: jpg@csn.es

SWEDEN

BLOMGREN, Jan
Dept. of Neutron Research
INF, Uppsala University
Box 525
751 20 UPPSALA

Tel: +46 18 471 37 88
Fax: +46 18 471 38 53
Eml: jan.blomgren@tsl.uu.se

UNITED KINGDOM

PEARCE, Andy
National Physical Laboratory
Hampton Road
Teddington
Middlesex TW11 0LW

Tel: +44 20 8943 6699
Fax: +44 20 8943 6161
Eml: andy.pearce@npl.co.uk

UNITED STATES

DE OLIVEIRA, Cassiano R.E.
Nuclear and Radiological Engineering Program
The George W. Woodruff school
of Mechanical Engineering
Georgia Institute of Technology
Atlanta, GA 30332-00405

Tel: +1 404 385 4928
Fax: +1 404 894 3733
Eml: cassiano.oliveira@nre.gatech.edu

INTERNATIONAL ORGANISATIONS

European Commission

COADOU, Jean
EC, DG TREN
Directorate Nuclear Energy,Unit H2,
1, rue Henry M. Schnadt
Office EUFO 4384
L-2920 Luxembourg
LUXEMBOURG
Tel: +352 4301 34034
Fax: +352 4301 30139
Eml: jean.coadou@ec.europa.eu

RULLHUSEN, Peter
EC - JRC - Institute for Reference
Materials and Measurements
Joint Research Center
Retieseweg 111
B-2440 GEEL
BELGIUM
Tel: +32 (14) 57 14 76
Fax: +32 (14) 57 18 62
Eml: peter.rullhusen@cec.eu.int

Nuclear Energy Agency (NEA)

DUJARDIN, Thierry
Deputy Director, Science and Development
Tel: +33 1 45 24 10 06
Eml: thierry.dujardin@oecd.org

NORDBORG, Claes
Head of Nuclear Science Section
Tel: +33 1 45 24 10 90
Eml: claes.nordborg@oecd.org

SARTORI, Enrico
Data Bank
Tel: +33 1 45 24 10 72
Eml: sartori@nea.fr

CHOI, Yong-Joon
Data Bank
Tel: +33 1 45 24 10 91
Eml: choi@nea.fr

GALAN, Juan
Data Bank
Tel: +33 1 45 24 10 08
Eml: galan@nea.fr

HENRIKSSON, Hans
Data Bank
Tel: +33 1 45 24 10 84
Eml: henriksson@nea.fr

KODELI, Ivo
IAEA representative at the NEA Data Bank
Tel: +33 1 45 24 10 74
Eml: ivo.kodeli@oecd.org

NAGEL, Pierre
Data Bank
Tel: +33 1 45 24 10 82
Eml: nagel@nea.fr

RUGAMA, Yolanda
Data Bank
Tel: +33 1 45 24 10 99
Eml: rugama@nea.fr